Publication No. 66

Evapotranspiration Estimates Based on Surface Temperature and Net Radiation: Development of Remote Sensing Methods

By

K. F. Heimberg
L. H. Allen, Jr.
W. C. Huber

Agronomy Department
University of Florida
Gainesville

EVAPOTRANSPIRATION ESTIMATES BASED ON SURFACE TEMPERATURE AND NET RADIATION: DEVELOPMENT OF REMOTE SENSING METHODS

K.F. Heimburg

Graduate Student Investigator

L.H. Allen, Jr.
and
W.C. Huber

Principal Investigators

Publication No. 66

Florida Water Resources Research Center

Research Project Technical Completion Report

Project Number A-040-FLA

Annual Allotment Agreement Numbers

14-34-0001-0110
14-34-0001-1110

Report Submitted: December 20, 1982

The work upon which this report is based was supported in part by funds provided by the United States Department of the Interior.

PREFACE

This report was also supported in part by Agriculture and Resources Inventory Surveys Through Aerospace Remote Sensing (AgRISTARS) funds through the U.S. Department of Agriculture, as well as several sources within the University of Florida. The report is based entirely upon the Ph.D. Dissertation of K.F. Heimburg, University of Florida, December, 1982.

ACKNOWLEDGMENTS

The work reported in this dissertation grew out of National Aeronautics and Space Administration (NASA) sponsored water resources research. It was primarily supported by a grant from the Office of Water Resources Technology in the U.S. Department of the Interior and Agriculture and Resources Inventory Surveys Through Aerospace Remote Sensing (AgRISTARS) program funds administered through the U.S. Department of Agriculture (USDA). Some support was also received in the form of an assistantship from the Agronomy Department at the University of Florida. All these sources of support are gratefully acknowledged.

I would especially like to thank Dr. Wayne C. Huber and Dr. L. Hartwell Allen, Jr. for signing the original research proposal as principal investigators and seeing this project through to its completion. Without their initial confidence in me and the day-to-day administrative efforts of Dr. Allen none of the work would have been possible. I would also like to thank them and the rest of my supervisory committee, Dr. Howard T. Odum, Dr. Ralph W. Swain, and Dr. James P. Heaney for improvements they made possible with their comments on the manuscript.

The research reported in this dissertation stretched over four years and required the help and cooperation of many people. Sensors and other equipment were borrowed from USDA, NASA, Center for Wetlands, Fruit Crops Department, and Environmental Engineering Sciences Department of the University of Florida. The Animal Science Department permitted ET measurements in part of one of its pastures and the Agronomy

Department provided space for an instrument room. The people I owe special thanks to are Bill Ocumpaugh and Fred McGraw for patiently working around the measurement equipment and giving up some space; Johnny Weldon for allowing me the use of the Agricultural Engineering Department machine shop; Jim Hales for use of his tools and advice in fabricating apparatus in the machine shop; Lester Burch for his fine machining; my brother Stephan Heimburg for conscientiously checking and adjusting the thermopile time constants; Mike Baker for designing and helping build the scanning valve control electronics, and repairing the dewpoint analyzer after a lightning strike; Wayne Wynn for help in maintaining the measurement system; Dan Ekdahl at the Digital Design Facility for electronics repairs--especially a lightning-damaged computer-controlled voltmeter and similarly damaged computer interface boards; and finally, Beth Chandler for expeditiously inking most of the figures in this dissertation.

I owe a debt of gratitude beyond words to three people who went miles out of their way to help me. Gene Hannah was invaluable in the original field installation and helped with problems throughout the course of the project. I'm thankful to Ferris Johnson for his tireless assistance in use of the computer system and trouble-shooting computer hardware problems. Finally, I enthusiastically acknowledge the work of Pattie Everett, who spared no effort and sacrificed evenings, weekends and holidays in moving this manuscript through countless drafts toward perfection.

TABLE OF CONTENTS

LIST OF FIGURES

Appendix D: Supplementary Figures

LIST OF TABLES

ABSTRACT

A generalized physical method is developed for making evapotranspiration (ET) estimates based on directly measured air temperature and remotely sensed surface temperature and net radiation data. The method is based on the correlation of surface-to-air temperature gradients and varying net radiation loads; the slope and intercept of this correlation are shown to be composite values of two groups of surface parameters. Five equations are developed to calculate ET from these composite values plus net radiation and some combination of two of the four surface parameters (bulk air transport, moisture availability, saturation deficit, and soil heat flux).

The method is validated using ET measurements made over a pasture surface using the energy budget/profile Bowen ratio technique. An automatic measurement system consisting of a computer-controlled data acquisition system and air sampling arrangement, time-constant-matched humidity, temperature, and radiation sensors, and four interacting programs was developed to measure and calculate half-hour average surface energy budgets and statistics. Data from 42 days in the spring and fall of 1981 are reported.

It was found that the radiation surface temperature is in general not the same as the effective heat transport surface temperature--it may be necessary to correct remote surface temperature measurements before using them with conventionally evaluated heat transport coefficients. Because parameters are assumed constant, instantaneous ET

estimates made with the developed method are at times systematically high or low, but these errors tend to cancel in cumulative estimates.

The method is shown to be well-suited for use with 1- to 3-hour time resolution satellite data. In effect it evaluates surface parameters such as moisture availability, requires no interpolation for ET estimates between data sets, is adapted to the inevitable cloud-caused loss of satellite surface temperature data, and reduces calculation of cumulative ET to estimating total positive net radiation and duration of positive net radiation in a particular estimation period. The method's ET estimates are shown to be as accurate as the state-of-the-art simple residual method, which does not have these advantages.

CHAPTER 1

INTRODUCTION

Potential for Remote Evapotranspiration Estimates

The loss of water from the earth's surface by either evaporation from soil and plant surfaces or transpiration by plants is called evapotranspiration (ET). Along with rainfall and runoff, it plays a very significant role in determining the availability of water at the earth's surface and the recharge to deep aquifers. Because water is critically important to man's existence, ET estimation methods are important in solving problems of water supply.

Water supply problems in relatively dry areas have long included the estimation of crop water requirements, evaporation from reservoirs, and evapotranspiration over aquifer recharge areas. As population has grown, the demand for water has increased and interest in estimation methods has become more widespread. Today, there is a growing need for evapotranspiration estimates even in relatively wet areas, such as Florida.

Present methods of measuring and estimating ET are diverse, depending upon the specific purposes of the estimates and available data. On the one hand are physically-based measurement techniques developed by scientists. They provide accurate instantaneous ET rates for a specific location, but require continuous measurements of such variables as air temperature and vapor pressure, net radiation, and soil heat flux. Examples of these techniques are the eddy flux correlation, energy

budget/profile Bowen ratio and Penman methods (American Society of Agricultural Engineers, 1966; Brutsaert, 1982).

On the other hand, water use planners and water supply engineers have developed methods which produce daily to monthly estimates for larger areas. In locations where such records are kept, these methods are based on climatologic data. They are generally founded on some physical correlation, but all involve empirical adjusting factors for vegetation type, air humidity, altitude and the like. Examples are the Blaney-Criddle method, the radiation method, the Penman method, and the pan evaporation methods (Doorenbos and Pruitt, 1977).

The weather stations which provide the base information for these methods are widely scattered. On the average, each station in the United States represents an area on the order of 100 mi square (Price, 1982). Regional estimates of evapotranspiration are thus difficult to make and of dubious accuracy. They are limited by insufficient data on highly variable surface parameters such as soil moisture conditions and vegetation types.

By comparison to the weather station network, today's satellites return remotely sensed information about the earth's surface with an unprecedented level of detail. The surface area element or pixel sizes and the time intervals between coverage of some of the satellites appropriate to regional scale studies are shown in Table 1-1. As a result of the availability of this type of data and modern high-speed computers, the potential exists to systematically monitor evapotranspiration on a regional scale.

Development of this potential could benefit a variety of research areas. If remote-sensing methods are also developed to estimate rainfall

Table 1-1. Spatial and Temporal Resolution in Satellites

Satellite Acronym	Orbit Type	Pixel Size	Time Intervals
Landsat	polar	80 x 80 m	18 da
HCMM	polar	.6 x .6 km	12 hr each 5 da
TIROS	polar	1 x 1 km	12 hr
GOES	geostationary	8 x 4 km	30 min

on a regional basis and if streamflow is gaged, aquifer recharge over wide areas can be estimated (Allen et al., 1980). The information on surface energy fluxes gained by an ET estimation technique could also be useful as boundary conditions for models of the atmosphere. It is also possible that large-scale changes on the earth's surface such as deforestation and desertification could be monitored by observing longer-term changes in ET patterns. Finally, the correlation of evapotranspiration and yield in agronomic crops may lead to large-scale yield predictions (Doorenbos and Pruitt, 1977; Chang, 1968).

The purpose of this research is to develop and test a generally applicable method for estimating evapotranspiration based as much as possible on remotely sensed data. Since it is ultimately intended for use with satellite data from large diverse areas, criteria for this method include that it be strictly physical, relatively easy to apply, and compatible with the format and limitations of satellite data. The research is also intended to identify factors critical to the accuracy of the estimates which require more research, and factors which may improve future satellite measurement for use in ET estimation.

Scope of the Research

Data returned from a satellite consist of the energy flux in a particular band of wavelengths coming from a particular surface area

element at a particular time. For environmental applications, the electromagnetic spectrum is usually resolved into visible and thermal bands. With a clear sky and proper consideration of atmospheric transmission properties, these measurements can be used to calculate the surface temperature and the net radiation absorbed by the surface.

Net radiation and surface temperature estimates should lead to good evapotranspiration estimates because they are very prominent variables in the heat exchange processes that take place at the earth's surface. Net radiation is the primary energy source used in changing water from liquid to vapor at the surface, while surface temperature--because it is a result of surface variables and energy exchange processes--is a composite measurement of the effects of these variables.

However, it is a long step from measurements of net radiation and surface temperature to an operational ET estimating system using satellite data. The following questions illustrate the range of problems faced in developing a method for such a system.

1. What is the best way to estimate net radiation from satellite pixel information? How does one treat clouds or haze?

2. How is the radiation temperature of a complex surface like that of vegetation interpreted? Does angle of view and height of vegetation make a difference? How does one handle a canopy underlain by a cool surface like a marsh or swamp? How does one treat mountainous topography?

3. Is an interpolation technique required to compensate for the temporal resolution of satellite data?

4. What level of detail is required in a practical ET estimation method? How does one get the most acceptably accurate estimate for the least effort in data collection and processing?

5. How are the effects of water availability, vegetation type, cloudiness, and wind related? And how do they influence ET? What is the minimum amount of data needed from ground-based observations?

6. Can estimates made with area average data be of reasonable accuracy when there are various vegetation types or net radiation regimes in the same pixel?

7. Ultimately, what factor most limits the accuracy of a given remote estimation scheme?

The work described in this report addresses many of these questions. The emphasis is on how to most efficiently account for all the factors affecting evapotranspiration, and how to extract as much information as possible about the surface and its environment from remote data. Practical limitations such as the fact that satellite data are available only at discrete time intervals and sometimes incomplete because clouds prevent a surface temperature measurement are considered. All ground-based measurements except air temperature were avoided; methods to eliminate this measurement are suggested, but their investigation was considered beyond the scope of this research.

It is assumed that estimates of net radiation and surface temperature are, barring clouds, available at regular time intervals. The question of complex radiation temperatures is side-stepped by considering a relatively simple pasture grass surface. Although a parameter that includes the effect of wind on evapotranspiration is used, its functional dependence on windspeed is not explored.

Research Approach

The overall approach to developing a remote evapotranspiration estimation scheme was to compare estimates made with trial methods to actual ET rates measured over a test surface. Accordingly, there were three main areas of effort: the collection of a base of accurate ET data, the theoretical development of an estimation method based on remotely sensed data, and the testing of that method against the actual ET measurements.

As suggested in the previous section, the enormous variety of terrain and vegetation types present on the earth's surface introduce a large number of complicating factors into ET estimation formulations. In order to clearly assess the potential of a general method, as many of these complicating factors as possible were avoided by choosing a relatively homogeneous flat area of pasture as a test surface. The approach was to develop a basic method which would work for simple surfaces; once it is proven successfult can be modified if necessary to deal with more complex situations like mountainous terrain or swamp.

A micrometeorologic measurement technique was used to measure actual ET so that surface processes were left as undisturbed as possible. The radiation surface temperature as well as net radiation was measured for later use in method-testing. A great deal of effort went into developing a data collection system to assure the reliability of the ET measurements. Special efforts were made to match the time constants of the sensors involved and to reduce electrical signal noise. Control of the measuring system, scheduling of the measurements, and calculations were all performed by computer to minimize human error.

The fundamental assumption in method development was that satellite data would be available in time intervals on the order of 1-3 hours. After this assumption, the emphasis was on operational criteria--a practical method must have general applicability, computational simplicity, and low data requirements. With these objectives in mind, an analytical approach, rather than a simulation approach, was chosen. In order to keep data requirements low yet take advantage of satellite data, the level of detail was chosen to be somewhat intermediate between the strictly physical ET measurement methods and the empirical estimation

methods. This required a set of assumptions, all of which are explicitly identified in the derivation of the method.

The general objective of the method-testing was to validate the general framework of the method and to assess the error contributions of various parts of the method on instantaneous and cumulative ET estimates. The assumptions made during the development of the method were individually examined; in this way, the relative importance of ground-gathered ancillary data such as air temperature, saturation water vapor deficit, windspeed, and soil temperature could be judged. The testing was done with ideally accurate on-site measurements of net radiation, surface temperature, air temperature, and evapotranspiration.

Experimental Site and Data Collection

An area of pasture at the University of Florida's Beef Research Unit was used as the research surface. The site is located northeast of Gainesville, Florida, as shown in Figure 1-1. It was chosen because it is typical of northern Florida pasture areas, and was amenable to micrometeorologic measurement of a surface energy budget. The area was flat with relatively uniform grass cover, and was large enough to ensure well-developed temperature and vapor pressure profiles. The test surface was a mixture of grasses: roughly 60-70% was bahiagrass (*Paspalum notatum*), about 20-40% was smutgrass (*Sporobolus poiretii*), and 5-10% was white clover (*Trifolium repens*).

Evapotranspiration was computed by an energy budget/profile Bowen ratio method from measurements of net radiation, soil heat flux, and gradients of temperature and water vapor pressure over the pasture surface. A Hewlett-Packard 2100 computer and low-speed data acquisition subsystem was used to automatically scan and measure the sensors,

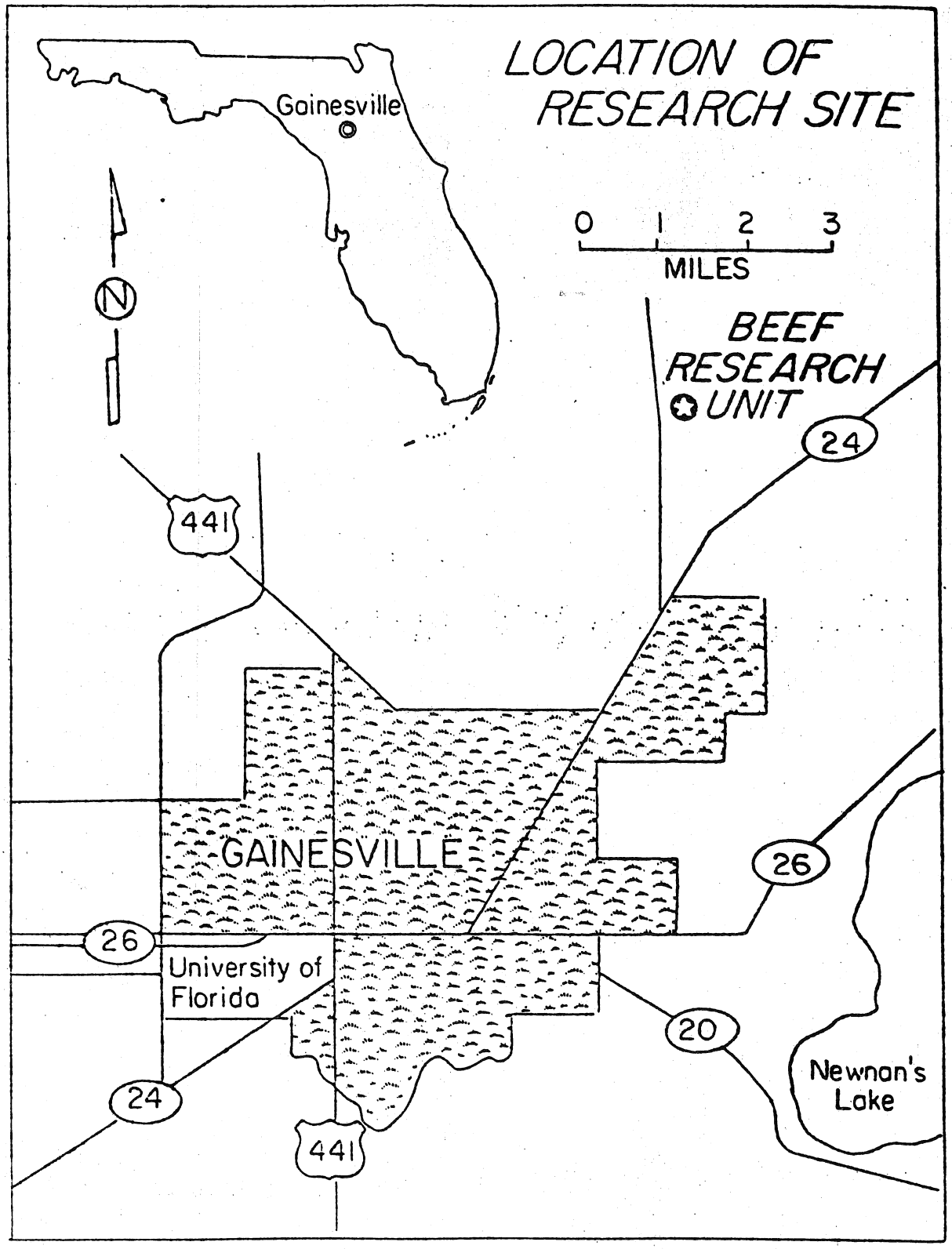

Figure 1-1. Location of the University of Florida Beef Research Unit.

convert the measurements to proper units, and compute averages. Average energy budget components and temperature and vapor pressure gradients were calculated and reported for half-hour periods.

The arrangement of sensors in the field is shown in Figure 1-2. Aspirated thermopiles and air sampling ports were mounted on arms of a 2.5-m mast. The area within a 10-m radius of this mast was completely unobstructed to meet the fetch requirements of the measurement method. Radiometers were attached to the end of a guyed boom about 2 m over the surface. The precision radiation thermometer was bolted to a camera tripod atop an antenna tower 9.5 m above the grass surface; the windspeed and direction sensors were mounted on the same tower at 7 m. A 14-m tower served as lightning protection for the entire group of instruments.

Shielded buried signal cable connected the sensors to the data acquisition system which was housed in a building about 90 m away from the sensors. For vapor pressure measurements, air samples from five separate levels in the field were pumped continuously back to the building through heated insulated tubing and mixing chambers to a dewpoint analyzer. Air samples were switched sequentially to this instrument by a scanning valve controlled by the measuring computer program. The dewpoint was measured after a half-minute delay to allow time for the analyzer to settle on the dewpoint of the sample from the new level.

Altogether, ET data from 42 days were used in verifying the remote ET estimation method developed. These data were collected in the spring and fall of 1981.

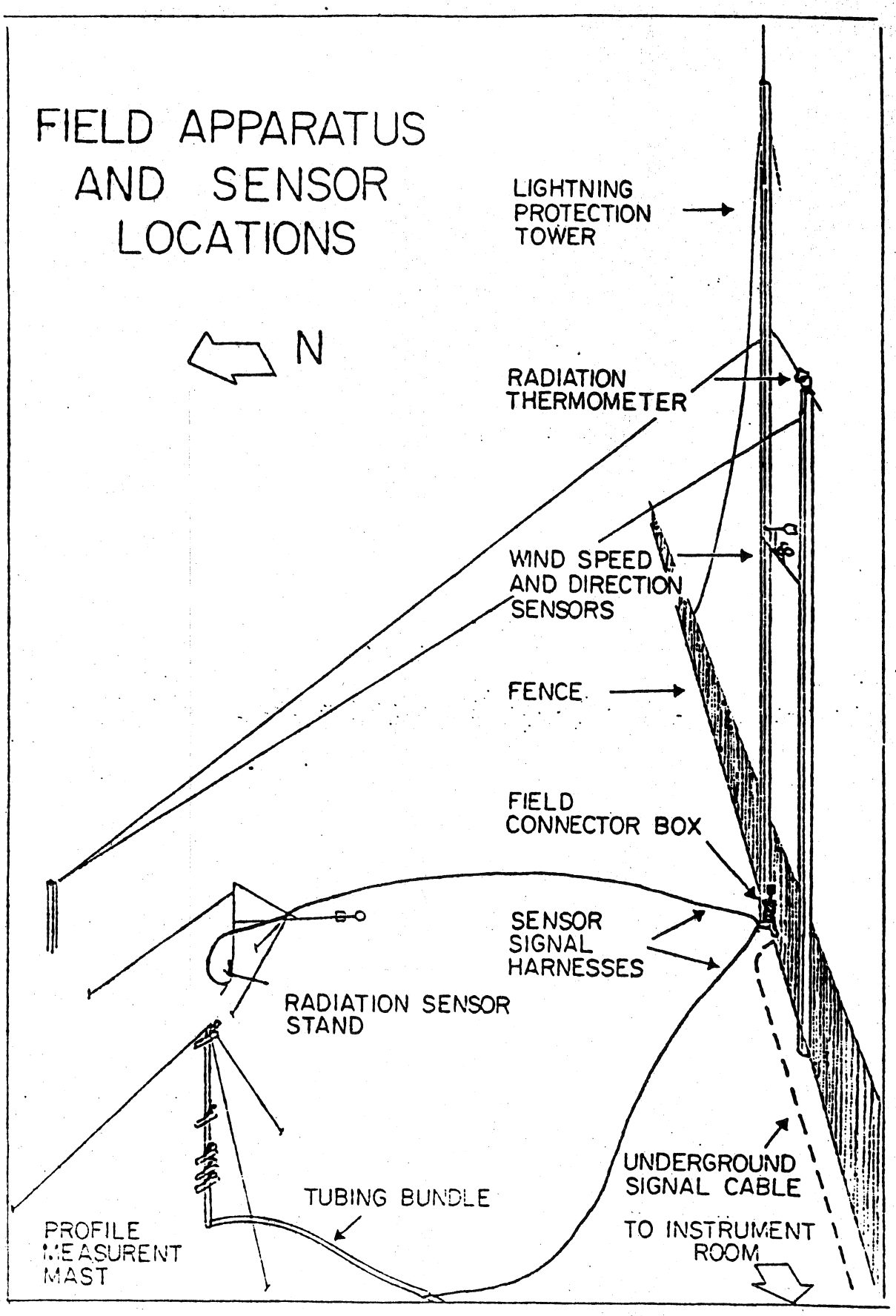

Figure 1-2. Field Apparatus and Sensor Locations. This diagram is not to scale.

Organization of Report

Basic concepts underlying current understanding of the evapotranspiration process are reviewed in Chapter 2. These concepts are fundamental to both the evapotranspiration measurement and method development portions of the study. Chapter 3 describes the computer-based evapotranspiration measurement system that was developed to collect a base of accurate ET data. This chapter contains the theory of the measurement technique, considerations made in designing the profile sensing systems, brief descriptions of the programs that operate the system, and an assessment of the strengths and weaknesses of the measurement system. Two methods of calculating ET based on remotely sensed data are derived in Chapter 4, one relatively rigorous with a minimum of added assumptions, and a grosser less detailed one with extensive approximations. Both methods are based on a temperature gradient model which uses net radiation and surface temperature data to determine surface parameters. The performance of this model and these methods is compared to actual ET measurements in Chapter 5. The method most suitable for use with satellite data is tested component by component to clearly evaluate its strengths and weaknesses. A summary of conclusions and suggestions for further research are contained in Chapter 6.

Repeatedly used symbols are defined in Appendix A. (All symbols are defined in the text where they are introduced.) Appendix B is a listing of the programs developed for the automatic ET measurement system, along with definitions of names for subroutines, functions, data arrays, and indexes. Appendix C is a summary listing of the data collected, and supplementary figures are presented in Appendix D.

CHAPTER 2

EVAPOTRANSPIRATION AND SATELLITE DATA

Overview

The availability of satellite images of the earth's surface and the resources to investigate their usefulness has resulted in a variety of remote-sensing research projects. In recent years, there have been programs in which evapotranspiration estimation procedures were the objective, notably a joint effort among the National Aeronautics and Space Administration (NASA), the Institute of Food and Agricultural Sciences at the University of Florida, the Florida Water Management Districts (Allen et al., 1980), and NASA's Heat Capacity Mapping Mission, or HCMM (Goddard Space Flight Center, 1978).

Since the estimation techniques need to be applicable to many different surfaces, physical rather than empirical approaches are required. The physical methods that have been developed, including the one presented in this work, are all based on the energy budget concept of the surface and on the similarity of transport among quantities in turbulent flow. These ideas and various approaches to solving the energy budget equation are developed in the first part of this chapter. Remote ET estimation techniques are reviewed in the second part, which concludes with an introduction to the new method.

The Evapotranspiration Process

At the interface between a liquid and a gas, molecules are continually breaking and reforming the intermolecular bonds which hold them at

the surface as a liquid. The energy of the random molecular collisions which cause the bonds to break is carried with the freed molecule; this thermal (heat) energy is lost by either liquid or gas molecules near the interface. Since this energy contributes only to the molecule's conversion to the vapor state and not its temperature, it is called the latent heat of vaporization. It is released to the molecules at the surface should a free molecule collide with and be captured by molecules in the liquid state.

When the concentration of vapor molecules is higher at the surface than at some distance away from it, there is a net flow of molecules and energy (in the form of latent heat) away from the surface. This process is evaporation.

Evapotranspiration is the evaporation of water from soil or plant surfaces together with transpiration by plants. In transpiration, water evaporates from internal plant surfaces and diffuses into the air around the plant through openings in the leaves (stomata). Like the process of evaporation, evapotranspiration consists of three fundamental elements: the absorption of thermal energy at a water-air interface, the change of state of water from liquid to vapor, and the resulting net loss of vapor molecules and their heat of vaporization from the surface due to a favorable vapor concentration gradient.

The heat energy consumed in the evapotranspiration process is lost from the vegetation biomass. Therefore, all the energy fluxes to and from the plant canopy and the factors influencing them play a part in determining the evapotranspiration rate. Figure 2-1 is a simplified diagram of the surface and its primary energy and water fluxes. It is presented in the diagramming language of Odum (1982), and embodies many of

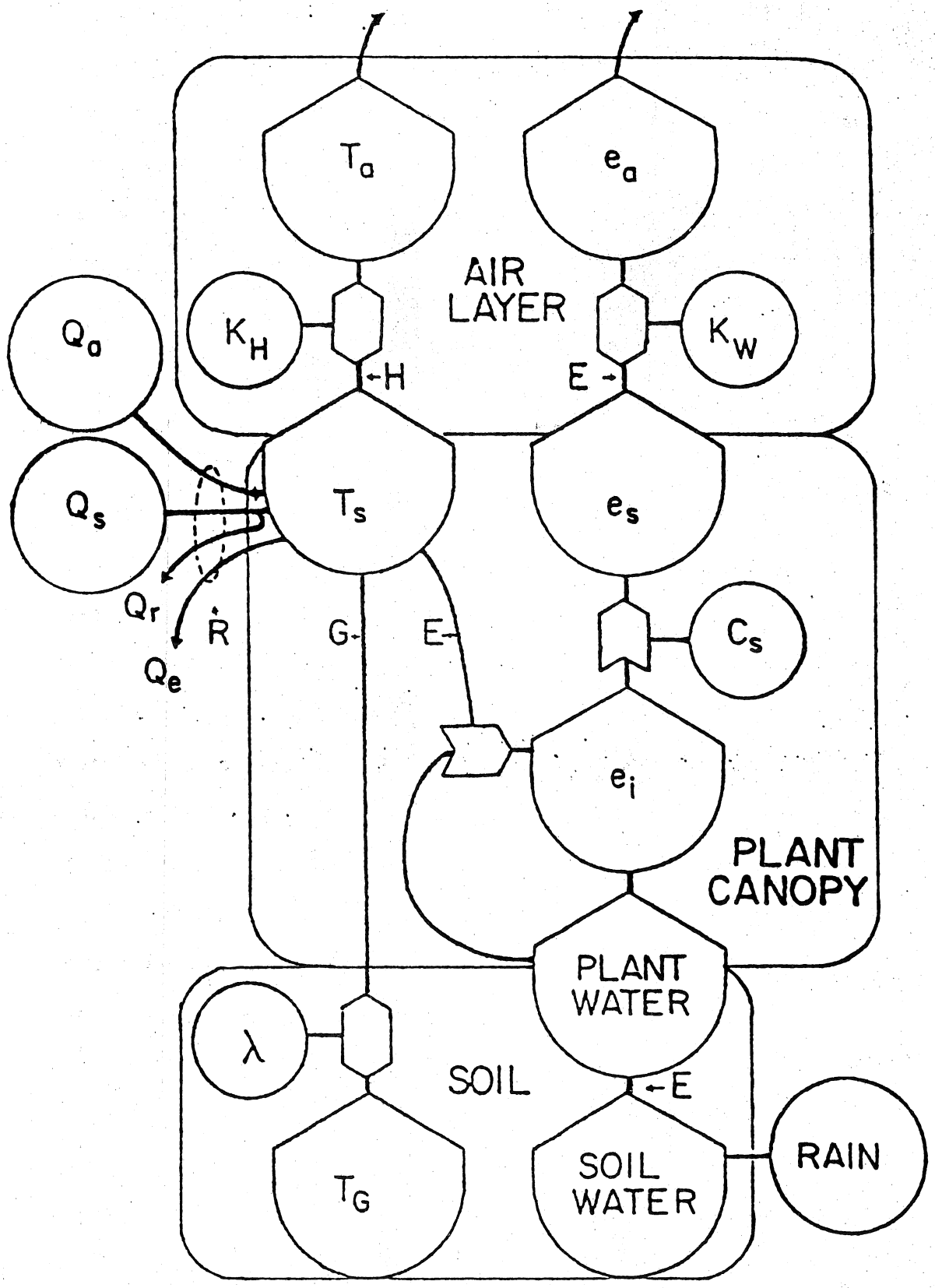

Figure 2-1. System Diagram of Generalized Evapotranspiring Surface. Symbols are from Odum (1982).

the concepts and simplifications conventionally applied in evapotranspiration theory.

The heat energy stored in the plant canopy is represented by its temperature (T_s). The bulk of this energy comes into the vegetation in the form of direct or scattered solar short wavelength (0.3 to 3 μm) radiation (Q_s); it also intercepts thermal or long wavelength (3 to 50 μm) radiation emitted by the atmosphere (Q_a). A substantial fraction of the shortwave radiation received by the surface is reflected (Q_r), a very small part is used to drive photosynthetic reactions in the plants, and the remainder becomes heat energy absorbed and stored temporarily in the biomass. Part of this energy is reradiated to the atmosphere (Q_e). The difference between the downwelling radiation (direct and atmospheric) and the upwelling radiation (reflected and emitted) is referred to as net radiation (R).

Besides these radiant energy fluxes, the vegetation exchanges energy with its environment in several other ways. Thermal energy exchanged with the air by the process of molecular conduction and turbulent diffusion is referred to as sensible heat flux (H); energy exchanged with the soil is soil heat flux (G). Energy used in the change of state from water to water vapor is transported with water vapor and is referred to as latent heat flux (E).

In this generalized view of the surface system, the plant canopy is considered to have a uniform temperature representative of its heat content. There are complex energy exchange processes that occur within the canopy because of differences in temperature. For example, radiation is exchanged between plant surfaces, and sensible heat released from one leaf may be reabsorbed and released from another as latent heat.

However, when the purpose is to make total evapotranspiration estimates, these exchanges are ignored, and only the energy fluxes entering or leaving its boundaries are considered.

Besides the radiant energy pathways (R) and heat energy stored in the plant canopy, Fig. 2-1 shows the dependence of the surface energy balance, and thus evapotranspiration, on factors in the environment of the surface. Heat that is lost to (or gained from) the air as sensible heat is not (is) available for evapotranspiration. This flux is dependent on the air temperature (T_a) and the thermal transport properties of the air, represented by the eddy thermal diffusivity (K_H) in the figure. When the air temperature is cooler than the surface temperature of the canopy, sensible heat moves from the canopy into the air. When the canopy is cooler than the air, it absorbs heat energy from the air. There is an analogous heat flux pathway to the soil, dependent on soil temperature (T_g) relative to the canopy temperature (T_s), and the thermal conductivity of the soil (λ).

The right half of Fig. 2-1 shows the pathway of water through the surface system. It originates in the soil and moves through plant tissues into the leaves, where it evaporates. Depending on the vapor pressure inside the leaves (e_i), the vapor pressure in the surface air layer outside the leaf (e_s), and the stomatal conductivity (C_s), water vapor then diffuses through stomata into the air around the leaves. From the surface layer water vapor diffuses into the air, depending on the relative vapor pressures of the surface layer and air (e_s and e_a) and the eddy water vapor diffusivity (K_W).

The Energy Balance Approach to ET Estimation

The Energy Budget Equation

The three elements of evapotranspiration (the absorption of water from the soil or plant surfaces, the absorption of thermal energy from the plant canopy, and the flux of water vapor through the air over the surface) provide at least three fundamental approaches to evapotranspiration measurement. These have been referred to as the water budget, energy budget, and aerodynamic approach, respectively. All previously developed remote ET estimation methods, the remote technique developed in this study, and the ground truth measurement technique used in this study are founded on the energy budget equation.

The energy balance of a vegetation and air layer can be written

$$R - E - H - G - P - S = 0 \quad , \qquad 2\text{-}1$$

where R is the net radiation flux absorbed (from p.15, $R = Q_s+Q_a-Q_r-Q_e$)
E is the latent heat flux,
H is the sensible heat flux,
G is the soil heat flux,
P is the photosynthetic heat flux, and
S is the time rate of heat flux storage in the vegetation/air layer.

Here energy "flux" is used to describe energy "flux density," i.e., the energy flow per unit time through a unit area. All terms are in these units.

Because of inherent measurement difficulty and sensor limitations, the energy budget components can only be measured to within about 10% of their actual values (Sinclair et al., 1975). Since some of the smaller components are actually indistinguishable from measurement error, they need not be considered.

Usually the smallest component is photosynthetic heat flux. It can be considered negligible because only 1 to 5% of the net radiation impinging on vegetation is absorbed in this way (Allen et al., 1964).

It can be shown by a "worst case" calculation that the storage term is also in the negligible range. Heat in the vegetation/air layer can be stored as sensible heat in the air, latent heat in the air, sensible heat in the biomass, and sensible heat in the litter surface layer. In a strict sense, these are evaluated as follows:

$$S = \int_0^l c_a(z) \frac{\partial T_a(z)}{\partial t} dz + \int_0^l \frac{c_a}{\gamma} \frac{\partial e_a(z)}{\partial t} dz + \int_0^l c_b(z) \frac{\partial T_b(z)}{\partial t} dz + \int_0^d c_g(z) \frac{\partial T_g(z)}{\partial t} dz \quad , \qquad 2\text{-}2$$

where $c_a(z)$, $c_b(z)$, and $c_g(z)$ are volumetric heat capacities (ρc) of canopy air, plant biomass, and surface soil, respectively,
$T_a(z)$, $T_b(z)$ and $T_g(z)$ are the temperatures of canopy air, canopy biomass, and surface soil, respectively,
$e_a(z)$ is the vapor pressure of canopy air,
γ is the psychrometric constant,
l is the vegetation height,
d is the depth of the surface litter layer, and
z is the vertical space coordinate.

Using averages for the spatial variables, Eq. 2-2 can be rewritten:

$$S = (\rho c_p)_a h \frac{\Delta \overline{T}_a}{\Delta t} + \frac{(\overline{\rho c_p})_a}{\gamma} h \frac{\overline{\Delta e_a}}{\Delta t} + (Vc)_b \frac{\overline{\Delta T_b}}{\Delta t} + (\rho c)_g d \frac{\overline{\Delta T_g}}{\Delta t} \quad , \qquad 2\text{-}3$$

where a, b, and g are subscripts referring to air, biomass, and soil specific heats, densities, and temperatures, and
V is the mass of vegetation per unit area.

total heat storage	=	sensible heat stored in canopy air	+	latent heat stored in canopy air	+	heat stored in vegetation	+	heat stored in top soil layer
S	=	$(\rho c_p)_a h \frac{\overline{\Delta T}_a}{\Delta t}$	+	$(\rho c_p)_a h \frac{1}{\gamma} \frac{\overline{\Delta e}_a}{\Delta t}$	+	$(Vc)_b \frac{\overline{\Delta T}_b}{\Delta t}$	+	$(\rho c)_g d \frac{\overline{\Delta T}_g}{\Delta t}$
S	=	$.0012 \frac{g}{cm^3} \times 0.24 \frac{cal}{g°C} \times 20\ cm \times \frac{24}{4} \frac{°C}{hr}$	+	$.0012 \frac{g}{cm^3} \times 0.24 \frac{cal}{g°C} \times 20\ cm \times 1.5 \frac{°C}{mb} \times 3 \frac{mb}{hr}$	+			
		$10{,}000 \frac{kg}{ha} \times 1.0 \frac{cal}{g°C} \times \frac{24}{4} \frac{°C}{hr}$	+	$1.5 \frac{g}{cm^3} \times 0.2 \frac{cal}{g°C} \times 1\ cm \times \frac{5}{4} \frac{°C}{hr}$				
S	=	$.0006 \frac{cal}{cm^2\ min}$	+	$.0004 \frac{cal}{cm^2\ min}$	+	$.01 \frac{cal}{cm^2\ min}$	+	$.006 \frac{cal}{cm^2\ min}$
S		$.02 \frac{cal}{cm^2\ min}$						

Figure 2-2. Rough Calculation of Heat Storage in Pasture Canopy.

This expression is evaluated in Fig. 2-2 using values typical for pasture grass. Heat storage in pasture biomass and the top litter layer is approximately two orders of magnitude less than peak net radiation loads; latent and sensible heat storage in the canopy air is about three orders of magnitude less.

Since the values of the photosynthetic heat flux and the time rate of canopy heat storage are negligibly small, the energy budget equation may be written

$$R - E - H - G = 0 \quad . \qquad 2\text{-}4$$

The ET measurement method and the remote estimation method are based on this simplified form of the equation. It is also the basis for all but the empirical remote-sensing ET estimation methods. The following subsections briefly review the fundamental analytical concepts and evaluation techniques which are common to previously developed evapotranspiration estimation methods based on the energy budget equation.

Transport Similarity and Wind Models

After the surface energy balance, the most important concept to ET estimation techniques is that of transport similarity among momentum, heat, and mass fluxes in the turbulent layer near the surface. This idea is used in all forms of the energy budget approach to ET estimation, both to evaluate transport properties and to avoid evaluating transport properties.

The fundamental equations for the one-dimensional transport of momentum, heat, and water vapor are (Eagleson, 1970)

$$\tau = \rho K_M \frac{\partial \bar{u}}{\partial z} \qquad 2\text{-}5$$

$$H = \rho c_p K_H \frac{\partial T}{\partial z} \qquad 2\text{-}6$$

$$E = \frac{\rho L \varepsilon}{p} K_W \frac{\partial e}{\partial z} \qquad 2\text{-}7$$

where τ is momentum flux,
H is sensible heat flux,
E is latent heat flux,
K_M, K_H, K_W are the eddy diffusivities of momentum, heat, and water vapor,
$\bar{u}$ is the average horizontal windspeed,
T is temperature,
e is vapor pressure,
ρ is the air density,
c_p is the air specific heat at constant pressure,
L is the latent heat of evaporation,
P is the atmospheric pressure, and
ε is the ratio of molecular weights of water and dry air.

The similarity hypothesis, which was developed in the last half of the nineteenth and early twentieth centuries (reviewed by Brutsaert, 1982), proposes that the eddy diffusivities of momentum, heat, and water vapor are all the same:

$$K_M = K_H = K_W \quad . \qquad 2\text{-}8$$

It was not until Prandtl's (1932) development of the mixing length concept that general analytical treatment of eddy diffusivity began. According to mixing length theory, it is argued that

$$K_M(z) = \ell^2 \frac{d\bar{u}}{dz} \quad , \qquad 2\text{-}9$$

where ℓ is the mixing length and
$\bar{u}$ is the average windspeed perpendicular to z (horizontal).

By postulating that the mixing length increased with distance from a surface ($\ell = \kappa z$, where κ is the von Karman constant), Prandtl went on to derive an expression that accurately describes the variation of windspeed near a surface, the simple log wind profile. With parameters for displacement height (D--with dense vegetation, that height above the surface where the windspeed vanishes) and roughness height (z_0--a

parameter included so that the windspeed is defined as zero when $z - D = 0$), the equation for the log profile can be written

$$\bar{u}(z) = \frac{1}{\kappa}\frac{\tau_0}{\rho} \ln\left(\frac{z - D + z_0}{z_0}\right) , \qquad 2\text{-}10$$

where τ_0 is the shear stress at the surface. With this wind profile, the eddy diffusivity can be evaluated between the surface and any level in the air with average windspeed $\bar{u}_a$:

$$K_M(z) = \frac{\kappa^2 \bar{u}_a (z - D + z_0)}{\ln\left(\frac{z - D + z_0}{z_0}\right)} . \qquad 2\text{-}11$$

With the assumption of transport similarity (Eq. 2-8), this expression can be used to evaluate K_H and K_W. Similar treatments of eddy diffusivity can be found in many texts (e.g., Brutsaert, 1982).

With very precise experimental work it has been determined that the turbulent transport of momentum, heat, and water vapor is strictly similar only under neutral stability conditions, e.g., Swinbank and Dyer (1967). To describe eddy diffusivities under other conditions, diabatic influence functions (ϕ_M, ϕ_H, ϕ_W) have been developed. They are defined such that

$$K_H = \frac{\phi_H}{\phi_M} K_M \quad \text{and} \qquad 2\text{-}12$$

$$K_W = \frac{\phi_W}{\phi_M} K_M . \qquad 2\text{-}13$$

These are experimentally determined and expressed in terms of dimensionless variables such as the Monin-Obukhov length or Richardson number (Morgan et al., 1971; Businger, 1973).

A number of wind profiles and corresponding eddy diffusivity treatments both with and without stability corrections have been developed. (These are referred to as wind models.) None are used in this study, but the fact that bulk air transport is theoretically and experimentally adequately understood is important in supporting the remote-sensing method developed. All remote-sensing methods involve a wind model of some kind to help evaluate sensible and latent heat fluxes.

Latent and Sensible Heat Flux Expressions

In application, the flux between two specific points (z_1 and z_2) that have a gradient between them must be evaluated. Since eddy diffusivity in general varies with the distance from a surface (Eq. 2-11), the latent and sensible heat transport equations (Eqs. 2-5, 2-6 and 2-7) must be integrated along the direction of transport and between the points of application (Monteith, 1973). Assuming that all parameters except diffusivity are constant between the two levels and that the flux in question is steady (or that flux storage in the layer between levels is negligible),

$$H = \frac{\rho c_p (T_1 - T_2)}{\int_{z_1}^{z_2} \frac{dz}{K_H(z)}} \quad \text{and} \qquad 2\text{-}14$$

$$E = \frac{\rho L \varepsilon}{p} \frac{(e_1 - e_2)}{\int_{z_1}^{z_2} \frac{dz}{K_W(z)}} \; . \qquad 2\text{-}15$$

The integral in the denominator of these equations, when evaluated, represents the lumped transport properties between points z_1 and z_2 away from the surface. From the preceding subsection, it is understood that these integrals can be evaluated with various wind models for $K_z(z)$.

The expressions for latent and sensible heat flux that are commonly used are simplified versions of Eqs. 2-14 and 2-15. For sensible heat flux from the surface to a reference level above the surface, the integral expression is abbreviated either as a bulk thermal conductivity or as a bulk air resistance:

$$H = \rho c_p K(T_s - T_a) = \frac{\rho c_p (T_s - T_a)}{r_a} \quad , \qquad 2\text{-}16$$

where T_s is the surface temperature,
T_a is the air temperature at a reference level above the surface,
K_a is the bulk thermal conductivity for the slab of air between the surface and the reference level, and
r_a is the bulk resistance to heat transport of the slab of air between the surface and the reference level.

In this study, the sensible heat flux expression is condensed even further to

$$H = h(T_s - T_a) \quad , \qquad 2\text{-}17$$

where h is referred to as the bulk heat transport coefficient. Since the fundamental definition of h is

$$h = \frac{\rho c_p}{\int_{z_s}^{z_a} \frac{dz}{K_H(z)}} \quad , \qquad 2\text{-}18$$

use of a wind model (to evaluate K_H) is implied any time the bulk heat transport coefficient or bulk air resistance is used (Monteith, 1973, 1975; Thom and Oliver, 1977).

Applying the similarity concept to a description of latent heat flux is complicated because it is impossible to measure the vapor pressure at the vegetation surface. The air inside the leaves is usually assumed to be at the saturation vapor pressure corresponding to the surface temperature [$e_s^* = e^*(T_s)$]. A unitless parameter M, which varies

from 0 to 1, can be introduced to account for subsaturation of the surface air:

$$M(e_s^* - e_a) = e_s - e_a \quad . \qquad 2\text{-}19$$

This formulation was suggested by Tanner and Pelton (1960) and applied by Outcalt (1972), Pandolfo and Jacobs (1973), Nappo (1975), and Carlson and Boland (1978), and in a slightly different form by Barton (1979). The equation for latent heat flux can then be written in terms of the heat transport coefficient and moisture availability parameter:

$$E = \frac{h}{\gamma} M(e_s^* - e_a) \quad , \qquad 2\text{-}20$$

where e_s^* is the saturation vapor pressure at the surface temperature,
e_a is the vapor pressure at the reference level a,
M^a is a unitless parameter interpreted as moisture availability,
h is the bulk heat transport coefficient, and
γ is the psychrometric constant ($\gamma = c_p P/L\varepsilon$).

The resistance formulation (Monteith, 1973) includes an additional resistance term, r_s, the bulk stomatal diffusion resistance (sometimes referred to as the canopy resistance, r_c) to account for the subsaturation of air at the surface:

$$E = \frac{\rho c_p (e_s^* - e_a)}{\gamma(r_a + r_s)} \quad . \qquad 2\text{-}21$$

Both of the transport coefficient resistance formulations are used in the ET literature; analytic evaluation of either type of expression is based on diffusivity integrals like those in Eqs. 2-14 and 2-15. These formulations can be substituted for one another with the following identities:

$$h = \frac{c_p}{r_a} \quad \text{and} \qquad 2\text{-}22$$

$$M = \frac{r_a}{r_a + r_s} \quad . \qquad 2\text{-}23$$

This study uses the conductivity formulation.

Energy Budget ET Estimation Strategies

There are two major ways in which the energy budget and gradient equations can be solved. The physically more realistic method is based on dynamic simulation of the heat transfer processes; the other method is based on a cruder description of the surface and steady-state analysis of the surface heat exchange processes.

Gradient expressions like those in Eqs. 2-5, 2-6 and 2-7 are used in both approaches. The difference is that in simulations the expressions are applied over arbitrarily short distances and time steps according to the level of detail required in the application. When transport is in one direction, as it is considered to be in most of the problems encountered in ET measurement or prediction, the medium through which the flux is transported is thought of as consisting of layers perpendicular to the direction of transport. Fluxes through each layer can then be computed individually for each time step, allowing the treatment of flux transients as well as the treatment of differing transport properties of the layers. In the steady-state approaches the gradient expressions are applied over the entire distance between measurements, and transients are ignored.

Simulation models consist of an interdependent system of equations which describe the exchange of latent, sensible, and soil heat flux with the vegetation layer and the air or soil, and also the transport of latent, sensible and soil heat between layers. This system of equations is solved iteratively using solar and atmospheric radiation data as a forcing function and quantities such as air temperature, vapor pressure, and soil temperature as boundary conditions. Generally, unknown surface parameters are chosen such that simulated surface temperatures match

observed surface temperatures. The simulated ET flux is then assumed to be the actual ET flux. Examples of evapotranspiration simulations are Waggoner et al. (1969), Stewart and Lemon (1969), Sinclair et al. (1971), Murphy and Knoerr (1970, 1972), Goudriaan and Waggoner (1972), Lemon et al. (1973), and Sinclair et al. (1976). Dynamic models of the surface heat transfer processes are computationally orders of magnitude more complex than the steady-state approaches, and were developed only after the introduction of the electronic computer.

The earliest physical models of the surface energy exchange process were based on steady-state analysis and the similarity of latent and sensible heat transport. Three steady-state strategies for solving the energy budget equation for evapotranspiration have been developed; they are referred to as the simple residual, Penman, and Bowen ratio methods. To more easily compare these methods, their equations have been written in the same notation. Soil heat flux is included even though this component is often assumed too small to be included for vegetated surfaces.

In the residual approach, the energy budget equation is solved for latent heat flux, and a simple gradient expression is used to evaluate sensible heat flux:

$$E = (R - G) - h(T_s - T_a) \quad . \qquad 2\text{-}24$$

The transport coefficient for air conductivity is estimated from empirically derived wind functions or physical wind models as described previously. The biggest advantage of this method is that it requires no information on the surface moisture status. Its disadvantage is that it is very sensitive to an accurate transport coefficient estimate. When the sensible heat flux term is written in terms of a resistance, this method is also called the resistance energy balance method (Rosenberg, 1974) .

The Penman (1948) approach is very closely related to the residual approach. In addition to the wind function, it includes an expression that relates the temperature gradient to the vapor pressure gradient via the linearized saturation vapor pressure curve,

$$e_s^* - e_a = s(T_s - T_a) + \delta e_a \quad , \qquad 2\text{-}25$$

where s is the slope of the saturation vapor pressure curve, and
δe_a is the saturation deficit of the air.

This approach has since been generalized to include subsaturated surfaces (Barton, 1978), which allows ET to be expressed as a function of net radiation, the moisture availability parameter (M), and the saturation deficit (δe_a):

$$E = \frac{M}{Ms + \gamma} [s(R - G) + h\delta e_a] \quad . \qquad 2\text{-}26$$

(See Chapter 4 for the full derivation.) Historically, Penman's method was the first to combine the energy budget equation with a wind model to evaluate ET. Although the residual approach also employs a wind model, in common usage it is the Penman method that is referred to as the combination method. The Penman method's main advantage is that it is not explicitly dependent on measurement of a temperature gradient; its principal disadvantage is that it requires information on moisture availability of the surface.

The Bowen ratio approach (Bowen, 1926) assumes that in the fully turbulent layer over the surface, transport of heat and water vapor are similar (i.e., $K_H = K_W$). This allows eddy diffusivities to be avoided altogether, and latent and sensible heat flux to be apportioned according to the relative strength of the temperature and water vapor pressure gradients:

$$E = \frac{(R - G)}{1 + \frac{\gamma(T_2 - T_1)}{(e_2 - e_1)}} \quad , \qquad 2\text{-}27$$

where subscripts 1 and 2 refer to two levels in the fully turbulent air layer. This approach is free of a wind model, but it requires very accurate measurement of temperature and vapor pressure gradients. It is discussed in detail in Chapter 3.

Remote ET Estimation Methods

Surface Temperature and Net Radiation

Satellite-borne sensors can measure the amount of radiant energy coming from a particular surface area element in a particular wavelength interval. For environmental applications, the wavelength intervals measured are divided into the visible, thermal, and microwave regions of the electromagnetic spectrum, yielding measurements of reflected solar, emitted thermal, and microwave radiation. So far, all ET estimation methods designed for use with satellite data only employ the visible and thermal wavelength ranges.

Net radiation is the largest component of the surface energy budget, and surface temperature plays a role in determining all the energy budget components. Usually, measurements of reflected solar and emitted thermal radiation measurements are used to estimate net radiation and surface temperature. Methods to estimate ET are then based on these net radiation and surface temperature estimates.

With a clear sky and proper consideration of the atmosphere's transmission properties, surface temperature can be determined directly from emitted thermal radiation:

$$Q_e = \varepsilon\sigma T_s^4 \quad , \qquad 2\text{-}28$$

where ε is the emissivity of the surface,
σ is the Stefan-Boltzmann constant, and
T is the surface temperature.

Solving for T_s,

$$T_s = \sqrt[4]{\frac{Q_e}{\varepsilon\sigma}} \quad . \qquad 2\text{-}29$$

In principle, net radiation is calculated according to the equation

$$R = Q_s + Q_a - Q_r - Q_e \quad . \qquad 2\text{-}30$$

The upwelling components, reflected (Q_r) and emitted (Q_e) radiation, are directly measurable by satellite given atmospheric transmission properties. The solar radiation incident at the surface (Q_s) is known as a function of date, time of day, location, and atmospheric absorption (Tennessee Valley Authority, 1972). Atmospheric radiation (Q_a) can be similarly estimated.

Some of the ET estimation methods discussed in the following sections are designed for use with satellites that provide only thermal data from the surface. These methods express the net shortwave radiation as a function of estimated incident solar radiation (R_s) and albedo (α):

$$Q_s - Q_r = (1 - \alpha)Q_s \quad . \qquad 2\text{-}31$$

Simulation Methods

In 1978, NASA launched the Heat Capacity Mapping Mission (HCMM). The polar orbit of the HCMM satellite was designed to collect maximum and minimum temperatures of the earth's surface, and groups worldwide were funded to study the maximum-minimum temperature data. Several groups adapted or developed simulation methods to bridge the long time intervals (12 hours) between data sets. Examples of models used are Carlson and Boland (1978), Soer (1977), and Rosema et al. (1978).

The Carlson model is very general, having been developed for study of urban and rural surfaces. It is based on the energy budget equation and gradient transport equations for latent, sensible, and soil heat flux. Soil thermal conductivity and heat capacitance are combined into a thermal inertia parameter which is evaluated with an empirical relationship to thermal conductivity. The model does not describe soil and plant water transport. It introduces a moisture availability parameter as shown in Eq. 2-19 to account for the subsaturation of the surface air. Eddy diffusivities for latent and sensible heat are iteratively computed using empirical stability corrections; there are, in fact, different atmospheric models for daytime and nighttime.

Use of the Carlson model to determine daily heat budget components is discussed in Carlson et al. (1980). Computed solar radiation is used to force the model; measured windspeed, air temperature and humidity, and soil temperature are used as boundary conditions. By varying two model parameters (thermal inertia and moisture availability) on successive model runs, sets of corresponding cumulative heat budget components and 24-hour maximum and minimum temperatures are generated. Then a regression equation expressing daily ET as a function of maximum and minimum temperatures is developed. Given the ground-measured data for the simulation and two extreme temperature maps from the HCMM satellite, a map of daily ET is produced.

The Soer model (named TERGRA) is much the same as the Carlson model, providing for stability conditions in the surface air layer and requiring temperature, vapor pressure, and windspeed as boundary conditions at a reference level. However, rather than a moisture availability parameter, soil and plant water transport is modelled in detail. (The

TERGRA model was designed for grasslands, making this more detailed approach feasible.) It uses pseudo-empirical expressions for soil water transport resistance and stomatal resistance, and requires a reference soil moisture pressure as well as a soil temperature as a boundary condition.

Use of the TERGRA model in obtaining cumulative ET estimates is explained in Soer (1980). The procedure requires data on the boundary conditions and radiation falling on the surface for the duration of the simulation periods, and values of various parameters like soil hydraulic conductivity and surface roughness. First, windspeed, roughness height, air temperature, and remotely measured surface temperature are used to compute the instantaneous ET rate for the time at which satellite data are available. This is done with the simple residual method (see previous subsection), which requires no knowledge of surface moisture. Then the TERGRA model is run with various soil moisture pressures to match the ET rate at the time of the satellite overflight. The modelled cumulative daily ET rates are then assigned to areas with matching instantaneous ET rates at the time of the overflight.

The Rosema et al. (1978) model (named TELL-US) is also constructed around the surface energy budget, and similarly computes latent, sensible, and soil fluxes based on measured gradients and calculated transport properties. It is more detailed in describing the surface; surface slope and slope direction must be specified. Its parameters are soil thermal inertia and surface relative humidity.

Given the daily course of boundary conditions and incident radiation, the model is used to compute daily maximum and minimum temperatures and cumulative daily evapotranspiration for various combinations

of thermal inertia and surface relative humidity. This procedure must be repeated for each combination of surface roughness, slope, and slope direction. Then satellite-measured maximum and minimum temperatures for specific areas are matched to the modelled values to determine daily ET for those areas.

Steady-State Methods

Most efforts to use remote-sensing data to estimate ET rates were made with the simple residual method (Eq. 2-24). Remotely sensed data were used to estimate net radiation, and sensible heat flux from the surface was evaluated with a remotely-sensed surface temperature and a ground-measured air temperature. Evapotranspiration was then calculated as the net radiation less the estimated sensible and soil heat flux. Studies that fall into this category are Allen et al. (1980), Seguin (1980), Soer (1980), and Price (1982). Soer and Price extend their methods to cumulative daily ET estimates with the help of simulation models described in the preceding subsection.

These methods differ primarily in how they treat the bulk heat transport coefficient or transport resistance of the surface air layer. Two methods of computing sensible heat flux were used in the Allen et al. (1980) approach. For short vegetation (mostly pasture), a stability-corrected thermal conductivity was computed using the log law wind model and dimensionless empirical relationships developed by a group at the University of California at Davis (Morgan et al., 1971). An empirical resistance equation based on leaf length, windspeed, shelter factor, and leaf area index (Monteith, 1965) was used for transport over areas covered with trees. By using measured windspeed and air temperature, the estimated tree resistances and a surface temperature map, it was

possible to construct a map of instantaneous evapotranspiration rates. For regional estimates, the rates computed for subareas were weighted by the total area with that particular ET rate and summed.

The Seguin (1980) approach to thermal conductivity in the surface air layer was formulated in terms of a resistance. It used the simple log law wind function with surface roughness to evaluate the resistance to sensible heat flux; no stability corrections were made. Measured windspeed, air and soil temperature, remotely measured surface temperature, and estimated albedo and soil conductivity were required to estimate instantaneous ET rates. Regional ET rates were estimated by multiplying areas with different surface temperature and surface roughness combinations by their individual ET rates.

Soer (1980) also used a resistance formulation of the sensible heat flux. It included stability corrections based on the Monin-Obukhov length and the Businger-Dyer semi-empirical mass and heat transport equations. In other particulars it is practically identical to the Seguin approach.

Price (1977, 1980) has developed the energy budget equation in terms of time averages in an effort to determine surface thermal inertia using remotely sensed maximum and minimum surface temperatures. He has since (Price, 1982) used this approach in conjunction with the TELL-US model to estimate daily ET rates. First a preliminary estimate is made with a residual equation like Eq. 2-24, except that time average air and surface temperatures and windspeed are used. The daily ET value obtained is then corrected with a regression equation developed from a set of corresponding Price method estimates and TELL-US simulation estimates.

A different approach to solving the residual equation was taken by Menenti (1980). In his approach, the simple residual equation is simplified by Taylor series expansion around some central ET rate at a given shortwave radiation level. All terms except those containing surface temperature and albedo are eliminated, leaving the ET rate for a particular surface a function of the central ET rate, its surface temperature, and its albedo. No means to make cumulative daily ET estimates were suggested.

Temperature Gradient Response Methods

The two ET estimation methods developed in this study are steady-state methods. They are based on the response of surface-to-air temperature gradients to varying levels of net radiation. One of these methods, the average temperature gradient response method, is suitable for use with satellite data.

The primary difference between this method and the simple residual method is that it expresses the vapor pressure gradient in terms of the temperature gradient, the slope of the saturation vapor pressure curve, and saturation deficit--an innovation first made in Penman's (1948) pioneering work. This addition gives the method some protection against "residual errors." For example, if the measured temperature gradient is erroneously high, both the latent and sensible heat fluxes will be affected; there will not just be an increase in sensible heat and an equal decrease in latent heat flux. Also, the method allows ET to be expressed as a function of net radiation and parameters only (without explicit mention of surface and air temperature). This feature makes ET calculable when surface temperatures cannot be measured remotely but net

radiation can be estimated, as when there is cloud cover or in between sets of satellite data.

A significant advantage of the estimation method developed is that it, in effect, determines surface parameters like moisture conditions almost completely from remote-sensing data. This is done with an equation (hereafter referred to as the temperature gradient model) that relates the surface-to-air temperature gradient to net radiation and parameters that describe the surface. By assuming that the parameters are constant, two of them (e.g., moisture availability and saturation deficit) can be determined from the correlation of the surface-to-air temperature gradient and net radiation. Although surface temperatures are required (implying clear skies) to determine parameters, they can be used with cloudy condition net radiation estimates for cloudy condition ET estimates.

The need for a surface-to-air temperature net radiation correlation calculation requires several daytime satellite data sets. Unlike the HCMM methods, the remote ET estimation method developed in this study is designed for use with satellite data that is available at least every 2 or 3 hours. At this time resolution, the average temperature gradient response method can make reasonably accurate cumulative daily ET estimates without the need for simulation. Because the parameters are considered constant, no interpolation scheme is needed to make cumulative ET estimates; only an estimate of the cumulative daytime net radiation is required.

CHAPTER 3

A SYSTEM FOR AUTOMATIC COLLECTION OF ET DATA

Overview

The energy budget/profile Bowen ratio technique was used to make the evapotranspiration measurements needed for a data base in this research. It was selected because it is one of the methods that least disturbs the surface being measured, and when correctly applied, permits measurements with an error on the order of 10% (Sinclair et al., 1975). The profile Bowen ratio method has been successfully applied to a variety of surfaces (Sinclair et al., 1975; Stewart and Thom, 1973; Black and McNaughton, 1972, 1971).

The theoretical basis of this method is developed first, followed by a discussion of considerations going into the choice and use of the sensors and other apparatus. Next, the automatic data collection system that is assembled to make and report energy budget measurements is described. It consists of a computer-controlled scanner, voltmeter, gas sampling arrangement, and a set of four interacting programs. The chapter concludes with a discussion of practical considerations that are important in maintaining a high level of accuracy in the measurements and the limitations of the data collection system.

Energy Budget/Profile Bowen Ratio Theory

As described in Chapter 2, the energy balance of a vegetated surface can be written:

$$R = E + H + G \,, \qquad 3\text{-}1$$

where R is net radiation absorbed by the surface,
E is the evapotranspirative or latent heat flux,
H is sensible heat flux, and
G is the soil heat flux.

It has already been shown that the rate of heat storage in the vegetation layer and the rate of photosynthetic assimilation are negligible in comparison to these terms.

The Bowen ratio is defined as the ratio of sensible heat flux to latent heat flux:

$$\beta = \frac{H}{E} \quad . \qquad 3\text{-}2$$

In the energy budget/profile Bowen ratio measurement technique, net radiation and soil heat flux are measured directly. Latent and sensible heat fluxes are determined indirectly by first measuring the Bowen ratio, and then computing the fluxes:

$$E = \frac{1}{\beta + 1} (R - G) \quad \text{and} \qquad 3\text{-}3$$

$$H = \frac{\beta}{\beta + 1} (R - G) \quad . \qquad 3\text{-}4$$

The Bowen ratio can be calculated from air temperature and water vapor pressure measurements at various heights over the surface, provided a number of experimental conditions are met. Over a uniform surface with adequate fetch, latent and sensible heat fluxes may be considered to exist in the vertical direction only (no flux divergence). In the turbulent boundary layer the fluxes at any instant can be described as follows:

$$H = -\rho c_p K_H \frac{\partial T}{\partial z} \quad , \qquad 3\text{-}5$$

$$E = \frac{-\varepsilon \rho L}{P} K_W \frac{\partial e}{\partial z} \quad , \qquad 3\text{-}6$$

where ρ is air density,
c_p is specific heat capacity at constant pressure,
ε is the ratio of molecular weights of water and dry air,
L is the latent heat of evaporation of water,
P is the atmospheric pressure,

K_H is the eddy thermal diffusivity,
K_W is the eddy vapor diffusivity,
T is the air temperature,
e is the vapor pressure, and
z is the vertical coordinate.

The Bowen ratio can then be written:

$$\beta = \frac{H}{E} = \frac{c_p P K_H \frac{\partial T}{\partial z}}{\varepsilon L K_W \frac{\partial e}{\partial z}} \quad . \qquad 3\text{-}7$$

If temperature and vapor pressure measurements are made at the same heights, the ∂z terms may be cancelled. If the measurements are made at the same instant, it can be assumed that the eddy diffusivity for water vapor and heat are the same ($K_H = K_W$). This in effect states that turbulent mixing is the dominant transport mechanism in the turbulent boundary layer, and that bouyancy and stability effects cause no significant differences in the transport of heat or water vapor (Dyer, 1967; Swinbank and Dyer, 1967; Webb, 1970; Dyer and Hicks, 1970; Garratt and Hicks, 1973). Incorporating these conditions into the expression for the Bowen ratio,

$$\beta = \left(\frac{c_p P}{\varepsilon L}\right)\frac{\partial T}{\partial e} = \gamma \frac{\partial T}{\partial e} \quad . \qquad 3\text{-}8$$

Since the terms in brackets are physical "constants" (abbreviated as the psychrometric constant, γ), only $\partial T/\partial e$ needs evaluation. This can be done with air temperature and vapor pressure measurements.

In this application of the energy budget/profile Bowen ratio concept, air and dewpoint temperatures were measured at five heights--35, 60, 85, 135, and 225 cm over the surface. Vapor pressure was calculated from the dewpoint temperature according to the Magnus-Tetens formula (Tennessee Valley Authority, 1972). The ratio $\partial T/\partial e$ was the slope of a two-independent-variable linear regression (Kendall, 1968) calculated

using temperature data as the ordinate and vapor pressure as the abscissa (see Fig. 3-1). In calculating the Bowen ratio, the specific heat of the air, the atmospheric pressure, and the ratio of molecular weights was considered constant; the latent heat of vaporization was a function of the average air temperature.

Sensor and Time Constant Considerations

Although simple in principle, a great deal of care is required in choosing sensors and collecting data for the calculation of the Bowen ratio. Temperature and vapor pressure vary randomly from instant-to-instant and level-to-level in the turbulent boundary layer, and the total temperature and dewpoint differences across the air layer to be measured are only 1 or 2°C. In order to calculate the relative strengths of the gradients, very precise measurements at several levels are required.

Sensors were chosen to eliminate, as much as possible, the error introduced by sensor-to-sensor variability. This was avoided entirely in the case of the vapor pressure profile; the same dewpoint analyzer was used to measure the dewpoint at each level by use of a gas sampling arrangement. In the case of the temperature profile, the effect of thermocouple-to-thermocouple differences was minimized by measuring temperature differences with thermopiles. Twenty-junction copper constantan thermopiles, arranged with 10 junctions at each level, were used to measure temperature differences between levels. The temperature at the lowest level was measured with a thermocouple using an Omega Engineering MCJ-T electronic icepoint reference. Temperatures at the other levels were obtained by adding the appropriate thermopile-measured temperature differences to the one reference temperature measurement.

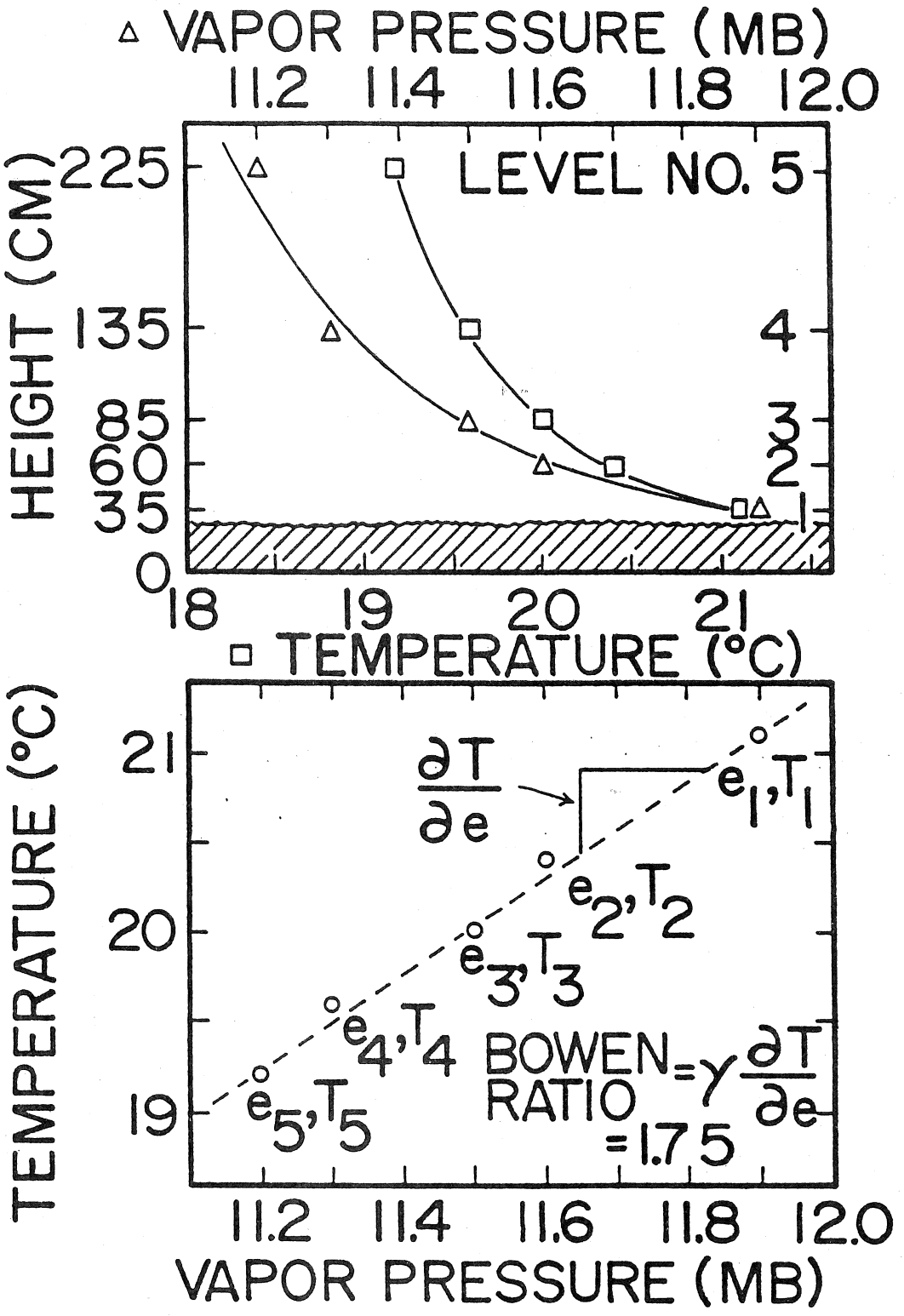

Figure 3-1. Bowen Ratio Calculation from Measurements of Vapor Pressure and Temperature. Note that the scale used to plot vapor pressure profile in upper graph is the same as the vapor pressure scale in the lower graph. Data are from October 20, 1981, 9:30 TST (see Fig. 3-6).

The apparatus used to collect temperature measurements and air samples was designed so that the sensors returned signals accurately representative of the air layers being sensed. The thermopiles were nested inside three aspirated radiation shields, with each shield wrapped in highly reflective aluminum foil. Air samples were pumped continuously from sampling ports near the thermopiles through about 100 m of 6-mm ID polypropylene tubing and 11.3-L mixing chambers in the instrument room. To prevent any danger of condensation, the air sampling system was heated from sampling mast to dewpoint analyzer. The bundle of five tubes from the mast was taped around a heater cable (3 W/ft) and packed inside a 1.3-cm-thick foam rubber insulation tube. The mixing chambers and the sampling valve were also heated.

The travel time of air samples from mast to instrument room was approximately 1 min. Therefore, the dewpoint measurement corresponding to a temperature measurement at a specific level was made 1 min later. Also, the dewpoint temperature measurements were pressure-corrected because the arrangement of the air sampling system caused the pressure rate at the dewpoint sensor to be ∿30 mb less than atmospheric pressure.

To ensure clean electrical signals, shielded signal cable with a single common ground was used. In spite of these precautions, the Beef Research Unit fence charger managed to induce significant voltage spikes on the low level signals (e.g., the 0-200 microvolt thermopile signals). This problem was solved with a filtering routine in the data collection program.

In addition to reducing the error sources from the sensors in every practicable way, the temperature and vapor pressure signals were physically smoothed. Smoothing was required because the measurement rate

was limited to one measurement every 2.5 min for the vapor pressure profile measurements.

Vapor pressure in the Bowen ratio data collection system was computed from a measurement of the dewpoint temperature. Since the same dewpoint sensor was used for all five levels and a delay had to be scheduled between measurements to allow the analyzer to settle on new dewpoints, the response of the dewpoint analyzer was the factor limiting the sampling rate. The analyzer, an EG&G Model 880 Dewpoint Hygrometer, was tuned so that it could "lock on" to small dewpoint temperature changes within about 15 sec. However, 30 sec per measurement were scheduled to allow the analyzer to stabilize on a given dewpoint under less than ideal conditions. Since there were five levels to measure, the time interval between measurements at the same level was 2.5 min.

The variability of temperature and vapor pressure in the turbulent air layer is well documented; at any point in this layer, instantaneous temperatures and dewpoints vary randomly (Desjardins et al., 1978). The higher-frequency temperature and dewpoint fluctuations were smoothed in order to get representative measurements with a sampling rate of one measurement every 2.5 min.

In the case of an air-sampling system, this smoothing is conveniently done by inserting a mixing chamber into the sample stream ahead of the analyzer. An abrupt (or step) change in an air sample is translated into a gradual, approximately exponential change by mixing in a chamber. The exponential change is characterized by a time constant, which is determined by the volume of the mixing chamber divided by the flow rate. By harmonic analysis, it was determined that a time constant of 4 min would damp random signal variations occurring more often than every 2.5

min to 10% or less of their amplitude. In the case of the dewpoint system, 11.5-L mixing chambers with a flow rate of 3 L/min were used.

To maintain the proper correlation between dewpoint and temperature readings, it was necessary to introduce the same time constant into the temperature-sensing system. The appropriate time constant was determined experimentally by varying the air flow rate over the aspirated thermopiles and subjecting them to different temperature differences. It was found that at a set air flow rate, measured time constants varied with the temperature difference applied to the thermopiles. As a result, the air flow rates were adjusted so that a 4-min time constant resulted for temperature differences in the average operating range--temperature differences in the range of 0.2 to 0.3°C.

The 4-min time constant was also introduced into the surface temperature and net radiation measurements. Sensor response was slowed digitally by using weighted averages of the most recent 25 sensor readings.

Each time a complete temperature and vapor pressure profile was measured (every 2.5 min), the correlation coefficient between temperature and dewpoint measurements was calculated. This provided a running check on the quality of the measurements and the current similarity of the profiles.

Data Collection Equipment

The overall schematic for the thermopile/air sampling system is shown in Fig. 3-2. The major parts are the data acquisition system, the air sampling mast, the mixing box, and the signal cables and tubing which connect them.

A computer-controlled data acquisition system was used because of the large number of measurements and extensive calculations that this

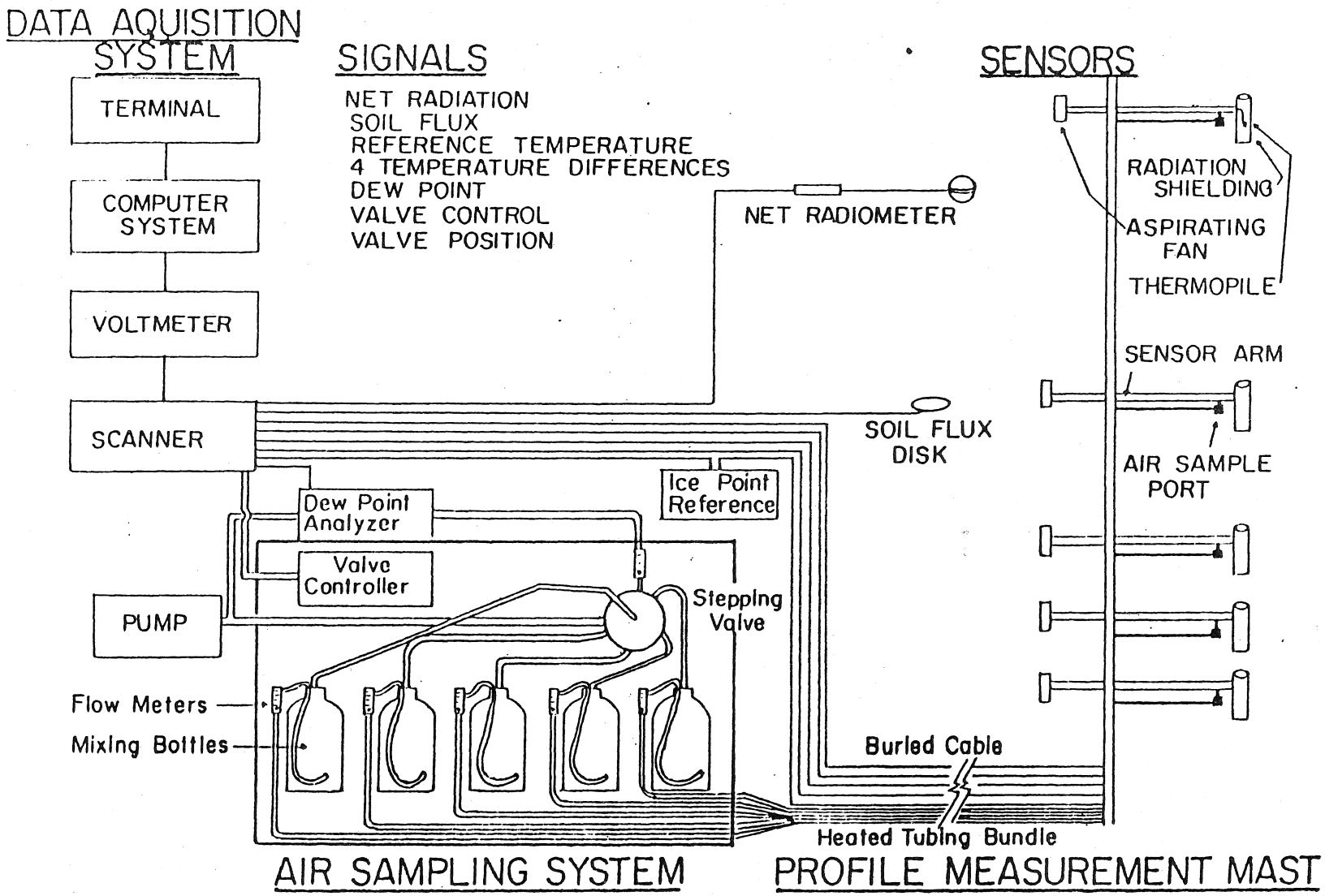

Figure 3-2. Schematic of ET Measurement System. Details of profile measurement and air sampling equipment are shown in Figs. 3-3 and 3-4.

technique requires. The central piece of equipment was a Hewlett-Packard 2100S Minicomputer with a disk resident Real Time Executive-2 operating system. The system allowed editing and compilation of programs, swapping programs between core and disk memory, scheduling programs for relative or absolute start times, and "simultaneous" running of programs according to priority. Input and output were by means of a HP-2126P terminal.

The peripheral equipment used in making the measurements and controlling the gas sampling valve is listed in Table 3-1. The controlling computer, disk drive, data acquisition equipment, and terminal were all housed in an air-conditioned room.

Table 3-1 Data Acquisition System Identification (All components are manufactured by Hewlett-Packard)

Component	Model No.	Serial No.
Minicomputer (32K Memory)	HP-2100S	1420A05546
Scanner	HP-2911A	737-00476
Scanner Controller	HP-2911B	832-00412
Integrating Digital Voltmeter	HP-2402A	1027A01060
Disk Drive	HP-7901A	1321A-00255
Terminal	HP-2621P	2102W03475

The field apparatus on the pasture site consisted of an air-sampling mast, a radiation sensor boom, and a 9.5-m tower supporting a precision radiation thermometer at its top, and windspeed and direction sensors at 7 m. Another taller tower was erected and equipped to protect all instrumentation from lightning.

The 2-m radiation sensor boom was supported by an aluminum tripod stand and guy wires about 1.8 m over the ground surface. Two Eppley pyranometers, oriented to measure incoming and reflected radiation, and a Swissteco net radiometer were mounted at its end. An aspirating pump and

dessicant container for the net radiometer were held in a weatherproof box at the base of the tripod.

The air sampling mast consisted of a 2.5-m steel channel to which five sensor arms (see Fig. 3-3) were attached at various levels. At one end of each arm, teflon spacers centered two clusters of 10 thermocouple junctions inside the smallest of three radiation shields. Individual junctions were kept in thermal contact with a metal oxide conducting paste. Air was drawn over the thermopiles, between radiation shields, and through the length of the arm by a small fan at the opposite end. Air samples were drawn from the air flowing through the arm. All wiring (four 20-junction thermopiles and one thermocouple) and tubing (5 sample lines) were contained inside the 3x3 cm channel down to its base, where they ended in wire and tubing connectors. The mast and sensor arms as well as the radiation shields were wrapped in highly reflective aluminum foil.

The sensors were connected to the scanner in the instrument room with shielded signal and thermocouple wire. In the field, leads from the sensors ran aboveground in wire harnesses to a junction box, where they were connected to a signal cable via screw connectors. This cable ran 100 m underground to another junction box in the instrument room. From this panel the signal lines were connected to one of two 50-pin connectors, which plugged into a short piece of cable tied directly into the scanner. The "quick-disconnect" plugs were included to rapidly isolate the data acquisition system from possible lightning strikes in severe weather; the junction boxes allowed signal problems to be quickly traced to sensors, underground cabling, or the data acquisition system. The sensors used are identified in Table 3-2.

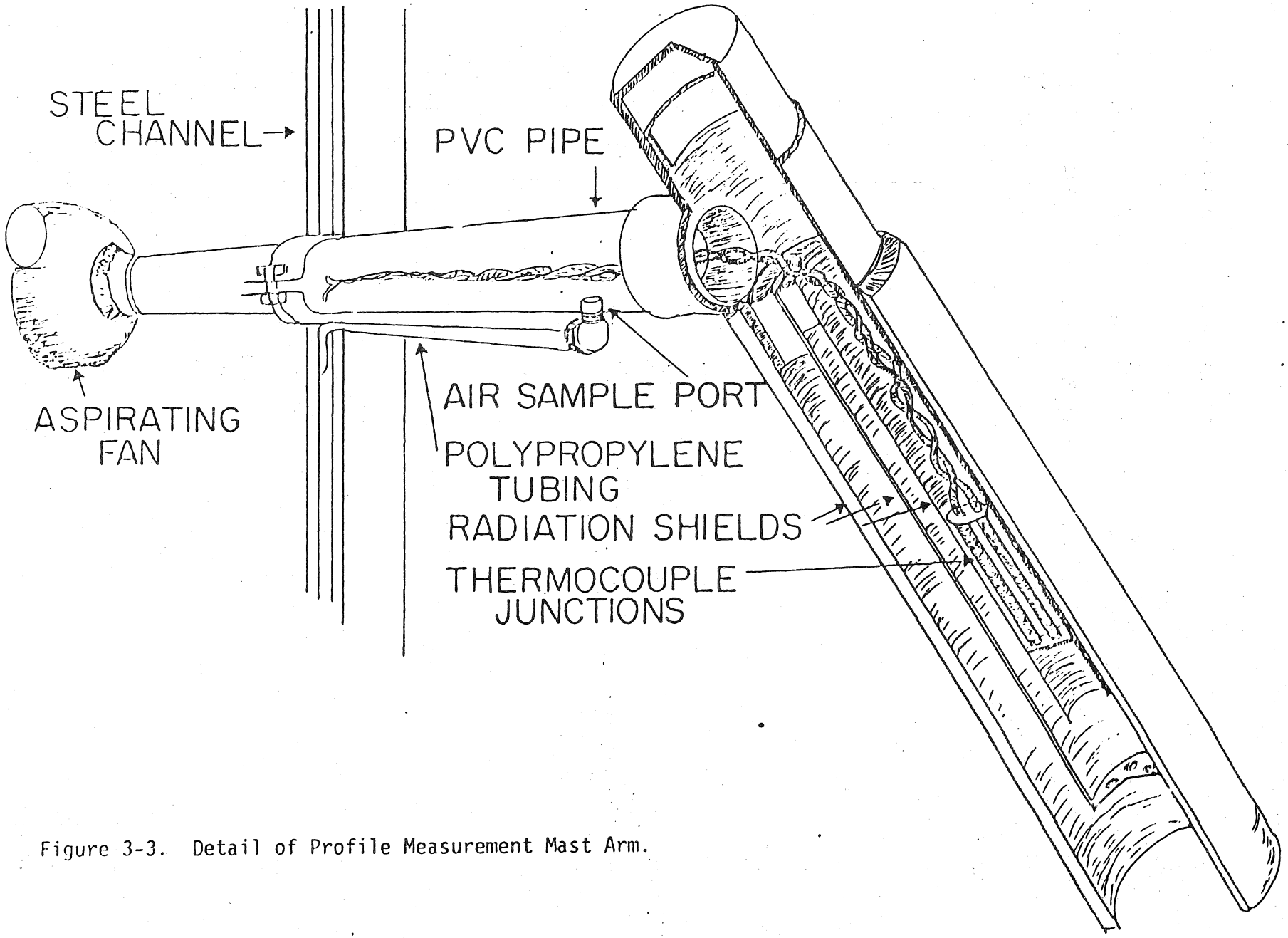

Figure 3-3. Detail of Profile Measurement Mast Arm.

Table 3-2 Sensor Identification

Measurement	Sensor Make & Model No.	Ser. No.
Net Radiation	Swissteco Net Radiometer	6990
Incoming Shortwave Radiation	Eppley Pyranometer 8-48	12876
Reflected Shortwave Radiation	Eppley Pyranometer 8-48	10000
Surface Temperature	Barnes IT-5 (Spring 1981)	--
	Barnes IT-3 (Fall 1981)	521
Dewpoint Temperature	EG&G 880-C1	1409
Windspeed and Direction	R.M. Young 6101 and 6301	--
Air Temperatures	Custom-made Thermopiles	--
Reference Temperature	Omega Engineering MCJ-T	--
Soil Heat Flux	Micromet Heat Flow Disk	282

Air was pumped continuously from each sample port on the mast through ~100 m of heated insulated polypropylene tubing and the gas sampling apparatus in the instrument room. In the "mixing box," air first passed through flowmeters, then the mixing chambers, the scanning valve, and the air pump. Samples from each level were drawn sequentially through a sampling port, a separate sample flowmeter, and the dewpoint analyzer. All equipment except the pump and analyzer were contained inside a heated, insulated plywood box (see Fig. 3-4) to prevent condensation problems.

The scanning valve was controlled from the data acquisition computer. The sampling port was turned from one air source port to the next by an electric motor powered for a precise fraction of a second. This was done by a relay control circuit that was designed to sense scanner closure. Thus a program statement calling for a measurement of the scanning valve control channel resulted in changing the position of the valve. After each change, the valve position was checked to ensure that the programs and valve were synchronized.

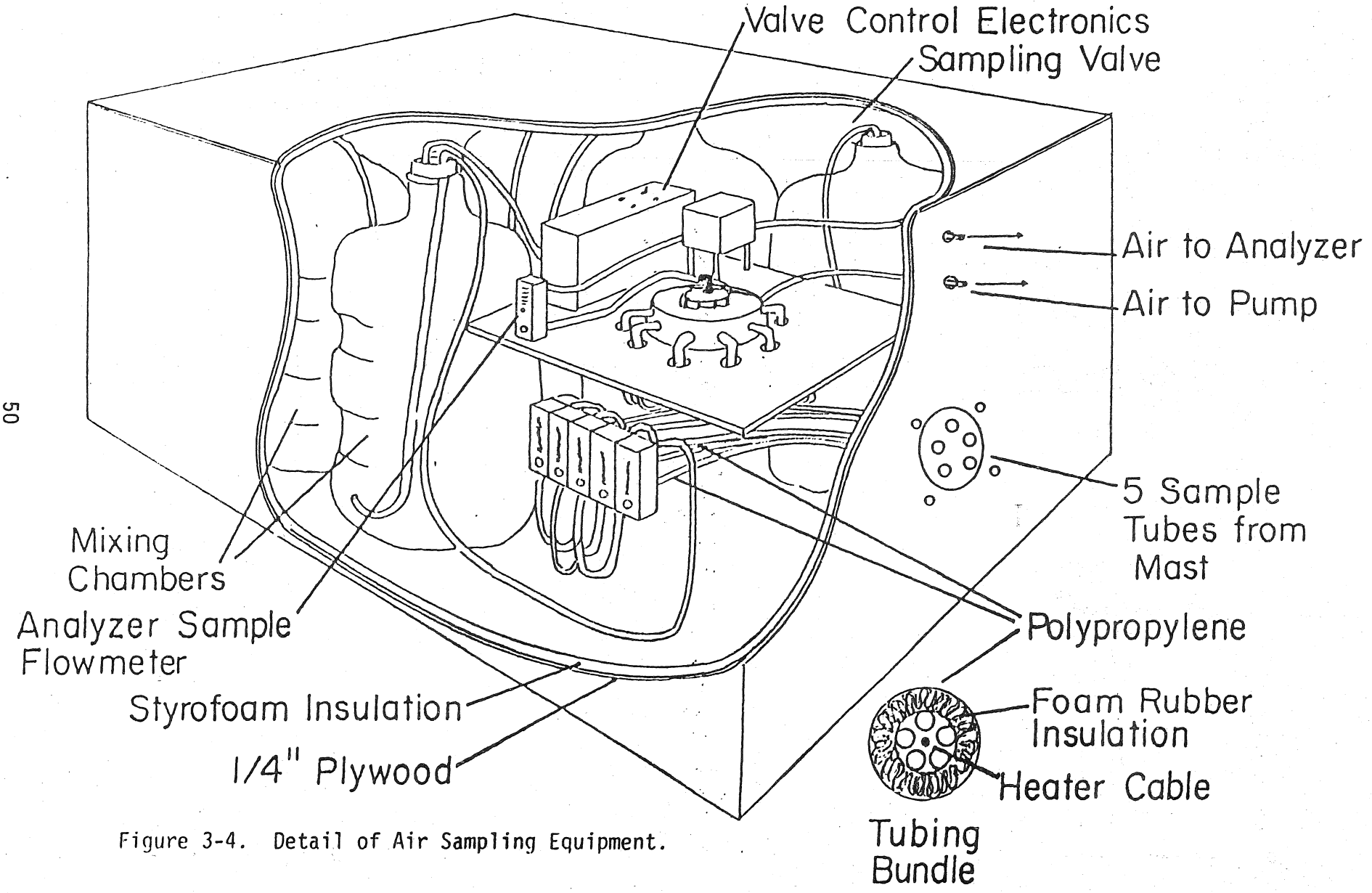

Figure 3-4. Detail of Air Sampling Equipment.

Data Collection Programs

A system of four programs was developed to collect, report, and analyze the data required for the test surface energy budget. Program MEASR makes the measurements and calculations, REPRT produces the half-hourly summary reports, ANALZ does some analysis of data and performs additional calculations, and SET schedules the other programs. Listings of these programs appear in Appendix B; brief descriptions of their functions and interactions follow.

Basically, all sensors are scanned in a computer program loop. Depending on the status of various indexes in this loop or the system clock, control is passed to specific calculation and/or reporting routines. This fundamental loop is in program MEASR; it is repeated approximately every 30 sec, the measuring rate determined by the dewpoint analyzer.

When a program calls for a measurement [i.e., CALL EXEC (1, 9, DATA, CHANNEL NUMBER, VOLTMETER PROGRAM WORD)] the channel number in the measurement program statement is passed to the scanner controller, and the program word indicating type of measurement, voltage range, and delay time is passed to the voltmeter. After the scanner has closed on the proper signal lines, the voltmeter has been set for the type of measurement, and a programmed delay is complete, the voltmeter integrates the signal for 1/60 second and passes the average back to the measuring program. It resumes execution with the next program step.

During each execution of the measurement loop, one air temperature, one dewpoint temperature, and all other sensors except soil thermocouples are scanned. Immediately after the dewpoint measurement, the scanning valve position is changed (Subroutine STEP) so that the dewpoint

instrument can begin to stabilize on a new dewpoint. A programmed delay makes up the balance of the 30 sec required between measurements. At the end of five scans (2.5 min), a complete temperature and dewpoint profile is available to compute a Bowen ratio. A report on that profile is printed at the option of the system operator (see Fig. 3-5).

To compensate for the approximately one-minute air sample travel time from field to mixing chamber, temperature and dewpoint measurements are offset by two levels. For example, the dewpoint at level 1 is measured in the same sensor scan as the temperature at level 3. This accounts for extra statements at the beginning of the program which ensure proper initialization, and for extra branching after sensor scans which deal with the offset completion times of the temperature and dewpoint profiles.

To guarantee that the dewpoint analyzer is receiving the air sample from the level called for in the program, a mark voltage channel is measured and checked in each scan of the sensors. In one particular position of the scanning valve, 12 volts are expected on this channel. If the voltage measured is low or 12 volts are measured when not expected, the data for the profile being collected are discarded and a message to the operator is printed. The program makes one attempt to reposition the valve and restart data collection. If this fails, another message is printed and the programs are terminated.

When temperature and dewpoint measurements at all five levels are complete, the data are passed to subroutine RATIO, which calculates a linear temperature versus dewpoint regression relationship. Its slope is multiplied by the appropriate constants (Eq. 3-8) to give the Bowen

PROF# 6	RAD.T.	23.27	TEMP	21.1	20.4	20.0	19.5	19.1	R = .999
9:16:27	NET R.	.45	DPT.	9.5	9.2	9.0	8.7	8.5	
B =1.723	W.SPD.	2.86	V.P.	11.9	11.6	11.5	11.3	11.1	
PROF# 7	RAD.T.	23.77	TEMP	21.2	20.5	20.2	19.7	19.3	R = .997
9:18:56	NET R.	.45	DPT.	9.6	9.3	9.1	8.9	8.7	
B =1.813	W.SPD.	2.18	V.P.	11.9	11.7	11.5	11.4	11.2	
PROF# 8	RAD.T.	24.25	TEMP	21.4	20.7	20.4	20.0	19.6	R = .997
9:21:26	NET R.	.46	DPT.	9.8	9.5	9.2	9.0	8.8	
B =1.612	W.SPD.	3.73	V.P.	12.1	11.8	11.7	11.5	11.3	
PROF# 9	RAD.T.	24.30	TEMP	21.7	21.0	20.6	20.1	19.8	R = .996
9:23:55	NET R.	.47	DPT.	9.8	9.6	9.2	9.0	8.8	
B =1.590	W.SPD.	3.54	V.P.	12.2	11.9	11.7	11.5	11.4	
PROF# 10	RAD.T.	24.49	TEMP	21.8	21.1	20.8	20.4	20.1	R = .988
9:26:24	NET R.	.47	DPT.	9.9	9.5	9.5	9.3	9.1	
B =1.904	W.SPD.	3.36	V.P.	12.2	11.9	11.9	11.7	11.5	
PROF# 11	RAD.T.	24.90	TEMP	22.2	21.5	21.1	20.6	20.3	R = .999
9:28:54	NET R.	.48	DPT.	10.1	9.8	9.6	9.4	9.2	
B =1.679	W.SPD.	2.85	V.P.	12.4	12.1	12.0	11.8	11.6	
PROF# 12	RAD.T.	25.28	TEMP	22.5	21.7	21.3	20.8	20.4	R =1.000
9:31:23	NET R.	.49	DPT.	10.3	9.9	9.7	9.5	9.3	
B =1.618	W.SPD.	2.94	V.P.	12.5	12.2	12.0	11.8	11.7	

Figure 3-5. Example of Intermediate Program Output. This report is printed if switch #3 on face of HP 2100 computer is on. Data are from the 15 min preceding half-hour report shown in Fig. 3-6.

ratio. The ratio and corresponding correlation coefficient are returned to the calling program.

Function FILT was added to MEASR after it was discovered that the shielding system did not prevent the Beef Research Unit electric fence charging system from inducing noticeable spikes on the signal lines. These 10-50 microvolt spikes were shorter than the voltmeter measurement cycle, and thus lent themselves to being filtered digitally. FILT takes 10 measurements, looks for three in a row that are the same within a tolerance, and compares the rest of the measurements to one of them. Any measurement varying more than a specified tolerance is dropped, and the average of the "good" measurements is passed back to MEASR. If more than half of the measurements are noisy (out of tolerance), a warning is printed to notify the operator.

Subroutine TMTCH is included to match the time constants of the net radiation and precision radiation thermometer to that of the temperature and dewpoint measurements. This matching is done by using the weighted average of the 25 most recent (collected in the last 12.5 min) measurements to calculate a matched measurement. The weights assigned to older measurements decrease exponentially with a time constant of 4 min. The same weighting scheme is used for the net radiation and surface temperature because their sensor response time constants are 8 and 2 seconds, respectively. At a sampling rate of one measurement every 30 sec, their responses are, in effect, instantaneous.

Program REPRT produces a half-hourly data summary report. It calculates half-hourly average profiles of the heat budget components, windspeed and direction, Bowen ratio, and profiles of soil and air temperature, air vapor pressure and relative humidity. Most of this program is

concerned with formating and printing the summary report. An example report is shown in Fig. 3-6, and Table 3-3 lists the variable names used.

Program ANALZ makes ancillary calculations and produces the last five lines of the half-hourly report. It has a search routine which computes the displacement height of the temperature and vapor pressure profiles. With an assumed value of the roughness parameter (z_0) and trial values of the displacement height (D), it computes the correlation of temperature or vapor pressure and height over the surface with

$$T,\ e = B \ln \left(\frac{z - D + z_0}{z_0} \right) + A \quad . \qquad 3\text{-}9$$

The assumed roughness height, the displacement height producing the best correlation, and other profile parameters are printed out.

ANALZ also computes a variety of other quantities which may be of use in data analysis or operation of the system. Among these are atmospheric and stomatal resistances, albedo, optical air mass and atmospheric transmission coefficient, zenith and hour angle of the sun, and the equation of time.

The fourth program, SET, is the executive program. It is used to properly start the acquisition of data and determine whether and when the other programs should be run. In a "cold" start, SET positions the scanning valve, initializes counters and statistics, and schedules MEASR to start so that profile collection is completed at specified times. On occasions other than a "cold" start, it determines whether the other programs should be run, depending on flags in MEASR or operator input via switches on the face of the HP-2100. Its most valuable function is to schedule MEASR to begin at an absolute clock time at the beginning of

BEEF RESEARCH UNIT ET PROJECT DATA

AVERAGES AND (PERCENT VARIATION) FOR HALF HOUR ENDING
TUESDAY, OCTOBER 20, 1981 (JULIAN DAY 293) TIME - 09:31:27 TST

NET RAD.	SOIL H.F.	SENS. H.F.	LAT. H.F.	N WINDS	RSQ.>.95	B.R.	AVG.R.
.45 LY/M	.02 LY/M	.28 LY/M	.16 LY/M	3.06 M/S	12 OF 12	1.753	.999

	RADIATION (LY/M)		AIR TEMP (CM)	(*C)	VAP PRESS (CM)	(MB)	REL HMDTY (CM)	(%)	SOIL TEMP (CM)	(*C)
NET	.451	(5.0)	225	19.2 (4.2)	225	11.2 (3.0)	225	50.2	0	16.8
ISW	.802	(4.1)	135	19.6 (4.1)	135	11.3 (2.9)	135	49.8	-2	17.6
RSW	.177	(3.7)	85	20.0 (4.1)	85	11.5 (2.8)	85	49.2	-5	18.2
NLW	.109	(16.)	60	20.4 (4.0)	60	11.6 (3.1)	60	48.6	-10	19.2
ILW	.616	(5.5)	35	21.1 (3.9)	35	11.9 (3.1)	35	47.6	-25	20.1
PT	.162	MM/HR	0	23.4 (5.5)	**.95+ BR =1.760,+OR-.115**				-50	21.7

ZO	TO	DH	U*H	RCH	EO	DE	U*E	RCE
1.	23.0	22.0	33.4	-1.000	12.8	17.0	12.8	-.999
2.	22.6	22.0	32.6	-1.000	12.6	18.0	12.4	-.999
3.	22.3	22.0	31.9	-1.000	12.5	19.0	12.2	-.999

RAIR,RSTM(S/M)	.238,4.350	.311,4.353	.348,4.350	.397,4.358	.436,4.365

ABDO	SWIO	OAM	ATC	ZNGL	HRNGL	EOT	E.S.T.	T.S.T.	DAY
.22	1.09	1.84	.85	57.3	-41.2	-.2579	9.48	9.25	293

Figure 3-6. Example of Half-Hourly Data Report. Variable names and units are listed in Table 3-3.

Table 3-3. Variable Names and Units for Half-Hour Reports

RSQ.>.95	Number of temperature and vapor pressure profiles with correlation coefficient better than .95
B.R.	Bowen Ratio
AVG.R.	Correlation coefficient of half-hour average profiles
NET	Net radiation (ly/min)
ISW	Incoming shortwave radiation (ly/min)
RSW	Reflected shortwave radiation (ly/min)
ALW	Atmospheric longwave radiation (ly/min)
ELW	Emitted longwave radiation (ly/min)
ET	Evapotranspiration rate (mm/h)
.95+BR	Average and standard deviation of individual profile Bowen ratios with greater than .95 correlation coefficient
ZO	Roughness height (cm)
TO	Temperature at ZO by temperature profile extrapolation (°C)
DH	Displacement height for heat (cm)
U*H	Friction velocity as determined by fit of profile (m/min)
RCH	Correlation coefficient for temperature profile
EO	Vapor pressure at ZO by vapor pressure profile extrapolation (mb)
DE	Displacement height for vapor pressure (cm)
U*E	Friction velocity as determined by fit of vapor pressure profile (m/min)
RCE	Correlation coefficient for vapor pressure profile
RAIR	Air diffusion resistance (s/m)
RSTM	Stomatal diffusion resistance (s/m)
ABDO	Albedo (fraction)
SWIO	Shortwave insolation without atmosphere (ly/min)
OAM	Optical air mass (atmospheric diameters)
ATC	Atmospheric transmission coefficient ISW = SWIO * (ATC * OAM) [absorption coefficient = -ln(ATC)]
ZNGL	Zenith angle of sun (degrees)
HRNGL	Hour angle of sun (degrees)
EOT	Equation of time (h)
E.S.T.	Eastern standard time
T.S.T.	True solar time
DAY	Day of year

each half hour. This prevents the data reports from precessing out of synchronization with the system clock.

SET also enables REPRT and ANALZ to be swapped between core and disk so as not to interfere with the measurement schedule. At the end of a typical half hour (1.5 min past the clock hour or half hour, when measurement of the twelfth profile has just been completed) MEASR calls for SET to run immediately and ends. SET schedules MEASR to start again at an absolute clock time, 2 min into the new half hour, or roughly 30 seconds after the last measurement made. It then loads and runs REPRT and ANALZ. When it is time for MEASR to start, whichever program is in core is moved back to disk, and MEASR is loaded. MEASR makes its first scan, and during the usual delay between scans, REPRT and/or ANALZ are reloaded and run to completion. MEASR is then swapped back to core to be continued at the end of the programmed delay.

The programs can be halted from the computer terminal or with switches on the face of the computer. When switches 1 and 2 are on, MEASR ends with the next profile and REPRT computes averages for all the data collected in that half hour. When only switch 2 is on, MEASR ends at the next normal half-hour reporting time.

Operational Considerations

The thermopile/air sampling system required a great deal of care in setting up and maintaining the instrumentation involved. It also required an awareness of the theoretical and practical limitations of the measurement method. Proper calibration and tuning of the dewpoint analyzer were most critical for good measurements. Sensor cleaning and output calibration procedures are well documented in the EG&G Model 880 Dewpoint Hygrometer Manual (1977). However, to achieve optimum response

times, it was necessary to tune the instrument slightly differently than Manual specifications. It was made more sensitive by setting the THK potentiometer so that voltage on the test points was 200-260 mV, and made faster by setting the GAIN potentiometer so that the test voltage was 150-210 mV. The new settings sacrificed dewpoint analyzer response time in large step changes in order to improve response time in the smaller step changes normally encountered in the profiles. To ensure that the dewpoint analyzer actually had time to settle on readings before being read by the voltmeter, its output was spot-monitored on a millivolt recorder.

The most difficult problem was the individual and cross-correlation of the dewpoint analyzer, the thermocouple/thermopile air temperature sensors, and the precision radiation thermometer. The dewpoint analyzer output was calibrated according to the EG&G manual. Temperatures at the bottom and top of the scale were simulated by substituting precision resistances for the mirror-temperature sensing thermistor; the analyzer output at these simulated temperatures was matched to the factory standard instrument output. The radiation thermometer was calibrated by measuring its output for known surface temperatures produced with a stirred constant-temperature bath. A regression equation for the temperature vs. output correlation was calculated and used in the programs.

It was not possible to cross-calibrate these temperature sensors until the system was run in a light drizzle on Nov. 5, 1981. This situation resulted in the same temperatures at all measured levels, near-zero net radiation, and air that was near saturation, so the dewpoint, air, and surface temperatures were approximately the same. The temperature differences between sensors were used to correct the rest of the data.

(It should be noted that this correction did not affect the Bowen ratio calculation, since it used only relative changes. The correction did affect surface temperatures, which were not used in computing the energy budget.)

The radiation sensors were calibrated against a recently purchased (and calibrated) Eppley Pyranometer.

On the whole, the thermopile/air sampling system developed worked very well and produced excellent data. However, there were some situations in which it could not function well. The system was protected from almost all of these situations because calculation of a complete energy budget was made conditional on temperature and dewpoint profile similarity. Latent and sensible heat fluxes were not calculated when the profile correlation coefficient was less than 0.95.

Profiles were regularly dissimilar for a few time periods in the early morning and late afternoon, while temperature and dewpoint profiles were reversing in direction. This dissimilarity occurred because changes in the temperature profile generally preceded changes in the dewpoint profile.

Sensible heat generated at the surface of the outermost radiation shields was usually carried away by the air flowing over them. At very low windspeeds, however, the warm air produced at the outer surface of the lowest radiation shields could become entrained in the aspiration air of mast arms above. This problem showed in profile correlation coefficients but was usually not so bad that energy budgets could not be calculated. Under clear skies this effect was not as marked, presumably because the radiation shields could more effectively radiate heat away.

When the system was run at night, some condensation took place in the air sample lines because the air sampling mast was not heated. Water accumulated in the tubing in proportion to the length of the tubing section in the mast. As a result, the fifth level produced obviously high dewpoint temperatures until the tubing had dried. The temperature dewpoint correlation made it obvious at what time all condensation had been evaporated from the sample lines.

The situation most hazardous to data quality occurred on very sunny, dry days. At these times, the air temperature of the instrument room (21-24°C) was quite a bit higher than the dewpoint temperature of the outside air. At some point the analyzer would no longer be able to cool its sensor mirror low enough to get dew formation. Since air samples from different levels have different temperatures, the coolest mirror temperatures possible varied also. A false dewpoint profile, which correlated very well with air temperatures, would be measured and thus passed through the correlation coefficient screen. Evidence for this condition was the brightly-lit cooling circuit lamp on the dewpoint analyzer. With experience this condition could be anticipated, and its effects minimized by unplugging the heater cables to the sampling lines and mixing box.

In spite of precautions taken, susceptibility to lightning damage was the system's greatest weakness. The system was damaged twice by lightning. In both cases, instrumentation and computer equipment was damaged by current surges in the AC power system, in spite of power-surge arrestors. The only solution was the most fundamental--unplugging all sensor cabling and all AC power cords.

CHAPTER 4

THEORETICAL BASIS OF THE TEMPERATURE GRADIENT RESPONSE ET ESTIMATION METHOD

Overview

The key problem in developing a remote ET estimation method is describing the vegetation and air layer at the surface so as much information as possible about its energy budget can be gained from the surface temperature and net radiation. In addition, there is the question of how much ancillary data is necessary for acceptable levels of accuracy in the estimates. Previous approaches to these problems were outlined in Chapter 2.

The methods developed in this chapter are based on the response of surface-to-air temperatures to varying net radiation loads. First, a functional relationship that describes the dependence of the surface-to-air temperature gradient on net radiation and other factors is derived. This temperature gradient response (TGR) model is used with surface temperature, air temperature and net radiation data to evaluate surface parameters, which are then used in an adapted version of the combination equation to estimate evapotranspiration. Two methods of making estimates are developed. The first is physically strict, with a minimum of assumptions; the second is more approximate with correspondingly fewer data requirements.

For the sake of simplicity, the derivations that follow are in terms of surface temperature (T_s) and net radiation (R) rather than the direct remote measurements, reflected (Q_r) and emitted (Q_e) radiation.

Also, in application, temperature differences are used to evaluate temperature gradients. For that reason, differences are used in the equations developed and are referred to interchangeably as differences and gradients.

Temperature Gradient Model

The simplified energy balance of a vegetated surface was developed in Chapter 2:

$$R = E + H + G \quad . \qquad 4\text{-}1$$

The purpose of this section is to express the components of the surface energy budget as much as possible in terms of net radiation and surface temperature, so that a useful relationship between the two can be derived.

Because of heat storage in the surface air layer, surface temperatures lag net radiation. This lag is complicated by the fact that the passage of clouds usually makes the net radiation absorbed by the system vary randomly. For this reason, a method containing time as a variable has been avoided. This was done by modeling the response of surface-to-air temperature gradients to changes in net radiation.

In describing heat flux using a surface temperature (i.e., between the surface and some plane above the surface), at least two layers with different transport properties must be considered (see Fig. 4-1). The first is the surface layer, in which molecular diffusion is the primary transport mechanism. It is the thin layer of air immediately next to the plant surfaces, represented by the layer between z_s and z_0 in the diagram. The second is the fully turbulent layer between z_0 and z_a, where turbulent eddies are the primary transport mechanism. Following the development shown in Chapter 2, the heat flux between the surface (at

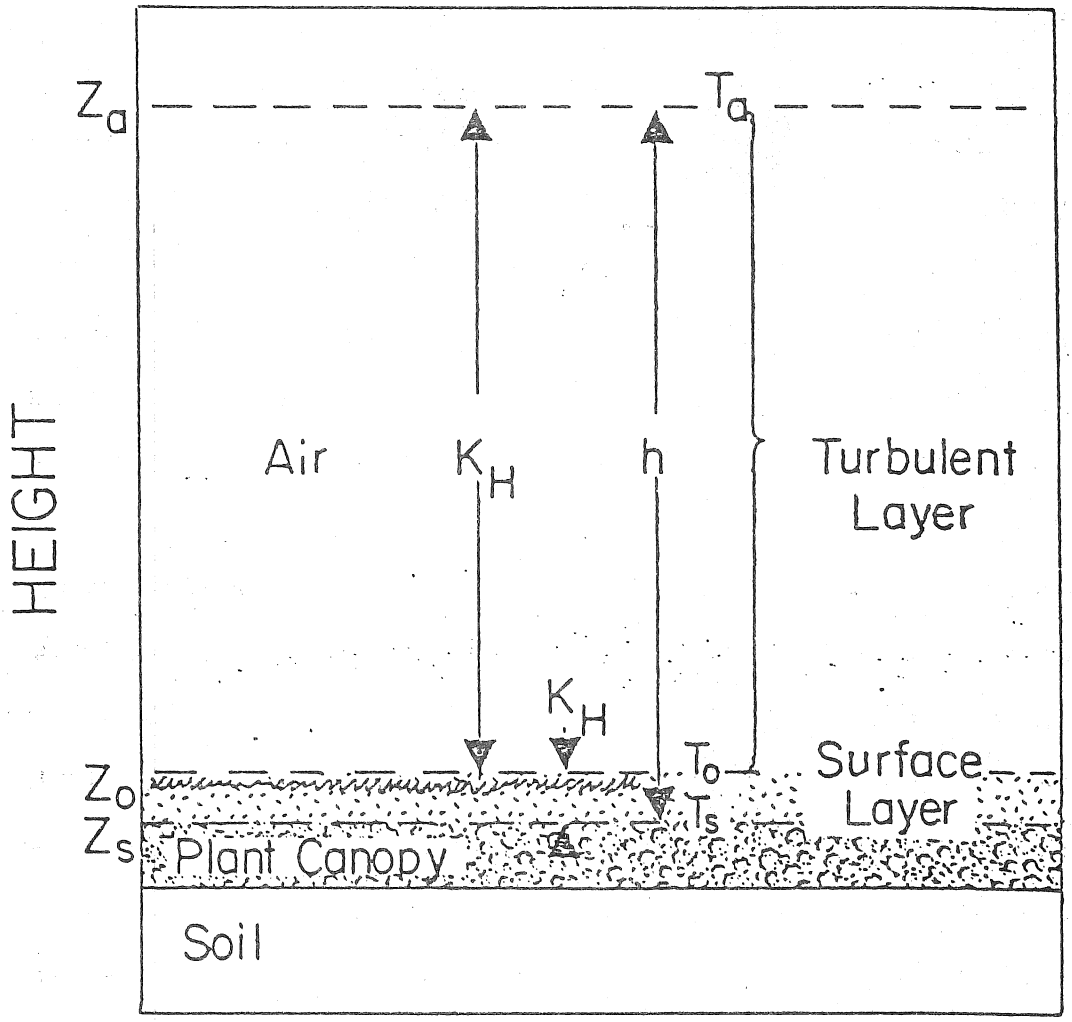

Figure 4-1. Definition Sketch for Transport Properties. The surface layer which is dominated by laminar air flow (molecular thermal diffusivity, k_H) is represented by the layer between z_s and z_a. The heat transport coefficient is used to represent the combined transport properties of both layers.

temperature T_s) and some level in the air above the surface (at T_a) is described by

$$H = \frac{(\rho c_p)_a (T_s - T_a)}{\int_{z_s}^{z_0} \frac{dz}{k_H} + \int_{z_0}^{z_a} \frac{dz}{K_H}} , \qquad 4\text{-}2$$

where ρ is air density,
c_p is the specific heat of air at constant pressure,
k_H is the molecular thermal diffusivity of air, and
K_H is the eddy thermal diffusivity of air.

(The first term in the denominator is equivalent to the resistance of the laminar surface air layer, and the second term in the denominator is equivalent to the resistance of the surface turbulent boundary layer.)

Treating latent heat flux analogously,

$$E = \frac{(\rho c_p)_a (e_s - e_a)}{\gamma\left(\int_{z_s}^{z_0} \frac{dz}{k_W} + \int_{z_0}^{z_a} \frac{dz}{K_W}\right)} , \qquad 4\text{-}3$$

where e is the water vapor pressure,
γ is the psychrometric constant ($\gamma = c_p P/L\varepsilon$),
k_W is the molecular water vapor diffusivity, and
K_W is the eddy water vapor diffusivity.

It has been shown that for a wide range of stability conditions normally found (Dyer, 1967; Swinbank and Dyer, 1967; Webb, 1970; Dyer and Hicks, 1970; Garratt and Hicks, 1973):

$$\int_{z_0}^{z_a} \frac{dz}{K_W} \simeq \int_{z_0}^{z_a} \frac{dz}{K_H} \qquad 4\text{-}4$$

For simplicity, it is also assumed that

$$\int_{z_s}^{z_0} \frac{dz}{k_W} \simeq \int_{z_s}^{z_0} \frac{dz}{k_H} \qquad 4\text{-}5$$

This assumption is unvalidated, but shared by the majority of theoretical treatments. Literature values for the molecular water vapor and thermal diffusivities are in fact at least approximately equal [e.g., Eagleson (1970) quotes values of 0.1 and 0.13 cm^2/sec, respectively].

With the above assumption, transport of latent and sensible heat can be considered similar from the surface to a reference level in the air. The simple expressions developed in Chapter 2 (Eqs. 2-17 and 2-20) can then be used to describe these fluxes:

$$H = h(T_s - T_a) \quad \text{and} \qquad 4\text{-}6$$

$$E = \frac{h}{\gamma} M(e_s^* - e_a) \quad . \qquad 4\text{-}7$$

The moisture availability parameter (M) is included to account for the subsaturation of the surface air layer. However, use of Eq. 4-7 as a hard equality will force M to include minor differences due to inequality of molecular diffusivities of latent and sensible heat (Jarvis et al., 1971), any differences due to stability effects, and any differences due to dissimilar sources and sinks of latent and sensible heat within the vegetation system.

The dependence of the vapor pressure gradient on the surface-to-air temperature gradient is shown in Fig. 4-2. It shows that the vapor pressure difference $(e_s^* - e_a)$ is in part due to the greater temperature of the surface relative to the air, and in part due to the saturation deficit of the air. Considering the saturation vapor pressure curve linear in the neighborhood of the surface and air temperatures,

$$e_s^* - e_a = s(T_s - T_a) + \delta e_a \quad . \qquad 4\text{-}8$$

where s is the slope of the saturation vapor pressure curve between T_s and T_a, and

δe_a is the saturation deficit of the air.

Substituting this expression into the latent heat flux equation (Eq. 4-7) gives the latent heat flux in terms of the temperature gradient:

$$E = \frac{h}{\gamma} M [s(T_s - T_a) + \delta e_a] \quad . \qquad 4\text{-}9$$

The hysteresis caused by changes in the slope of the saturation vapor pressure curve and saturation deficit is often masked by relatively large changes in moisture availability. When there is heavy dew, as on Oct. 17, 1981, more evaporation takes place in the morning, causing temperature gradients to remain small relative to afternoon gradients at equivalent radiation loads. In the afternoon, moisture availability has decreased and temperature gradients are pushed higher. The extreme changes in M in the early morning are what cause the belly in the graph.

Figure 5-12 shows data from a clear day in spring which had a much smaller range of moisture availabilities. Very little dew accumulated during the previous night because of a steady post-cold front northeast breeze. In this case, morning temperature gradients are higher than corresponding afternoon gradients because the variations in the slope of the saturation vapor pressure curve and saturation deficit outweighed changes in moisture availability.

The morning-afternoon hysteresis in Figs. 5-7 and 5-12 is most extreme on clear days which have the temperature extremes to cause relatively large variations in s. Variations in the parameters are lessened on partly cloudy days; Fig. 5-13 shows the parameters and temperature gradient/net radiation correlation for a partly cloudy day. Clouds narrow the range of surface and air temperatures and concurrent s, thus lessening the variation between morning and afternoon temperature gradients.

Variations in the fraction of net radiation going into soil heat flux have a negligible effect on the surface-to-air temperature gradients because soil heat flux is a very small component of the heat

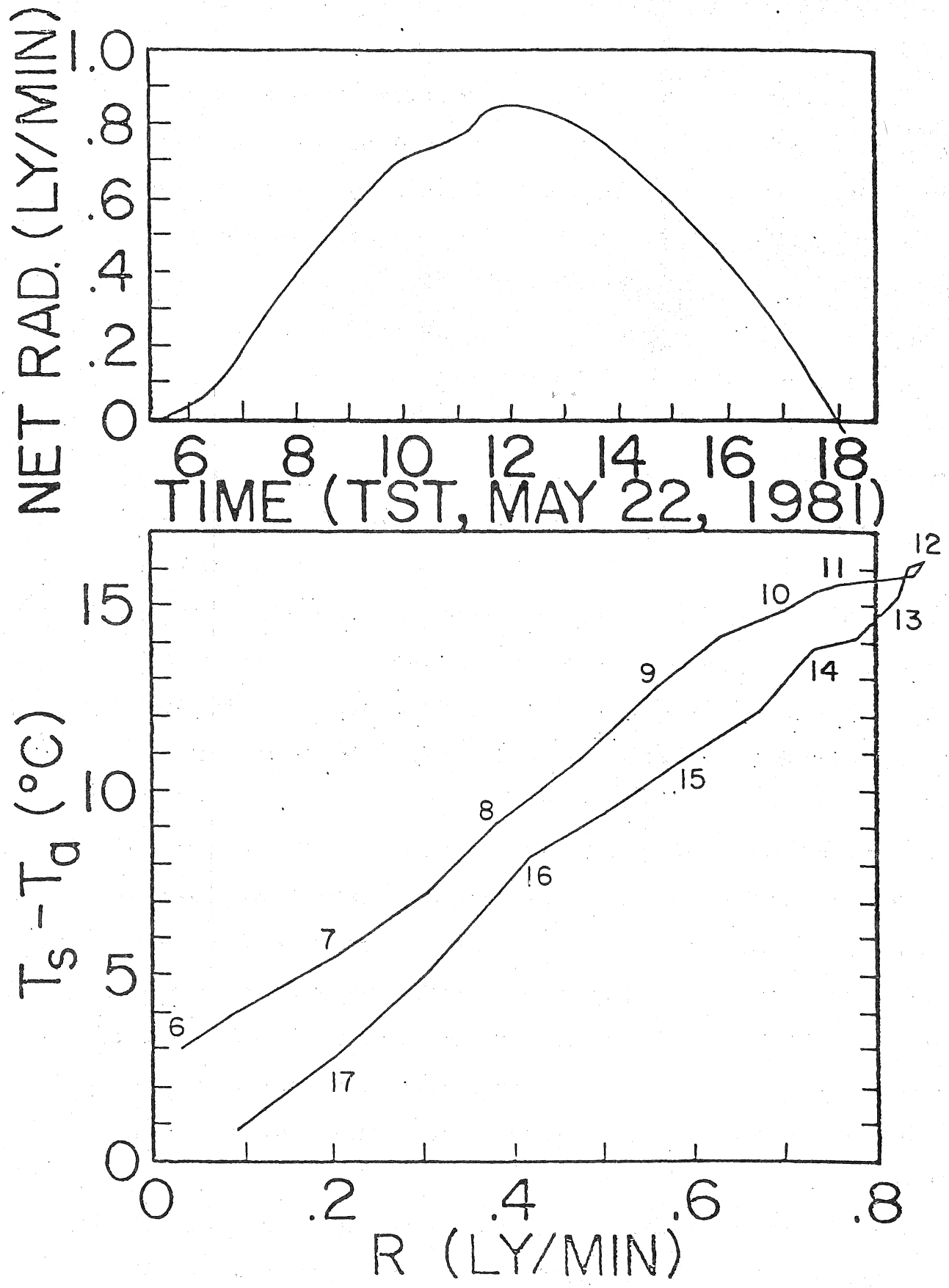

Figure 5-12. Temperature Gradient Response of a Clear Day with Constant Moisture Availability. The temperature gradient hysteresis is the opposite of that for October 17, 1981 (Fig. 5-7) which had decreasing moisture availability.

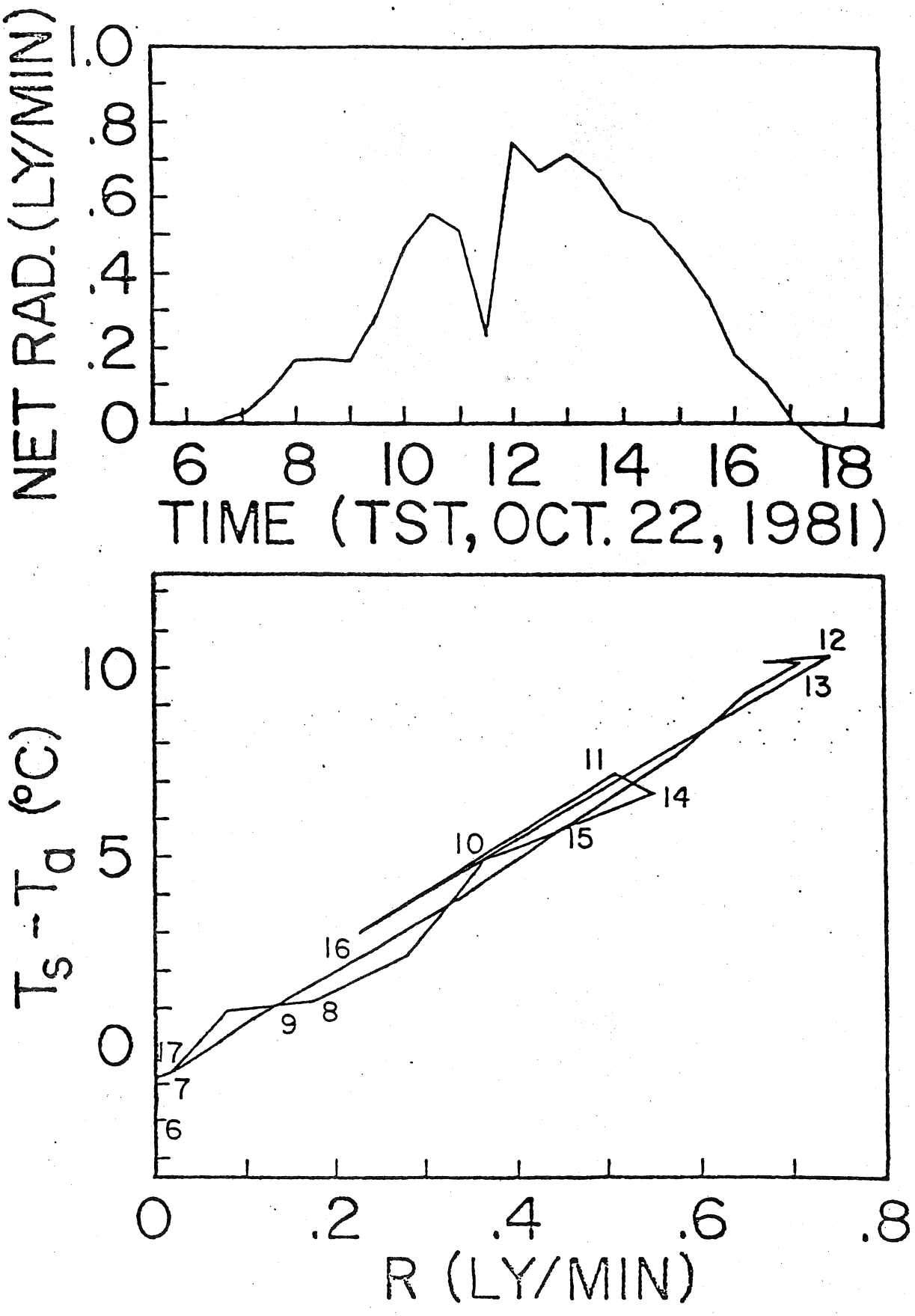

Figure 5-13. Temperature Gradient Response of a Partly Cloudy Day.

budget--here less than 10% of net radiation. The noisy character of air bulk thermal conductivity also does not seem to show in the temperature gradient/net radiation correlation. This and the fact that considering h constant leads to more reasonable moisture availability estimates suggests that variations in thermal conductivity have an insignificant effect on temperature gradients. For the most part, the pattern in the temperature gradient/net radiation correlation is a result of the interaction of moisture availability and the vapor pressure parameters.

Generality of the ATGR Latent/Sensible Partition

Another argument in favor of the ATGR method is that it correctly reproduces the general pattern of change in latent and sensible heat fluxes. Even though instantaneous ET rates are sometimes slightly over- and underestimated because the parameters are considered constant, the ATGR partition matches the daily pattern of other partition measures, such as the Bowen ratio.

Figure 5-14 shows an idealized ATGR latent/sensible heat flux partition and the resulting idealized daily time course of the Bowen ratio and E/R, another widely used dimensionless partition ratio. The ratios were computed according to

$$\beta = \frac{H}{E} = \frac{hAR - hB}{(f - hA)R + hB} \quad \text{and} \qquad 5\text{-}14$$

$$\frac{E}{R} = \frac{(f - hA)R + hB}{R} \quad , \text{ with} \qquad 5\text{-}15$$

$$R = R_0 \cos\left(\frac{2\pi}{24} TST - \pi\right) \quad , \qquad 5\text{-}16$$

where TST is true solar time ($6 \leq TST \leq 18$), and
R_0 is an arbitrary maximum net radiation load.

These patterns have been observed and reported for clear days by other researchers (e.g., Pruitt, 1964). The gradient response partition also

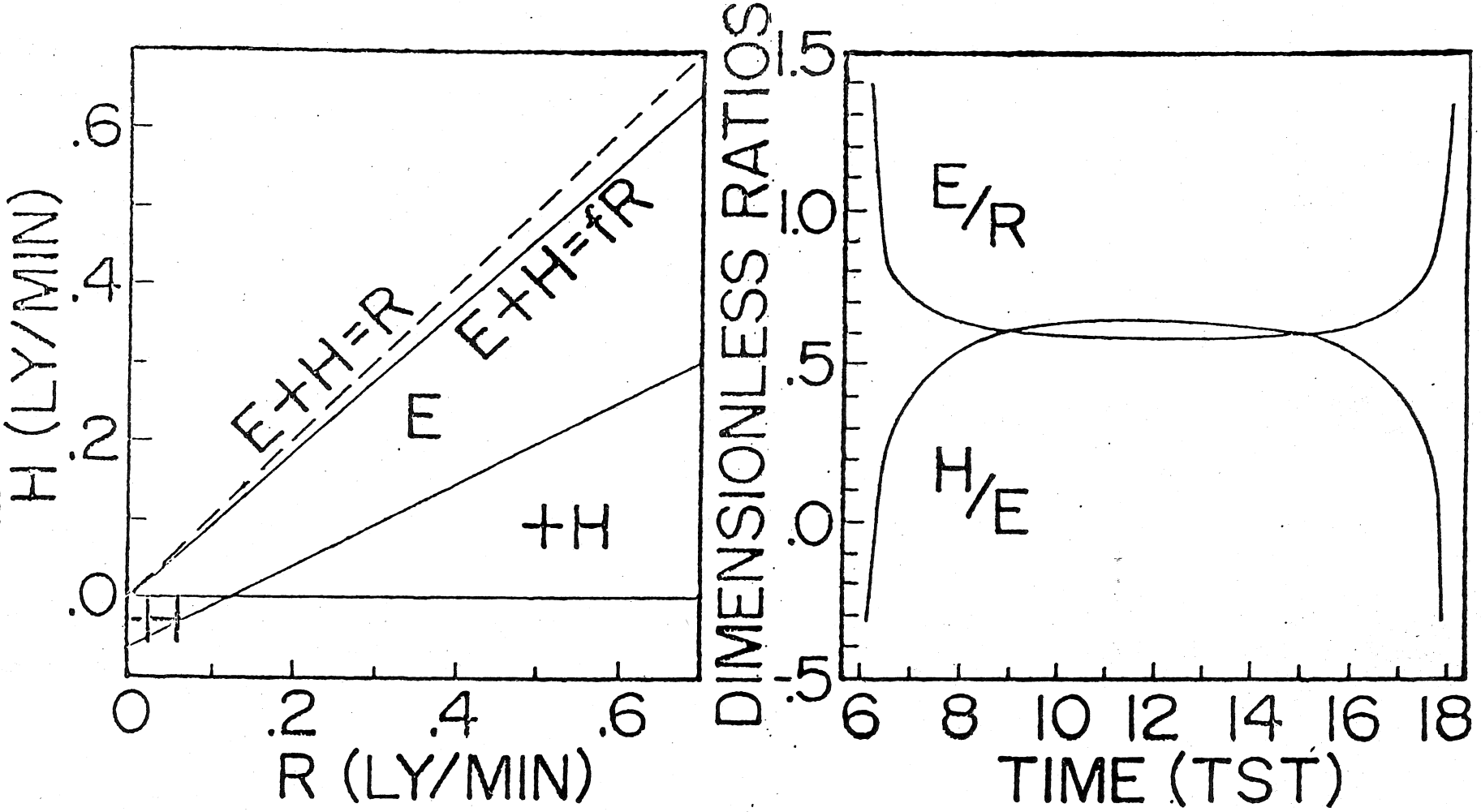

Figure 5-14. Generalized Clear Day H/E and E/R Patterns. The patterns in (b) were generated with the average temperature gradient response in (a) and a sinusoidal net radiation pattern. When the intercept in (a) is zero (negligible saturation deficit), E/R and H/E are constant (see Fig. 5-12). The curvature in the patterns of these ratios increases as the intercept becomes more negative (saturation deficit increases).

correctly reproduces the complex Bowen ratio patterns of partly cloudy days, as shown in the middle section of Fig. 5-15 (same day as shown in Fig. 5-13).

The relative magnitudes of sensible and latent heat flux vary with the amount of net radiation received by the surface because of the saturation deficit term in the equation for evapotranspiration. If there were no saturation deficit, the intercept (B) of the temperature gradient/net radiation correlation would be zero, reducing the expressions for the dimensionless ratios (Eqs. 5-13 and 5-14) to constants:

$$\beta = \frac{hA}{f - hA} \qquad 5\text{-}17$$

$$\frac{E}{R} = f - hA \quad . \qquad 5\text{-}18$$

The greater the role of the saturation deficit in driving ET, the greater the variations in the dimensionless ratios.

The fact that the average temperature gradient/net radiation correlation coefficients A and B explain general patterns and can be considered roughly constant suggest they may be useful in some form of climate index. They are more representative of the surface and surface environment than the Bowen ratio or other ratios, which are representative only of the particular time at which they were measured.

Tests of the ATGR Method

The purpose of this section is to show that the temperature gradient/net radiation correlation does reflect the average values of the parameters during the time of the measurements, and that the ATGR method produces reasonably accurate ET estimates. This is done with data collected in the fall of 1981.

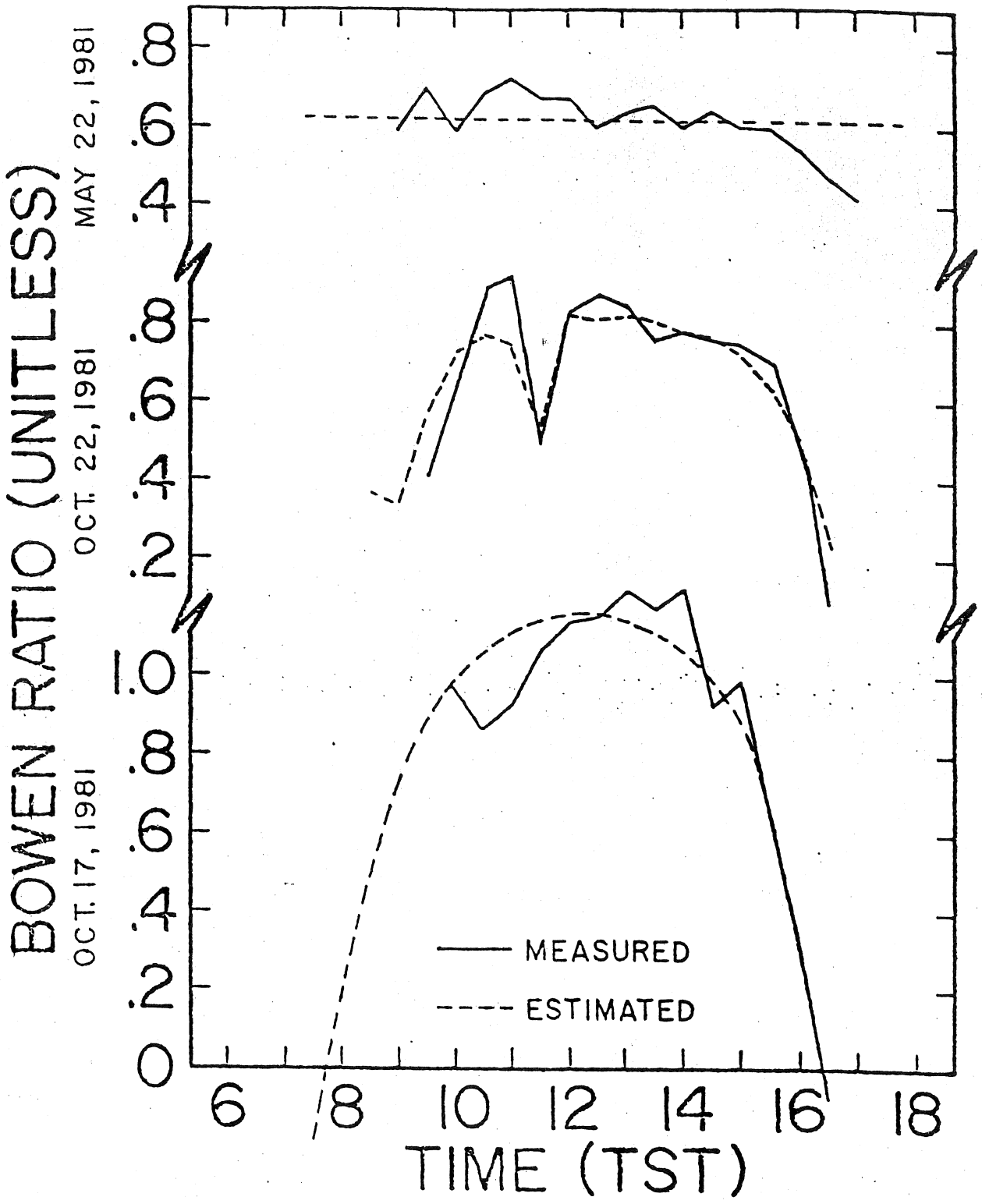

Figure 5-15. Comparison of Measured and Estimated Bowen Ratios. Bowen ratios were estimated with Eq. 5-14. Note the increasing curvature in the pattern with increasing saturation deficits, and the change in Bowen ratio with clouds on Oct. 22, 1981. (The temperature gradient responses of these days were shown in Figs. 5-7, 5-12, and 5-13.)

It can be shown that the temperature gradient/net radiation correlation is a result of the average parameters by comparing estimates of A and B computed using independently estimated values of the parameters to A and B computed by regression equations. Table 5-2 lists average parameter values for most of the fall days on which data were collected and corresponding A's and B's calculated by Eqs. 4-28 and 4-29 (using averaged parameters) and by Eqs. 4-30 and 4-31 (using measured net radiation and surface-to-air temperature gradients).

Table 5-2. Comparison of Average and Correlation Estimated A and B. Numbers in parentheses are the coefficients of variation of the parameters expressed as percentages.

Oct	h	M	f	s	δe_a	A_{avg}	A_{corr}	B_{avg}	B_{corr}
17	.034 (13)	.13 (17)	.92 (2)	2.6 (7)	21 (9)	18.2	17.5	2.6	2.2
18	.037 (16)	.13 (28)	.92 (4)	2.6 (7)	20 (10)	16.7	12.8	2.6	0.8
20	.038 (23)	.13 (14)	.94 (2)	2.0 (13)	16 (18)	17.7	14.0	2.2	0.6
21	.033 (11)	.15 (18)	.92 (4)	2.3 (6)	17 (11)	18.2	14.5	2.6	1.0
22	.031 (12)	.18 (32)	.94 (1)	2.6 (12)	18 (25)	18.2	16.5	2.8	1.7
23	.026 (36)	.24 (52)	.91 (4)	2.8 (10)	21 (21)	20.2	14.9	3.8	0.4
28	.033 (11)	.18 (26)	.98 (3)	2.1 (18)	11 (28)	19.0	15.7	1.8	0.6
29	.031 (14)	.15 (16)	.96 (2)	2.2 (10)	12 (13)	20.3	13.7	1.9	0.2
31	.041 (32)	.33 (87)	1.05 (12)	1.4 (5)	2 (65)	15.0	8.9	0.5	-0.3

The parameters were calculated for each time period (according to Eqs. 5-2, 5-5, 5-6, 5-7, and 5-9) and then averaged. This calculation is equivalent to the line-fitting procedure used in Figs. 5-3, 5-4, 5-5, and 5-6. The parameter data and temperature gradient/net radiation correlation for five of the days listed in Table 5-2 are graphed in the (a), (b), (c), (d), and (f) parts of Figs. 8, 9, 10, 11, and 12 in Appendix D.

The calculated and observed values of A show a better degree of agreement than do the values of B. This can be traced to the cross-calibration of the surface and air temperature sensors. If they are not in agreement, the temperature difference due to lack of cross-calibration becomes part of the surface-to-air temperature difference. This systematic error directly affects the intercept (B) of the temperature gradient/net radiation correlation. Indirectly, it also affects the value of A calculated using an average value of the air transport coefficient. For example, if the surface temperature is slightly high relative to the air temperature, temperature gradients will be overestimated, and the value of B obtained from the temperature gradient/net radiation correlation will be high. This means that B will be less negative than it ought to be, or too small in absolute value. Indirectly, a high surface temperature measurement will result in a low air transport coefficient, which will produce a correspondingly high calculated value of A (Eq. 4-28). The surface and air temperature cross-calibration used in this analysis was obtained from time periods in which there was little net radiation and immeasurably small temperature gradients, as described on p. 59.

The accuracy of ET estimates made using the ATGR method is evaluated in Table 5-3. This is done by calculating the correlation between measured ET rates and ATGR method estimates (Eq. 4-35). The first three numbers after the date indicate the slope, intercept, and correlation coefficient of a simple regression line fit to the measurements and estimates. If the correlation was perfect, the slope would be 1, the intercept would be 0, and the correlation coefficient would be 1. The latter is a measure of the scatter between measured and estimated ET rates; the departure of the slope and intercept from 1 and 0 is an indication of systematic differences between measured and estimated ET rates. These systematic differences probably occur because of the lack of data at low net radiation levels. Morning ET data were generally missing because of condensation in the air sampling mast, so temperature gradient/net radiation correlations are biased toward afternoon conditions.

The comparison of ET estimates to measurements is presented graphically for five days in graphs (g), (h), and (i) in Figs. 8, 9, 10, 11, and 12 of Appendix D. Estimates made with the simple residual method (Eq. 2-24) are also shown for comparison. This method represents the state-of-the-art in remote ET estimation methods.

Graph (g) in each of the figures compares the daily course of measured Bowen ratios, ratios calculated via the ATGR method (Eq. 5-14) and ratios calculated by the simple residual method. The latter was calculated according to:

$$\beta = \frac{h(T_s - T_a)}{fR - h(T_s - T_a)} \quad . \qquad 5\text{-}19$$

In both cases, the average heat transfer coefficient of the particular day graphed was used in computations. The ATGR method Bowen ratio is

Table 5-3. Quality of ET Estimates made with the ATGR Method. The table below gives two measures of the quality of ET estimates for each of two methods of calculating instantaneous ET. The first measure of quality is the slope intercept and regression coefficient of a line fit to the relationship between ET estimates and measured ET rates. The second is the slope of a line describing the same relationship, except forced through the origin.

Date	Calculated with daily average h and f				Calculated with average conditions h and f			
Oct.	Slope	Intercept	R^2	Cum. Err.	Slope	Intercept	R^2	Cum. Err.
17	.88	.03	.96	.99	.84	.03	.96	.97
18	.52	.04	.97	.68	.86	.04	.97	.99
20	.98	.01	.92	1.02	1.09	.00	.92	1.11
21	.94	.01	.98	.98	.90	.01	.98	.95
22	.93	.02	.99	.99	.77	.03	.99	.88
23	1.14	-.03	.98	1.05	.79	-.01	.98	.74
28	1.14	-.02	1.00	1.06	1.07	-.02	1.00	1.00
29	1.23	-.03	1.00	1.09	1.11	-.03	1.00	.99

better at following the general pattern of the measured Bowen ratio. The residual method Bowen ratio is noisy by comparison because it is very responsive to small variations in temperature gradients; whenever the numerator in Eq. 5-19 is reduced, the denominator is increased by an equal amount, and vice versa.

Instantaneous ET estimates made by the ATGR and residual methods are compared in graph (h) of each of the figures. In these calculations an average conditions value is used for the heat transport coefficient (.035 ly/min°C). Both methods produce estimates of the same quality, since they use essentially the same information to produce estimates. Both appear to have the same sensitivity to the heat transport coefficient value. Figure 11(h) shows a day (Oct. 22, 1981) on which the heat transport coefficient averaged about 15% less than the average conditions value, causing both methods to underestimate ET. Graph (i) in Figs. 8, 9, 10, 11 and 12 shows the same data as graph (h) plotted against time. This presentation of the data more clearly shows the systematic departure of ATGR estimates from measured ET rates.

Finally, the accuracy of cumulative ATGR method ET estimates are compared to measurements. The simplest comparison is shown in the fourth column of Table 5-3. It is the slope of a line passing through the origin and the center of the measured vs. estimated ET points, as shown in graph (h) of Figs. 8, 9, 10, 11, and 12 in Appendix D. If the slope is 1.11, for example, the cumulative ET estimate is 11% too high. The second set of numbers in Table 5-3 was calculated under more realistic estimating constraints--"average conditions" values for the air heat transfer coefficient (.035 ly/min°C) and the soil heat flux

parameter (.94) were used for all estimates. Although errors in estimates for individual days change, the overall error level does not.

The overall error level of the cumulative ET estimates can most easily be seen in Fig. 5-16. It graphically compares ET estimates made with the ATGR method (using "average conditions" h and f) and residual methods. In general, cumulative estimates are more accurate than instantaneous estimates, and days on which the ATGR method performance is worst are generally overcast days for which it was very difficult to obtain representative values of A and B.

From the calculations presented in this chapter it can be concluded that the average temperature gradient response is a measure of the average surface parameters, and that the slope and intercept of the temperature gradient/net radiation correlation can be used to make reasonably accurate ET estimates. It must be noted that the cross-calibration of the surface and air temperature sensors is of critical importance in application of the ATGR method. In these calculations it appears that the surface temperature may have been slightly high relative to the air temperature measurement.

Cumulative ET estimates made with the ATGR method are exactly as accurate as estimates made with the state-of-the-art simple residual method. However, unlike the simple residual method, it is useful for any time period(s) for which a net radiation estimate is available--its application is thus not limited to clear time periods. Both methods seem equally susceptible to errors in the value of the heat transport coefficient used in making estimates; estimates that agree least closely with measured ET amounts generally have a heat transfer coefficient substantially different from the average conditions value used.

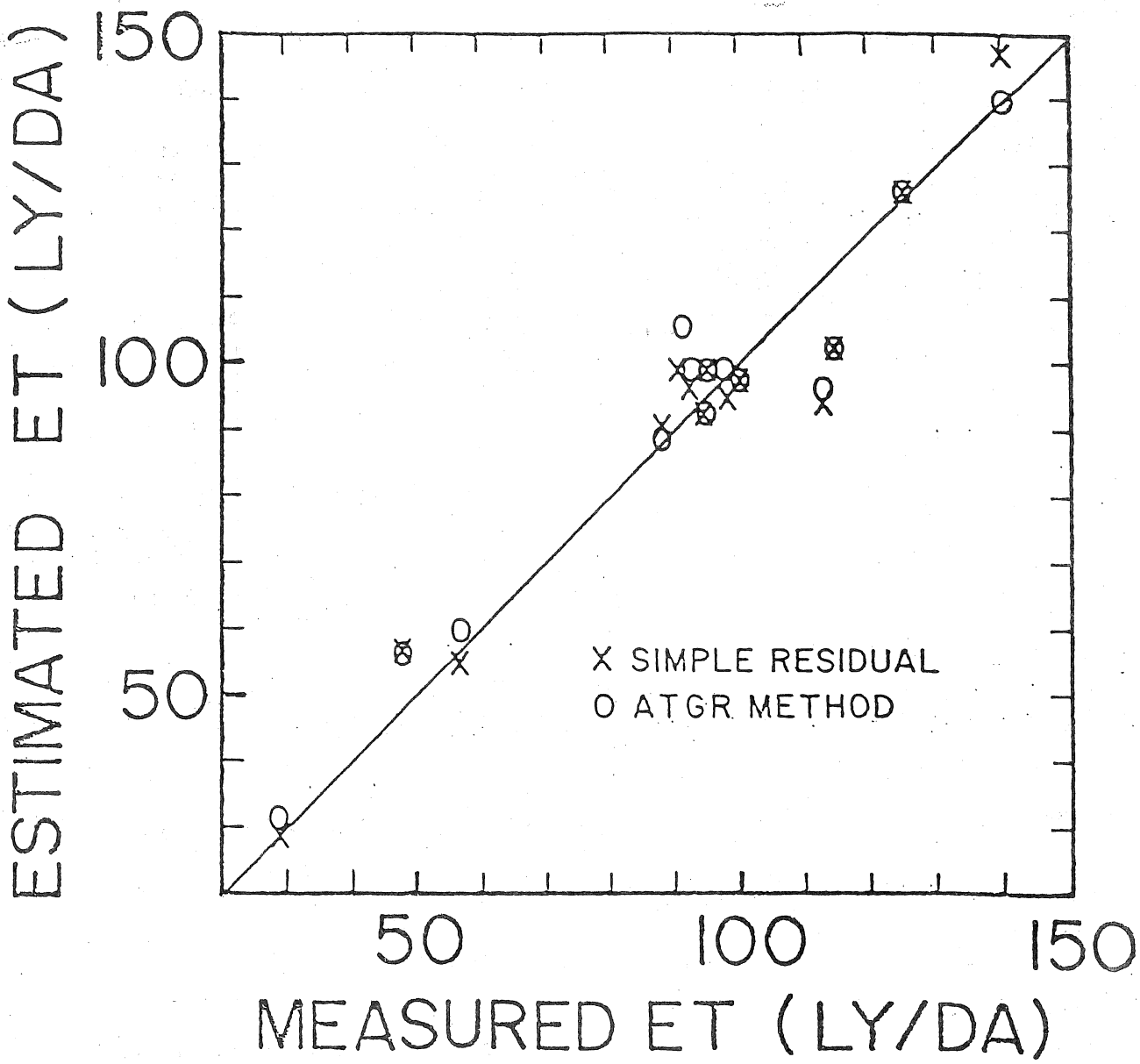

Figure 5-16. Cumulative ET Estimates by the Residual and ATGR Methods. Only the periods for which measured ET was available were used in comparing estimated daily ET with measured daily ET. Data from 15 days between October 17 and November 6, 1981, are shown.

CHAPTER 6

CONCLUSIONS

Summary of Results

The Average Temperature Gradient Response Method

The challenge in developing a general ET estimation method for use with satellite data is to find the method that delivers the most acceptably accurate ET estimate for the least in data collection and data processing costs. The average temperature gradient response (ATGR) method, the primary result of this research, is directed at these practical considerations.

The ATGR method is based on a steady-state model of the surface developed to describe the relationship of temperature gradients and net radiation over a surface. This model,

$$T_s - T_a = \frac{1}{h(Ms + \gamma)} (\gamma f R - Mh\delta e_a) \quad , \qquad 4\text{-}25$$

characterizes the surface with parameters for heat transport through the near-surface air layer (h), surface moisture availability (M), the temperature dependent slope of the saturation vapor pressure curve (s), the fraction of net radiation available to be converted into latent or sensible heat (f), and the saturation deficit (δe_a). By considering the parameters (and the psychrometric constant, γ) stationary over some time period, the average temperature gradient/net radiation correlation

$$T_s - T_a = AR - B \qquad 4\text{-}27$$

can be used to obtain a composite measurement of the average parameters:

$$A = \frac{\gamma f}{h(Ms + \gamma)} \quad \text{and} \qquad 4\text{-}28$$

$$B = \frac{M\delta e_a}{(Ms + \gamma)} \quad . \qquad 4\text{-}29$$

With independent evaluation of two of the parameters, for example, the heat transfer coefficient (h) and the fraction of net radiation available for latent or sensible heat (f), the composite parameters can be used to estimate evapotranspiration:

$$E = (f - hA)R + hB \quad . \qquad 4\text{-}35$$

This is one of five equations for latent heat flux developed, each for a different combination of unknown parameters (see Table 4-1).

Making an ET estimate with the ATGR method is a two-stage process. First, individual remote net radiation and surface temperature measurements and ground-gathered air temperature data are used to calculate the temperature gradient/net radiation correlation (i.e., A and B). This requires data from clear time periods when surface temperatures are observable. The second stage consists of making the ET estimates. With A and B determined, only a net radiation estimate and the two independently estimated parameters are required. For instantaneous ET estimates, these values are simply substituted into Eqs. 4-33, 4-34, 4-35, 4-36, or 4-37.

Since the parameters are considered constant, making cumulative ET estimates is also relatively convenient. Only an estimate of the total positive net radiation during the estimating period (R_p) and the duration of positive net radiation during the estimation period (t_p) are required. For the particular parameter combination in Eq. 4-35, the cumulative ET over the estimating period is

$$E_p = (f - hA)R_p + hBt_p \quad . \qquad 5\text{-}13$$

The two-stage method solves the problem of cloudy skies and the problem of interpolating between data sets. Although there may be some cost in the form of reduced accuracy for instantaneous ET estimates, the considerable data collected over Florida pasture (including net radiation and surface-to-air temperature gradient measurements under partly cloudy and cloudy skies) indicate that the ATGR approach is a good approximation. Cumulative ET estimates were as good as estimates made by the simple residual method (Chapter 2), which requires the same amount of data but has no physically based method of dealing with clouds and the time resolution of satellite data.

Method Limitations and Strengths

In principle, the ATGR method is a descendant of the Penman method and many of the criticisms of the Penman method are relevant to it. The Penman equation has been faulted for including a heat transport coefficient which is an empirical function of wind (Thom and Oliver, 1977). In its generalized form (for unsaturated surfaces) the Penman equation is difficult to use because it requires knowledge of the dryness of the surface in the form of a moisture availability parameter (Barton, 1979) or a bulk stomatal diffusion resistance (Monteith, 1973). Methods of predicting these parameters are all empirical, ranging from an air temperature weighting factor (Doorenbos and Pruitt, 1977) to resistance functions for various plant species (e.g., American Society of Agricultural Engineers, 1966). Finally, the Penman method has been criticized for its use with average daily data; the Penman equation is considered strictly correct only instantaneously (Van Bavel, 1966).

The issue of the correct wind model to use in evaluating the heat transport coefficient is not addressed in this research, although

attention is called to the fact that the radiation surface temperature may not be the same as the effective heat transfer surface temperature. Caution should be exercised in adapting a wind model from the literature; the need for a surface temperature correction procedure for more complex surfaces than pasture, like swamp or mountainous terrain, cannot be ruled out.

The primary advantage in using the ATGR method is that it can obtain a measure of the surface moisture availability from the temperature gradient/net radiation correlation. In fact, with an average measure of the saturation deficit (δe_a) or bulk transfer coefficient (h) and the correlation parameters (A and B), both moisture availability and bulk stomatal diffusion resistance should be calculable:

$$M = \frac{\gamma f}{\delta e_a - Bs} = \frac{(f - hA)}{hAs} \quad \text{and} \qquad 4\text{-}28,29$$

$$r_s = \frac{\rho c_p A \delta e_a (\delta e_a - Bs - B\gamma)}{B\gamma f(\delta e_a - Bs)} \; . \qquad 6\text{-}1$$

(Equation 6-1 was obtained by simultaneous solution of Eqs. 2-23, 4-28 and 4-29.)

The data presented in Chapter 5 make a good case in favor of using daily average data in the Penman equation. The reason this approach works is that the factors which affect the ET rate (h, M, s, f, and δe_a) are constant enough to allow good cumulative ET estimates. The ATGR method has an additional advantage: the process of fitting a line to the temperature gradient/net radiation correlation minimizes the errors caused by considering the parameters constant. With several sets of data per day, it is likely that the ATGR method will be more accurately representative of a particular day than the Penman method, and produce better ET estimates. Usually, daily maximum and minimum temperatures and an

estimate of wind run are the basis for a daily ET estimate with the Penman method. The ATGR method uses several sets of net radiation and corresponding surface-to-air temperature gradients, in effect evaluating surface moisture conditions. As with the Penman method, the ATGR method estimates should improve as they are applied to longer time periods.

The principal limitation of the ATGR method is that it is not yet dependent on remote data alone; it still requires ground-measured air temperatures and independent estimates of two surface parameters. However, air temperatures are dependent on surface temperatures, so at least pseudoempirical methods of estimating air temperature with surface temperatures can be developed (Idso, 1981). Soil heat flux is quite small for areas with closed vegetation canopies and thus does not present a significant problem with regard to the accuracy of the estimate. Potential problems with the heat transport coefficient have been identified, and it can probably be evaluated with one of the wind models in the literature (Thom and Oliver, 1977), possibly with a preliminary surface temperature correction.

The ATGR approach and the approaches developed for the HCMM program suggest a tradeoff between the amount of satellite and ground data collected and the amount of data processing required in producing ET estimates. The simulation approaches require only one or two sets of remote data per day, but require a lot of ground-measured data to force and provide boundary conditions for dynamic models. They also require a good deal of computation to match ancillary data, trial values of surface conditions, and model results to observed surface temperatures. The ATGR approach requires roughly ten times as much remote data, but

needs only concurrent ground-measured air temperatures and the solution of regression equations to make ET estimates.

Because of the directness and simplicity of the ATGR approach, it is the opinion of the author that developing the combination of high time resolution satellite data and relatively simple steady-state methods for ET estimates is preferable to the combination of low time resolution satellite data and complex simulation methods. The major advantage of the steady-state approach lies in the reduced total effort involved in the ET estimates. The cruder surface description of the ATGR method seems better matched to the strengths and limitations of the satellite data source. Another practical advantage of the use of higher time resolution satellite data is that it offers more opportunities to acquire data under clear sky conditions, which are required in both approaches.

Recommendations for Future Research

An estimation procedure can be no more accurate than allowed by its weakest part. From this perspective, the most important area for future research is development of operational methods to determine surface temperature and net radiation from satellite data. This development includes solutions to the problems of image registration and atmospheric absorption corrections. The ability to accurately overlay visible and infrared data collected at different times from the same area on the earth's surface is critical to all remote-sensing methods, as is the ability to correct temperature and net radiation estimates for atmospheric effects. The success with which these "raw" data estimates can be made under realistic operational conditions (varying levels of cloudiness) will determine the overall potential accuracy of an estimation

method. The level of detail of other parts of the method does not need to be greater than can be justified by this potential accuracy.

There are also a number of questions directly related to the ATGR method which need to be addressed. The surface-to-air temperature gradient/net radiation correlation needs to be observed over other surfaces to determine whether the ATGR method can be applied in the same way. For a more complex vegetation canopy, the influence of the sun to surface to remote sensor radiation geometry needs to be investigated. If the radiation temperature of complex surfaces like swamp or mountains is significantly different than the effective heat transfer surface temperature, a correcting technique will need to be developed for surface temperature measurements.

Further research is required to determine a general method of estimating the bulk heat transport coefficient. The primary question to be investigated is whether complication of obtaining average surface roughness and windspeed data is justified with the accuracy levels anticipated in the raw data, or whether an "average conditions" value is adequate.

Making the ATGR method depend as much as possible on remote data is another area that needs investigation. How to obtain surface-to-air temperature gradients from surface temperatures alone is the most important area, but the possibility of estimating the other parameters from remote data should also be investigated.

Eventually a study must be made to determine the magnitude of errors introduced when average net radiation and surface temperature values from nonhomogeneous pixels are used to compute ET. From the equations it would appear that this would not be too great a problem

except in areas where the surface moisture in parts of the same pixel are radically different, as in irrigated fields surrounded by very dry areas.

Besides building the method one step at a time for more complex estimating problems, the remote ET estimation problem might also be approached by applying the ATGR method as is. The ATGR method's ET estimates for research watersheds can be compared to ET estimates made by other methods. It would also be productive to examine the stationarity and distribution of the temperature/net radiation correlation coefficients, A and B. An idea of the behavior of these coefficients and the problems associated with their calculation would help in developing operational data processing methods. If A and B can be legitimately constrained to reasonable values, use of the more numerically sensitive equations for ET might prove feasible.

Clearly there are many potential problem areas that remain to be investigated before the general applicability of the ATGR method is proven. The ATGR method is reasonably simple and theoretically sound, and in this study is shown to work for a simple pasture surface. The number of parameters needed to describe a vegetated surface has been reduced to a minimum, and the temperature gradient model correctly describes their interrelationship and relationship to remotely sensed data. On that basis, the method can definitely be used as a framework for further research toward a practical regional ET estimation method.

REFERENCES

Allen, L.H. Jr., C.S. Yocum, and E.R. Lemon. 1964. Photosynthesis Under Field Conditions. VII. Radiant Energy Exchanges Within a Corn Crop Canopy and Implications in Water Use Efficiency. Agron. J. 56: 253-259.

Allen, L.H. Jr., J.F. Bartholic, R.G. Bill, Jr., A.F. Cook, H.E. Hannah, K.F. Heimburg, W.H. Henry, K. Hokkanen, F.G. Johnson and J.W. Jones. 1980. Chapter 5.6, Evapotranspiration Measurements. In Florida Water Resources, NAS10-9348 Final Report, IFAS, University of Florida, in cooperation with NASA and the South Florida Water Management District. pp. 5.6-1-88. (Technical Research Report).

American Society of Agricultural Engineers. 1966. Evapotranspiration and its role in water resources management. Proceedings, Chicago, IL, Dec. 5-6, 1966. ASAE, St. Joseph, MI.

Barton, I.J. 1979. A parameterization of the evaporation from non-saturated surfaces. J. Appl. Met. 18:43-47.

Black, T.A. and K.G. McNaughton. 1971. Psychrometric apparatus for Bowen-ratio determination over forests. Bound. Layer Met. 2:246-254.

Black, T.A. and K.G. McNaughton. 1972. Average Bowen-ratio methods of calculating evapotranspiration applied to a Douglas fir forest. Bound. Layer Met. 3:466:475.

Bosen, J.F. 1960. A formula for approximation of saturation vapor pressure over water. Monthly Weather Rev. 88:275-276.

Bowen, I.S. 1926. The ratio of heat losses by conduction and by evaporation from any water surface. Phys. Rev. 27:779-87.

Brutsaert, W. 1982. Evaporation into the Atmosphere. Theory, History and Applications. D. Reidel Publ. Co. Boston. 283 pp.

Businger, J.A. 1973. Aerodynamics of vegetated surfaces. In Heat and Mass Transfer in the Biosphere, De Vries, D.A. and Afgan, N.H., eds., Scripts Book Co., Washington, D.C. 594 pp.

Carlson, T.N. and F.E. Boland. 1978. Analysis of urban-rural canopy using a surface heat flux/temperature model. J. Appl. Met. 17:998-1013.

Carlson, T.N., J.K. Dodd, S.G. Benjamin and J.N. Cooper. 1981. Satellite estimation of the surface energy balance, moisture availability and thermal inertia. J. Appl. Met. 20:67-87.

Chang, J. 1968. Climate and Agriculture. Aldine Publishing Co., Chicago, IL. 303 pp.

Desjardins, R.L., L.H. Allen, Jr. and E.R. Lemon. 1978. Variations of carbon dioxide, air temperature, and horizontal wind within and above a maize crop. Boundary-Layer Met. 14:369-380

Doorenbos, J. and W.D. Pruitt. 1977. Guidelines for predicting crop water requirements. Food and Agriculture Organization of the United Nations, Irrigation and Drainage Paper No. 24. 144 pp.

Dyer, A.J. 1967. The turbulent transport of heat and water vapor in an unstable atmosphere. Quart. J. Roy. Met. Soc. 93:501-508.

Dyer, A.J. and B.B. Hicks. 1970. Flux-gradient relationships in the constant flux layer. Quart. J. Roy. Met. Soc. 96:715-721.

Eagleson, P.S. 1970. Dynamic Hydrology. McGraw-Hill Book Co., New York, NY. 462 pp.

EG&G International, Inc. 1977. The Dew Point Hygrometer Model 880 Instruction Manual TM 71-174. Waltham, MA.

Garratt, J.R. and B.B. Hicks. 1973. Momentum, heat and water vapor transfer to and from natural and artificial surfaces. Quart. J. Roy. Met. Soc. 99:680-687.

Goddard Space Flight Center. 1980. Heat Capacity Mapping Mission (HCMM) Data User's Handbook for Applications Explorer Mission-A (AEM). National Aeronautics and Space Administration (NASA), Greenbelt, MD. 120 pp.

Goudriaan, J. and Waggoner, P.E. 1972. Simulating both aerial microclimate and soil temperature from observations above the foliar canopy. Neth. J. Agric. Sci. 20:104-124.

Idso, S.B. 1982. A surface air temperature response function for earth's atmosphere. Boundary-Layer Met. 22:227-232.

Jackson, R.D., S.B. Idso, R.J. Reginato and P.J. Pinter, Jr. 1980. Remotely sensed crop temperatures and reflectances as inputs to irrigation scheduling. Proc. Spec. Conf. on Irrig. and Drain. ASCE, Boise, Idaho, July 23-25, 1980.

Jarvis, P.G. 1971. The estimation of resistances to carbon dioxide transfer. In Plant Photosynthetic Production, Sestak, Z., J. Catsky, and Jarvis, P.G., eds, Dr. W. Junk N.V., The Hague, Netherlands. 818 pp.

Kendall, M.G. 1968. A course in multivariate analysis. In Statistical Monographs and Courses. Charles Griffin & Co. LTD, London, UK.

Lemon, E.R., D.W. Stewart, R.W. Shawcroft and S.E. Jensen. 1973. Experiments in predicting evapotranspiration by simulation with a soil-plant-atmosphere model (SPAM). In Field Soil Water Regime, Soil Sci. Soc. Amer., Madison, WI.

Menenti, M. 1980. Defining relationships between surface characteristics and actual evaporation rate. NTIS #E80-10335, U.S. Dept. Commerce, Springfield, VA.

Monteith, J.L. 1965. Evaporation and environment. Symp. Soc. Exp. Biol. 19:205-234.

Monteith, J.L. 1973. Principles of Environmental Physics. Edward Arnold, London. 241 pp.

Monteith, J.L. 1975. Vegetation and the Atmosphere. Vol. 1. Academic Press, London, UK. 273 pp.

Morgan, D.L., W.O. Pruitt and F.J. Lourence. 1971. Analysis of energy and mass transfers above vegetative surfaces. Res. & Devel. Tech. Rept. ECOM 68-G10-F by Univ. of Calif.-Davis for U.S. Army Electronics Command, Atmos. Sciences Lab., Ft. Huachuca, AZ. AD 721-301. 128 pp.

Murphy, C.E., Jr. and K.R. Knoerr. 1970. A general model for the energy exchange and microclimate of plant communities. Proc. Summer Computer Simul. Conf., Simul. Council, Inc., La Jolla, CA. pp. 786-797.

Murphy, C.E., Jr. and K.R. Knoerr. 1972. Modeling the energy balance processes of natural ecosystems. E. Decid. Forest Biome. Memo Rept. No. 72-10. Oak Ridge Natl. Lab., Oak Ridge, TN.

Nappo, C.J. 1975. Parameterization of surface moisture and evaporation rate in a planetary boundary layer model. J. Appl. Met. 14:289-296.

Odum, H.T. 1982. Systems Ecology: An Introduction. John Wiley & Sons, NY. 614 pp.

Outcalt, S.I. 1972. The development and application of a simple digital surface-climate simulator. J. Appl. Met. 11:629-636.

Pandolfo, J.P. and C.A. Jacobs. 1973. Test of an urban meteorological pollutant model using CO validation data in the Los Angeles metropolitan area. Vol. I, CEM-4121-490A, The Ctr. for the Environ. and Man, Hartford, CT. 176 pp.

Penman, H.L. 1948. Natural evaporation from open water, bare soil and grass. Proc. Roy. Soc. A. 199:120-145.

Prandtl, L. 1932. Meteorologische Anwendungen der Strömungslehre. Beitr. Phys. Fr. Atmosph. 19:188-202.

Price, J.C. 1977. Thermal inertia mapping: a new view of the earth. J. Geophy. Res. 82:2582-2590.

Price, J.C. 1980. The potential of remotely sensed thermal infrared data to infer surface soil moisture and evaporation. Water Resources Res. 16:787-795.

Price, J.C. 1982. Estimation of regional scale evapotranspiration through analysis of satellite thermal infrared data. IEE Transactions of Geoscience & Remote Sens. GE-20 #3, July 1982.

Pruitt, W.O. 1964. Cyclic relations between evapotranspiration and radiation. Paper No. 61-716, presented at Am. Soc. Agr. Eng. Winter Mtg., Chicago, IL, Dec. 1961.

Rosema, A., J.H. Bijleveld, P. Reiniger, G. Tassone, K. Blyth and J. Gurney. 1978. TELL-US, a combined surface temperature, soil moisture and evaporation mapping approach. Presented at 12th Int. Symp. on Remote Sens. of Environ., Environ. Res. Inst. of MI, Manila, Philippines, 1978.

Rosenberg, N.J. 1974. Micro-climate, the Biological Environment. John Wiley & Sons, NY. 315 pp.

Seguin, B. 1980. Détermination de l'évaporation réelle dans les bilans hydrologiques par la télédétection en thermographie infra-rouge. Bull. Sci. Hydrol. 25:143-153.

Sinclair, T.R., L.H. Allen, Jr. and E.R. Lemon. 1975. An analysis of errors in the calculation of energy flux densities above vegetation by a Bowen-ratio profile method. Boundary-Layer Met. 8:129-139.

Sinclair, T.R., L.H. Allen, Jr. and D.W. Stewart. 1971. A simulation model for crop-environmental interactions and its use in improving crop productivity. Proc. Summer Computer Simul. Conf., Simul. Council, Inc., La Jolla, CA. pp. 784-794.

Sinclair, T.R., C.E. Murphey, Jr. and K.R. Knoerr. 1976. Development and evaluation of simplified models for simulating canopy photosynthesis and transpiration. J. Appl. Ecol. 13:813-829.

Soer, G.J.R. 1977. The Tergra model, a mathematical model for the simulation of the daily behaviour of crop surface temperature and actual evapotranspiration. NIWARS publ. 46, Delft, Netherlands.

Soer, G.J.R. 1980. Estimation of regional evapotranspiration and soil moisture conditions using remotely sensed crop surface temperatures. Remote Sensing Environ. 9:27-45.

Stewart, D.W. and E.R. Lemon. 1969. The energy budget at the earth's surface: a simulation of net photosynthesis of field. U.S. Army ECOM Tech. Rept. 2-68-1-6. U.S. Army Electronics Command, Ft. Huachuca, AZ. 132 pp.

Stewart, J.B. and A.S. Thom. 1973. Energy budgets in pine forest. Quart. J. Roy. Met. Soc. 99:154-170.

Swinbank, W.C. and A.J. Dyer. 1967. An experimental study in micrometeorology. Quart. J. Roy. Met. Soc. 93:494-500.

Tanner, C.B. and M. Fuchs. 1968. Evaporation from unsaturated surfaces: a generalized combination method. J. Geophys. Res. 73:1299-1304.

Tanner, C.B. and W.L. Pelton. 1960. Potential evapotranspiration estimates by the approximate energy balance method of Penman. J. Geophys. Res. 65:3391-3413.

Tennessee Valley Authority. 1972. Heat and mass transfer between a water surface and the atmosphere. Water Resources Res. Lab. Rept. #14 (TVA Rept. #0-6803), Norris, TN.

Thom, A.S. and H.R. Oliver. 1977. On Penman's equation for estimating regional evaporation. Quart. J. Roy. Met. Soc. 103:345-357.

van Bavel, C.H.M. 1966. Potential evaporation: the combination concept and its experimental verification. Water Resources Res. 2:455-467.

Waggoner, P.E., G.M. Furnival and W.E. Reifsnyder. 1969. Simulation of the microclimate in a forest. Forest Sci. 15:37-45.

Webb, E.K. 1970. Profile relationships: the log-linear extension to strong stability. Quart. J. Roy. Met. Soc. 96:67-90.

APPENDIX A

LIST OF SYMBOLS

The following is a list of the most frequently used symbols.

A	Slope of the line fit to the surface-to-air temperature gradient/net radiation correlation
B	Intercept of the line fit to the surface-to-air temperature gradient/net radiation correlation
C	Generalized coefficient of net radiation in evapotranspiration formulae. Computed from A, B, and estimates of two parameters, as shown in Table 4-1
c_p	Specific heat of air at constant pressure
D	Generalized constant term in evapotranspiration formulae. Computed from A, B, and estimates of two parameters, as shown in Table 4-1
E	Latent heat flux, evapotranspiration rate, or ET
E_p	Cumulative ET over an estimating period
e_a	Water vapor pressure at a reference level in the air above the surface
e_s	Vapor pressure at plant surfaces corresponding to the surface temperature; not measurable
e_s^*	Saturation vapor pressure at the surface temperature
f	Unitless soil heat flux parameter ($f = 1 - G/R$)
G	Soil heat flux
H	Sensible heat flux
h	Bulk heat transport coefficient
L	Latent heat of evaporation
M	Unitless parameter for moisture availability $M(e_s^* - e_a) = e_s - e_a$
P	Atmospheric pressure

Q_a Radiation emitted by the atmosphere

Q_e Radiation emitted by the surface

Q_r Radiation reflected by the surface

Q_s Solar radiation incident on the surface (direct and scattered)

R Net radiation absorbed by the surface ($R = Q_s + Q_a - Q_r - Q_e$)

R_p Cumulative positive net radiation over an estimating period

R_0 Arbitrary maximum net radiation load

r_a Bulk resistance to heat transport of the slab of air between the surface and a reference level

r_s Bulk stomatal diffusion resistance

s Slope of the saturation vapor pressure curve (a known function of temperature, e.g., Eq. 5-6)

T Temperature

T_a Air temperature at a reference level above the surface

T_s Radiation surface temperature

T_0 Temperature at the hypothetical boundary between the laminar layer next to the vegetation and the turbulent layer above. Arbitrarily taken to be the lowest temperature measurement (35 cm) for calculations

TST True solar time

t_p Duration of positive net radiation during the estimating period

z Vertical space coordinate

β Bowen ratio

γ Psychrometric constant ($\gamma = c_p P/L\varepsilon$)

δe_a Saturation deficit of the air

ε Ratio of molecular weights of water and dry air

ρ Air density

σ Stefan-Boltzmann constant

APPENDIX B

PROGRAM LISTING AND DEFINITION OF NAMES USED

Programs SET, MEASR, REPRT, and ANALZ are listed in the following pages. They are written in Fortran IV and run under Hewlett-Packard's Real Time Executive (RTE-2) operating system. Calls to RTE-2 (CALL EXEC) were used to schedule programs, delay program execution between program statements, make measurements, and determine the system time. Names of subroutines, functions, data arrays, and indexes are defined in the pages following the programs.

```
      PROGRAM SET(3,90)
C*****SET SCHEDULES PROGRAM MEASR FOR UNIFORM MEASUREMENT TIMING AND
C*****RUNS PROGRAMS REPRT AND ANALZ AT 12 PROFILE (HALF HOUR) INTERVALS
      COMMON DUMMY(27),AST(6),AT(5,2),AE(5,2),ARAD(6,2),AWSPD,ND(8),
     *NBR,NPROF,BR(2),KFLAG,NVALV,LEVEL,VMARK,RAD(6,2),DPTCOR,NADV,
     *WSPD,T(10),NMEAS
      DIMENSION ITIME(5),MEASR(3)
      INTEGER ANALZ(3),REPRT(3)
      DATA MEASR/2HME,2HAS,2HR /,
     *REPRT/2HRE,2HPR,2HT /,ANALZ/2HAN,2HAL,2HZ /
      IF(ISSW(2))40,1
    1 LAG = 29
      GO TO(2,5,30,35)KFLAG
    2 NADV = 2
      NMEAS = 0
      D = .85
      P = 29.92
      DPTCOR = P/(P-D)
      WRITE(1,3)
    3 FORMAT(1X,"SENSOR PLUGS IN ?  PUMP, DEW POINT",
     *" INSTRUMENT, MIXING BOX, MAST FANS ON?")
      READ(1,4)IANS
      IF(IANS .EQ. 2HYE)5,1
    4 FORMAT(A2)
C*****CHECK POSITION OF ROTARY VALVE
    5 CALL EXEC(1,9,DATA,2,110,4045B)
      VMARK = CONV(DATA)
      IF(VMARK .GT. 6.)20,10
   10 CALL FIND(VMARK)
C*****INITIALIZE COUNTERS AND PROFILE AVERAGES FOR COLD START
   20 NVALV = -NADV
      LEVEL = -NADV
      VMARK = 0.0
      NPROF = 0
      CALL ZERO(AST,ARAD,AE,AT,AWSPD,ND,BR,NBR)
      DO 25 K=1,6
      RAD(K,1) = 0.0
      RAD(K,2) = 0.0
   25 CONTINUE
      WSPD = 0.0
C*****DELAY PROGRAM MEASR START FOR UNIFORM REPORT TIMING
      CALL EXEC(11,ITIME)
      K = ITIME(3)*60+ITIME(2)
      LAG = 150-MOD(K,150)+62
      IF(LAG .GT. 150) LAG = LAG-150
   30 CALL EXEC(12,MEASR,2,0,-LAG)
      IF(KFLAG .LT. 3)45,40
   35 CALL EXEC(11,ITIME)
      MIN = 2
```

```
      IF(ITIME(3) .GT. 3) MIN = 32
      CALL EXEC(12,MEASR,2,0,ITIME(4),MIN,3,0)
   40 CALL EXEC(10,REPRT,1)
      CALL EXEC(10,ANALZ,1)
   45 KFLAG = 0
      END
      SUBROUTINE ZERO(AST,ARAD,AE,AT,AWSPD,ND,BR,NBR)
C*****ZERO INITIALIZES SUMMATIONS USED IN CALCULATING AVERAGES
      DIMENSION AST(6),ARAD(6,2),AE(5,2),AT(5,2),ND(8),BR(2)
      DO 50 I=1,2
      BR(I) = 0.0
      DO 50 K=1,5
      AE(K,I) = 0.0
      AT(K,I) = 0.0
   50 CONTINUE
      AWSPD = 0.0
      DO 55 K=1,8
      ND(K) = 0
   55 CONTINUE
      DO 60 K=1,6
      AST(K) = 0.0
      ARAD(K,1) = 0.0
      ARAD(K,2) = 0.0
   60 CONTINUE
      NBR = 0
      RETURN
      END
      SUBROUTINE FIND(VMARK)
C*****FIND TURNS SELECTOR VALVE ONE PORT AND RETURNS MARK VOLTAGE
      DO 65 K=1,10
      CALL EXEC(1,9,DATA,2,19,4043B)
      CALL EXEC(1,9,DATA,2,0,4043B)
      CALL EXEC(12,0,2,0,-2)
      CALL EXEC(1,9,DATA,2,110,4045B)
      VMARK = CONV(DATA)
      IF(VMARK .GT. 6.0)RETURN
   65 CONTINUE
      WRITE(6,70)
   70 FORMAT(1X,"NO MARK VOLTAGE. CHECK PANEL PLUGS AND POWER TO BOX.")
      STOP 0001
      END
      END$
```

```
      PROGRAM MEASR(3,90)
C*****MEASR CONTROLS AIR SAMPLE FLOW TO DEWPOINT ANALYZER, SCHEDULES
C*****AND MAKES ALL MEASUREMENTS AND PERFORMS PRELIMINARY CALCULATIONS
      COMMON CST(6),CAT(5),CAE(5),CRAD(6),TSURF,HSENS,HLTNT,CWSP,R
     *AST(6),AT(5,2),AE(5,2),ARAD(6,2),AWSPD,ND(8),NBR,NTOT,BR(2),
     *KFLAG,NVALV,LEVEL,VMARK,RAD(6,2),DPTCOR,NADV,WSPD,T(10),
     *NMEAS,DAT(26,2)
      DIMENSION E(5),ITIME(5),DPT(5),
     *TRAD(6),CB(7),CA(7),IPGM2(6),IWAIT(5)
      INTEGER CHAN1(4),CHAN2(6),ANALZ(3),REPRT(3),SET(3)
      DATA CHAN1/111,112,113,115/,CHAN2/14,101,102,100,104,109/,
     *REPRT/2HRE,2HPR,2HT /,ANALZ/2HAN,2HAL,2HZ /,SET/2HSE,2HT ,2H  /
      DATA CA/29.40,127.88,142.04,35.4,3210.,104.5,9.37/,
     *CB/0.,0.,0.,0.,59.5,0.,0./,IPGM2/3042B,3042B,3042B,3042B,
     *3043B,3042B/,IWAIT/-30,-15,-14,-12,-16/
      HV(T) = 597.3-.566*T
      GO TO 30
   25 CALL EXEC(12,0,2,0,-23)
C*****VALVE POSITION CHECK(USUAL RETURN, START OF EACH MEAS. SEQUENCE)
   30 IF(VMARK .GT. 6.)35,45
   35 WRITE(6,40)
   40 FORMAT(1X,"VALVE POSITION NOT IN SYNC WITH PROGRAM.WILL TRY ",
     *"RESTART")
      KFLAG = 2
      GO TO 140
   45 NVALV = NVALV+1
      LEVEL = LEVEL+1
      LEVT = LEVEL+NADV
C*****SUSPEND PROGRAM EXECUTION BETWEEN MEASUREMENTS
      IF((NPROF .EQ. 0) .AND. (LEVEL .EQ. 1))55,50
   50 CALL EXEC(12,0,2,0,IWAIT(LEVEL))
   55 TBASE = 0.0
      DTEMP = 0.0
C*****MEASURE TEMPERATURE AT PROFILE BASE
      AVG = FILT(108,3042B,.000002)
      TBASE = CUCON(AVG,-1)
      IF((LEVT .EQ. 1) .OR. (LEVT .EQ. 6))68,60
C*****LOOP TO DETERMINE TEMPERATURE AT LEVT VIA THERMOPILES
   60 NDT = LEVT-1
      IF(LEVT .GT. 6) NDT = LEVT-6
      DO 64 K=1,NDT
      DTEMP = DTEMP+2451.*FILT(CHAN1(K),3042B,.000002)
   64 CONTINUE
   68 T(LEVT) = TBASE-DTEMP
C*****LOOP TO MAKE OTHER MEASUREMENTS
      NMEAS = NMEAS + 1
      DO 72 I=1,6
      DATA = FILT(CHAN2(I),IPGM2(I),.000002)
      DATA = (CA(I)*DATA+CB(I))
```

```
      SVAL = DATA
      IF(I .EQ. 1) CALL TMTCH(DATA,1,NMEAS,SVAL,DAT)
      IF(I. EQ. 5) CALL TMTCH(DATA,2,NMEAS,SVAL,DAT)
      DATA = SVAL
      IF(I. NE. 4) GO TO 70
      AVG = FILT(13,3042B,.000002)
      AVG = CUCON(AVG,-1)
      DATA = DATA+.00000000008131*AVG**4
   70 RAD(I,1) = RAD(I,1)+.2*DATA
      RAD(I,2) = RAD(I,2)+DATA**2
   72 CONTINUE
      CALL EXEC(1,9,DATA,2,106,7044B)
      W = CONV(DATA)
      IF((W .GE. 9.375) .OR.  (W .LT. 0.625)) ND(1)=ND(1)+1
      IF((W .GE. 0.625) .AND. (W .LT. 1.875)) ND(5)=ND(5)+1
      IF((W .GE. 1.875) .AND. (W .LT. 3.125)) ND(2)=ND(2)+1
      IF((W .GE. 3.125) .AND. (W .LT. 4.375)) ND(6)=ND(6)+1
      IF((W .GE. 4.375) .AND. (W .LT. 5.625)) ND(3)=ND(3)+1
      IF((W .GE. 5.625) .AND. (W .LT. 6.875)) ND(7)=ND(7)+1
      IF((W .GE. 6.875) .AND. (W .LT. 8.125)) ND(4)=ND(4)+1
      IF((W .GE. 8.125) .AND. (W .LT. 9.375)) ND(8)=ND(8)+1
      CALL EXEC(1,9,DATA,2,105,7043B)
      DATA = CONV(DATA)
      WSPD = WSPD+.2*(CA(7)*DATA+CB(7))
C*****IF INITIAL (COLD START) MEASUREMENTS COMPLETE, CONTINUE
      IF(LEVEL)25,25,74
C*****MAKE DEW POINT MEASUREMENT AND STEP VALVE TO NEXT LEVEL
   74 EGG = FILT(107,4042B,.000002)
      CALL EXEC(11,ITIME)
      CALL STEP(VMARK)
      DPT(LEVEL) = (1508.*EGG-32.768)*DPTCOR
      E(LEVEL) = 10.**((7.5*DPT(LEVEL))/(DPT(LEVEL)+237.3)+.7858)
      IF (ISSW(0))76,80
   76 WRITE(1,78)ITIME(4),ITIME(3),ITIME(2),VMARK,T(LEVEL),
     *DPT(LEVEL),E(LEVEL),TBASE,DTEMP,T(LEVT),NVALV,LEVEL,LEVT,NDT,K
   78 FORMAT(1X,I2,":",I2,":",I2,F7.3,6F7.1,5I4)
C*****IF REAL TIME PROFILE COMPLETE, SAVE AVERAGES FOR PROFILE REPORT
   80 IF(LEVT .NE. 5) GO TO 95
C*****AT START OF HALF HOUR, MAKE SURE THAT REPRT HAS ZEROED AVERAGES
      IF((NPROF .EQ. 0) .AND. (NBR .NE. 0)) STOP 0002
   85 DO 90 K=1,6
      DATA = FILT(K,3042B,.000002)
      AST(K) = AST(K)+CUCON(DATA,-1)
      ARAD(K,1) = ARAD(K,1)+RAD(K,1)
      ARAD(K,2) = ARAD(K,2)+RAD(K,2)
      TRAD(K) = RAD(K,1)
      RAD(K,1) = 0.0
      RAD(K,2) = 0.0
   90 CONTINUE
      AWSPD = AWSPD+WSPD
      TWSPD = WSPD
      WSPD = 0.0
```

```
      AWDIR = AWDIR+WDIR
      WDIR = 0.0
C*****IF LAGGED DEW POINT PROFILE COMPLETE, COMPUTE BOWEN RATIO,
C*****REPORT PROFILE DATA, AND ADD IT TO HALF HOUR SUMS
   95 IF(LEVEL .EQ. 5)100,30
  100 NPROF = NPROF+1
      CALL RATIO(E,T,B,C)
      B = (391.7*B)/HV(TRAD(5))
      CD = ABS(C)
      IF(CD-.95)106,106,104
  104 NBR = NBR+1
      BR(1) = BR(1)+B
      BR(2) = BR(2)+B**2
  106 IF(ISSW(3))107,109
  107 WRITE(6,108)NPROF,TRAD(5),T(1),T(2),T(3),T(4),T(5),C,
     *ITIME(4),ITIME(3),ITIME(2),
     *TRAD(1),DPT(1),DPT(2),DPT(3),DPT(4),DPT(5),B,TWSPD,E(1),E(2),
     *E(3),E(4),E(5)
  108 FORMAT(/,4X,"PROF#",I3,"    RAD.T.",FT.2,"    TEMP",5F6.1,
     *"   R = ",F5.3,/,4X,I2,":",I2,":",I2,"    NET R.",F7.2,
     *"    DPT.",5F6.1,/,4X,"B =",F5.3,"    W.SPD.",F7.2,
     *"    V.P.",5F6.1)
C*****TRIMMER DELAY
      CALL EXEC(12,0,1,0,-32)
      GO TO 110
  109 CALL EXEC(12,0,1,0,-49)
C*****SUM PROFILE DATA FOR AVERAGES, ROLL DOWN ADVANCE TEMPERATURE
C*****READINGS
  110 DO 115 K=1,5
      AT(K,1) = AT(K,1)+T(K)
      AT(K,2) = AT(K,2)+T(K)**2
      T(K) = T(K+5)
      AE(K,1) = AE(K,1)+E(K)
      AE(K,2) = AE(K,2)+E(K)**2
  115 CONTINUE
      LEVEL = 0
      IF(NVALV .EQ. 10)120,130
  120 IF(VMARK .GT. 6.)125,35
  125 NVALV = 0
      VMARK = 0.0
  130 IF(ISSW(1))132,134
  132 KFLAG = 3
      GO TO 138
C*****AT END OF HALF HOUR, COMPUTE AVERAGES AND REPORT
  134 IF(((ITIME(3) .GE. 0) .AND. (ITIME(3) .LT. 3)) .OR.
     *((ITIME(3) .GE. 30) .AND. (ITIME(3) .LT. 33)))136,30
  136 KFLAG = 4
  138 NTOT = NPROF
      IF(NTOT .GT. 5) NMEAS = 25
      NPROF = 0
  140 CALL EXEC(9,SET,1)
      END
```

```
      FUNCTION FILT(NCHAN,IPGM,TOL)
C*****FUNCTION FILT THROWS OUT MEASUREMENTS CONTAINING NOISE
C*****CAUSED BY ELECTRIC CATTLE FENCE CHARGER.
      DIMENSION DAT(12)
      DO 145 M1=1,10
      CALL EXEC(1,9,DAT(M1),2,NCHAN,IPGM)
      DAT(M1) = CONV(DAT(M1))
  145 CONTINUE
      DAT(11) = DAT(1)
      DAT(12) = DAT(2)
      DIF1 = ABS(DAT(1)-DAT(2))
      DO 155 M2=1,10
      DIF2 = ABS(DAT(M2+1)-DAT(M2+2))
      IF (DIF1 .LT. TOL) .AND. (DIF2 .LT. TOL))160,150
  150 DIF1 = DIF2
  155 CONTINUE
  160 TOT = DAT(M2)
      NGD = 1
      GD = DAT(M2+1)
      DO 170 M3=M2,10
      DIF2 = ABS(GD-DAT(M3+2))
      IF(DIF2 .LT. TOL)165,170
  165 TOT = TOT+GD
      GD = DAT(M3+2)
      NGD = NGD+1
  170 CONTINUE
      RGD = NGD
      RMEAS = NMEAS
      DQ = RGD/RMEAS
      FILT = TOT/RGD
      IF(DQ .LT. .5) 175,185
  175 WRITE(6,180) NCHAN
  180 FORMAT(1X,"CHANNEL ",I3," IS SUSPICIOUSLY NOISY - CHECK IT OUT")
  185 RETURN
      END
      SUBROUTINE STEP(VMARK)
C*****STEP TURNS SELECTOR VALVE ONE PORT AND RETURNS MARK VOLTAGE
      CALL EXEC(1,9,DATA,2,19,4043B)
      CALL EXEC(1,9,DATA,2,0,4043B)
      CALL EXEC(12,0,2,0,-2)
      CALL EXEC(1,9,DATA,2,110,4045B)
      VMARK = CONV(DATA)
      RETURN
      END
```

```
      SUBROUTINE TMTCH(DATA,L,NMEAS,SVAL,DAT)
C*****TMATCH SLOWS SENSOR RESPONSE TO MATCH TEMPERATURE AND DEW
C*****POINT MEASUREMENTS BY WEIGHTED AVERAGES
      DIMENSION DAT(26,2),W(25)
      DATA W/.137,.119,.104,.090,.077,.067,.058,.050,.044,.038,
     *.033,.028,.025,.021,.018,.016,.014,.012,.010,.009,
     *.008,.007,.006,.005,.004/
      IF(NMEAS .LT. 25)190,195
  190 K = 26 - NMEAS
      DAT(K,L) = DATA
      GO TO 200
  195 DAT(1,L) = DATA
      SVAL = 0.0
      DO 200 I=25,1,-1
      SVAL = SVAL + DAT(I,L)*W(I)
      DAT(I+1,L) = DAT(I,L)
  200 CONTINUE
      RETURN
      END
      SUBROUTINE RATIO(E,T,B,C)
C*****RATIO COMPUTES SLOPE OF T(LEVEL)VS.E(LEVEL) BY DIAGONAL REGRESSION
      DIMENSION E(5),T(5),SUM(5)
      DO 210 K=1,5
      SUM(K) = 0.0
  210 CONTINUE
      DO 220 K=1,5
      SUM(1) = SUM(1)+T(K)
      SUM(2) = SUM(2)+E(K)
      SUM(3) = SUM(3)+T(K)**2
      SUM(4) = SUM(4)+E(K)**2
      SUM(5) = SUM(5)+T(K)*E(K)
  220 CONTINUE
      ST = SUM(3)-(SUM(1)**2)/5.
      SE = SUM(4)-(SUM(2)**2)/5.
      SET = SUM(5)-(SUM(1)*SUM(2))/5.
      B = (ST-SE)/(2.*SET)
      IF(SET)225,230,230
  225 B = B-SQRT(1.+B**2)
      GO TO 235
  230 B = B+SQRT(1.+B**2)
  235 C = SET/SQRT(SE*ST)
      RETURN
      END
      END$
```

```
      PROGRAM REPRT(3,94)
C*****REPRT COMPUTES AND REPORTS HALF HOUR AVERAGE HEAT BUDGET AND
C*****PROFILES
      COMMON CST(6),CAT(5),CAE(5),CRAD(6),TSURF,HSENS,HLTNT,CWSP,
     *RCOEF,AST(6),AT(5,2),AE(5,2),ARAD(6,2),AWSPD,ND(8),NBR,NPROF
     *BR(2)
      DIMENSION RH(5),NS(6),NA(6),NAM(12),NDA(8),VCE(5),VCT(5),VCR(6)
      INTEGER DTIME(3),DIR(2)
      DATA NS/0,-2,-5,-10,-25,-50/,NA/225,135,85,60,35,0/,
     *NAM/2H N,2H I,2H R,2H A,2H E,2H  ,2HET,2HSW,2HSW,2HLW,2HLW,
     *2H  /,NDA/2H N,2H E,2H S,2H W,2HNE,2HSE,2HSW,2HNW/
      DATA DTIME/2HDT,2HIM,2HE /
      VC(SS,AVG,RN) = 100.*(SQRT(SS/RN-AVG**2))/AVG
      PROF = NPROF
      DO 5 K=1,6
      ARAD(K,2) = ARAD(K,2)/5.
      CRAD(K) = ARAD(K,1)/PROF
      VCR(K) = VC(ARAD(K,2),CRAD(K),PROF)
      CST(K) = AST(K)/PROF
    5 CONTINUE
      HV = 597.3-.566*CRAD(5)
      DO 10 K=1,5
      CAE(K) = AE(K,1)/PROF
      VCE(K) = VC(AE(K,2),CAE(K),PROF)
      CAT(K) = AT(K,1)/PROF
      VCT(K) = VC(AT(K,2),CAT(K),PROF)
      RH(K) = 100.*CAE(K)/(10.**(7.5*CAT(K)/(CAT(K)+237.3)+.7858))
   10 CONTINUE
      CWSP = AWSPD/PROF
      NDL = 1
      NDE = 1
      DIR(1) = 2H
      DO 30 K=2,8
      IF(ND(NDL) .LE. ND(K))15,30
   15 IF(ND(NDL) .EQ. ND(K))20,25
   20 NDE = NDL
   25 NDL = K
   30 CONTINUE
      IF((ND(NDE) .EQ. ND(NDL)) .AND. (NDE .NE. NDL)) DIR(1)=NDA(NDE)
      DIR(2) = NDA(NDL)
      RNET = CRAD(1)
      SFLX = CRAD(6)
      IF(NBR .EQ. 0)35,38
   35 R = 0.0
      BR = 0.0
      GO TO 40
   38 ABR = BR(1)/NBR
      R = SQRT(BR(2)/NBR-ABR**2)
   40 CALL RATIO(CAE,CAT,BNR,RCOEF)
```

```
      IF(ABS(RCOEF) .LT. .85)42,44
   42 HLTNT = 0.0
      HSENS = 0.0
      GO TO 75
   44 BNR = (391.7*BNR)/HV
      HLTNT = (RNET-SFLX)/(1.+BNR)
      HSENS = BNR*(RNET-SFLX)/(1.+BNR)
      IF(BNR .GE. 0.0)45,60
   45 IF(AT(1) .GT. AT(5))75,50
   50 HLTNT = -ABS(HLTNT)
      HSENS = -ABS(HSENS)
      GO TO 75
   60 IF(AT(1) .GT. AT(5))65,70
   65 HSENS = ABS(HSENS)
      HLTNT = -ABS(HLTNT)
      GO TO 75
   70 HSENS = -ABS(HSENS)
      HLTNT = ABS(HLTNT)
   75 WRITE(6,95)
      ET = 600.*HLTNT/HV
      CALL EXEC(9,DTIME,1)
      WRITE(6,80)DIR
      WRITE(6,85)RNET,SFLX,HSENS,HLTNT,CWSP,NBR,NPROF,BNR,RCOEF
   80 FORMAT(/,1X,"NET  RAD.  SOIL H.F.  SENS. H.F. LAT. H.F.",
     *2A2," WINDS  RSQ.>.95  B.R.  AVG.R.",/,78("-"))
   85 FORMAT(F4.2," LY/M",F6.2," LY/M",F6.2," LY/M",F6.2," LY/M",
     *F7.2," M/S  ",I2," OF ",I2,F6.3,F7.3)
      TSURF = CRAD(5)
      CRAD(5) = 273.2+CRAD(5)
      CRAD(5) = .98*.00000000008131*(CRAD(5)**4)
      WRITE(6,100)
      DO 90 K=1,5
      WRITE(6,105)NAM(K),NAM(K+6),CRAD(K),VCR(K),NA(K),
     *CAT(6-K),VCT(6-K),NA(K),CAE(6-K),VCE(6-K),NA(K),RH(6-K),
     *NS(K),CST(K)
   90 CONTINUE
      WRITE(6,110)ET,NA(6),TSURF,VCR(5),ABR,R,NS(6),CST(6)
   95 FORMAT(2/,22X,"BEEF RESEARCH UNIT ET PROJECT DATA",2/,2X,
     *"AVERAGES AND ( PERCENT VARIATION ) FOR HALF HOUR ENDING")
  100 FORMAT(1/,4X,"RADIATION",6X,"AIR  TEMP",9X,"VAP PRESS",9X,
     *"REL HMDTY",3X,"SOIL TEMP",/,5X,"(LY/M)",8X,"(CM) (*C)",
     *9X,"(CM) (MB)",9X,"(CM) (%)",4X,"(CM) (*C)",/,78("-"))
  105 FORMAT(A2,A2,F6.3," (",F3.1,")",2(I6,F6.1," (",F3.1,")"),
     *2(I6,F6.1))
  110 FORMAT(" ET ",F6.3," MM/HR",I6,F6.1," (",F3.1,")",2X,
     *" **.95+ BR =",F5.3,",+OR-",F4.3,"**",I6,F6.1,1/)
      DO 115 K=1,6
      AST(K) = 0.0
      ARAD(K,1) = 0.0
      ARAD(K,2) = 0.0
  115 CONTINUE
      DO 120 I=1,2
```

```
      DO 120 K=1,5
      AE(K,I) = 0.0
      AT(K,I) = 0.0
  120 CONTINUE
      AWSPD = 0.0
      DO 125 K=1,8
      ND(K) = 0
  125 CONTINUE
      BR(1) = 0.0
      BR(2) = 0.0
      NBR = 0
      END
      SUBROUTINE RATIO(E,T,B,C)
C*****RATIO COMPUTES DT/DE BY DIAGONAL REGRESSION
      DIMENSION E(5),T(5),SUM(5)
      DO 210 L1=1,5
      SUM(L1) = 0.0
  210 CONTINUE
      DO 220 L2=1,5
      SUM(1) = SUM(1)+T(L2)
      SUM(2) = SUM(2)+E(L2)
      SUM(3) = SUM(3)+T(L2)**2
      SUM(4) = SUM(4)+E(L2)**2
      SUM(5) = SUM(5)+E(L2)*T(L2)
  220 CONTINUE
      ST = SUM(3)-(SUM(1)**2)/5.
      SE = SUM(4)-(SUM(2)**2)/5.
      SET = SUM(5)-(SUM(1)*SUM(2))/5.
      B = (ST-SE)/(2.*SET)
      IF(SET)225,230,230
  225 B = B-SQRT(1.+B**2)
      GO TO 235
  230 B = B+SQRT(1.+B**2)
  235 C = SET/SQRT(SE*ST)
      RETURN
      END
      END$
```

```
      PROGRAM ANALZ(3,99)
C*****ANALZ TAKES DATA COLLECTED BY SET AND COMPUTES OTHER
C*****PARAMETERS THAT MAY BE OF INTEREST
      COMMON CST(6),T(5),E(5),RNET,SWI,RSW,ALW,ELW,SFLX,
     *TSURF,HSENS,HLTNT,CWSP,R
      DIMENSION ITIME(5),RSTM(5),RATM(5)
      HV = 597.3-.566*TSURF
      WRITE(6,2)
    2 FORMAT(1X,"ZO",10X,"TO",6X,"DH",6X,"U*H",5X,"RCH",
     *9X,"EO",6X,"DE",6X,"U*E",5X,"RCE")
      RHO = .0012832-.00000389*T(3)
      DO 5 I=L,3
      ZO = I
      CALL PROFT(T,TO,ZO,DH,BH,RH)
      UH = HSENS/(.24*RHO*.4*BH*100.)
      CALL PROFT(E,EO,ZO,DE,BE,RE)
      UE = HLTNT*1013./(RHO*.622*HV*.4*BH*100.)
      WRITE(6,4) ZO,TO,DH,UH,RH,EO,DE,UE,RE
    4 FORMAT(F3.0,1X,2(F12.1,2F8.1,F8.3))
    5 CONTINUE
      IF((RH .LT. -.95) .AND. (TSURF .GT. T(1)))10,15
   10 SVP = 10,**((7.5*TSURF)/(TSURF+237.3)+.7858)
      DO 12 I=1,5
      RHO = .0012832-.00000389*((TSURF+T(I))/2.)
      RTOT = 100.*.622*RHO*HV*(SVP-E(I))/(1013.*HLTNT)
      RATM(I) = 100.*.240*RHO*(TSURF-T(I))/HSENS
      RSTM(I) = RTOT - RATM(I)
   12 CONTINUE
      WRITE(6,14)(RATM(I),RSTM(I),I=1,5)
   14 FORMAT(/," RAIR,RSTM(S/M) ",5(F6.3,",",F5.3))
   15 CALL EXEC(11,ITIME)
      D = ITIME(5)
      TST = ITIME(4)+.25
      IF(ITIME(3) .LT. 10)TST = TST-.5
C*****TVA REPORT, APPENDIX B
      YA = .0172028*(D-1.)
      SYA = SIN(YA)
      CYA = COS(YA)
      S2Y = SIN(2.*YA)
      C2Y = COS(2.*YA)
      SIG = 4.885784+D+.03342*SYA-.001388*CYA+.000348*S2Y-.000028*C2Y
      SIND = .3978686*SIN(SIG)
      EOT = .004289*CYA-.12357*SYA-.153809*S2Y-.060783*C2Y
C*****TVA REPORT 5.5
      EST = TST+.48467-EOT
      COST = COS(.2618*(TST-12.))
      SIND = SIN(.40928*(COS(.017214*(172.-D))))
      COSD = SQRT(1.-SIND**2)
      SINA = .49606*SIND+.86794*COSD*COST
```

```
      COSA = SQRT(1.-SINA**2)
      ZNGL = 90.-57.2958*ATAN(SINA/COSA)
      HRNGL = 15.*(TST-12.)
C*****TVA REPORT 2.24
      OAM = 1./(SINA+.15*(93.885-ZNGL)**(-1.253))
C*****TVA REPORT 2.4
      AESR = 1.+.017*COS(.01721*(186.-D))
      SWIO = (2.*SINA)/(AESR**2)
      ATC = (SWI/SWIO)**SINA
      ABDO = RSW/SWI
      WRITE(6,20)
   20 FORMAT(/," ABDO    SWIO    OAM    ATC      ZNGL    HRNGL    EOT   ",
     *" E.S.T.  T.S.T.    DAY")
      WRITE(6,30)ABDO,SWIO,OAM,ATC,ZNGL,HRNGL,EOT,EST,TST,ITIME(5)
   30 FORMAT(F4.2,1X,3F7.2,2F9.1,F8.4,2F8.2,I8)
      END
      SUBROUTINE PROFT(V,VO,ZO,DV,BV,RV)
C*****PROFT FITS TEMPERATURE AND VAPOR PRESSURE PROFILES BY LINEAR
      REGRESSION.  DISPLACEMENT HEIGHTS CHOSEN BY BEST REGRESSION FIT.
      DIMENSION SUM(5),V(5),X(5),Z(5)
      DATA Z/35.,60.,85.,135.,225./
      RP = 5.0
      ROLD = 0.0
      RK = 0.0
      DO 135 J = 2,22,4
      BSTEP = J
      GO TO 105
  100 RK = RK+1.0
  105 D = BSTEP - RK
      IF(D)140,140,108
  108 DO 110 L2 = 1,5
      SUM(L2) = 0.0
  110 CONTINUE
      DO 120 L3 = 1,5
      IF(Z(L3) .LE. D)118,116
  116 X(L3) = ALOG((Z(L3)-D+ZO)/ZO)
      SUM(1) = SUM(1)+V(L3)
      SUM(2) = SUM(2)+V(L3)**2
      SUM(3) = SUM(3)+X(L3)
      SUM(4) = SUM(4)+X(L3)**2
      SUM(5) = SUM(5)+V(L3)*X(L3)
      GO TO 120
  118 RP = RP-1
  120 CONTINUE
      B = (RP*SUM(5)-SUM(1)*SUM(3))/(RP*SUM(4)-SUM(3)**2)
      A = (SUM(1)-B*SUM(3))/RP
      SDZ = SQRT(SUM(4)-(SUM(3)**2)/RP)
      SDV = SQRT(SUM(2)-(SUM(1)**2)/RP)
      RCOEF = B*(SDZ/SDV)
      IF(ISSW(5))121,123
  121 WRITE(6,122)ZO,D,A,B,RCOEF
  122 FORMAT(1X,5F12.5)
```

```
123 IF(ABS(RCOEF)-ROLD)130,130,125
125 ROLD = ABS(RCOEF)
    VO = A
    DV = D
    BV = ABS(B)
    RV = RCOEF
    IF(RK)135,135,100
130 ROLD = ABS(RCOEF)
    IF(RK)100,100,140
135 CONTINUE
140 RETURN
    END
    END$
```

Definition of Names

Subroutines and Functions

CUCON(VOLTS,-1) Hewlett-Packard library function which converts voltage from a copper-constantan thermocouple with ice point reference temperature into degrees Centrigrade

FILT(NCHAN,IPGM,TOL) Function used to filter fence charger voltage spikes out of low level signals. Argument requires channel number (NCHAN), voltmeter program word (IPGM), and noise tolerance (TOL).

FIND(VMARK) Subroutine used in Program SET to position air sampling valve for first vapor pressure measurement. It returns mark voltage to SET.

HV(T) Function that calculates heat of vaporization as a function of temperature.

PROFT(V,VO,ZO,DV,BV,RV) Subroutine in Program ANALZ which fits 5-level profile (V) and calculates displacement height (DV) given roughness height (ZO). Other arguments: VO is V at Z=0, BV is the slope of the profile, and RV is the correlation coefficient.

RATIO(E,T,B,C) Subroutine in Programs MEASR and REPRT which computes Bowen ratio (B) with diagonal regression of vapor pressure (E) and temperature (T) profiles. Also returns correlation coefficient (C).

STEP(VMARK) Subroutine used in Program MEASR to change position of sampling valve and return mark voltage from air sampling valve.

TMTCH(DATA,L,NMEAS,SVAL,DAT) Subroutine which imposes a 4 min time constant on surface temperature and net radiation measurements by calculating a weighted average of past 25 measurements. The last measurement (DATA) and sensor identification (L) are sent to the subroutine, and it returns a "slowed" value (SVAL) to the main program. In order that measurements made in the preceding half hour survive the program swapping that takes place during the half-hour reporting sequence (see Chapter 3), they are placed in COMMON via DAT(25,2). When the system is started, NMEAS is used to monitor the past data array to see if it has been filled--after NMEAS=25 weighted averages are reported.

ZERO(AST,ARAD,AE,AT,AWSPD,ND,BR,NBR) Subroutine in Program SET that initializes all summations used in calculating half-hour averages.

Main Data Arrays

E(5)*	Air vapor pressure for 5 levels (mb)
ND(8)	Number of occurrences per wind direction octant: ND(1), N; ND(2), E; ND(3), S; ND(4), W; ND(5), NE; ND(6), SE; ND(7), SW; ND(8), NW
DPT(5)	Dewpoint temperature for 5 levels (°C)
RAD(1,1)*	Net radiation (ly/min)
RAD(2,1)	Solar shortwave radiation (ly/min)
RAD(3,1)	Reflected shortwave radiation (ly/min)
RAD(4,1)	Atmospheric longwave radiation (ly/min)
RAD(5,1)	Emitted longwave radiation (ly/min)
RAD(6,1)	Soil heat flux (ly/min)
ST(6)	Soil temperature for 6 levels (°C)
T(10)*	Air temperature for 5 levels (°C). Completed temperature profiles are stored in T(6) through T(10) until corresponding vapor pressure profile is completely measured. Prefixed versions of this array (see below) have only 5 values.
WSP	Windspeed (m/s)

These array names may be prefixed by A, C, or T. Measurements are first loaded into the nonprefixed array. Arrays that are prefixed by T are "temporary" and hold values used in the intermediate data reports. Half-hour "average" values are summed in arrays prefixed with A, and these values are stored for analysis in the following half hour in "common" arrays prefixed with a C. The A-prefixed version of the asterisked arrays has a second column for squared measurements, like RAD does. These statistics are used to compute percent variations for the half-hour report.

Other Names and Indexes

ABDO	Albedo
ABR	Average of Bowen ratios with greater than .95 correlation coefficient
ATC	Atmospheric transmission coefficient
AVG	Filtered average voltage of reference thermocouple at level 1 on profile measurement mast
B	Bowen ratio returned by RATIO
BR(2)	Bowen ratio statistics summations
C	Correlation coefficient returned by RATIO

CA(7)	Sensor calibration factor-slope for the 6 sensors in RAD(6,2) and the windspeed sensor
CB(7)	Sensor calibration factor-intercept for the 6 sensors in RAD(6,2) and the windspeed sensor
D	Pressure correction for dewpoint measurement (in Hg)
DAT(12)	Array of sensor readings checked for voltage spikes in FILT
DAT(25,2)	Array of last 25 surface temperature and net radiation readings in TMTCH
DATA	Temporary name for measurements returned by voltmeter
DPTCOR	Pressure correction for dewpoint temperature reading
DTEMP	Temperature difference calculated from the vapor pressure profile (m/min)
EGG	Voltage from EG&G Dewpoint Analyzer
EOT	Equation of time (hrs)
GD	Number of good measurements made by FILT
HLTNT	Latent heat flux (ly/min)
HRNGL	Hour angle of the sun (degrees)
HSENS	Sensible heat flux (ly/min)
HV(T)	A function that calculates heat of vaporization as a function of temperature
IPGM2(6)	Voltmeter program word for the 6 measurements in RAD(6,2). Each is coded for type of measurement, delay time, and range of measurement
ISSW(N) ISSW(0)	Sense switch number N on face of HP-2100 Minicomputer: When on, causes Program MEASR to print the time, all measurements and indexes for each measurement cycle
ISSW(1)	When on, causes MEASR to produce full half-hour report with all data collected since last half-hour report
ISSW(2)	When on, causes MEASR to stop at end of next half-hour report
ISSW(3)	When on, causes MEASR to print data from each set of profiles collected
ISSW(5)	When on, causes Program ANALZ to print complete profile-fitting search
ITIME(5)	Time: ITIME(5), Day of year; ITIME(4), hour; ITIME(3), minute; ITIME(2), second; ITIME(1), centisecond

IWAIT(5)	Delay between measurements: IWAIT(1) is delay between levels 5 and 1, IWAIT(2) delay between levels 1 and 2, IWAIT(3) delay between levels 2 and 3, etc.
LAG	Delay time (in seconds) used to schedule MEASR when ISSW(1) is on.
LEVEL	Level at which dewpoint is currently being measured
LEVT	Level at which temperature is currently being measured
KFLAG	Flags for program SET: 0 default value 1 to prepare system for "cold" start 2 to recover when sampling valve is out of sync with program 3 to run REPRT and ANALZ immediately, restart MEASR after a delay when ISSW(1) is on 4 to run REPRT and ANALZ immediately, and schedule MEASR for absolute start time at beginning of half-hour period. Usual half-hour transition KFLAG
NADV	Number of levels temperature is measured in advance of vapor pressure to compensate for air sample travel time
NBR	Number of Bowen ratios with greater than .95 correlation coefficient
NCHAN	Channel number to be measured by FILT
NDA(8)	Array containing letter abbreviations for wind direction octants: NDA(1), N; NDA(2), E; NDA(3), S; NDA(4), W; NDA(5), NE; NDA(6), SE; NDA(7), SW; NDA(8), NW
NDE	Wind direction octant with greatest number of occurrences
NDL	Wind direction octant with number of occurrences less than or equal to NDE
NGD	Number of bad (noisy) measurements made by FILT
NMEAS	Number of measurements in subroutine TMTCH data array. When 25 or over, TMTCH returns weighted averages.
NPROF	Chronological number of profile being collected, starting at beginning of half-hour period
NTOT	Name used to save NPROF in COMMON
NVALV	Current scanning valve position (ranges from 1 through 10)
OAM	Optical air mass (unitless)
P	Atmospheric pressure (in Hg)

PROF	Number of profiles collected in last half-hour period (floating point NPROF)
R	Average correlation coefficient of profiles collected in last half hour
RATM	Atmospheric diffusion resistance (s/m)
RCOEF	Correlation coefficient of half-hour average profiles
RH(5)	Relative humidity for 5 levels (%)
RHO	Air density (g/cm^3)
RNET	Half-hour average net radiation (ly/min)
RSTM	Bulk stomatal diffusion resistance (s/m)
RTOT	Total resistance to vapor pressure transport (s/m)
SFLX	Half-hour average soil heat flux (ly/min)
SUM(5)	Regression summations in RATIO and PROFT
SVAL	Weighted average returned by subroutine TMTCH
SWIO	Intensity of solar shortwave radiation without atmosphere
TBASE	Air temperature at lowest level (1) on profile measurement mast
TOT	Used to sum good readings in subroutine FILT
TST	True solar time
TSURF	Half-hour average surface temperature (°C)
UH	Friction velocity calculated from the temperature profile (m/min)
UE	Friction velocity calculated from the vapor pressure profile (m/min)
VCE(5)	Variation coefficient for vapor pressure at 5 levels (%)
VCR(6)	Variation coefficient for readings in RAD (%)
VCT(5)	Variation coefficient for temperature at 5 levels (%)
VMARK	Mark voltage from scanning valve (0 or 12 volts)
W	Voltage from wind direction sensor (between 0-10 volts)
ZO	Roughness height (cm)
ZNGL	Zenith angle of the sun (degrees)

APPENDIX C

SUMMARY OF ENERGY BUDGET DATA

This appendix contains most of the energy budget data collected in the spring and fall of 1981. The table below is a catalog of the data.

It should be noted that different radiation thermometers were used in spring and fall (see Table 2-2), and that only the fall surface temperatures have been cross-calibrated to the air temperatures (1.5°C was added to surface temperature measurements). Subroutine TMTCH, which imposed a 4 min time constant on the radiation sensors, was in use only in the fall. Windspeed was measured 7 m over the pasture surface in both measuring periods.

The number at the far right on the data tables is the correlation coefficient for the temperature and vapor pressure gradients for each half hour period. On some occasions correlation coefficients greater than 1 are reported; these are for time periods when gradients were very small, causing numerical problems in computing the coefficient.

Spring 1981		
Day	Date	No. of Periods
139	May 19	20
140	20	14
141	21	23
142	22	24
143	23	24
145	25	19
147	27	8
148	28	18
149	29	23
150	30	21
151	31	22
152	Jun 1	17
153	2	21
155	4	11
160	9	11
161	10	21
162	11	11

Fall 1981		
Day	Date	No. of Periods
279	Oct 6	14
280	7	16
285	12	18
286	13	21
287	14	21
288	15	21
289	16	16
290	17	21
291	18	20
293	20	21
294	21	21
295	22	21
296	23	21
301	28	16
302	29	20
303	30	20
304	31	20
305	Nov 1	21
306	2	20
307	3	20
308	4	19
309	5	19
310	6	19
311	7	19
312	8	19

Day	Time	Net Rad	Soil Heat Flux	Sens Heat Flux	Lat Heat Flux	Wind	Air Temp	Surf Temp	Vap Pres	Prof Corr
	EDT	LY/M	LY/M	LY/M	LY/M	M/S	°C	°C	MB	
139	900	0.30	0.03	--	--	0.00	22.5	30.9	33.3	.513
	930	0.37	0.03	0.08	0.26	3.48	26.1	32.8	34.1	.983
	1000	0.30	0.04	0.08	0.19	3.91	26.9	32.7	32.1	.979
	1030	0.47	0.04	0.11	0.31	4.09	27.4	35.8	32.9	.986
	1100	0.44	0.05	0.13	0.25	5.12	27.9	36.2	32.4	.990
	1130	0.51	0.06	0.12	0.34	5.62	27.8	36.7	32.4	.986
	1200	0.54	0.06	0.14	0.34	4.82	28.1	38.2	32.2	.999
	1230	0.55	0.08	0.12	0.36	4.26	29.1	39.6	31.6	.991
	1300	0.50	0.06	0.10	0.34	4.68	29.5	38.2	29.4	.969
	1330	0.93	0.12	0.23	0.58	5.10	30.9	45.4	29.2	.998
	1400	0.67	0.10	0.17	0.40	5.86	31.1	42.0	27.9	.984
	1430	0.84	0.12	0.23	0.48	6.59	31.8	44.4	25.2	.985
	1500	0.69	0.10	0.17	0.41	6.62	31.8	42.7	19.8	.987
	1530	0.62	0.09	0.17	0.39	5.64	31.9	42.1	20.1	.985
	1600	0.52	0.08	0.13	0.30	5.79	31.7	40.2	20.2	.978
	1630	0.35	0.05	0.08	0.22	6.25	31.1	36.3	19.9	.963
	1700	0.29	0.04	0.08	0.17	5.51	30.9	35.2	22.2	.953
	1730	0.18	0.03	0.03	0.12	5.68	30.0	32.2	25.3	.977
	1800	0.12	0.02	0.02	0.08	5.38	28.9	30.4	26.9	.950
	1830	0.06	0.01	--	--	4.78	28.2	28.8	26.4	.787
140	1130	0.45	0.07	0.14	0.24	6.37	29.5	--	31.5	.994
	1200	0.77	0.09	0.21	0.48	5.41	30.1	--	31.1	.999
	1230	0.75	0.11	0.23	0.41	6.75	31.1	22.6	29.4	.996
	1300	0.65	0.09	0.21	0.36	6.65	30.7	39.7	28.6	.992
	1330	0.50	0.07	0.14	0.29	6.47	30.6	38.0	28.0	.990
	1400	0.56	0.07	0.15	0.33	5.60	30.5	38.4	29.2	.983
	1430	0.68	0.09	0.21	0.38	6.96	30.8	40.3	29.7	.989
	1500	0.59	0.09	0.19	0.31	6.70	30.9	38.9	29.9	.998
	1530	0.73	0.09	0.24	0.40	7.59	30.9	39.6	28.4	.990
	1600	0.63	0.09	0.20	0.34	7.30	30.9	39.0	29.3	.993
	1630	0.55	0.08	0.20	0.28	7.56	30.6	37.8	27.8	.996
	1700	0.43	0.06	0.14	0.23	6.45	30.1	35.8	28.1	.984
	1730	0.37	0.05	0.11	0.21	6.42	29.8	34.5	27.5	.989
	1800	0.28	0.03	0.10	0.15	6.33	29.2	32.2	27.1	.975
141	800	0.06	-0.01	--	--	3.87	15.8	17.8	21.6	-.714
	830	0.15	-0.00	0.03	0.12	4.03	16.4	19.9	21.3	.990
	900	0.17	-0.00	0.06	0.12	4.37	16.7	21.2	20.9	.994
	930	0.31	0.01	0.12	0.18	4.13	17.4	25.1	20.7	.997
	1000	0.40	0.01	0.18	0.20	3.71	17.4	27.1	20.4	.996
	1030	0.52	0.03	0.24	0.26	3.61	18.6	30.9	20.6	.998
	1100	0.55	0.03	0.25	0.27	3.91	18.9	31.7	20.3	.999
	1130	0.56	0.04	0.24	0.28	3.24	19.8	34.5	20.4	.998
	1200	0.70	0.05	0.28	0.37	3.28	20.8	37.1	20.5	.997
	1230	0.82	0.08	0.31	0.44	3.14	22.1	40.8	20.7	.997

Day	Time	Net Rad	Soil Heat Flux	Sens Heat Flux	Lat Heat Flux	Wind	Air Temp	Surf Temp	Vap Pres	Prof Corr
	EDT	LY/M	LY/M	LY/M	LY/M	M/S	°C	°C	MB	
141	1300	0.86	0.09	0.31	0.46	3.82	23.3	41.8	20.4	.998
	1330	0.83	0.09	0.30	0.44	3.74	23.8	41.5	19.7	.999
	1400	0.86	0.09	0.30	0.46	4.18	24.4	41.9	19.5	.998
	1430	0.85	0.09	0.31	0.45	4.25	25.2	42.1	19.7	.998
	1500	0.80	0.09	0.28	0.43	3.53	25.4	41.8	19.1	.999
	1530	0.76	0.09	0.27	0.41	4.17	25.8	41.4	19.8	.999
	1600	0.69	0.07	0.23	0.38	4.54	25.8	40.1	18.9	998
	1630	0.60	0.06	0.22	0.32	3.88	25.9	39.2	18.4	.998
	1700	0.49	0.04	0.18	0.27	4.65	25.9	36.4	19.0	.997
	1730	0.41	0.03	0.14	0.24	4.27	25.4	34.2	18.7	.996
	1800	0.31	0.02	0.11	0.18	4.60	25.3	31.3	18.5	.995
	1830	0.20	0.02	0.07	0.12	4.76	24.8	28.8	18.4	.994
	1900	0.10	0.01	0.02	0.07	4.12	24.0	26.5	18.6	.987
142	730	0.03	-0.02	--	--	-0.00	7.1	10.1	--	.740
	800	0.09	-0.01	--	--	0.47	10.5	14.5	--	.913
	830	0.20	0.00	--	--	1.08	13.8	19.3	--	.706
	900	0.30	0.01	--	--	2.04	16.6	23.8	--	-.458
	930	0.38	0.02	--	--	1.52	19.7	28.9	--	.845
	1000	0.47	0.03	--	--	2.33	21.8	32.6	--	-.762
	1030	0.56	0.05	0.19	0.32	2.63	23.2	36.0	16.5	.948
	1100	0.63	0.06	0.24	0.33	3.03	23.9	38.1	15.9	.996
	1130	0.70	0.07	0.23	0.39	3.04	24.6	39.5	14.3	.997
	1200	0.73	0.09	0.26	0.38	2.99	25.4	40.8	14.2	.991
	1230	0.76	0.08	0.29	0.38	3.15	25.5	41.1	14.2	.997
	1300	0.84	0.11	0.30	0.44	4.13	26.5	42.4	14.4	.992
	1330	0.85	0.11	0.29	0.44	3.28	26.9	43.2	14.2	.996
	1400	0.83	0.12	0.27	0.45	3.29	27.4	43.5	14.9	.994
	1430	0.82	0.11	0.28	0.43	3.50	27.8	43.1	14.7	.996
	1500	0.78	0.11	0.27	0.41	3.37	28.4	42.6	13.9	.991
	1530	0.73	0.10	0.23	0.40	2.94	28.6	42.4	13.7	.992
	1600	0.67	0.09	0.22	0.35	3.48	29.0	41.2	14.2	.987
	1630	0.59	0.08	0.19	0.32	3.62	29.0	39.9	14.1	.988
	1700	0.50	0.06	0.17	0.28	4.25	28.7	38.1	14.1	.989
	1730	0.41	0.05	0.13	0.23	3.63	28.5	36.7	14.2	.985
	1800	0.30	0.03	0.09	0.19	4.28	28.2	33.2	14.5	.981
	1830	0.20	0.03	0.05	0.12	4.17	27.7	30.4	14.5	.964
	1900	0.09	0.01	--	--	3.51	26.9	27.7	14.0	-.618
143	730	0.04	-0.02	--	--	-0.00	9.3	11.2	--	.896
	800	0.11	-0.00	--	--	-0.00	12.3	15.8	--	.854
	830	0.18	0.01	0.17	0.00	-0.00	16.8	21.2	--	.949
	900	0.28	0.02	--	--	0.44	20.8	26.8	--	-.128
	930	0.35	0.03	--	--	2.35	23.1	29.8	--	.848
	1000	0.49	0.04	0.21	0.24	3.64	23.9	32.9	23.1	.975
	1030	0.59	0.06	0.23	0.30	2.98	24.9	36.6	22.3	.976

Day	Time	Net Rad	Soil Heat Flux	Sens Heat Flux	Lat Heat Flux	Wind	Air Temp	Surf Temp	Vap Pres	Prof Corr
	EDT	LY/M	LY/M	LY/M	LY/M	M/S	°C	°C	MB	
143	1100	0.66	0.07	0.26	0.32	2.79	25.7	38.3	20.9	.985
	1130	0.65	0.08	0.26	0.32	2.47	26.0	38.7	20.7	.977
	1200	0.59	0.08	0.18	0.33	2.16	26.4	38.5	20.6	.992
	1230	0.82	0.11	0.28	0.44	2.41	27.2	41.8	19.9	.983
	1300	0.90	0.13	0.25	0.52	1.80	28.3	43.7	18.7	.946
	1330	0.92	0.14	0.30	0.48	1.95	28.8	44.3	19.6	.990
	1400	0.65	0.11	0.25	0.29	2.62	28.9	40.8	19.0	.962
	1430	0.43	0.06	0.15	0.22	2.91	28.4	36.6	18.8	.934
	1500	0.87	0.11	0.34	0.43	2.42	29.6	43.4	18.3	.967
	1530	0.77	0.11	0.29	0.38	2.51	30.1	42.7	17.5	.980
	1600	0.39	0.07	0.12	0.21	2.19	29.4	37.8	16.2	.991
	1630	0.21	0.04	0.05	0.13	1.65	29.0	34.1	16.9	.916
	1700	0.26	0.04	--	--	1.42	29.1	33.9	17.9	.680
	1730	0.29	0.05	--	--	2.11	29.5	34.8	18.6	.899
	1800	0.20	0.03	--	--	0.77	29.2	32.9	18.7	.669
	1830	0.10	0.02	--	--	0.79	28.4	29.7	19.3	.307
	1900	0.06	0.02	--	--	0.66	27.9	27.9	20.5	-.939
145	800	0.31	0.03	0.10	0.18	3.13	25.1	28.1	28.3	.989
	830	0.36	0.03	0.12	0.21	3.85	25.7	31.8	27.3	.967
	900	0.50	0.05	0.16	0.30	3.67	26.5	35.6	26.9	.980
	930	0.62	0.06	0.21	0.35	3.42	27.4	37.6	24.8	.982
	1000	0.64	0.07	0.21	0.37	3.19	28.1	38.9	25.5	.977
	1030	0.77	0.09	0.21	0.47	2.68	29.2	41.7	25.6	.995
	1100	0.62	0.10	0.16	0.36	2.33	29.6	40.2	26.1	.975
	1130	0.83	0.10	0.21	0.52	2.84	30.1	42.4	24.1	.975
	1200	0.92	0.13	0.27	0.52	2.98	30.8	44.3	22.9	.991
	1230	0.61	0.11	0.17	0.33	3.15	30.8	40.6	22.7	.984
	1300	0.84	0.12	0.27	0.46	3.41	31.3	42.9	22.8	.970
	1330	0.85	0.12	0.26	0.47	2.36	31.7	43.6	22.8	.975
	1400	0.50	0.08	0.14	0.29	2.23	31.2	39.1	22.0	.960
	1430	0.62	0.09	0.19	0.33	3.02	31.6	40.6	22.8	.981
	1500	0.42	0.05	0.10	0.26	3.59	30.8	36.8	23.8	.987
	1530	0.32	0.05	0.07	0.21	3.02	31.0	35.3	23.9	.975
	1600	0.40	0.05	0.10	0.25	3.34	31.9	36.8	22.9	.953
	1630	0.26	0.03	0.10	0.15	3.59	31.6	34.5	22.4	.940
	1700	0.20	0.03	--	--	3.56	31.4	33.1	22.1	.785
147	830	0.53	0.03	0.09	0.40	2.78	25.3	28.1	36.4	.949
	900	0.58	0.04	0.11	0.44	3.12	26.2	30.1	37.2	.968
	930	0.60	0.04	0.11	0.44	3.25	27.1	32.1	37.2	.987
	1000	0.66	0.05	0.13	0.48	3.26	28.3	34.2	37.7	.991
	1030	0.71	0.05	0.14	0.52	4.48	28.8	34.8	37.9	.997
	1100	0.53	0.06	0.13	0.34	4.05	27.9	34.8	38.3	.942
	1130	0.44	0.08	--	--	4.70	24.2	37.0	37.8	.913
	1200	0.32	0.07	--	--	4.99	25.8	36.2	36.3	.819

Day	Time	Net Rad	Soil Heat Flux	Sens Heat Flux	Lat Heat Flux	Wind	Air Temp	Surf Temp	Vap Pres	Prof Corr
	EDT	LY/M	LY/M	LY/M	LY/M	M/S	°C	°C	MB	
148	930	0.62	0.04	0.14	0.43	2.05	27.0	35.4	31.8	.988
	1000	0.69	0.05	0.16	0.48	2.35	27.8	36.7	31.3	.990
	1030	0.65	0.04	0.15	0.46	2.97	28.1	36.1	30.8	.996
	1100	0.82	0.06	0.18	0.57	2.89	28.9	38.6	29.8	.994
	1130	0.72	0.07	0.15	0.50	2.97	28.8	37.6	28.2	.996
	1200	0.76	0.08	0.16	0.52	2.84	29.4	38.4	27.0	.997
	1230	0.66	0.07	0.13	0.46	2.42	29.7	37.7	26.8	.993
	1300	0.79	0.08	0.16	0.55	2.95	30.0	38.6	26.1	.991
	1330	0.84	0.10	0.19	0.56	2.99	30.4	39.4	26.0	.992
	1400	0.86	0.10	0.19	0.57	2.72	31.1	39.9	25.9	.991
	1430	0.71	0.09	0.15	0.47	2.89	30.8	38.2	26.1	.994
	1500	0.68	0.08	0.15	0.45	2.83	30.8	37.6	26.2	.994
	1530	0.44	0.06	0.09	0.29	2.20	30.5	34.9	25.7	.979
	1600	0.39	0.05	0.08	0.27	2.24	30.5	34.3	26.5	.984
	1630	0.29	0.03	0.05	0.20	1.78	30.2	32.9	26.3	.950
	1700	0.22	0.03	--	--	1.51	30.2	31.6	25.5	.811
	1730	0.10	0.02	--	--	1.01	29.6	28.7	25.3	-.938
	1800	0.03	0.01	--	--	0.83	29.0	26.3	25.1	-.998
149	630	0.10	0.01	--	--	0.71	20.9	22.6	--	-.418
	700	0.17	0.01	--	--	1.27	21.8	23.3	--	-.526
	730	0.29	0.02	--	--	1.48	23.5	25.3	--	.713
	800	0.39	0.02	0.06	0.31	1.38	24.8	28.8	30.8	.975
	830	0.48	0.03	0.10	0.35	1.21	26.5	33.3	29.6	.984
	900	0.57	0.05	0.12	0.41	1.13	27.7	35.6	28.2	.976
	930	0.65	0.05	0.15	0.45	1.71	28.5	36.9	26.1	.991
	1000	0.73	0.06	0.17	0.50	2.29	29.3	37.9	24.4	.995
	1030	0.66	0.07	0.15	0.44	2.46	29.5	37.1	24.2	.994
	1100	0.84	0.09	0.17	0.58	1.85	30.3	39.6	22.1	.983
	1130	0.79	0.09	0.17	0.54	2.40	30.5	39.0	22.5	.990
	1200	0.72	0.10	0.16	0.46	2.82	30.8	38.2	22.8	.992
	1230	0.76	0.09	0.15	0.51	2.21	30.9	38.5	22.9	.993
	1300	0.85	0.11	0.20	0.54	2.25	31.7	40.1	22.8	.986
	1330	0.75	0.10	0.16	0.49	1.96	31.5	39.1	23.2	.990
	1400	0.73	0.11	0.15	0.48	1.55	32.2	39.4	23.2	.971
	1430	0.66	0.08	0.14	0.44	2.44	31.8	37.9	23.6	.988
	1500	0.59	0.07	0.12	0.39	2.41	31.9	37.0	23.9	.985
	1530	0.50	0.06	0.10	0.34	2.66	31.8	35.8	23.3	.986
	1600	0.40	0.06	0.06	0.28	1.66	32.2	35.3	22.9	.951
	1630	0.25	0.03	0.04	0.18	2.00	31.5	33.0	22.9	.925
	1700	0.15	0.03	--	--	1.05	31.2	31.5	23.0	-.317
	1730	0.08	0.02	--	--	1.06	30.7	29.3	24.2	-.965

Day	Time	Net Rad	Soil Heat Flux	Sens Heat Flux	Lat Heat Flux	Wind	Air Temp	Surf Temp	Vap Pres	Prof Corr
	EDT	LY/M	LY/M	LY/M	LY/M	M/S	°C	°C	MB	
150	800	0.37	0.03	0.08	0.26	0.58	25.7	32.3	34.6	.947
	830	0.44	0.04	0.09	0.31	0.68	27.1	34.6	35.0	.966
	900	0.54	0.05	0.09	0.39	0.72	28.7	36.1	33.6	.968
	930	0.63	0.06	--	--	0.42	29.8	37.4	30.4	.889
	1000	0.70	0.07	0.11	0.52	0.53	30.6	38.5	28.1	.940
	1030	0.77	0.08	0.14	0.55	0.97	31.4	39.5	28.4	.967
	1100	0.68	0.08	0.13	0.47	1.20	31.3	38.7	27.4	.989
	1130	0.80	0.10	0.15	0.64	1.88	32.3	40.6	27.2	.988
	1200	0.90	0.12	0.15	0.63	1.04	32.7	41.4	25.7	.989
	1230	0.87	0.12	0.15	0.60	1.87	33.3	40.9	24.8	.941
	1300	0.85	0.12	0.16	0.57	1.23	33.3	41.1	24.3	.978
	1330	0.84	0.12	0.15	0.56	1.44	34.1	41.1	24.0	.957
	1400	0.71	0.10	0.13	0.48	1.71	33.8	39.4	25.1	.979
	1430	0.69	0.09	0.12	0.48	2.01	33.8	39.0	25.1	.986
	1500	0.26	0.05	--	--	1.42	33.2	33.7	24.4	.691
	1530	0.32	0.06	--	--	1.31	33.5	34.4	25.1	.719
	1600	0.39	0.06	--	--	0.79	33.8	35.1	25.0	.212
	1630	0.28	0.04	--	--	2.26	33.8	33.7	26.0	.739
	1700	0.18	0.03	--	--	1.71	33.3	32.3	26.3	-.383
	1730	0.10	0.03	--	--	1.37	33.1	30.7	26.3	-.837
	1800	0.03	0.02	-0.00	0.02	0.91	32.3	28.3	27.5	-.992
151	730	0.27	0.03	--	--	1.25	25.1	28.6	36.0	.796
	800	0.36	0.03	--	--	1.01	26.5	31.7	35.8	.908
	830	0.46	0.04	0.10	0.32	1.35	27.9	34.0	36.1	.936
	900	0.56	0.05	0.11	0.39	1.55	29.0	35.7	36.5	.970
	930	0.64	0.07	0.12	0.45	1.68	29.9	36.9	35.3	.982
	1000	0.71	0.08	0.14	0.50	1.45	30.9	38.4	35.2	.962
	1030	0.77	0.09	0.14	0.53	1.40	31.9	39.7	34.2	.959
	1100	0.78	0.09	0.18	0.51	1.39	32.4	40.0	33.9	.967
	1130	0.82	0.10	0.19	0.52	1.70	33.2	40.5	32.7	.966
	1200	0.67	0.11	0.15	0.42	1.55	33.2	39.4	33.1	.971
	1230	0.59	0.08	0.13	0.38	2.10	33.1	37.5	34.0	.943
	1300	0.61	0.09	0.11	0.41	2.35	33.5	38.2	33.2	.962
	1330	0.49	0.07	0.09	0.32	2.46	33.5	36.4	31.4	.953
	1400	0.45	0.07	0.07	0.31	2.03	33.7	36.0	31.0	.900
	1430	0.37	0.06	0.08	0.24	2.27	33.5	35.3	32.2	.912
	1500	0.49	0.06	--	--	1.74	33.9	36.4	32.8	.842
	1530	0.56	0.08	0.15	0.34	2.89	34.5	37.4	33.7	.949
	1600	0.45	0.07	0.13	0.26	2.37	34.4	36.1	33.9	.943
	1630	0.28	0.04	0.07	0.16	2.81	33.8	34.1	34.2	.940
	1700	0.15	0.03	--	--	2.27	33.2	32.5	34.1	.574
	1730	0.11	0.03	--	--	2.24	32.9	31.6	32.4	.602
	1800	0.03	0.01	--	--	2.91	31.9	29.4	28.5	-.925

Day	Time	Net Rad	Soil Heat Flux	Sens Heat Flux	Lat Heat Flux	Wind	Air Temp	Surf Temp	Vap Pres	Prof Corr
	EDT	LY/M	LY/M	LY/M	LY/M	M/S	°C	°C	MB	
152	730	0.30	0.02	--	--	0.06	24.4	29.7	--	.884
	800	0.40	0.03	--	--	0.56	26.4	32.9	--	.828
	830	0.46	0.04	0.11	0.31	1.73	27.5	33.9	37.1	.965
	900	0.57	0.05	0.14	0.38	1.55	28.0	35.5	37.1	.974
	930	0.66	0.07	0.15	0.43	1.84	29.1	36.9	36.5	.979
	1000	0.72	0.08	0.17	0.48	1.64	29.7	38.2	36.0	.979
	1030	0.75	0.08	0.17	0.50	2.07	30.5	39.0	35.9	.992
	1100	0.60	0.09	0.11	0.41	1.08	31.0	37.9	35.4	.955
	1130	0.70	0.08	0.14	0.47	1.14	31.3	38.5	34.9	.968
	1200	0.81	0.11	0.16	0.53	1.55	32.4	40.7	34.0	.989
	1230	0.71	0.10	0.13	0.48	1.63	32.9	39.5	34.0	.975
	1300	0.60	0.09	0.12	0.39	1.38	33.0	38.5	33.7	.978
	1330	0.65	0.09	0.13	0.44	1.61	33.5	38.7	34.1	.948
	1400	0.47	0.09	0.10	0.28	1.50	33.5	37.3	34.4	.974
	1430	0.10	-0.02	--	--	3.46	28.4	25.7	37.9	.536
	1500	0.16	-0.05	--	--	4.54	24.0	22.5	36.0	-.897
	1530	0.10	-0.01	-0.02	0.14	3.02	23.7	23.0	36.8	-.955
153	700	0.22	0.01	--	--	1.41	23.7	24.4	--	.007
	730	0.31	0.02	--	--	2.14	25.0	25.6	--	.824
	800	0.42	0.03	--	--	2.05	26.1	27.5	--	.919
	830	0.53	0.04	0.10	0.39	2.20	27.2	30.0	41.0	.959
	900	0.61	0.05	0.12	0.44	2.62	27.8	31.9	41.0	.984
	930	0.63	0.05	0.12	0.46	2.73	28.4	32.7	40.7	.975
	1000	0.76	0.05	0.14	0.57	2.61	29.1	34.4	40.3	.981
	1030	0.81	0.06	0.15	0.60	2.84	29.8	35.5	39.0	.989
	1100	0.89	0.07	0.16	0.67	2.77	30.6	36.8	38.2	.984
	1130	0.89	0.07	0.16	0.65	2.81	30.8	37.2	37.4	.986
	1200	0.91	0.09	0.16	0.66	2.37	31.5	38.0	36.1	.988
	1230	0.91	0.09	0.20	0.62	2.85	31.9	37.9	36.2	.980
	1300	0.88	0.07	0.24	0.57	3.10	32.3	37.8	36.3	.987
	1330	0.86	0.07	0.22	0.57	2.92	32.8	37.7	35.9	.980
	1400	0.79	0.06	0.20	0.53	3.10	33.1	37.0	36.0	.977
	1430	0.72	0.06	0.18	0.49	2.76	33.7	36.5	36.1	.969
	1500	0.58	0.04	0.16	0.38	3.03	33.5	35.0	37.0	.943
	1530	0.47	0.03	--	--	2.60	33.5	34.1	38.8	.917
	1600	0.26	0.02	--	--	2.20	33.1	32.1	39.4	.742
	1630	0.04	0.00	--	--	1.44	31.9	28.4	39.4	-.821
	1700	0.04	0.00	--	--	0.93	31.4	28.0	40.6	-.900

Day	Time	Net Rad	Soil Heat Flux	Sens Heat Flux	Lat Heat Flux	Wind	Air Temp	Surf Temp	Vap Pres	Prof Corr
	EDT	LY/M	LY/M	LY/M	LY/M	M/S	°C	°C	MB	
155	930	0.90	0.07	0.19	0.63	3.73	30.6	37.0	40.1	.987
	1000	0.77	0.06	0.18	0.53	3.12	30.5	36.6	40.1	.990
	1030	0.79	0.07	0.16	0.56	4.12	31.0	36.4	39.8	.987
	1100	0.89	0.09	0.16	0.63	3.50	31.5	37.7	40.0	.983
	1130	0.92	0.10	0.16	0.66	4.00	32.0	38.2	38.9	.979
	1200	0.96	0.12	0.18	0.66	4.05	32.6	39.1	38.3	.992
	1230	1.00	0.14	0.16	0.70	3.39	33.2	39.8	38.7	.982
	1300	0.88	0.13	0.16	0.60	2.33	33.5	38.7	38.1	.950
	1330	0.88	0.12	0.15	0.61	2.43	33.9	38.6	37.7	.970
	1400	0.81	0.11	0.17	0.53	2.34	34.2	38.0	38.4	.956
	1430	0.72	0.10	0.18	0.44	2.28	34.3	37.1	39.9	.964
160	800	0.45	0.04	--	--	3.78	29.1	30.0	--	-.190
	830	0.52	0.05	0.19	0.28	4.34	29.7	31.2	31.3	.957
	900	0.53	0.05	0.16	0.32	3.96	30.5	32.2	30.5	.972
	930	0.57	0.05	0.17	0.35	3.58	31.0	32.7	29.4	.967
	1000	0.54	0.05	0.15	0.34	3.89	31.4	32.8	28.8	.992
	1030	0.82	0.06	0.21	0.54	3.18	29.9	34.3	26.3	.985
	1100	0.70	0.08	0.16	0.46	3.11	31.2	34.5	29.4	.994
	1130	1.00	0.12	0.26	0.61	4.88	32.3	36.7	30.1	.985
	1200	0.97	0.14	0.27	0.56	5.53	32.7	36.6	29.9	.981
	1230	0.85	0.15	0.27	0.43	5.13	33.3	36.0	30.6	.991
	1300	0.53	0.09	--	--	4.73	32.9	33.3	31.9	.925
161	730	0.36	0.03	--	--	3.33	28.5	28.8	--	.117
	800	0.42	0.04	--	--	4.09	29.1	30.1	--	-.263
	830	0.47	0.04	0.14	0.29	4.42	29.7	31.0	30.7	.967
	900	0.37	0.03	0.09	0.24	3.70	29.9	30.9	29.9	.985
	930	0.73	0.06	0.20	0.47	4.36	31.1	33.7	28.9	.982
	1000	0.65	0.06	0.15	0.43	3.95	31.2	33.3	28.9	.980
	1030	0.62	0.07	0.15	0.40	4.46	31.4	33.5	28.3	.995
	1100	0.90	0.10	0.21	0.59	4.49	32.3	36.2	29.0	.983
	1130	0.69	0.10	0.14	0.46	4.21	32.8	34.8	28.0	.985
	1200	0.50	0.08	0.09	0.33	4.95	32.4	33.1	27.7	.982
	1230	0.90	0.13	0.17	0.60	5.82	33.7	36.4	26.4	.984
	1300	0.89	0.14	0.19	0.56	5.50	34.7	36.8	26.4	.988
	1330	0.62	0.10	0.12	0.40	5.41	34.0	34.4	25.6	.991
	1400	0.75	0.11	0.13	0.51	5.31	34.4	35.4	25.3	.983
	1430	0.70	0.11	0.14	0.45	5.59	34.7	35.3	25.2	.990
	1500	0.50	0.08	0.10	0.32	5.43	34.3	33.6	25.0	.985
	1530	0.55	0.07	0.07	0.40	5.11	34.1	33.4	25.9	.966
	1600	0.31	0.05	0.07	0.19	5.57	33.4	31.6	25.6	.991
	1630	0.23	0.03	0.05	0.16	3.57	30.2	29.9	25.8	.971
	1700	0.11	0.02	--	--	2.23	29.2	28.8	26.3	.133
	1730	0.03	0.01	--	--	2.58	28.2	26.5	25.6	-.886

Day	Time	Net Rad	Soil Heat Flux	Sens Heat Flux	Lat Heat Flux	Wind	Air Temp	Surf Temp	Vap Pres	Prof Corr
	EDT	LY/M	LY/M	LY/M	LY/M	M/S	°C	°C	MB	
162	730	0.41	0.04	--	--	3.45	28.7	30.5	--	-.651
	800	0.54	0.05	--	--	3.21	29.8	31.6	--	-.270
	830	0.51	0.05	0.17	0.29	2.72	30.2	32.1	32.2	.992
	900	0.56	0.05	0.17	0.34	3.22	31.0	32.9	30.8	.965
	930	0.63	0.06	0.15	0.42	2.74	31.6	34.0	29.1	.977
	1000	0.58	0.06	0.11	0.42	2.49	31.8	33.9	27.8	.982
	1030	0.91	0.09	0.17	0.65	2.54	33.0	36.9	26.7	.974
	1100	0.80	0.10	0.15	0.56	2.73	33.2	36.5	25.8	.987
	1130	0.89	0.11	0.16	0.61	2.49	34.0	37.5	25.4	.981
	1200	0.74	0.11	0.14	0.49	2.33	34.1	36.5	25.3	.989
	1230	0.46	0.08	0.07	0.30	2.84	33.9	33.7	25.8	.966

Day	Time	Net Rad	Soil Heat Flux	Sens Heat Flux	Lat Heat Flux	Wind	Air Temp	Surf Temp	Vap Pres	Prof Corr
	EDT	LY/M	LY/M	LY/M	LY/M	M/S	°C	°C	MB	
279	1030	0.65	0.03	0.19	0.42	1.12	25.8	35.0	18.5	.985
	1100	0.70	0.04	0.22	0.45	1.58	26.2	37.5	18.4	.997
	1130	0.77	0.04	0.24	0.49	1.97	26.9	39.6	18.1	.998
	1200	0.81	0.05	0.26	0.50	2.10	27.4	40.6	17.9	.998
	1230	0.83	0.05	0.27	0.52	1.96	27.7	41.1	18.0	.997
	1300	0.78	0.05	0.23	0.51	1.60	27.9	40.4	18.0	.993
	1330	0.73	0.04	0.21	0.48	2.32	28.3	40.0	17.5	.993
	1400	0.66	0.04	0.19	0.44	2.02	28.7	38.8	16.9	.984
	1430	0.58	0.03	0.14	0.41	1.47	28.9	37.8	17.1	.973
	1500	0.49	0.03	0.11	0.35	1.64	29.1	36.1	17.5	.966
	1530	0.39	0.03	0.06	0.31	1.10	28.9	34.5	17.0	.937
	1600	0.28	0.02	--	--	1.33	29.4	32.7	16.9	.873
	1630	0.16	0.02	--	--	1.01	29.4	30.6	17.1	-.373
	1700	0.04	0.01	-0.01	0.04	0.95	28.9	27.6	17.0	-.974
280	700	0.03	-0.00	--	--	0.06	17.8	17.3	--	.766
	1000	0.55	0.03	0.19	0.33	3.16	26.1	33.9	23.6	.996
	1030	0.63	0.03	0.24	0.36	3.37	26.9	35.7	23.2	.993
	1100	0.70	0.04	0.23	0.43	2.89	27.6	38.6	23.3	.996
	1130	0.69	0.04	0.21	0.44	3.22	28.1	38.8	22.8	.997
	1200	0.77	0.04	0.23	0.49	2.99	28.8	40.9	22.2	.996
	1230	0.60	0.04	0.15	0.40	2.55	29.1	38.6	21.9	.996
	1300	0.65	0.04	0.18	0.44	2.81	29.5	39.8	21.1	.997
	1330	0.68	0.04	0.18	0.46	2.72	29.9	39.9	21.0	.998
	1400	0.48	0.03	0.09	0.35	1.80	29.8	37.1	20.9	.988
	1430	0.41	0.03	0.08	0.30	2.70	30.2	36.3	21.0	.994
	1500	0.34	0.03	0.04	0.27	1.96	29.9	34.9	21.6	.974
	1530	0.37	0.03	0.05	0.29	2.43	29.8	34.8	21.7	.975
	1600	0.28	0.03	0.03	0.22	2.19	30.0	33.9	21.8	.936
	1630	0.12	0.02	--	--	2.22	29.7	31.2	21.7	-.919
	1700	0.01	0.01	-0.00	0.01	0.65	28.5	28.0	22.3	-.996
285	830	0.30	-0.01	0.11	0.19	3.55	18.8	--	18.4	.989
	900	0.38	-0.00	0.16	0.22	4.30	19.8	30.1	18.4	.996
	930	0.47	0.00	0.22	0.25	3.93	20.9	26.2	18.7	.996
	1000	0.57	0.01	0.25	0.30	4.23	22.1	28.6	18.6	.996
	1030	0.64	0.01	0.30	0.33	3.57	22.5	30.2	18.9	.999
	1100	0.55	0.01	0.24	0.30	3.93	22.5	29.7	18.8	.996
	1130	0.73	0.02	0.32	0.40	3.95	23.3	33.0	18.4	.998
	1200	0.81	0.02	0.35	0.43	4.02	23.8	34.6	18.3	.998
	1230	0.61	0.01	0.25	0.34	4.00	23.6	32.8	17.8	.997
	1300	0.61	0.01	0.24	0.36	3.53	23.6	32.0	17.0	.996
	1330	0.62	0.01	0.25	0.36	3.69	24.1	32.8	16.9	.999
	1400	0.55	0.01	0.22	0.32	4.07	23.9	31.8	16.6	.995
	1430	0.58	0.01	0.24	0.33	3.72	23.7	31.6	16.4	.996
	1500	0.42	0.00	0.18	0.24	4.06	23.5	29.5	16.4	.994

Day	Time	Net Rad	Soil Heat Flux	Sens Heat Flux	Lat Heat Flux	Wind	Air Temp	Surf Temp	Vap Pres	Prof Corr
	EDT	LY/M	LY/M	LY/M	LY/M	M/S	°C	°C	MB	
285	1530	0.35	-0.00	0.15	0.20	4.58	23.1	27.9	16.2	.993
	1600	0.27	-0.01	0.11	0.17	3.88	22.8	26.7	15.8	.990
	1630	0.12	-0.01	0.04	0.09	3.82	22.2	24.4	15.8	.987
	1700	0.03	-0.01	--	--	3.74	21.2	22.3	16.2	.787
286	730	0.05	-0.02	--	--	2.63	14.8	15.2	--	.029
	800	0.16	-0.01	0.04	0.12	3.29	16.1	17.0	16.0	.982
	830	0.27	-0.01	0.10	0.18	4.83	17.5	19.2	16.6	.994
	900	0.35	-0.00	0.16	0.19	6.03	18.3	21.0	16.7	.996
	930	0.40	-0.00	0.19	0.20	5.51	19.0	22.6	16.7	.999
	1000	0.53	0.01	0.28	0.25	5.03	19.8	25.8	16.6	.996
	1030	0.45	0.00	0.24	0.21	5.37	19.8	25.0	16.1	.998
	1100	0.38	0.00	0.20	0.18	4.70	19.6	24.4	15.9	.998
	1130	0.37	0.00	0.19	0.17	4.54	19.5	24.5	15.7	.997
	1200	0.42	0.00	0.22	0.20	4.20	19.7	25.8	15.6	.997
	1230	0.64	0.01	0.34	0.29	5.36	20.4	28.8	15.8	.998
	1300	0.70	0.01	0.39	0.30	4.95	20.7	30.8	15.8	.999
	1330	0.74	0.01	0.41	0.32	4.92	21.2	31.4	15.8	.998
	1400	0.54	0.01	0.29	0.24	4.28	21.2	29.3	15.8	.998
	1430	0.52	0.01	0.28	0.23	4.91	21.1	28.5	15.7	.997
	1500	0.32	0.00	0.17	0.15	5.02	20.7	25.6	15.6	.996
	1530	0.21	-0.00	0.10	0.11	4.34	20.1	23.8	15.5	.995
	1600	0.19	-0.00	0.10	0.09	4.70	19.8	23.3	15.6	1.000
	1630	0.08	-0.00	0.04	0.05	3.97	19.2	21.5	15.6	.999
	1700	0.02	-0.01	0.01	0.02	3.95	18.5	20.0	15.3	.994
	1730	0.02	-0.01	0.01	0.02	3.65	18.0	19.5	15.3	.992
287	730	0.06	-0.01	0.01	0.06	2.45	16.0	16.8	18.3	.956
	800	0.16	-0.00	0.05	0.11	2.66	17.5	18.8	19.4	.998
	830	0.26	0.00	0.10	0.16	3.32	19.3	21.4	20.7	.993
	900	0.26	0.01	0.11	0.15	3.85	20.7	23.1	21.6	.996
	930	0.31	0.01	0.14	0.16	3.96	21.4	25.0	21.9	.996
	1000	0.29	0.01	0.11	0.16	4.07	22.1	25.5	21.9	.997
	1030	0.47	0.02	0.21	0.24	4.77	22.5	27.2	22.2	.999
	1100	0.70	0.02	0.30	0.38	4.13	22.8	31.8	22.9	.999
	1130	0.41	0.01	0.17	0.22	4.78	22.9	28.2	21.8	1.000
	1200	0.55	0.02	0.23	0.31	4.20	24.0	30.9	21.5	.997
	1230	0.37	0.01	0.13	0.23	4.84	22.8	26.9	22.0	.997
	1300	0.72	0.02	0.37	0.34	5.28	23.8	33.0	22.1	.999
	1330	0.35	0.01	0.16	0.18	5.09	22.3	26.9	22.0	.998
	1400	0.27	0.01	0.10	0.16	4.50	22.2	26.4	21.7	.995
	1430	0.18	0.01	0.05	0.13	3.42	21.4	24.2	21.9	.987
	1500	0.23	0.01	0.09	0.13	4.53	22.6	26.3	21.3	.998
	1530	0.37	0.01	0.18	0.17	5.48	22.9	27.5	20.8	.996

Day	Time	Net Rad	Soil Heat Flux	Sens Heat Flux	Lat Heat Flux	Wind	Air Temp	Surf Temp	Vap Pres	Prof Corr
	EDT	LY/M	LY/M	LY/M	LY/M	M/S	°C	°C	MB	
287	1600	0.22	0.01	0.12	0.10	5.88	22.3	25.6	20.3	.994
	1630	0.11	0.00	0.05	0.05	4.87	21.0	23.2	20.0	.995
	1700	0.06	-0.00	0.03	0.03	4.23	20.3	22.3	19.9	.993
	1730	0.01	-0.00	0.01	0.01	4.09	19.6	21.2	19.6	1.000
288	700	0.02	-0.02	--	--	2.05	13.2	13.5	17.0	.937
	730	0.09	-0.01	--	--	2.87	14.1	15.0	18.0	.502
	800	0.17	-0.01	--	--	3.02	15.3	16.6	18.5	.824
	830	0.26	-0.00	0.06	0.21	3.03	17.2	18.9	18.8	.991
	900	0.37	0.00	0.13	0.23	2.85	18.8	21.8	19.5	.997
	930	0.47	0.01	0.21	0.25	3.33	20.2	25.0	19.7	.997
	1000	0.55	0.02	0.27	0.26	3.11	21.6	28.5	20.0	.998
	1030	0.63	0.02	0.32	0.29	3.71	22.7	31.0	20.1	.999
	1100	0.67	0.02	0.36	0.29	3.44	23.2	33.5	20.1	.999
	1130	0.55	0.02	0.27	0.26	3.09	23.5	32.5	20.1	.999
	1200	0.75	0.03	0.36	0.36	3.14	24.4	36.0	20.0	.998
	1230	0.54	0.03	0.25	0.27	2.74	24.2	33.6	19.6	.997
	1300	0.65	0.03	0.31	0.31	2.90	24.7	35.0	19.4	.996
	1330	0.43	0.03	0.19	0.22	2.88	24.6	31.8	19.7	.996
	1400	0.51	0.02	0.21	0.27	3.36	24.9	32.4	18.7	.997
	1430	0.41	0.02	0.15	0.24	3.28	24.8	31.2	17.7	.992
	1500	0.39	0.02	0.14	0.23	3.30	25.0	30.5	16.8	.991
	1530	0.35	0.02	0.13	0.21	2.93	25.0	30.2	16.1	.989
	1600	0.25	0.01	0.08	0.16	2.76	24.8	28.4	16.0	.987
	1630	0.12	0.01	--	--	2.89	24.3	26.0	15.7	.906
	1700	0.02	0.00	--	--	2.24	23.7	23.8	15.6	-.915
289	730	0.06	-0.02	--	--	0.31	11.8	11.7	--	-.789
	800	0.16	-0.01	--	--	1.65	14.2	14.8	--	-.508
	830	0.26	0.00	--	--	1.26	16.3	17.9	--	-.670
	900	0.36	0.01	--	--	1.52	18.9	21.8	--	-.917
	930	0.45	0.01	--	--	2.43	20.9	25.7	--	-.353
	1200	0.69	0.04	0.29	0.36	1.84	25.6	36.6	13.2	.996
	1230	0.69	0.04	0.28	0.36	1.06	25.8	36.7	13.2	.999
	1300	0.67	0.04	0.26	0.37	1.45	26.3	36.8	13.0	.996
	1330	0.64	0.04	0.24	0.35	1.33	26.8	36.4	12.9	.993
	1400	0.58	0.04	0.24	0.31	1.45	27.3	35.6	13.2	.994
	1430	0.51	0.03	0.20	0.28	1.66	27.5	34.6	13.5	.991
	1500	0.42	0.03	0.18	0.22	0.92	27.5	32.9	13.6	.977
	1530	0.33	0.02	0.13	0.18	0.91	27.7	31.5	13.9	.932
	1600	0.23	0.02	--	--	1.13	27.5	29.6	13.8	.895
	1630	0.11	0.02	--	--	0.40	27.3	27.2	13.7	-.149
	1700	0.02	0.01	-0.01	0.01	0.99	26.5	24.4	14.2	-.975

Day	Time	Net Rad	Soil Heat Flux	Sens Heat Flux	Lat Heat Flux	Wind	Air Temp	Surf Temp	Vap Pres	Prof Corr
	EDT	LY/M	LY/M	LY/M	LY/M	M/S	°C	°C	MB	
290	700	0.01	-0.02	--	--	0.00	10.7	9.3	--	.937
	730	0.07	-0.01	--	--	0.00	12.5	12.3	--	.150
	800	0.15	-0.00	--	--	0.00	15.3	15.6	--	-.523
	830	0.24	0.01	--	--	0.35	18.3	19.7	--	-.826
	900	0.34	0.02	--	--	1.65	21.9	23.9	--	-.569
	930	0.43	0.02	--	--	2.65	23.6	27.5	--	.595
	1000	0.51	0.03	0.24	0.25	2.20	24.6	30.4	13.7	.997
	1030	0.58	0.04	0.25	0.29	1.26	25.5	33.0	14.4	.997
	1100	0.64	0.04	0.28	0.31	2.25	26.3	35.1	14.5	.998
	1130	0.67	0.04	0.32	0.31	2.42	26.5	36.0	15.3	.998
	1200	0.69	0.05	0.34	0.30	1.79	27.0	37.4	16.1	.997
	1230	0.69	0.05	0.34	0.30	1.56	27.4	37.7	16.3	.997
	1300	0.67	0.05	0.34	0.28	1.48	27.7	37.5	16.3	.994
	1330	0.63	0.05	0.31	0.27	1.12	28.2	36.9	16.5	.988
	1400	0.58	0.04	0.30	0.24	1.66	28.4	36.2	16.5	.990
	1430	0.51	0.04	0.23	0.25	1.53	28.6	35.1	16.5	.992
	1500	0.43	0.03	0.20	0.20	1.28	28.7	34.0	16.6	.973
	1530	0.32	0.03	0.12	0.18	0.70	28.7	32.4	16.6	.956
	1600	0.21	0.03	0.04	0.14	1.17	28.6	30.4	16.8	.923
	1630	0.11	0.02	--	--	0.59	28.1	28.4	17.0	.457
	1700	0.02	0.01	--	0.01	0.79	27.5	26.0	17.2	-.980
291	700	0.02	-0.01	--	--	0.00	13.7	13.5	--	1.084
	730	0.04	-0.00	--	--	0.00	15.6	15.7	--	.950
	800	0.06	0.00	--	--	0.06	17.4	17.5	--	.699
	830	0.20	0.01	--	--	1.77	19.2	20.5	--	-.759
	900	0.31	0.02	--	--	2.95	21.7	24.0	--	-.877
	930	0.43	0.03	--	--	3.02	24.3	28.3	--	.078
	1000	0.52	0.03	--	--	4.09	25.7	30.7	--	.602
	1030	0.59	0.03	0.28	0.27	3.55	26.8	33.2	19.3	.998
	1100	0.62	0.04	0.28	0.30	3.88	27.8	34.9	19.5	.998
	1130	0.44	0.03	0.16	0.24	4.11	27.6	32.3	19.3	.997
	1200	0.68	0.04	0.27	0.38	4.79	28.7	36.9	18.8	.997
	1230	0.50	0.04	0.18	0.28	4.05	28.6	34.5	18.0	.997
	1300	0.46	0.04	0.16	0.26	3.81	28.7	34.5	18.8	.999
	1330	0.63	0.04	0.24	0.36	4.88	29.1	35.9	18.6	.996
	1400	0.49	0.04	0.19	0.26	4.33	29.2	34.8	18.6	.999
	1430	0.48	0.03	0.21	0.24	4.72	29.3	34.5	18.7	.992
	1500	0.41	0.03	0.18	0.19	4.62	29.4	33.8	18.8	.998
	1530	0.29	0.03	0.12	0.15	4.21	28.5	31.1	18.8	.989
	1600	0.20	0.02	0.07	0.11	4.62	28.2	29.9	19.1	.995
	1630	0.11	0.02	0.02	0.07	3.99	27.6	28.3	19.5	.955
	1700	0.02	0.01	--	--	3.33	26.7	26.2	19.9	-.877

Day	Time	Net Rad	Soil Heat Flux	Sens Heat Flux	Lat Heat Flux	Wind	Air Temp	Surf Temp	Vap Pres	Prof Corr
	EDT	LY/M	LY/M	LY/M	LY/M	M/S	°C	°C	MB	
293	700	0.02	-0.04	--	--	1.10	6.0	3.8	--	.919
	730	0.11	-0.02	--	--	2.42	9.6	9.6	--	.808
	800	0.17	-0.01	--	--	2.36	11.5	11.7	--	-.767
	830	0.27	-0.00	--	--	2.76	14.0	15.6	--	-.557
	900	0.37	0.01	0.22	0.13	2.60	16.8	20.6	10.3	.999
	930	0.45	0.02	0.28	0.16	3.06	19.2	24.9	11.2	.999
	1000	0.53	0.03	0.30	0.20	3.59	21.3	27.9	12.2	1.000
	1030	0.59	0.03	0.31	0.25	3.69	22.5	30.2	12.9	.997
	1100	0.65	0.04	0.33	0.28	4.45	23.5	31.9	12.9	.998
	1130	0.70	0.04	0.39	0.27	5.38	24.0	32.9	12.8	.998
	1200	0.45	0.03	0.22	0.20	4.61	23.9	30.6	13.0	.998
	1230	0.37	0.03	0.15	0.19	4.68	23.8	28.4	13.0	.997
	1300	0.51	0.03	0.24	0.24	4.99	24.6	31.1	13.3	.999
	1330	0.63	0.04	0.29	0.31	3.75	25.3	33.5	13.0	.994
	1400	0.48	0.03	0.24	0.21	4.43	25.2	31.8	12.9	.995
	1430	0.43	0.02	0.19	0.22	5.33	24.8	29.4	13.4	.995
	1500	0.15	0.02	0.04	0.09	4.91	23.8	25.6	13.7	.996
	1530	0.24	0.02	0.09	0.14	5.23	24.3	26.9	13.6	.993
	1600	0.15	0.01	0.03	0.11	4.22	23.8	25.1	13.6	.941
	1630	0.08	0.01	--	--	3.59	23.3	24.0	13.9	.916
	1700	0.02	0.01	--	--	4.20	22.8	22.8	13.8	-.861
294	700	-0.01	-0.02	--	--	1.31	12.1	10.5	--	.855
	730	0.08	-0.01	--	--	1.67	13.4	14.0	--	-.415
	800	0.11	-0.00	--	--	1.42	14.8	15.9	--	-.704
	830	0.29	0.01	--	--	2.00	17.2	19.4	--	-.769
	900	0.35	0.01	--	--	2.53	19.5	22.6	--	-.796
	930	0.44	0.02	--	--	2.52	21.9	26.9	19.6	-.168
	1000	0.52	0.03	0.24	0.25	2.82	23.8	30.1	17.3	.995
	1030	0.58	0.03	0.28	0.27	3.79	24.9	32.2	17.3	.999
	1100	0.55	0.03	0.24	0.27	4.28	25.8	32.5	16.7	.999
	1130	0.55	0.03	0.23	0.29	4.29	26.3	33.3	16.2	.999
	1200	0.57	0.04	0.26	0.28	4.60	26.4	34.5	16.2	.999
	1230	0.50	0.03	0.22	0.26	4.40	26.3	32.9	16.5	.999
	1300	0.51	0.03	0.20	0.27	4.71	26.7	33.2	17.1	.998
	1330	0.51	0.03	0.21	0.26	4.64	27.1	33.3	17.5	.999
	1400	0.30	0.03	0.10	0.18	3.95	26.8	30.8	17.4	.995
	1430	0.47	0.03	0.17	0.27	4.57	27.2	32.3	17.4	.992
	1500	0.32	0.03	0.12	0.18	4.97	27.1	30.6	17.3	.995
	1530	0.32	0.02	0.12	0.18	5.11	27.1	30.3	17.4	.993
	1600	0.27	0.02	0.09	0.16	4.99	27.1	29.7	17.4	.991
	1630	0.10	0.02	0.02	0.06	4.43	26.1	26.8	17.3	.961
	1700	0.01	0.01	0.00	0.00	3.99	25.1	24.8	17.2	-.970

Day	Time	Net Rad	Soil Heat Flux	Sens Heat Flux	Lat Heat Flux	Wind	Air Temp	Surf Temp	Vap Pres	Prof Corr
	EDT	LY/M	LY/M	LY/M	LY/M	M/S	°C	°C	MB	
295	700	0.02	-0.00	--	--	0.50	17.7	16.9	--	.893
	730	0.08	0.00	--	--	1.19	18.8	19.7	--	-.016
	800	0.17	0.01	--	--	2.03	20.3	21.4	--	-.469
	830	0.17	0.01	--	--	1.54	21.7	22.5	--	-.684
	900	0.16	0.01	--	--	1.45	22.8	23.6	--	.226
	930	0.28	0.02	0.07	0.19	1.87	24.2	26.5	22.8	.984
	1000	0.46	0.03	0.17	0.27	2.37	25.8	30.6	22.3	.992
	1030	0.55	0.03	0.25	0.28	3.24	26.8	33.4	21.2	.997
	1100	0.51	0.03	0.23	0.25	2.65	27.1	34.3	20.8	.998
	1130	0.23	0.02	0.07	0.14	2.13	26.7	29.7	20.4	.991
	1200	0.74	0.04	0.31	0.38	2.79	28.0	38.3	20.2	.997
	1230	0.67	0.04	0.29	0.34	3.17	28.4	38.6	20.3	.998
	1300	0.71	0.04	0.30	0.36	3.63	28.7	38.9	19.8	.997
	1330	0.65	0.04	0.26	0.35	3.00	29.1	38.4	19.1	.996
	1400	0.57	0.04	0.23	0.30	3.50	29.0	36.6	19.4	.996
	1430	0.54	0.03	0.22	0.29	3.38	29.2	36.4	19.4	.995
	1500	0.45	0.03	0.18	0.24	4.08	29.1	34.8	18.7	.993
	1530	0.33	0.02	0.13	0.18	3.89	28.9	32.7	18.1	.993
	1600	0.23	0.02	0.06	0.14	3.51	28.7	31.0	18.1	.978
	1630	0.11	0.02	0.02	0.08	4.01	27.9	28.6	17.9	.913
	1700	0.02	0.01	-0.00	0.00	3.00	27.2	26.4	17.9	-.969
296	700	0.01	-0.02	--	--	0.00	14.1	13.1	--	.890
	730	0.05	-0.01	--	--	0.00	15.1	15.2	--	-.034
	800	0.13	0.00	--	--	0.51	17.5	18.3	--	-.691
	830	0.24	0.01	--	--	0.26	19.4	21.6	--	-.844
	900	0.34	0.02	--	--	0.26	21.2	25.3	--	-.946
	930	0.43	0.03	--	--	0.83	23.9	29.3	--	-.610
	1000	0.51	0.03	0.22	0.26	1.28	25.7	32.0	21.7	.953
	1030	0.56	0.04	0.24	0.29	1.07	26.9	34.8	20.6	.994
	1100	0.63	0.04	0.26	0.32	1.06	27.8	36.4	20.2	.990
	1130	0.48	0.04	0.18	0.27	0.87	28.3	35.4	19.4	.993
	1200	0.65	0.04	0.23	0.38	1.31	28.9	38.2	18.7	.994
	1230	0.75	0.05	0.28	0.42	0.84	29.5	40.7	18.2	.996
	1300	0.55	0.04	0.19	0.32	2.27	29.6	37.8	17.0	.996
	1330	0.72	0.05	0.27	0.40	1.95	30.4	40.7	16.9	.998
	1400	0.62	0.04	0.22	0.35	2.61	30.6	39.5	16.9	.997
	1430	0.30	0.03	0.07	0.20	1.11	29.5	34.0	17.6	.991
	1500	0.21	0.03	0.03	0.15	1.17	29.0	31.8	17.4	.976
	1530	0.17	0.03	0.01	0.13	1.27	29.1	31.1	17.5	.947
	1600	0.19	0.03	0.02	0.15	1.39	29.1	31.1	18.1	.924
	1630	0.06	0.02	-0.01	0.04	1.42	28.5	28.4	18.0	-.979
	1700	0.00	0.01	-0.01	0.02	0.15	27.4	16.1	19.4	-.998

Day	Time	Net Rad	Soil Heat Flux	Sens Heat Flux	Lat Heat Flux	Wind	Air Temp	Surf Temp	Vap Pres	Prof Corr
	EDT	LY/M	LY/M	LY/M	LY/M	M/S	°C	°C	MB	
301	900	0.19	-0.01	0.08	0.11	1.87	16.8	19.1	14.6	.999
	930	0.25	0.00	0.11	0.14	2.11	17.7	20.9	14.8	.997
	1000	0.29	0.00	0.14	0.15	1.82	18.8	22.9	15.1	.996
	1030	0.37	0.01	0.18	0.18	1.58	20.2	25.5	15.8	.994
	1100	0.51	0.02	0.25	0.24	1.88	21.9	28.6	16.8	.995
	1130	0.61	0.02	0.33	0.26	1.95	23.2	32.3	18.2	.998
	1200	0.67	0.03	0.34	0.30	1.66	24.2	34.7	19.7	.996
	1230	0.67	0.03	0.35	0.29	2.24	24.6	34.6	19.7	.997
	1300	0.67	0.03	0.34	0.30	2.23	25.3	35.1	20.2	.997
	1330	0.60	0.02	0.30	0.28	1.89	25.3	34.3	19.9	.996
	1400	0.56	0.02	0.28	0.26	2.23	25.7	33.9	19.8	.996
	1430	0.48	0.01	0.24	0.23	2.25	25.9	33.0	19.8	.994
	1500	0.40	0.01	0.19	0.20	1.72	25.9	31.7	19.6	.987
	1530	0.30	0.01	0.14	0.15	2.03	26.1	30.3	19.8	.986
	1600	0.19	0.01	0.08	0.11	2.22	25.8	28.4	19.8	.976
	1630	0.09	0.00	0.02	0.06	2.01	25.3	26.3	20.0	.947
	1700	-0.01	-0.00	-0.00	0.01	1.32	24.6	23.8	19.9	-.890
302	730	0.05	-0.01	--	--	1.99	16.1	16.7	--	.024
	800	0.06	-0.01	--	--	1.89	16.6	17.4	--	-.921
	830	0.18	-0.00	--	--	2.35	17.8	19.5	--	-.704
	900	0.20	0.00	--	--	2.59	18.6	20.3	--	-.682
	930	0.25	0.01	--	--	2.32	19.8	21.9	--	-.898
	1000	0.31	0.01	--	--	2.47	21.2	24.0	--	-.868
	1030	0.49	0.02	--	--	3.09	22.9	28.2	--	-.607
	1100	0.48	0.02	--	--	3.47	24.2	29.9	--	.897
	1130	0.33	0.02	0.15	0.17	3.30	24.4	28.4	21.3	.991
	1200	0.47	0.02	0.22	0.23	3.41	25.1	30.9	21.6	.997
	1230	0.67	0.03	0.32	0.31	3.52	26.0	35.3	21.4	.998
	1300	0.67	0.03	0.32	0.32	3.64	26.8	35.7	21.1	.996
	1330	0.42	0.02	0.19	0.22	3.70	26.6	32.2	20.6	.995
	1400	0.23	0.01	0.09	0.13	3.69	26.2	29.3	20.4	.997
	1430	0.22	0.01	0.07	0.14	3.50	26.0	28.6	20.3	.991
	1500	0.18	0.01	0.06	0.12	3.33	26.1	28.5	20.3	.992
	1530	0.19	0.01	0.07	0.11	4.44	25.8	28.1	20.5	.998
	1600	0.08	0.00	0.03	0.05	4.75	24.9	26.0	20.7	.991
	1630	0.10	0.00	0.03	0.07	4.58	24.7	25.8	20.3	.964
	1700	-0.01	-0.00	--	--	4.85	23.8	23.8	20.1	-.898
303	730	0.02	-0.00	0.01	0.02	4.78	20.4	20.9	21.8	.995
	800	0.02	-0.00	0.01	0.01	4.36	20.4	21.0	22.0	1.029
	830	0.04	-0.00	--	--	3.62	20.6	21.4	22.3	-.749
	900	0.09	0.00	0.04	0.04	4.41	21.0	22.2	22.6	1.009
	930	0.11	0.00	0.06	0.05	4.03	21.3	23.0	22.8	.971
	1000	0.10	0.00	0.06	0.04	3.94	21.4	23.0	22.9	.991
	1030	0.20	0.01	0.11	0.09	4.29	22.1	24.6	23.2	.988
	1100	0.29	0.01	--	--	4.64	22.9	26.4	23.4	-.047

Day	Time	Net Rad	Soil Heat Flux	Sens Heat Flux	Lat Heat Flux	Wind	Air Temp	Surf Temp	Vap Pres	Prof Corr
	EDT	LY/M	LY/M	LY/M	LY/M	M/S	°C	°C	MB	
303	1200	0.19	0.01	0.10	0.07	4.72	23.1	25.8	23.5	.988
	1230	0.19	0.01	0.11	0.07	5.69	22.7	25.3	23.5	.987
	1300	0.24	0.01	0.14	0.09	5.11	22.4	25.9	23.6	.990
	1330	0.13	0.00	0.08	0.04	5.09	22.1	24.5	23.3	.990
	1400	0.09	0.00	0.04	0.06	4.96	21.0	22.4	23.2	.993
	1430	0.16	0.00	0.05	0.11	4.63	20.9	22.8	23.5	.999
	1500	0.08	0.00	0.02	0.06	4.90	20.7	22.0	23.2	1.001
	1530	0.06	-0.00	0.01	0.05	3.79	20.4	21.5	22.9	1.005
	1600	0.06	-0.00	0.01	0.05	3.72	20.6	21.6	22.4	.920
	1630	0.05	-0.00	--	--	5.84	21.1	22.1	21.9	.846
	1700	0.01	-0.00	--	--	5.47	21.0	21.7	21.4	.803
304	730	0.02	-0.01	0.01	0.01	5.47	17.2	17.9	19.0	.967
	800	0.04	-0.01	0.03	0.02	5.36	17.4	18.2	19.0	.963
	830	0.09	-0.01	0.06	0.04	5.49	17.9	19.0	19.0	.991
	900	0.14	-0.00	0.09	0.06	6.13	18.2	19.8	19.3	1.003
	930	0.22	-0.00	0.13	0.08	7.10	18.7	21.0	19.3	1.001
	1000	0.21	-0.00	0.16	0.05	7.40	18.7	21.2	19.3	.973
	1030	0.15	-0.00	0.10	0.04	6.30	18.1	20.1	19.5	.965
	1100	0.11	-0.00	0.04	0.07	6.02	17.4	18.5	19.8	.993
	1130	0.09	-0.01	0.03	0.07	5.34	17.4	18.5	19.8	.995
	1200	0.11	-0.00	0.05	0.07	6.06	17.7	18.9	20.2	.979
	1230	0.11	-0.00	0.04	0.08	5.55	17.9	19.1	20.1	.959
	1300	0.13	-0.00	0.05	0.08	5.98	18.4	19.7	20.1	.993
	1330	0.15	-0.00	0.06	0.08	6.15	19.1	20.3	20.2	.975
	1400	0.12	-0.00	0.06	0.06	5.97	19.6	20.6	20.3	.994
	1430	0.10	-0.00	0.05	0.05	6.03	19.7	20.8	20.3	.979
	1500	0.07	-0.00	0.03	0.04	5.59	19.7	20.6	20.2	.992
	1530	0.06	-0.00	0.03	0.04	5.85	19.8	20.7	20.1	.975
	1600	0.06	-0.00	0.03	0.04	5.83	19.9	20.6	19.9	1.003
	1630	0.04	-0.00	0.02	0.03	5.62	19.9	20.6	19.8	.988
	1700	0.02	-0.00	0.01	0.02	6.33	19.8	20.3	19.6	.993
305	730	0.01	-0.01	--	--	3.55	18.2	18.5	20.8	.354
	800	0.04	-0.00	0.02	0.02	3.97	18.5	19.1	20.9	1.032
	830	0.09	-0.00	0.05	0.04	4.39	18.6	19.8	21.1	.992
	900	0.05	-0.01	0.02	0.03	3.06	17.8	18.4	21.2	.983
	930	0.05	-0.01	0.03	0.03	2.12	17.8	18.7	21.3	.989
	1000	0.08	-0.01	0.03	0.05	4.16	17.8	18.8	21.2	.993
	1030	0.10	-0.01	0.04	0.07	3.71	17.9	19.1	21.3	.999
	1100	0.10	-0.01	0.04	0.07	3.24	18.0	19.1	21.3	.996
	1130	0.14	-0.00	0.05	0.09	4.00	18.3	19.6	21.5	.992
	1200	0.17	-0.00	0.07	0.10	4.92	18.7	19.9	21.8	.996
	1230	0.28	0.00	0.12	0.16	4.79	19.4	21.5	22.3	.998
	1300	0.43	0.01	0.20	0.22	5.16	20.8	23.8	23.0	.995
	1330	0.35	0.00	0.17	0.17	5.66	20.9	23.3	22.5	.991

Day	Time	Net Rad	Soil Heat Flux	Sens Heat Flux	Lat Heat Flux	Wind	Air Temp	Surf Temp	Vap Pres	Prof Corr
	EDT	LY/M	LY/M	LY/M	LY/M	M/S	°C	°C	MB	
305	1400	0.25	0.00	0.13	0.02	5.14	20.9	22.9	22.4	.992
	1430	0.14	-0.00	0.07	0.07	5.44	20.5	21.8	22.2	.978
	1500	0.11	-0.00	0.05	0.06	5.49	19.8	20.6	22.3	.981
	1530	0.12	-0.00	0.04	0.08	4.62	19.3	20.4	22.5	.994
	1600	0.12	-0.00	0.04	0.09	5.12	19.2	20.3	22.2	.994
	1630	0.07	-0.01	0.03	0.05	4.40	19.0	19.9	22.2	.978
	1700	0.04	-0.01	0.01	0.03	3.69	19.0	19.7	22.0	.993
	1730	0.01	-0.01	0.00	0.02	3.43	18.7	19.2	20.4	.916
306	730	0.02	-0.01	0.00	0.02	2.91	18.0	18.4	19.9	.976
	800	0.08	-0.01	0.02	0.07	2.78	18.3	19.3	20.1	.988
	830	0.17	-0.00	0.05	0.12	3.12	18.9	20.3	20.2	.994
	900	0.29	0.00	0.10	0.19	3.23	20.1	22.3	20.3	.997
	930	0.40	0.01	0.15	0.24	3.19	21.4	24.7	20.5	.998
	1000	0.50	0.01	0.19	0.30	3.82	22.7	26.3	20.3	.996
	1030	0.57	0.01	0.23	0.32	4.45	23.8	28.5	19.9	.996
	1100	0.63	0.02	0.28	0.34	4.41	24.8	30.2	20.2	.999
	1130	0.64	0.02	0.29	0.33	6.26	25.3	30.8	20.0	.998
	1200	0.36	0.01	0.15	0.20	5.44	23.8	26.7	20.7	.998
	1230	0.67	0.02	0.27	0.38	4.27	24.5	32.2	21.6	1.000
	1300	0.63	0.02	0.29	0.32	5.74	25.8	32.3	20.5	.996
	1330	0.53	0.02	0.26	0.25	5.47	25.7	31.1	20.4	.994
	1400	0.26	0.01	0.12	0.12	5.07	25.0	27.6	20.7	.997
	1430	0.25	0.00	-0.02	0.26	3.84	23.3	23.7	21.1	-.948
	1500	0.30	0.00	0.06	0.23	5.72	23.4	24.4	21.1	.999
	1530	0.10	-0.01	0.01	0.10	3.32	19.9	21.0	21.0	.987
	1600	0.14	0.00	0.02	0.11	2.73	20.7	22.2	22.0	.988
	1630	0.08	-0.01	--	--	4.75	20.8	21.0	20.7	-.879
	1700	0.02	-0.01	-0.01	0.04	2.66	20.9	20.6	19.9	-.982
307	730	0.03	-0.01	--	--	2.38	17.9	18.2	--	-.921
	800	0.08	-0.00	--	--	2.46	18.1	19.1	--	-.329
	830	0.19	0.00	--	--	2.43	19.0	20.6	--	-.731
	900	0.29	0.01	--	--	3.14	20.9	22.9	--	-.979
	930	0.39	0.01	--	--	4.10	23.0	25.1	--	-.407
	1000	0.50	0.02	0.17	0.31	4.19	24.1	27.1	20.1	.999
	1030	0.58	0.02	0.22	0.34	5.71	24.9	28.9	19.1	.996
	1100	0.48	0.01	0.18	0.29	5.60	25.0	27.9	17.7	.995
	1130	0.57	0.02	0.23	0.32	4.80	25.7	30.4	17.3	.998
	1200	0.63	0.02	0.27	0.34	5.06	26.2	32.4	17.4	.998
	1230	0.51	0.02	0.21	0.28	5.12	26.4	31.2	18.0	.996
	1300	0.44	0.02	0.18	0.25	4.80	26.2	30.5	18.2	.997
	1330	0.48	0.02	0.20	0.26	3.90	26.4	31.6	18.5	.999
	1400	0.38	0.02	0.19	0.17	4.74	25.8	29.9	19.5	.999
	1430	0.18	0.01	0.07	0.10	3.34	25.0	27.1	19.8	.995
	1500	0.13	0.01	0.05	0.07	2.44	24.5	26.4	19.5	.997

Day	Time	Net Rad	Soil Heat Flux	Sens Heat Flux	Lat Heat Flux	Wind	Air Temp	Surf Temp	Vap Pres	Prof Corr
	EDT	LY/M	LY/M	LY/M	LY/M	M/S	°C	°C	MB	
307	1530	0.09	0.01	0.03	0.06	2.62	24.1	25.5	19.8	.991
	1600	0.06	-0.00	0.02	0.04	3.04	23.4	24.2	18.3	.988
	1630	0.03	-0.00	0.00	0.03	2.00	23.2	23.7	18.4	.954
	1700	0.02	-0.00	-0.00	0.02	2.64	23.1	23.2	18.6	-1.022
308	730	0.01	-0.00	--	--	1.92	19.8	20.0	22.5	-.359
	800	0.06	-0.00	--	--	2.34	20.0	20.7	22.9	.846
	830	0.14	0.00	0.04	0.10	3.19	20.4	21.6	23.1	.999
	900	0.28	0.01	0.07	0.20	2.58	21.4	23.6	23.6	.996
	930	0.43	0.02	0.13	0.28	2.96	22.8	25.9	24.1	.997
	1000	0.40	0.02	0.13	0.25	2.45	23.6	26.8	24.1	.989
	1030	0.57	0.02	0.19	0.35	3.69	25.5	29.7	23.4	.992
	1100	0.55	0.02	0.21	0.32	4.37	25.6	29.3	22.0	.996
	1130	0.51	0.02	0.21	0.29	3.70	26.0	30.0	21.8	.996
	1200	0.44	0.02	0.16	0.26	3.15	26.2	30.0	21.4	.996
	1230	0.46	0.02	0.17	0.27	3.01	26.6	31.4	20.9	.993
	1300	0.31	0.02	0.11	0.19	3.40	26.4	29.0	20.3	.994
	1330	0.34	0.02	0.12	0.20	2.73	26.7	29.9	20.9	.996
	1400	0.28	0.02	0.11	0.15	3.68	26.3	29.3	21.9	.998
	1430	0.22	0.01	0.09	0.12	3.57	25.8	28.4	22.5	.994
	1500	0.11	0.01	0.04	0.06	4.30	24.8	26.3	22.7	.985
	1530	0.10	0.01	0.04	0.05	4.22	24.1	25.6	23.4	.992
	1600	0.05	0.00	0.02	0.03	3.61	23.5	24.8	23.7	.967
	1630	0.03	0.00	0.01	0.02	3.88	22.8	23.7	23.5	1.000
309	800	0.03	-0.00	0.01	0.02	2.67	20.3	20.7	23.2	1.039
	830	0.02	-0.00	0.01	0.02	2.51	20.6	21.0	23.6	1.024
	900	0.03	-0.00	0.01	0.03	2.16	20.8	21.2	23.7	.940
	930	0.05	-0.00	0.01	0.03	2.61	20.9	21.3	23.9	.983
	1000	0.05	0.00	0.01	0.04	2.62	21.1	21.5	24.2	.993
	1030	0.02	-0.00	0.00	0.01	2.96	21.1	21.2	24.0	.860
	1100	0.02	-0.00	0.00	0.02	2.50	20.8	20.9	23.6	.870
	1130	0.01	-0.00	--	--	2.36	20.7	20.7	23.5	.594
	1200	0.02	-0.00	0.00	0.02	2.16	20.8	20.8	23.5	.957
	1230	0.03	-0.00	0.01	0.03	2.63	20.8	20.9	23.6	.900
	1300	0.02	-0.00	0.00	0.02	3.29	20.9	21.1	23.9	1.010
	1330	0.03	-0.00	0.01	0.03	3.57	21.0	21.1	23.9	.926
	1400	0.02	-0.00	0.00	0.02	2.70	20.9	21.2	23.8	.899
	1430	0.02	-0.00	0.00	0.02	3.63	20.8	21.0	23.7	1.161
	1500	0.07	-0.00	0.02	0.05	3.62	20.7	21.2	23.5	.995
	1530	0.07	-0.00	0.01	0.06	4.06	20.5	21.1	23.3	.985
	1600	0.05	-0.00	0.01	0.04	3.31	20.3	20.9	22.8	1.013
	1630	0.10	-0.00	0.02	0.08	2.95	20.5	21.2	22.9	1.003
	1700	0.03	-0.00	0.01	0.03	3.11	20.3	20.7	22.7	.979

Day	Time	Net Rad	Soil Heat Flux	Sens Heat Flux	Lat Heat Flux	Wind	Air Temp	Surf Temp	Vap Pres	Prof Corr
	EDT	LY/M	LY/M	LY/M	LY/M	M/S	°C	°C	MB	
310	730	0.02	-0.01	--	--	1.93	18.1	18.3	19.5	.791
	800	0.05	-0.01	0.01	0.05	1.50	18.4	18.9	19.7	.981
	830	0.11	-0.00	0.02	0.10	2.61	18.9	19.6	19.8	1.000
	900	0.18	-0.00	0.03	0.15	3.46	19.3	20.1	19.4	1.001
	930	0.37	-0.00	0.09	0.28	4.00	20.0	22.0	18.9	.997
	1000	0.46	0.00	0.14	0.31	3.29	20.8	23.6	18.5	.999
	1030	0.55	0.01	0.19	0.35	3.38	21.6	25.9	18.2	.998
	1100	0.63	0.01	0.24	0.38	3.36	22.3	27.0	17.4	.997
	1130	0.66	0.01	0.26	0.39	3.78	23.0	28.9	16.6	.998
	1200	0.68	0.01	0.29	0.38	3.73	23.4	30.0	15.8	.998
	1230	0.68	0.01	0.30	0.37	4.22	23.5	30.3	15.0	.997
	1300	0.66	0.01	0.29	0.36	4.16	24.0	31.0	14.8	.996
	1330	0.59	0.01	0.26	0.32	4.14	24.0	30.0	13.2	.993
	1400	0.56	0.00	0.26	0.30	4.05	24.0	29.8	12.4	.996
	1430	0.48	-0.00	0.22	0.26	4.04	23.9	28.9	11.6	.995
	1500	0.39	-0.01	0.17	0.23	4.47	23.7	27.4	10.5	.994
	1530	0.29	-0.01	0.12	0.17	3.59	23.5	26.0	10.6	.997
	1600	0.17	-0.01	0.06	0.12	3.33	23.1	24.2	11.1	.992
	1630	0.06	-0.01	--	--	2.34	22.6	22.2	11.1	.150
311	730	0.05	-0.04	--	--	0.02	6.1	6.2	--	-.913
	800	0.14	-0.03	--	--	0.61	9.1	9.4	--	.249
	830	0.19	-0.02	--	--	2.31	11.7	11.6	--	.782
	900	0.31	-0.02	0.07	0.26	3.83	12.8	13.5	8.2	.971
	930	0.40	-0.01	0.18	0.23	3.65	13.9	16.7	7.7	.998
	1000	0.48	-0.01	0.30	0.18	3.44	15.0	19.5	7.5	.999
	1030	0.53	-0.00	0.37	0.17	2.68	15.8	23.1	7.5	.999
	1100	0.59	0.00	0.39	0.20	1.66	16.6	24.6	7.6	.999
	1130	0.62	0.01	0.40	0.22	2.03	17.5	26.9	7.6	.999
	1200	0.64	0.01	0.41	0.21	1.35	17.9	28.5	7.5	.999
	1230	0.63	0.01	0.41	0.21	1.18	18.6	29.2	7.5	.998
	1300	0.62	0.01	0.39	0.22	1.62	19.3	29.3	7.6	.999
	1330	0.58	0.01	0.35	0.22	1.61	19.7	29.0	7.7	.999
	1400	0.52	0.00	0.31	0.21	1.88	20.6	28.5	7.8	.999
	1430	0.45	0.00	0.25	0.19	1.93	21.1	27.6	7.8	.999
	1500	0.36	-0.00	0.20	0.16	2.07	21.3	26.3	7.6	.997
	1530	0.26	-0.00	0.14	0.13	1.75	21.4	24.7	7.6	.992
	1600	0.15	-0.00	0.07	0.09	1.44	21.2	22.6	7.6	.973
	1630	0.04	-0.01	--	--	1.58	20.5	20.0	7.6	.617
312	730	0.06	-0.03	--	--	0.00	3.9	4.5	--	.549
	800	0.15	-0.02	--	--	0.00	7.2	7.9	--	-.648
	830	0.20	-0.00	--	--	0.04	11.1	12.1	--	-.611
	900	0.30	0.01	--	--	1.37	14.7	16.0	--	-.593
	930	0.39	0.02	--	--	1.16	17.5	19.8	--	-.669
	1000	0.45	0.02	--	--	1.37	19.1	23.2	--	-.837

Day	Time	Net Rad	Soil Heat Flux	Sens Heat Flux	Lat Heat Flux	Wind	Air Temp	Surf Temp	Vap Pres	Prof Corr
	EDT	LY/M	LY/M	LY/M	LY/M	M/S	°C	°C	MB	
312	1030	0.51	0.02	--	--	2.23	20.1	26.5	--	-.491
	1100	0.58	0.03	--	--	1.86	20.7	27.7	--	.520
	1130	0.62	0.03	0.35	0.24	2.22	21.5	30.2	12.1	.999
	1200	0.64	0.03	0.36	0.25	2.86	21.9	31.4	11.9	.998
	1230	0.64	0.03	0.36	0.25	2.87	22.5	32.2	11.9	.999
	1300	0.62	0.03	0.35	0.25	2.80	23.0	32.4	12.2	.996
	1330	0.59	0.02	0.32	0.25	2.94	23.5	31.7	11.7	.994
	1400	0.53	0.02	0.21	0.29	2.46	23.8	31.2	11.1	.904
	1430	0.46	0.01	0.24	0.20	2.33	24.1	23.9	11.9	.991
	1500	0.36	0.01	0.19	0.17	2.47	24.3	28.6	12.4	.989
	1530	0.27	0.01	0.13	0.13	2.17	24.4	27.0	12.0	.981
	1600	0.15	0.01	0.06	0.09	1.66	24.2	24.9	11.8	.969
	1630	0.03	0.00	--	--	0.83	23.8	22.1	12.3	.300

APPENDIX D

SUPPLEMENTARY FIGURES

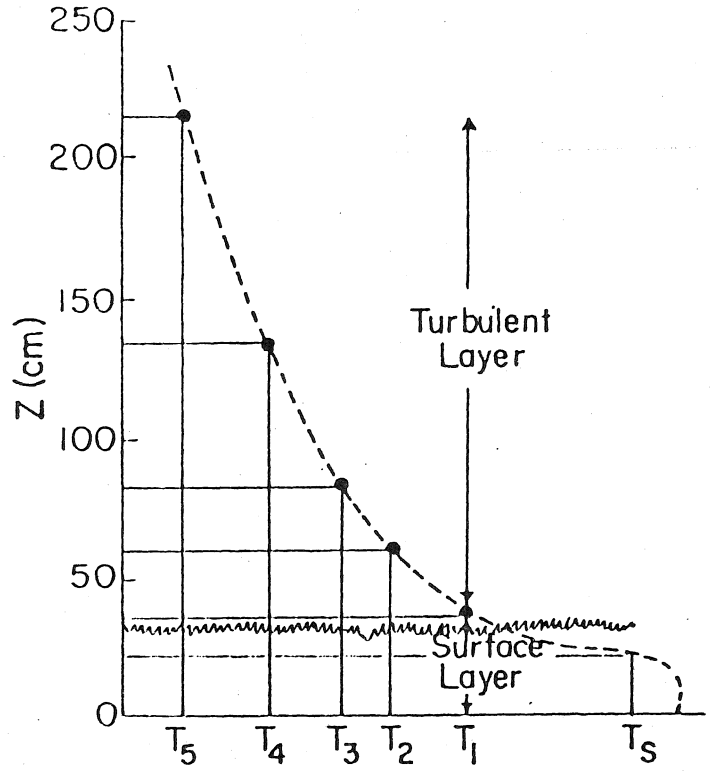

Figure 1. Hypothetical Daytime Temperature Profile. The various levels at which temperature measurements for the Bowen ratio calculation were made is also shown, as surfact temperature is plotted at an arbitrary height within the canopy.

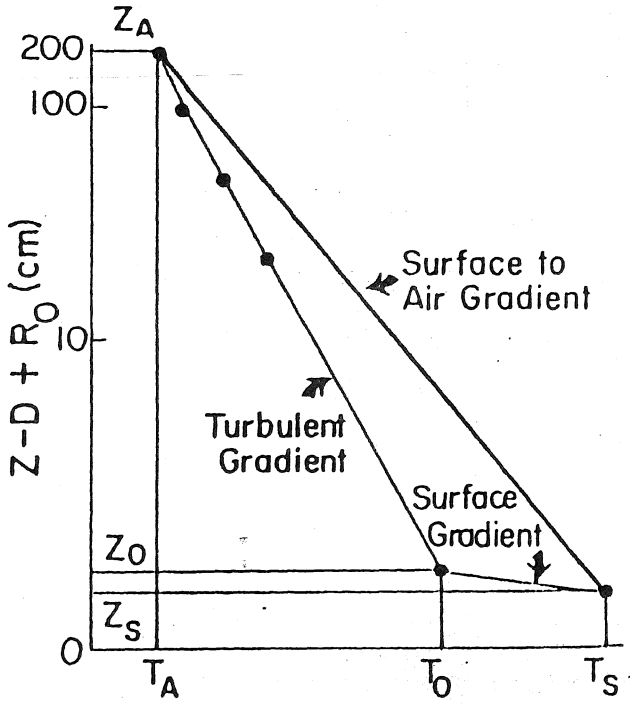

Figure 2. Simplified Temperature Profile. T_A is the air temperature measured at level 5 in the profile, T_0 is the temperature at the surface/turbulent layer interface and T_S is the radiation temperature. The displacement height (D) is 35 cm, and the roughness height (R_0) is 1 cm.

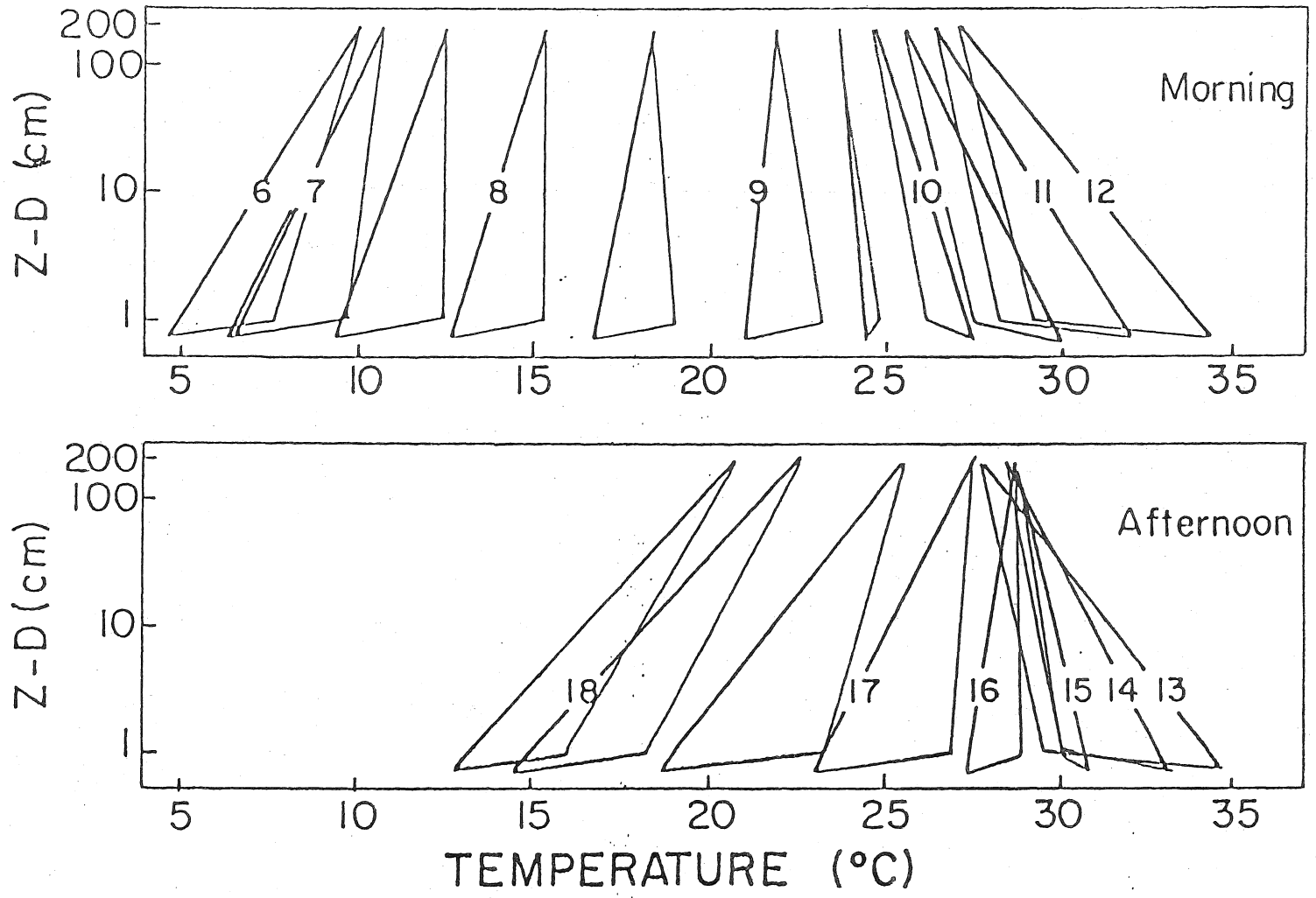

Figure 3. Simplified Temperature Profiles for a Clear Day. Temperature gradients are represented as in Fig. 2. The heavy lines are the average surface-to-air temperature gradients measured on October 17, 1981. They are labeled with the true solar time at the end of the half-hour period in which they were collected. The turbulent and surface segments are shown in light lines.

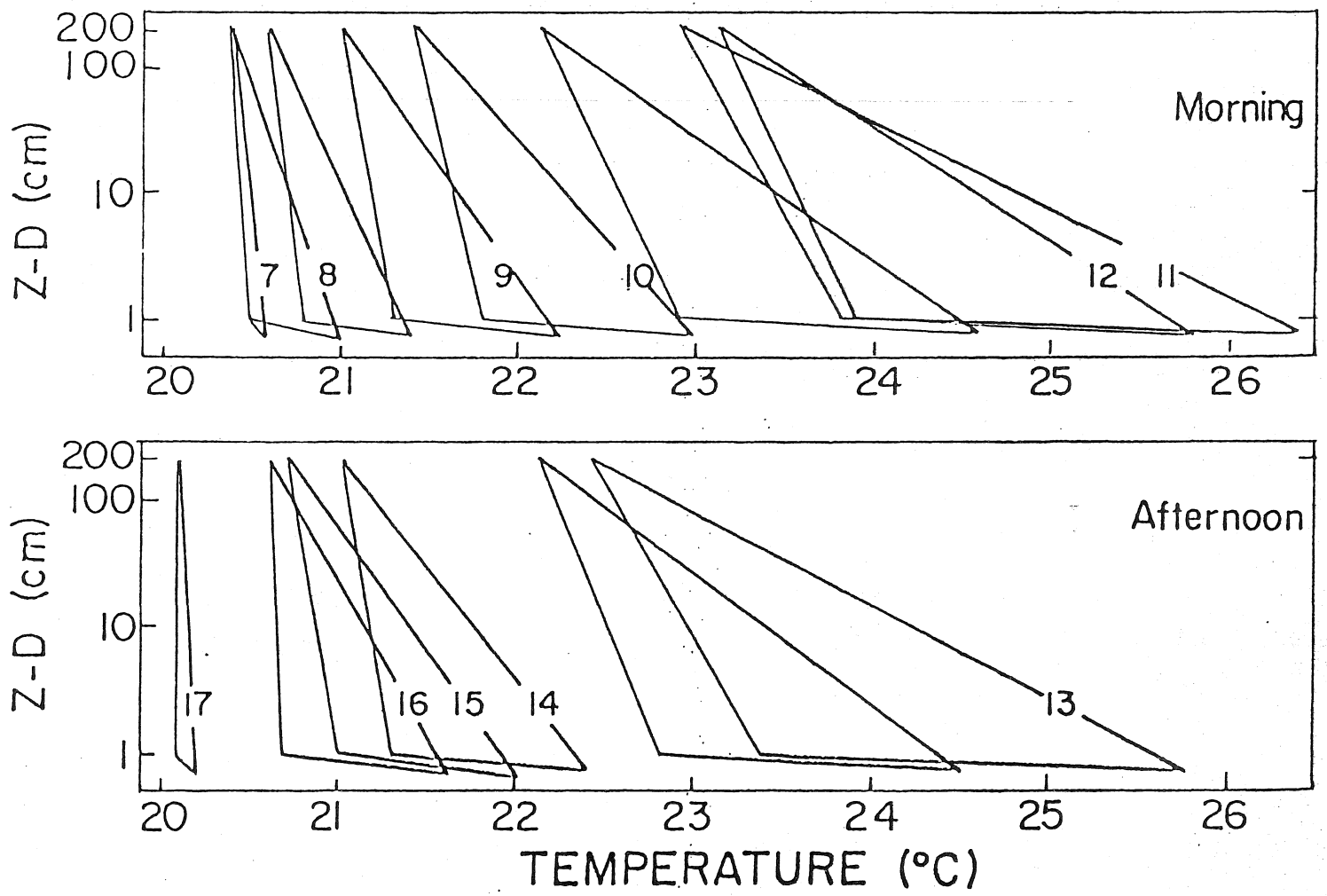

Figure 4. Simplified Temperature Profiles for an Overcast Day. These gradients were measured on October 30, 1981. Note the difference in temperature scale when comparing to Figure 3. The rapid afternoon cooling was caused by intermittent drizzle.

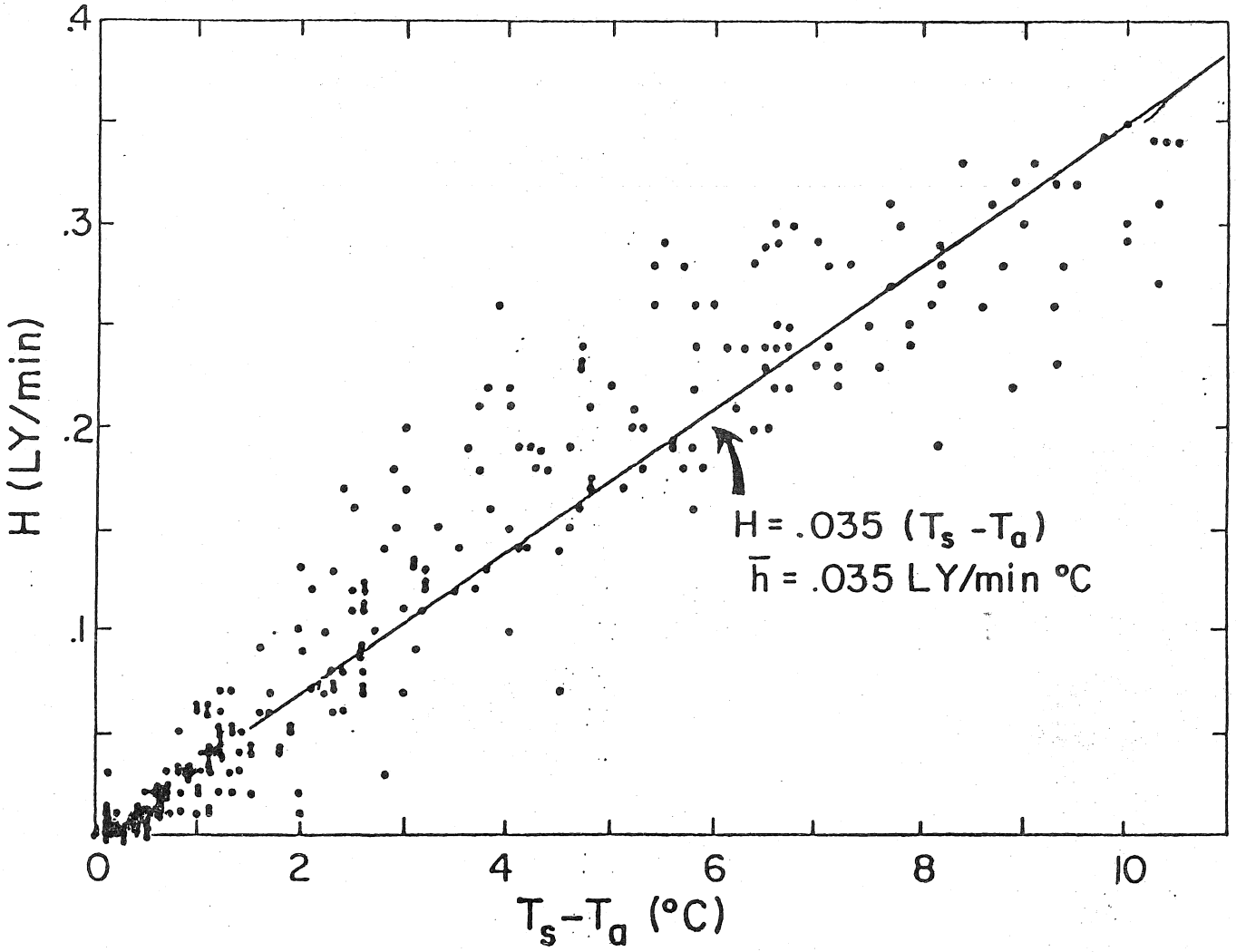

Figure 5. Air Transport Coefficient for Average Conditions. Data are from days 290-310 inclusive except days 297-300 inclusive, on which no data were collected.

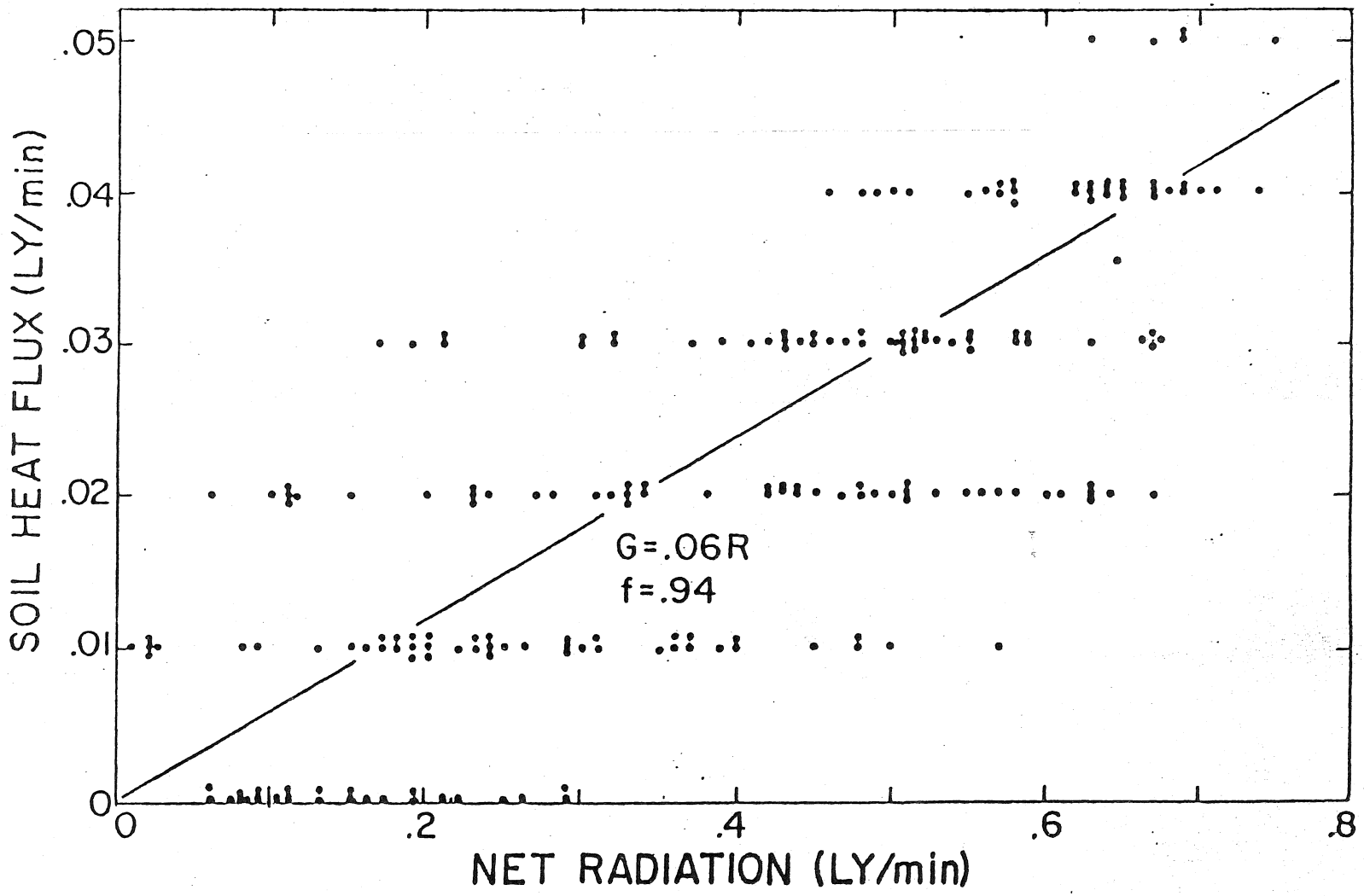

Figure 6. Soil Heat Flux Parameter for Average Conditions. Data are from days 290-310 inclusive except days 297-300 inclusive, on which no data were collected. Data are grouped because soil heat flux data were recorded in hundredths of ly/min.

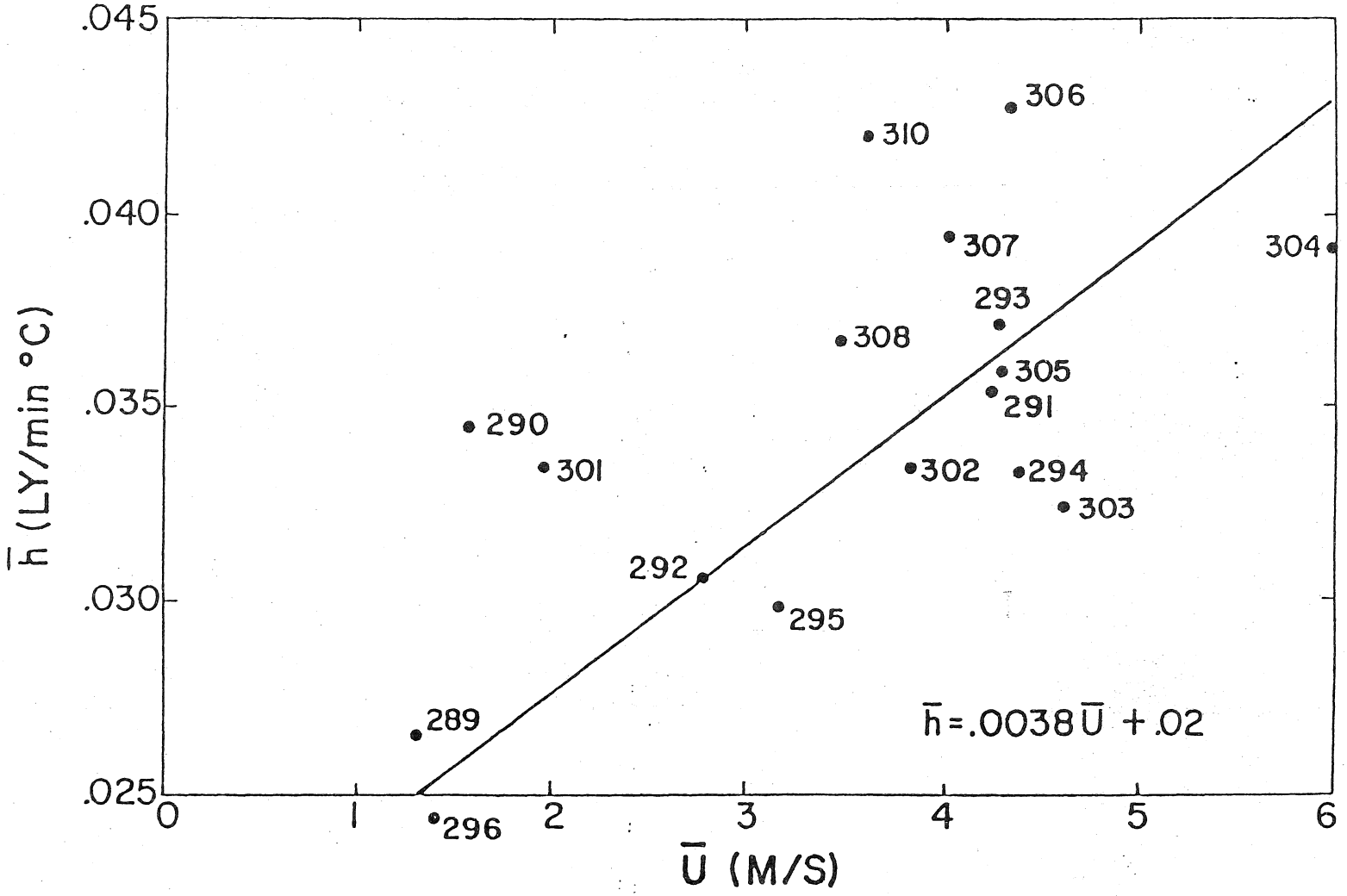

Figure 7. Variation of the Daily Average Heat Transport Coefficient with the Daily Average Windspeed.

Figures 8, 9, 10, 11, and 12. Data and ET Estimates for October 17, 18, 21, 22, and 23, 1981. Each figure presents one day's data in 9 graphs on 5 pages. The numbers on the graphs indicate the true solar time at the end of the half hour averaging period that the corresponding point represents. The graphs are labelled (a) through (i), and are described below:

(a) Sensible Heat Flux vs. Surface-to-Air Temperature Difference. The slope of the line passing through the origin and the data points is the average heat transport coefficient.

(b) Latent Heat Flux vs. Surface-to-Air Vapor Pressure Difference. The surface vapor pressure is the saturation vapor pressure at the surface temperature. The slope of the line passing through the origin and data points is the average vapor pressure transport coefficient, from which average moisture availability can be computed.

(c) Vapor Pressure Gradient vs. Temperature Gradient. The slope of the line fitted to the points is the slope of the saturation vapor pressure curve at the average temperature, and the intercept is the average vapor pressure deficit.

(d) Soil Heat Flux vs. Net Radiation. The slope of the line passing through the origin and the data points is equal to the average fraction of net radiation conducted into the soil (G/R). The soil heat flux parameter (f) is calculated from $f = 1 - G/R$.

(e) Daily Course of Net Radiation. This graph shows the general cloudiness of the day in question.

(f) Surface-to-Air Temperature Gradient/Net Radiation Relationship. The equation in the lower right corner has been "eye fit" to the data.

(g) Comparison of Bowen Ratios in Time. The solid line ratios were calculated from half-hour average temperature and vapor pressure profiles; the data plotted are from periods in which the profile correlation was at least .95. The dotted ratios were computed by the simple residual method, and the dashed using the correlation developed from the temperature gradient/net radiation correlation. The heat transport coefficient used in the latter two methods was constant (the same for each time period) but separately determined for the day in question.

(h) Comparison of Instantaneous ET Estimates. Estimates by the simple residual method and the ATGR method are compared to actual ET rates under more realistic estimation conditions. The residual and ATGR estimates are calculated using an "average conditions" heat transfer coefficient ($h = .035$ ly/min°C) and soil heat flux parameter ($f = .94$); see Figs. 5 and 6 for "average conditions" plots.

(i) Comparison of Instantaneous Measurements and Estimates over Time.

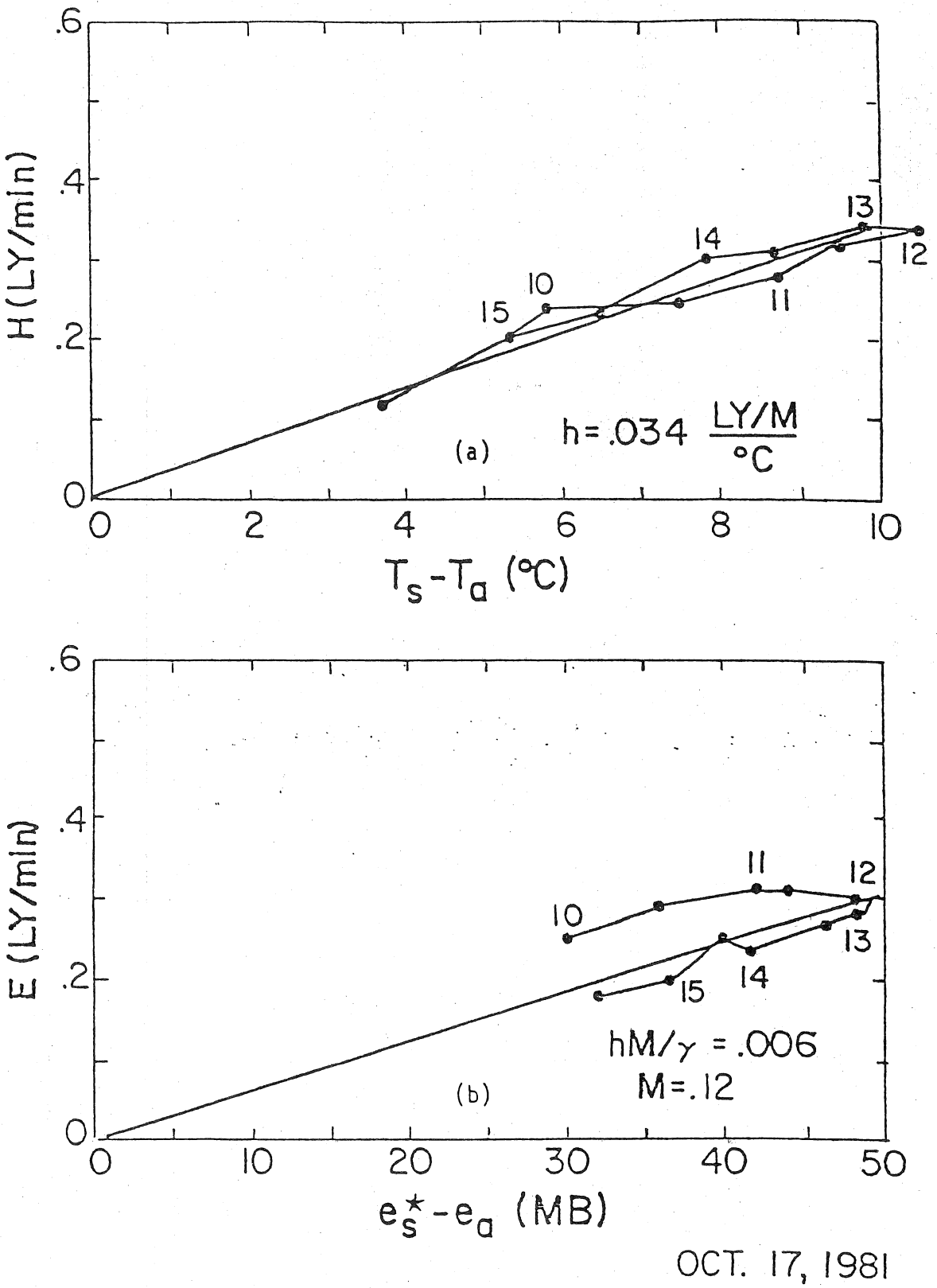

Figure 8. Data and ET Estimates for Oct. 17, 1981. See p. 185 for brief explanation of individual graphs.

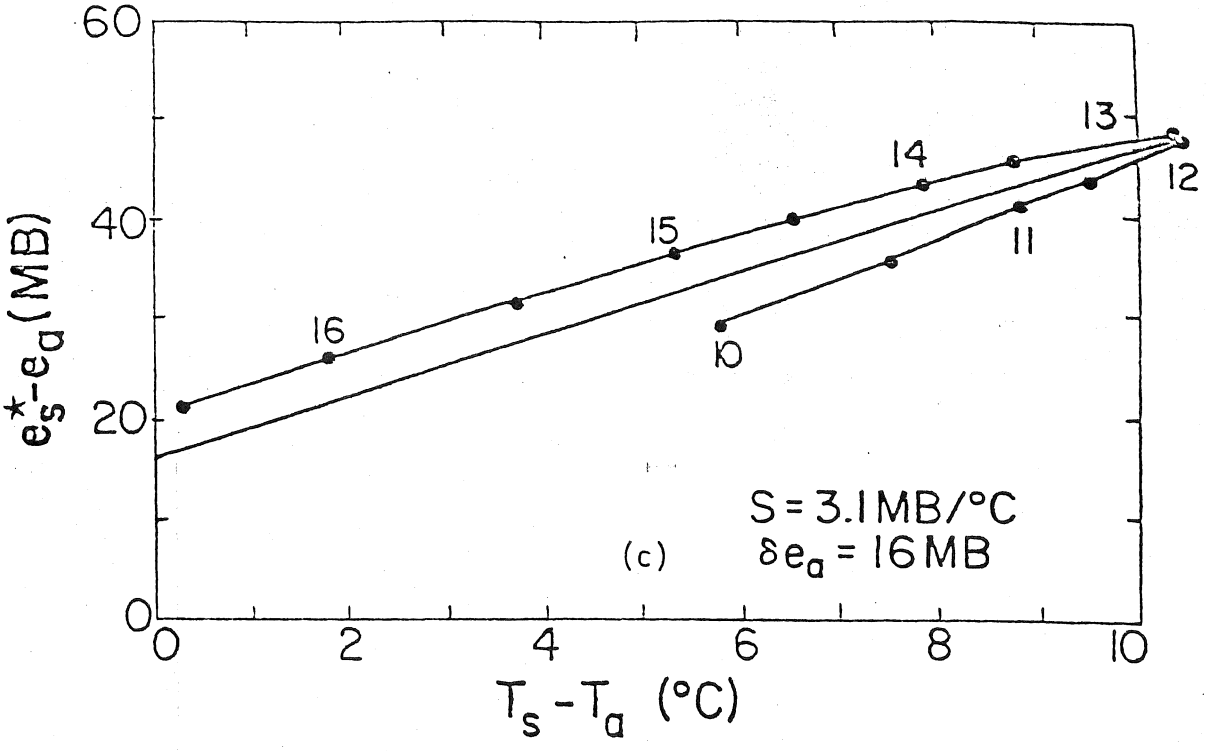

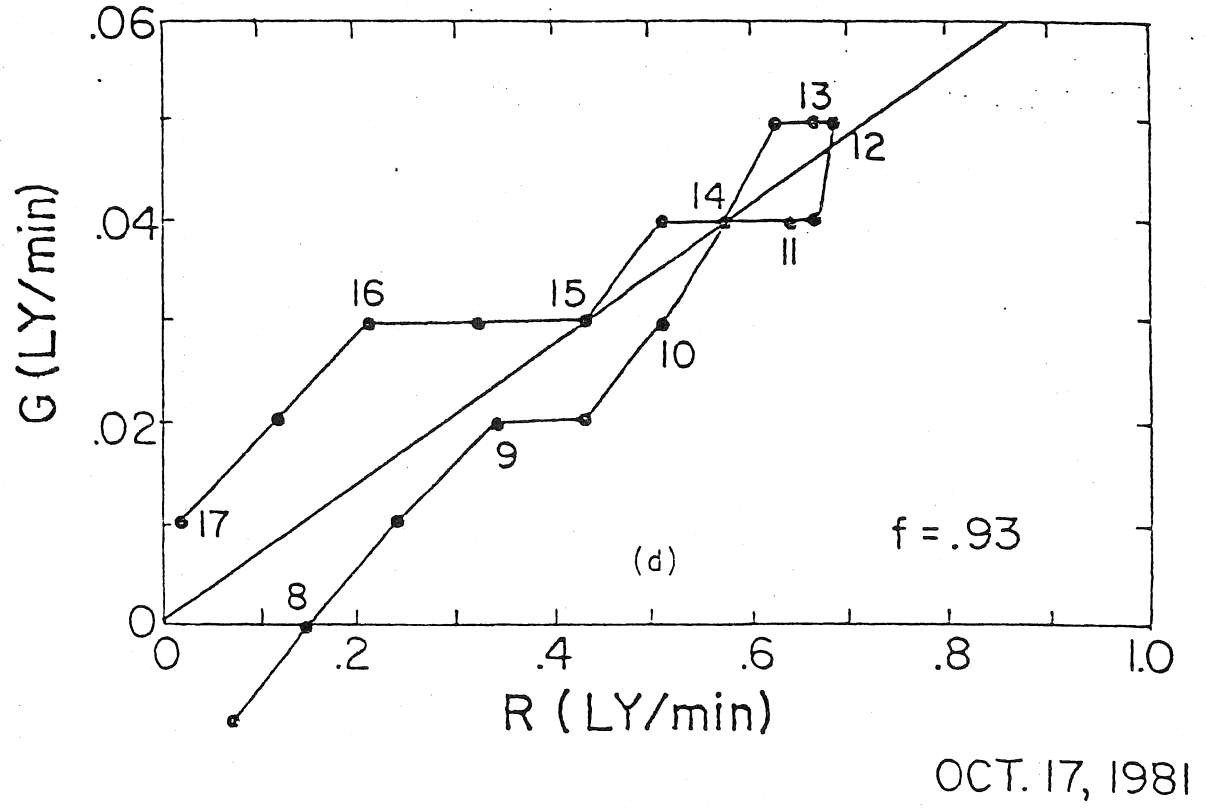

Figure 8. (cont.)

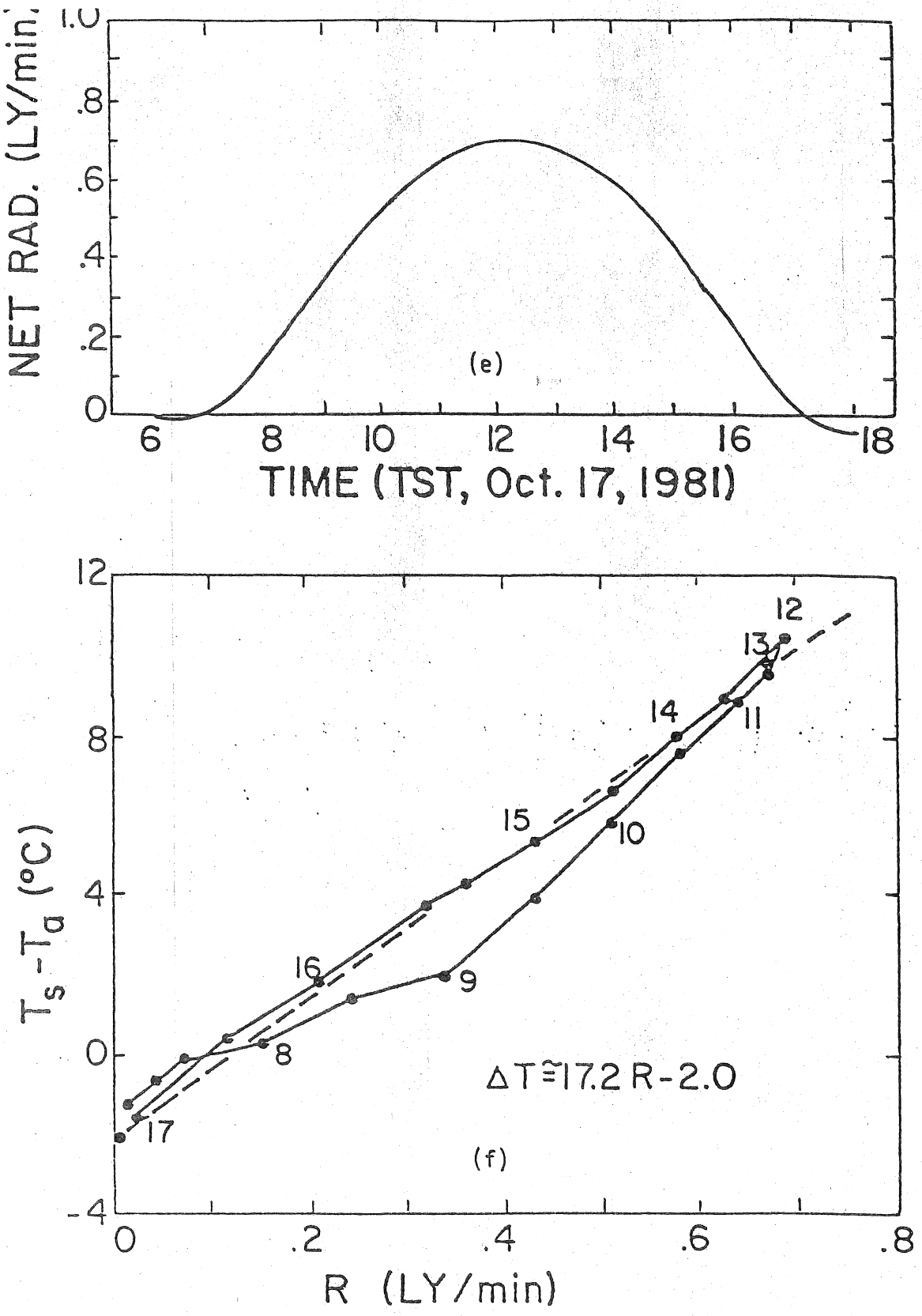

Figure 8. (cont.)

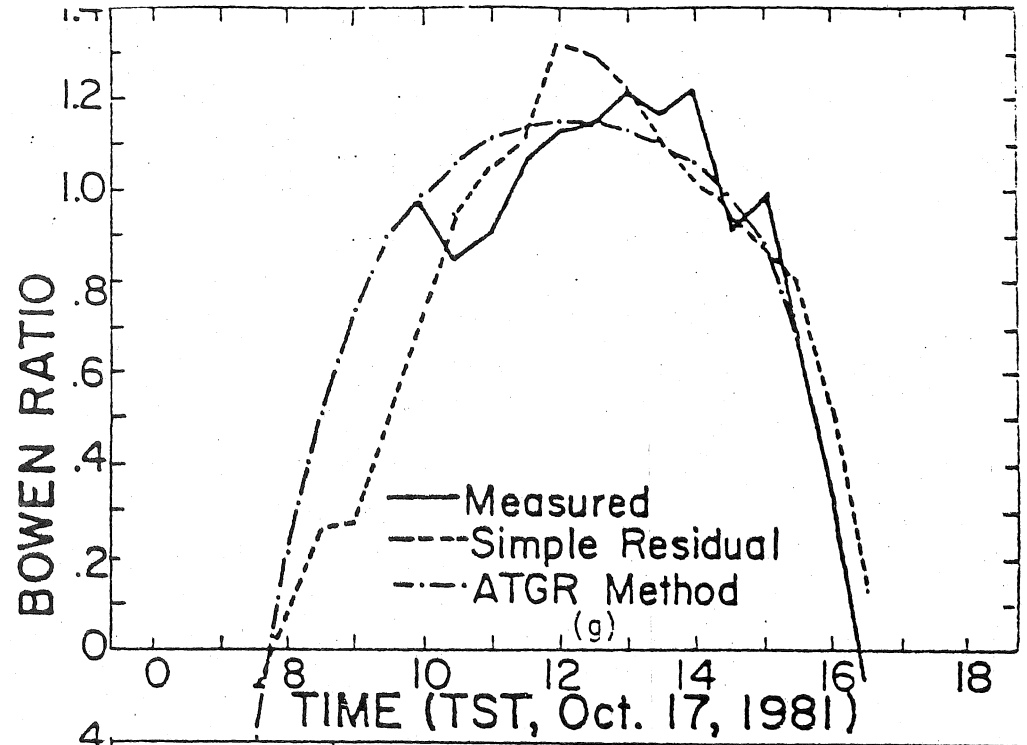

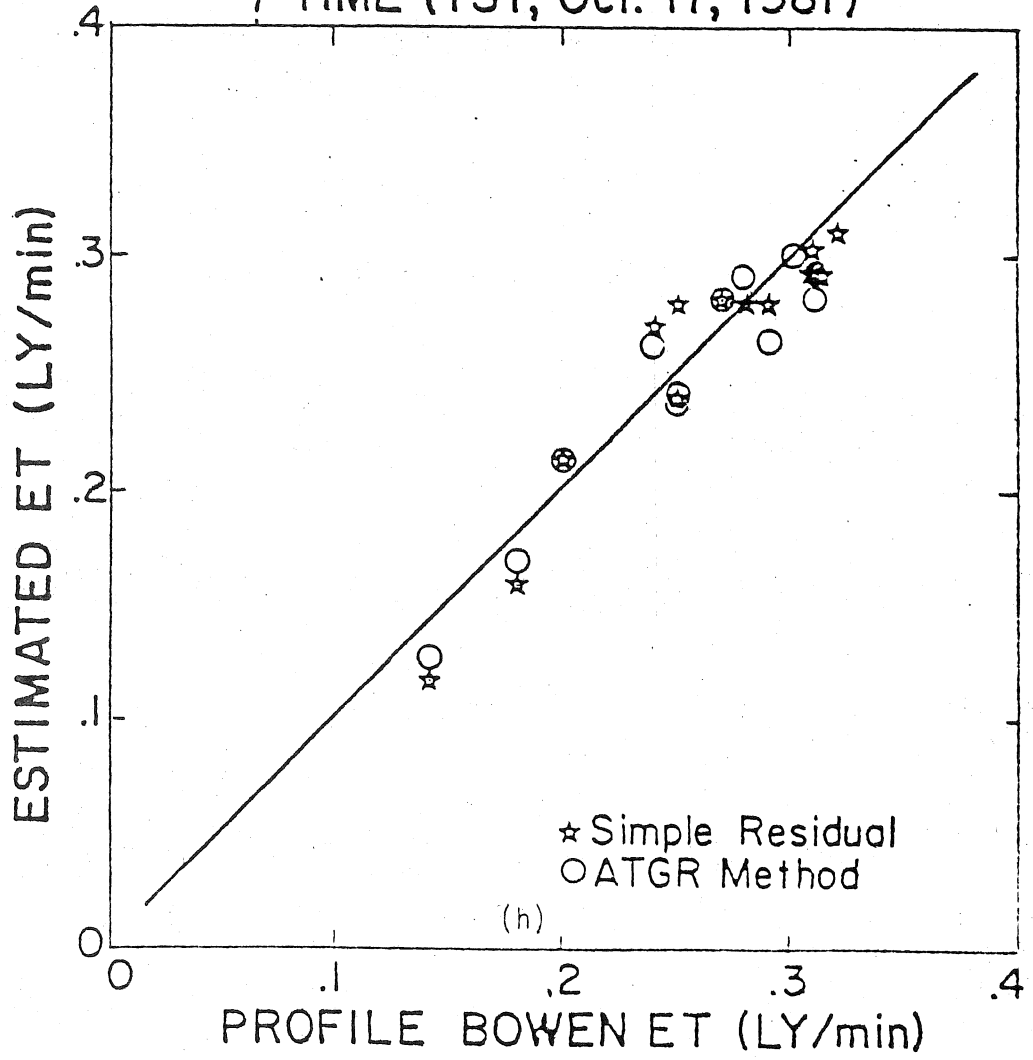

Figure 8. (cont.)

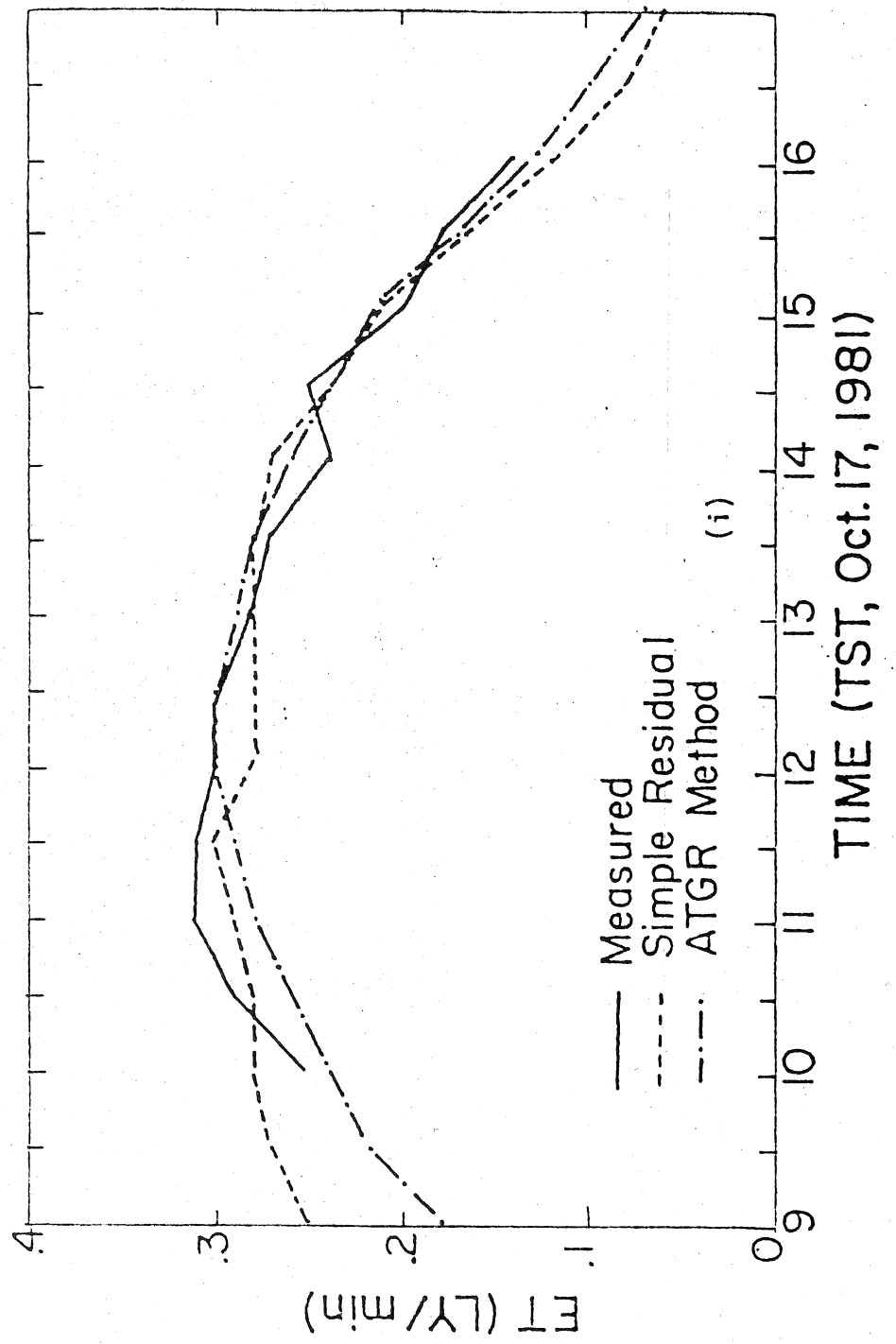

Figure 8. (cont.)

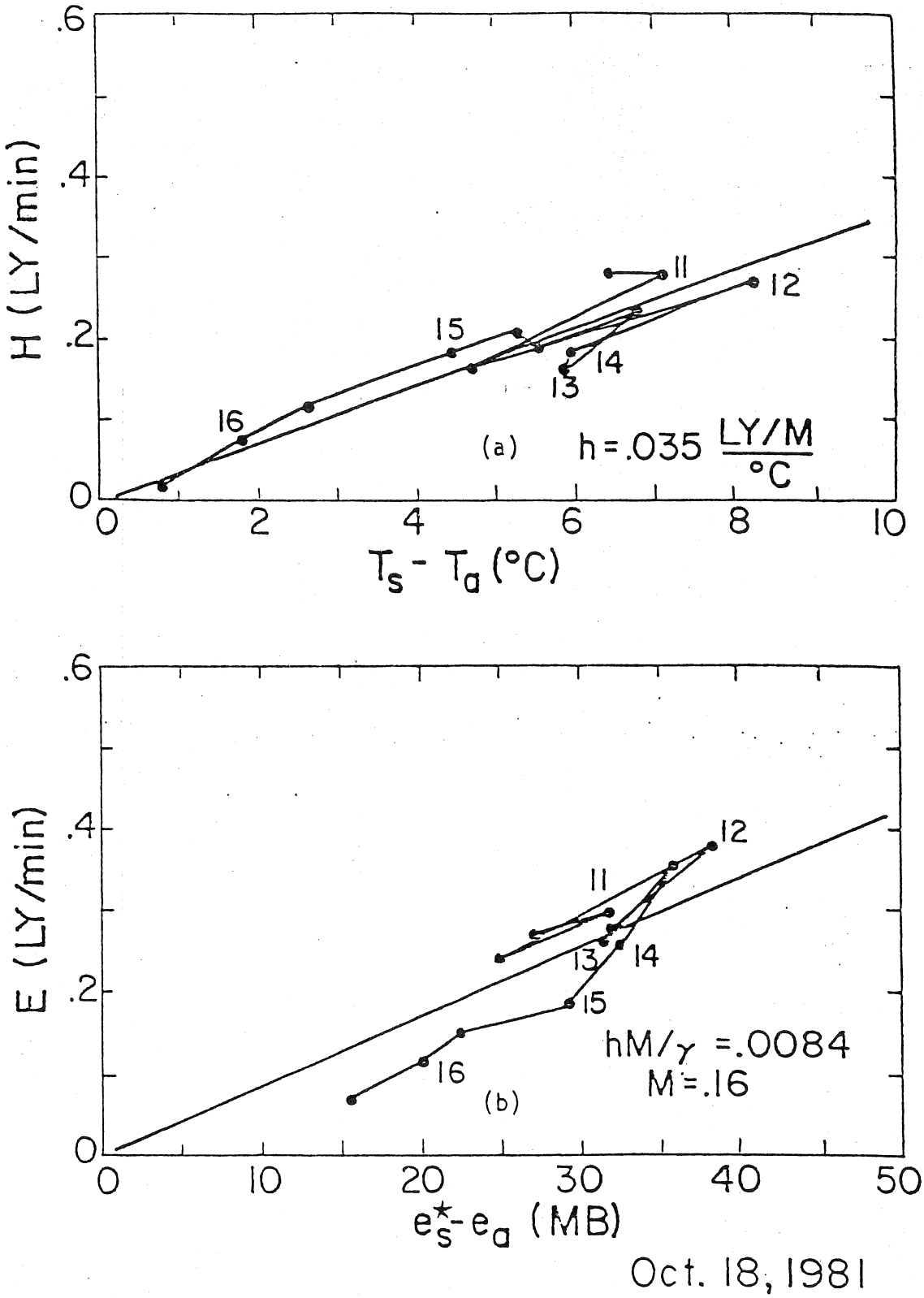

Figure 9. Data and ET Estimates for Oct. 18, 1981. See p. 185 for brief explanation of individual graphs.

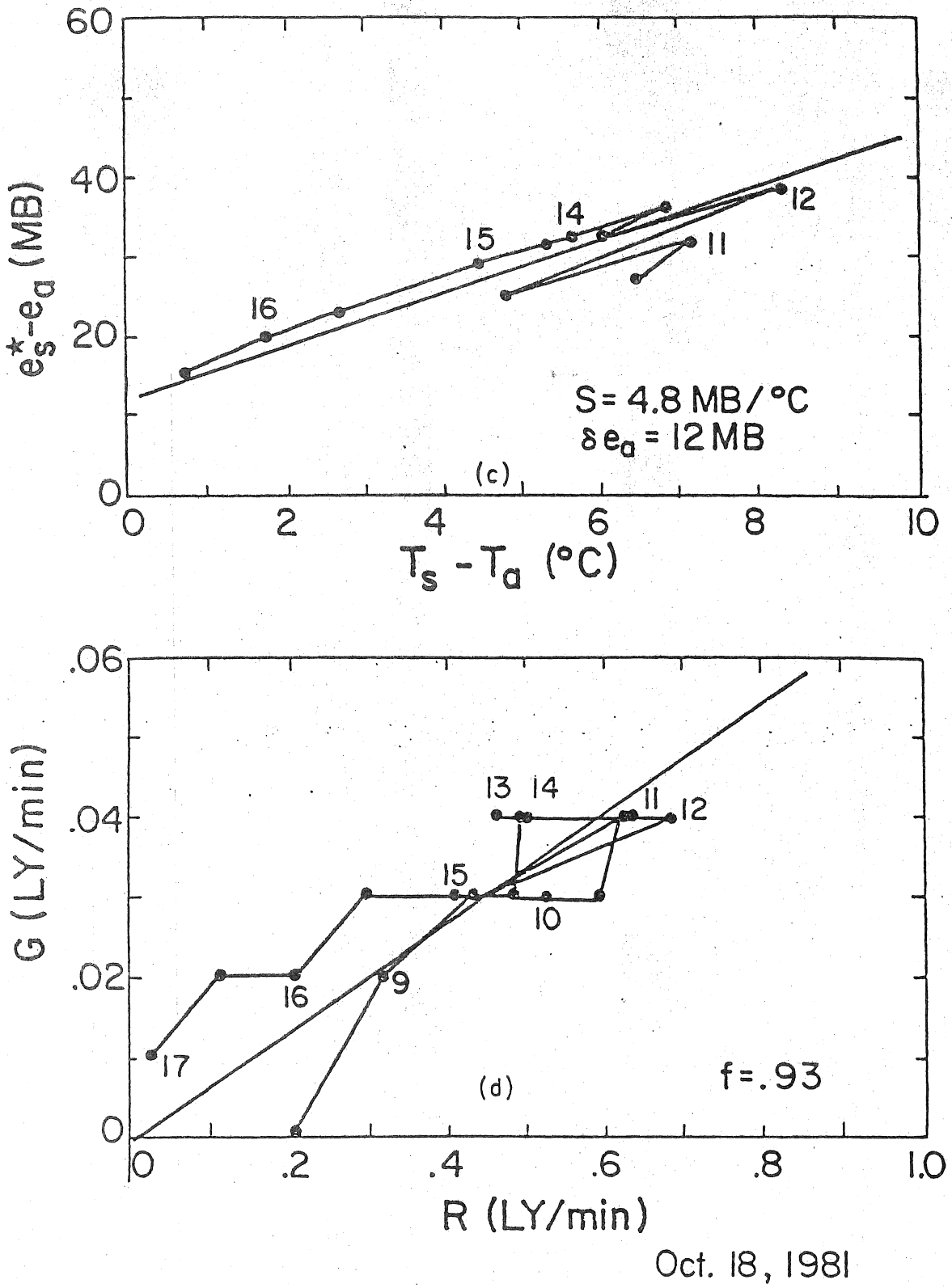

Figure 9. (cont.)

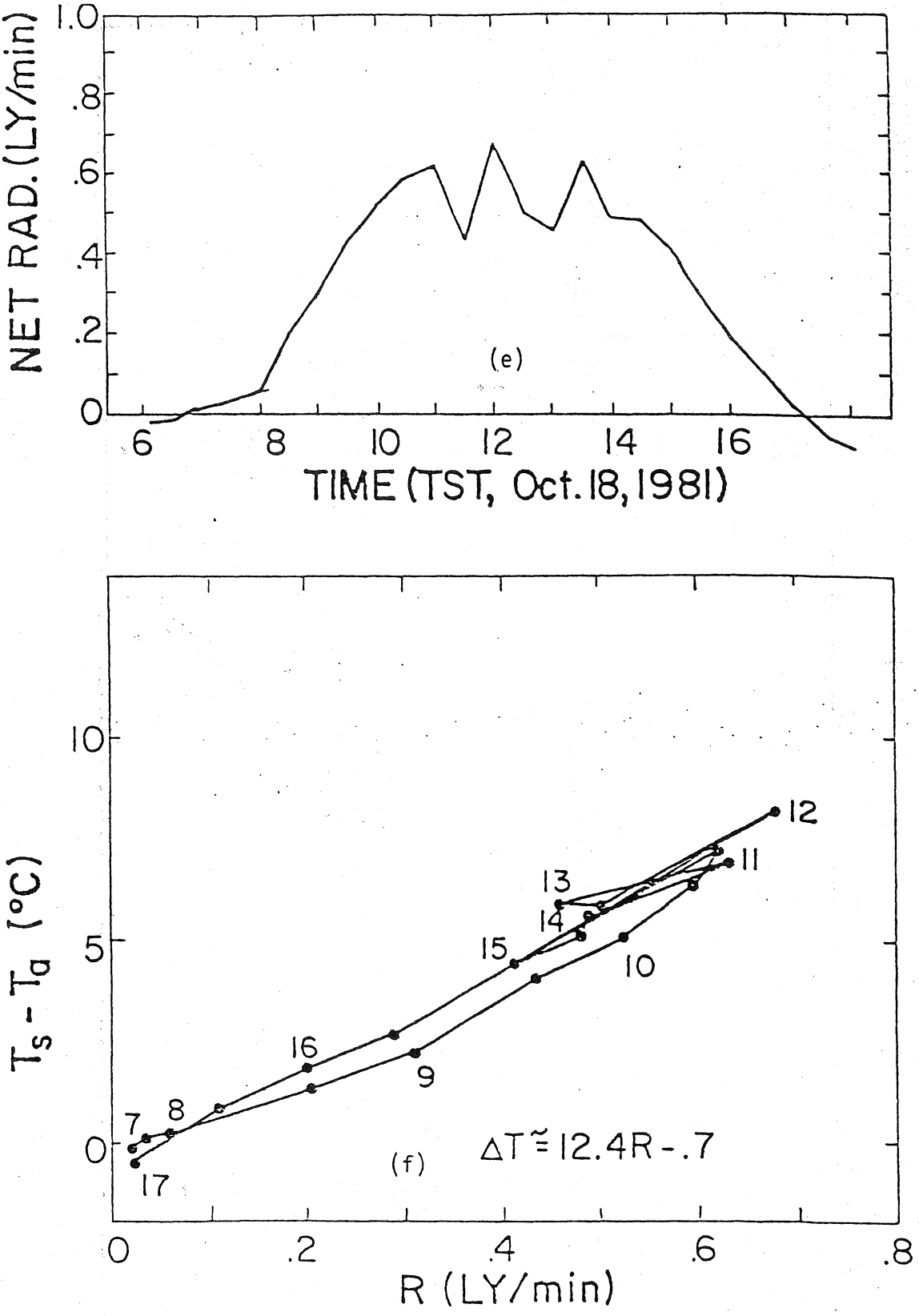

Figure 9. (cont.)

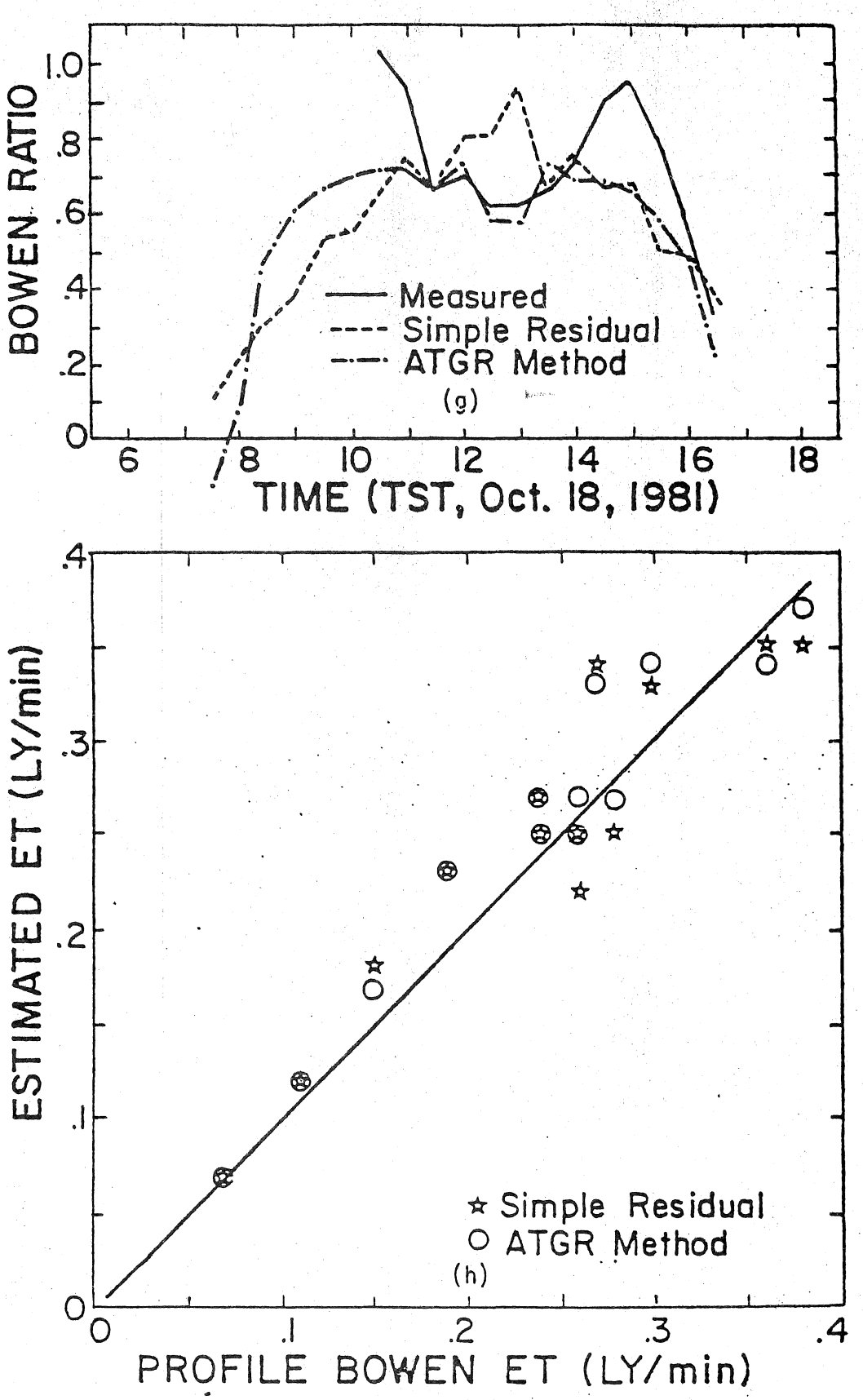

Figure 9. (cont.)

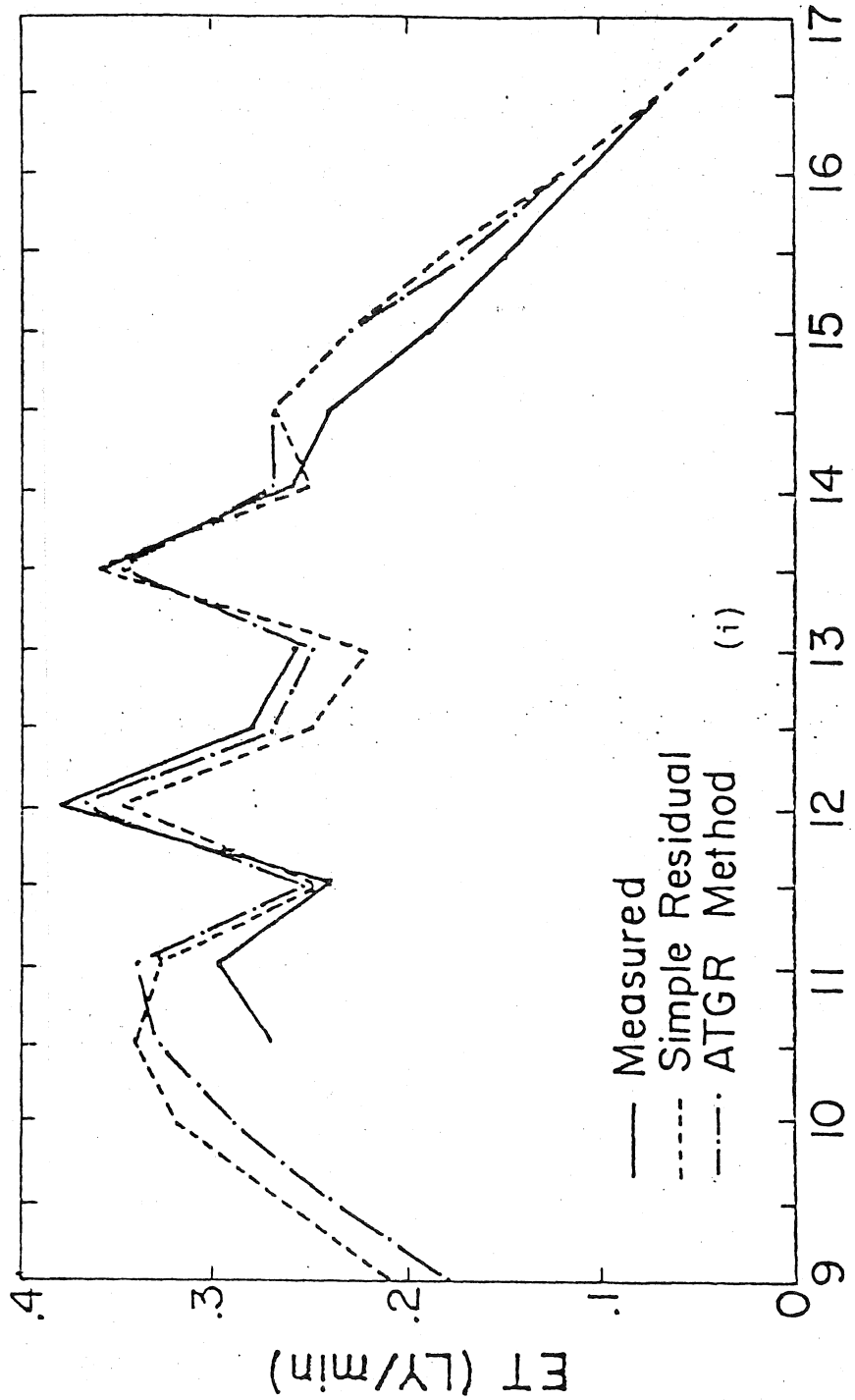

Figure 9. (cont.)

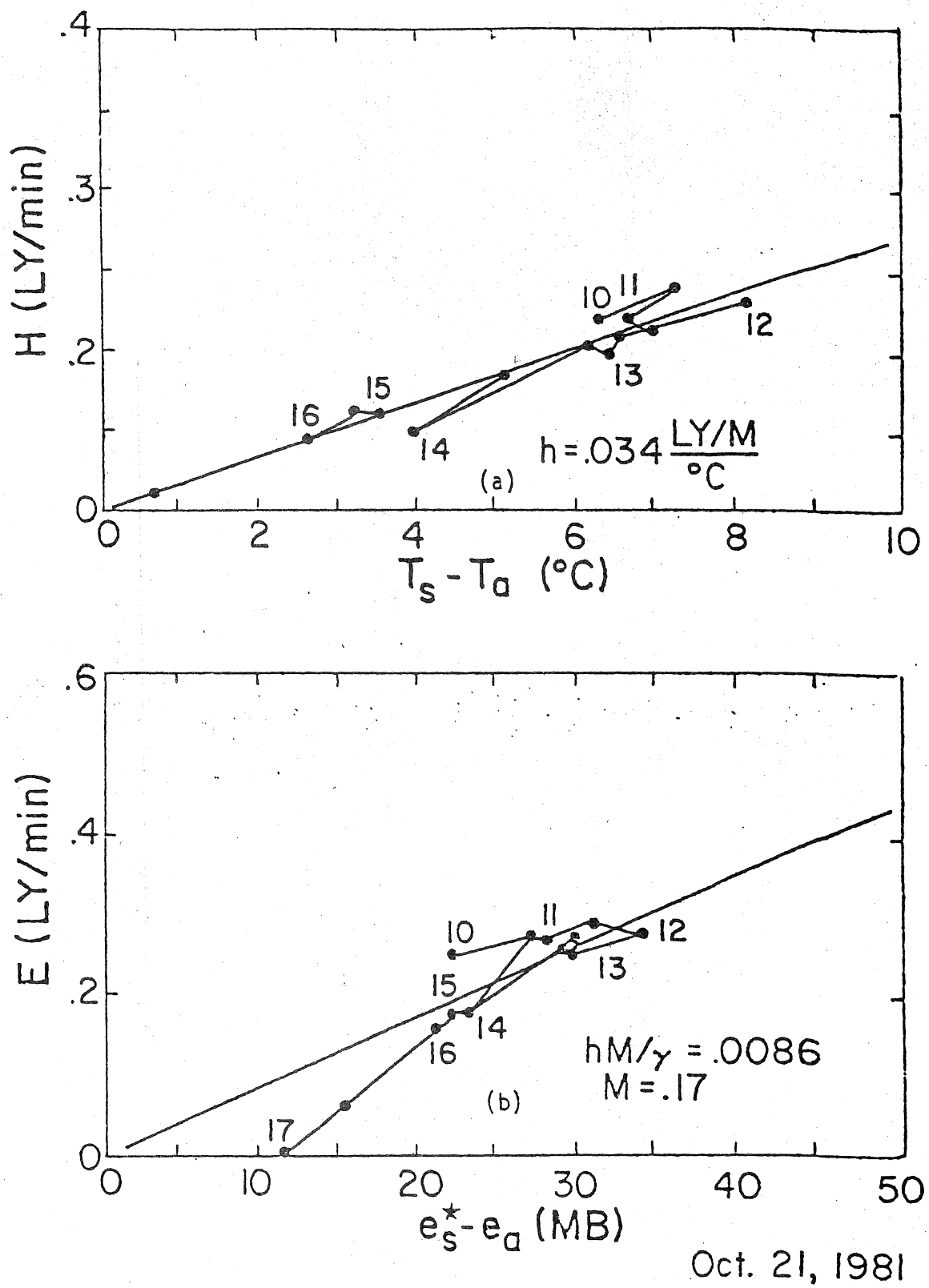

Figure 10. Data and ET Estimates for Oct. 21, 1981. See p. 185 for brief explanation of individual graphs.

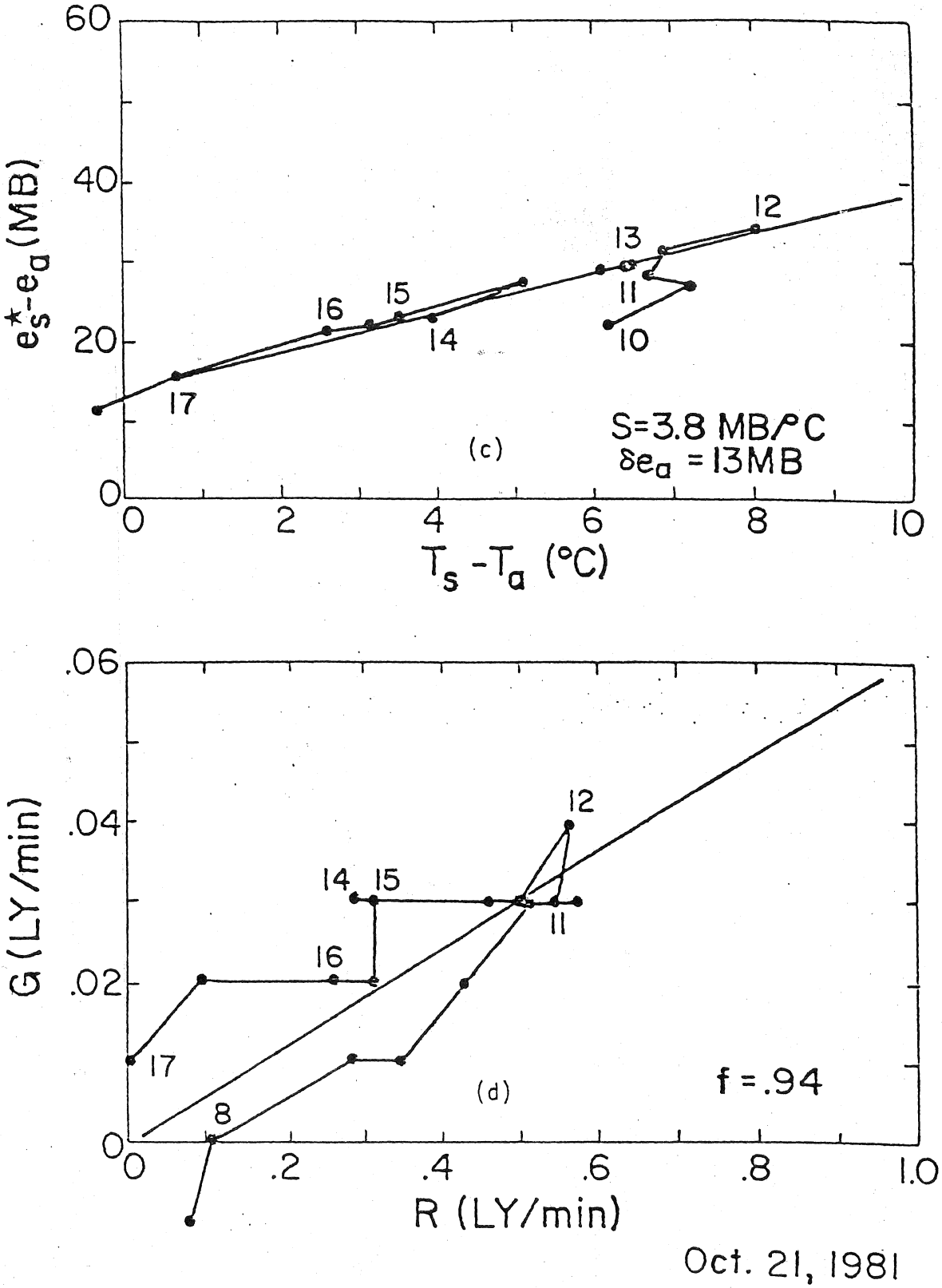

Figure 10. (cont.)

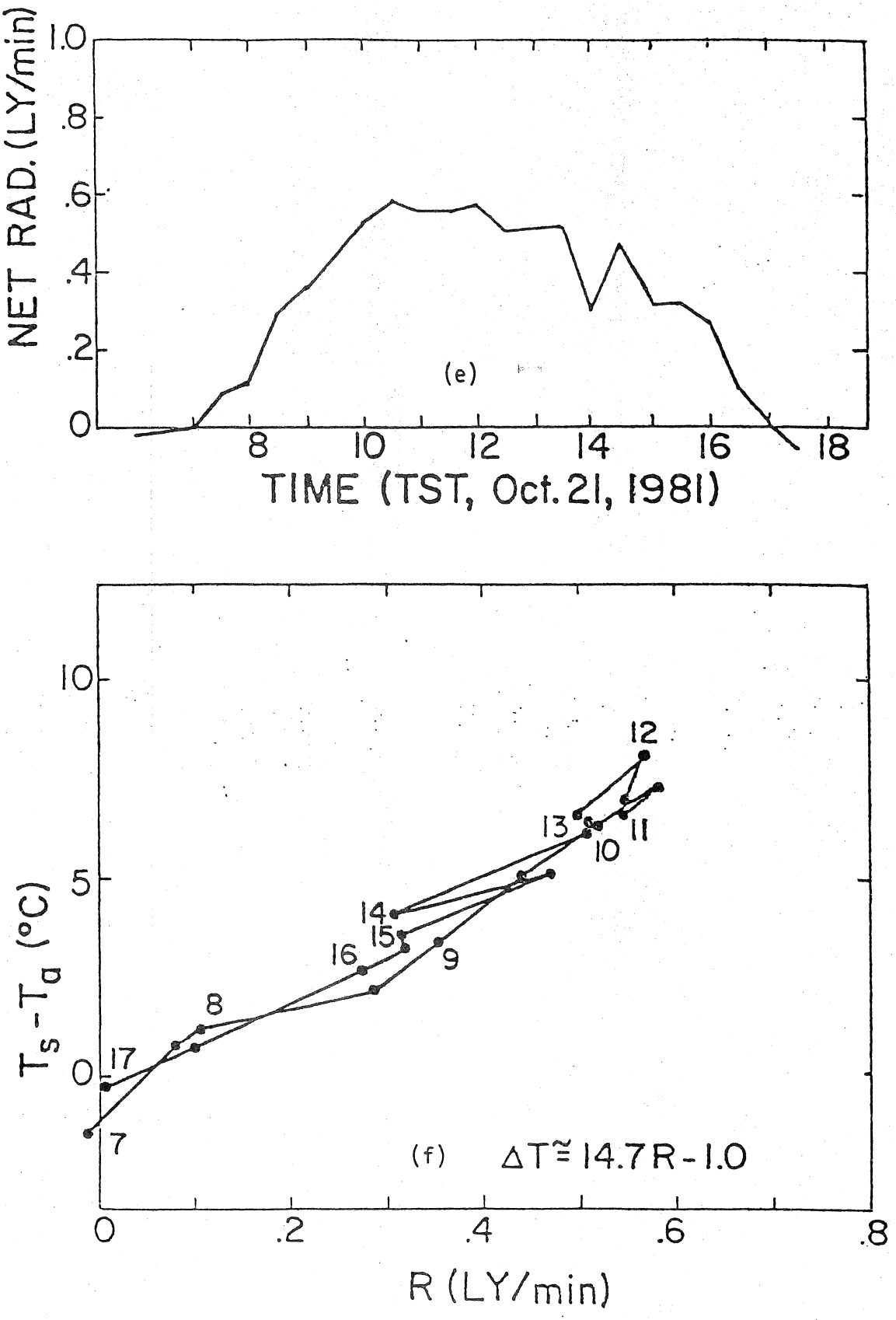

Figure 10. (cont.)

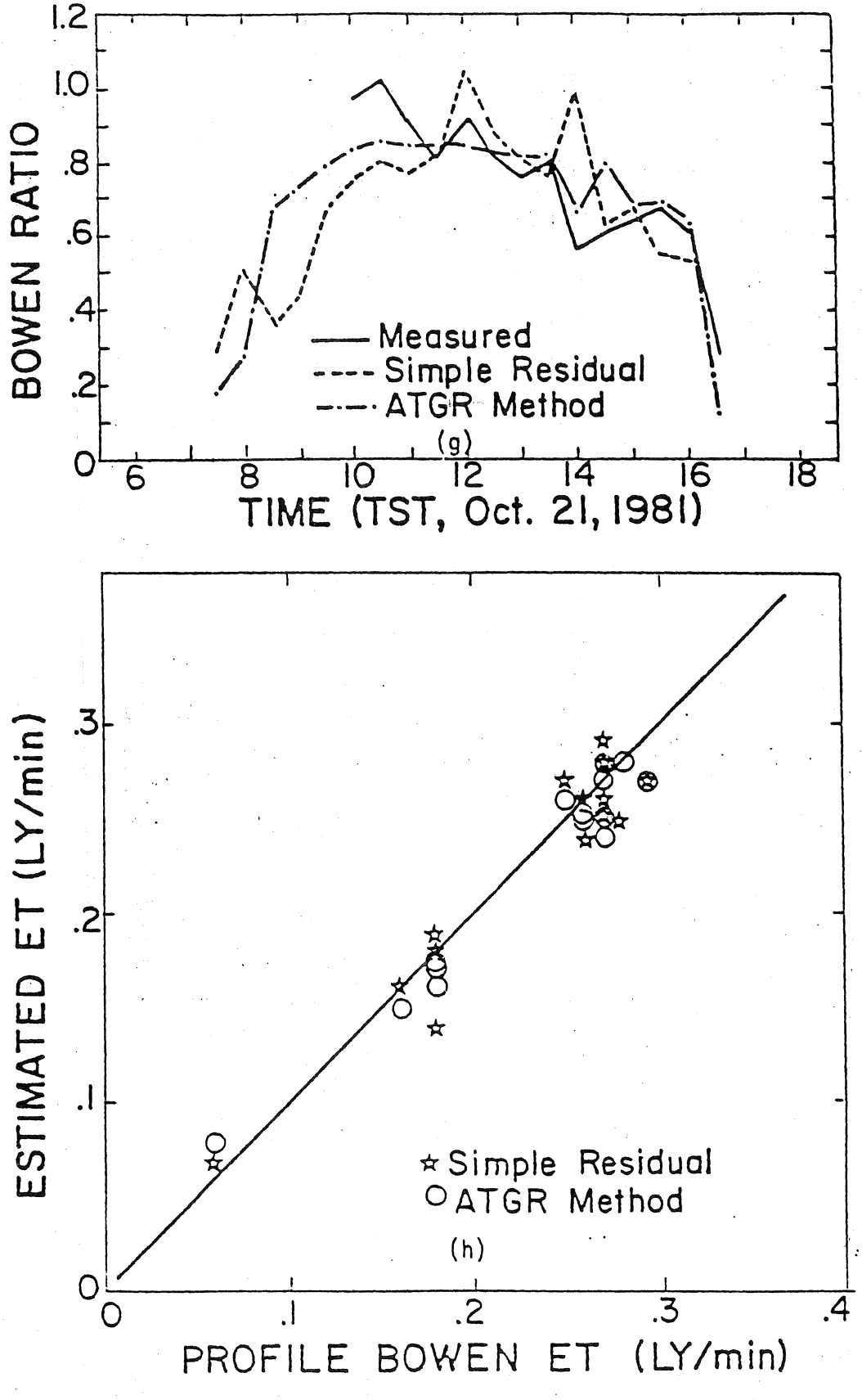

Figure 10. (cont.)

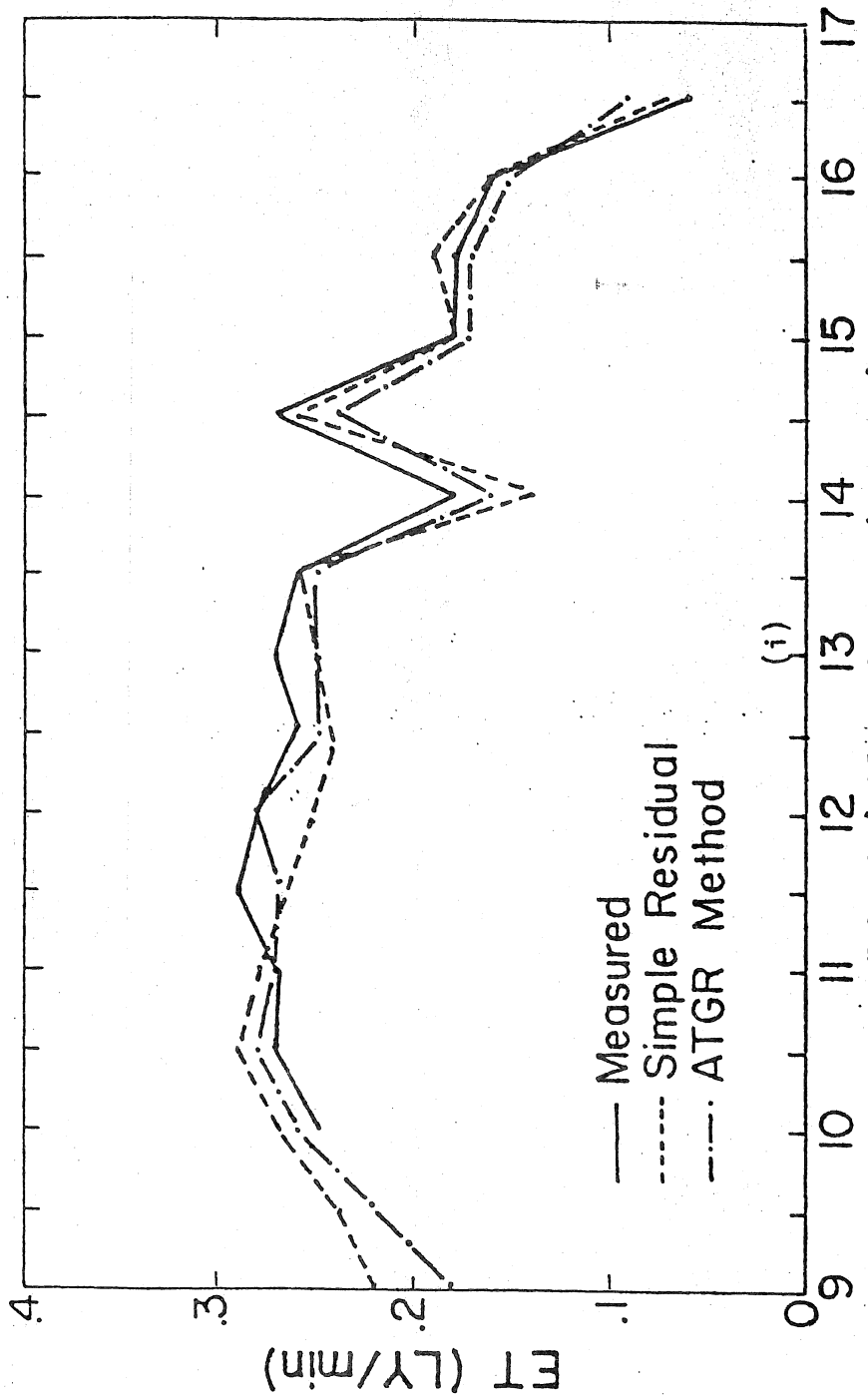

Figure 10. (cont.)

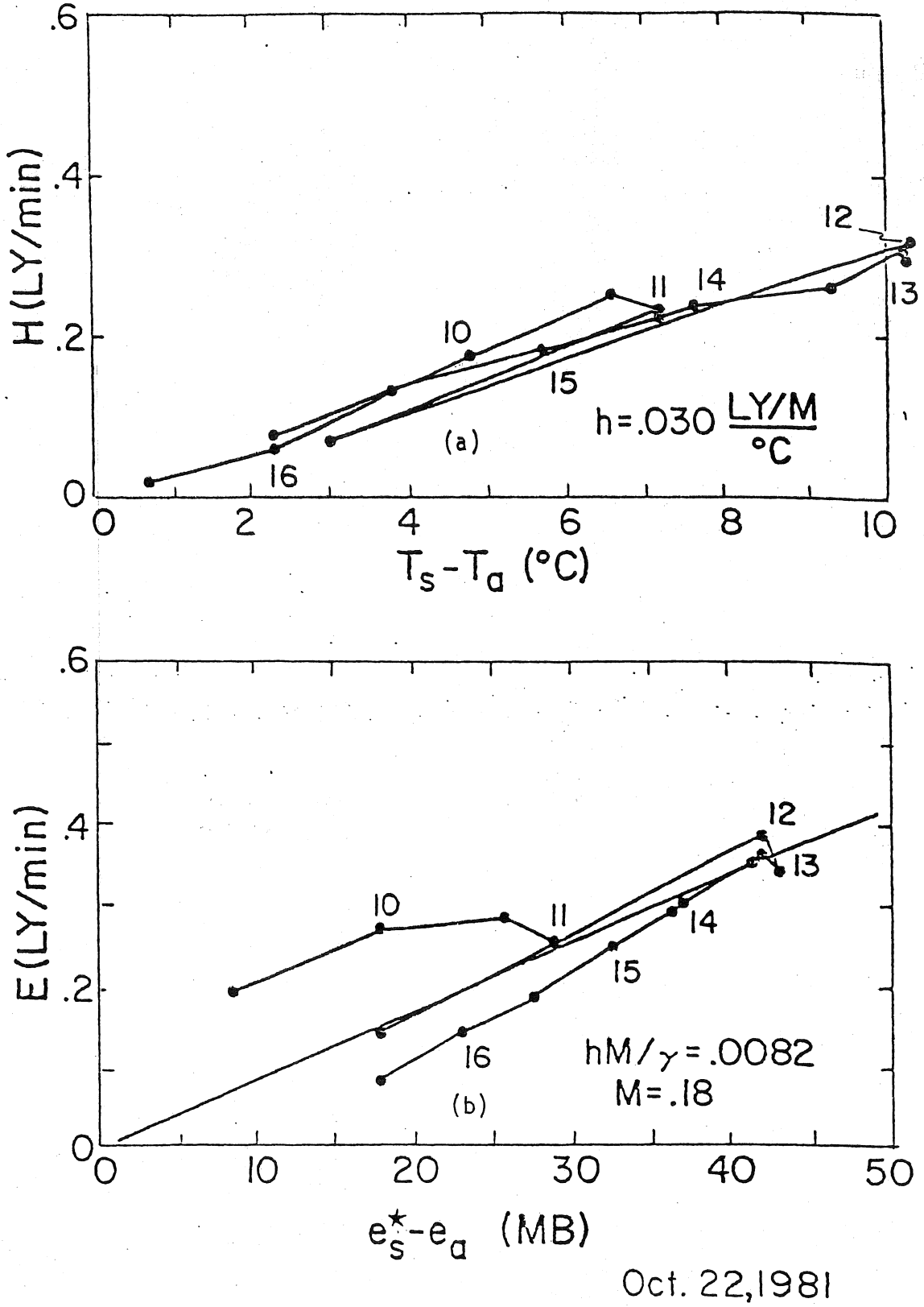

Figure 11. Data and ET Estimates for Oct. 22, 1981. See p. 185 for brief explanation of individual graphs.

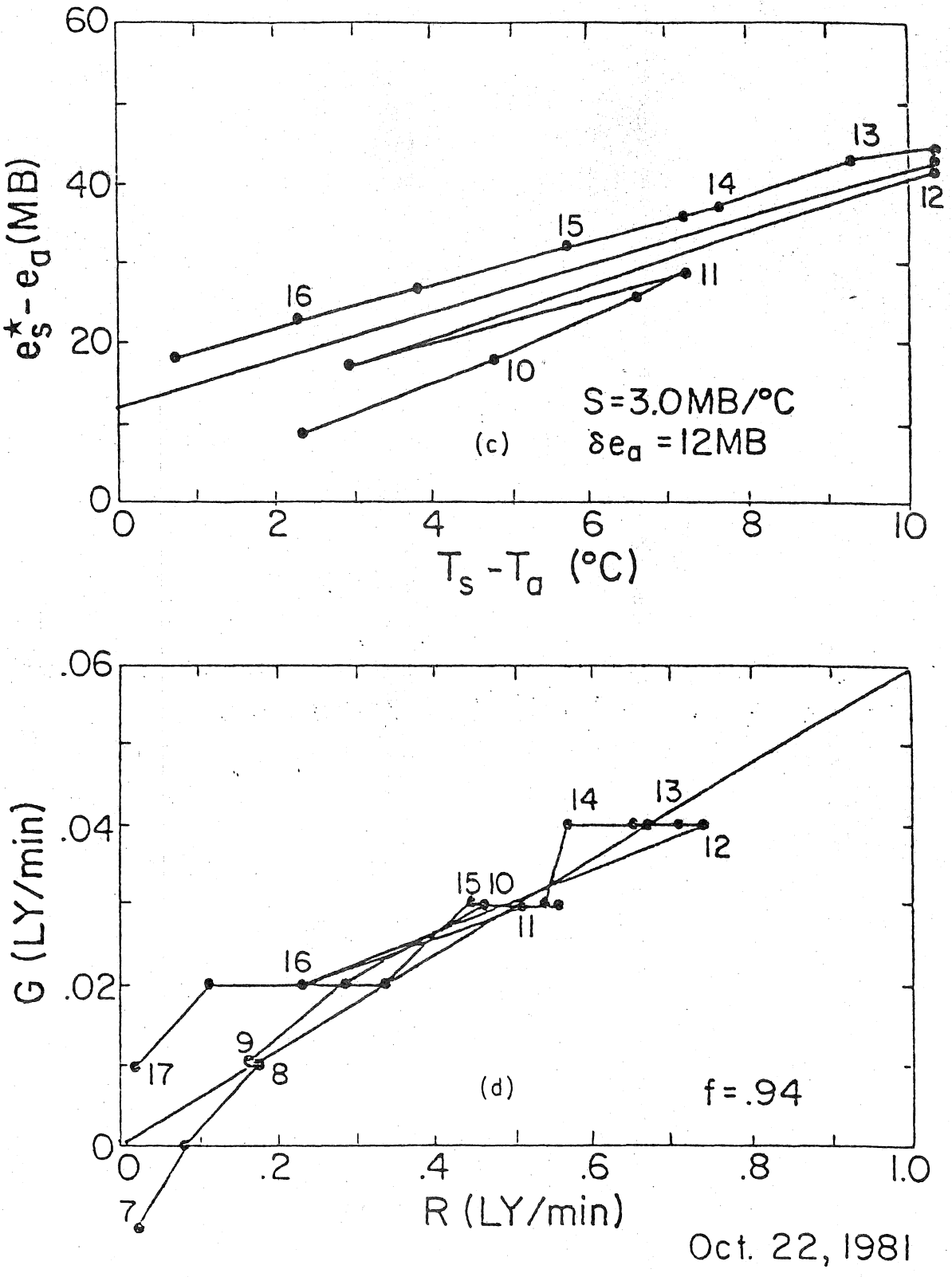

Figure 11. (cont.)

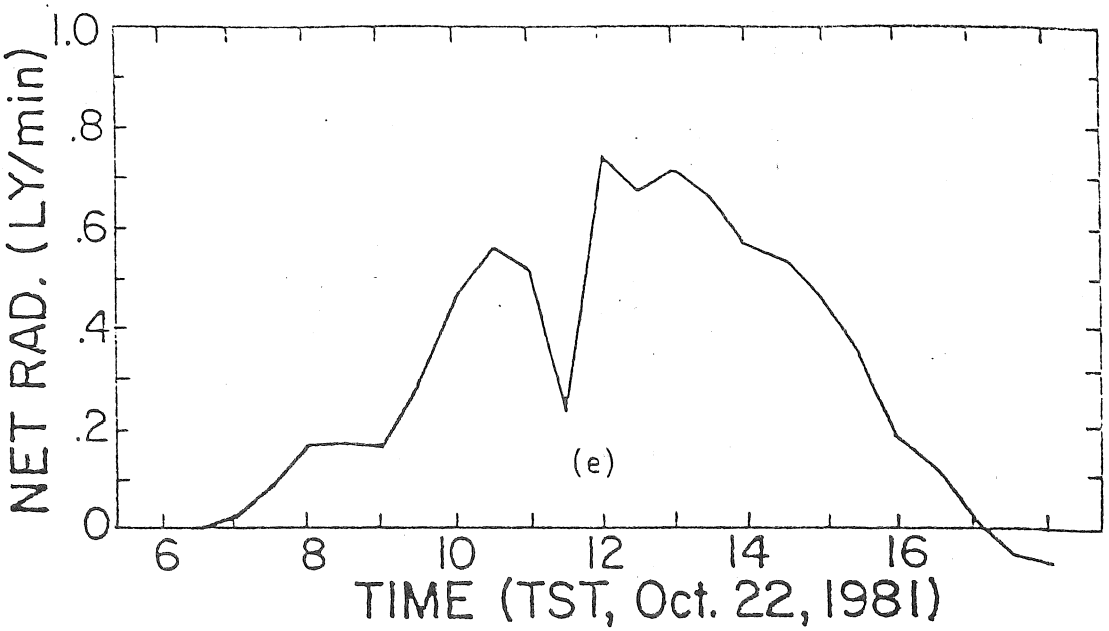

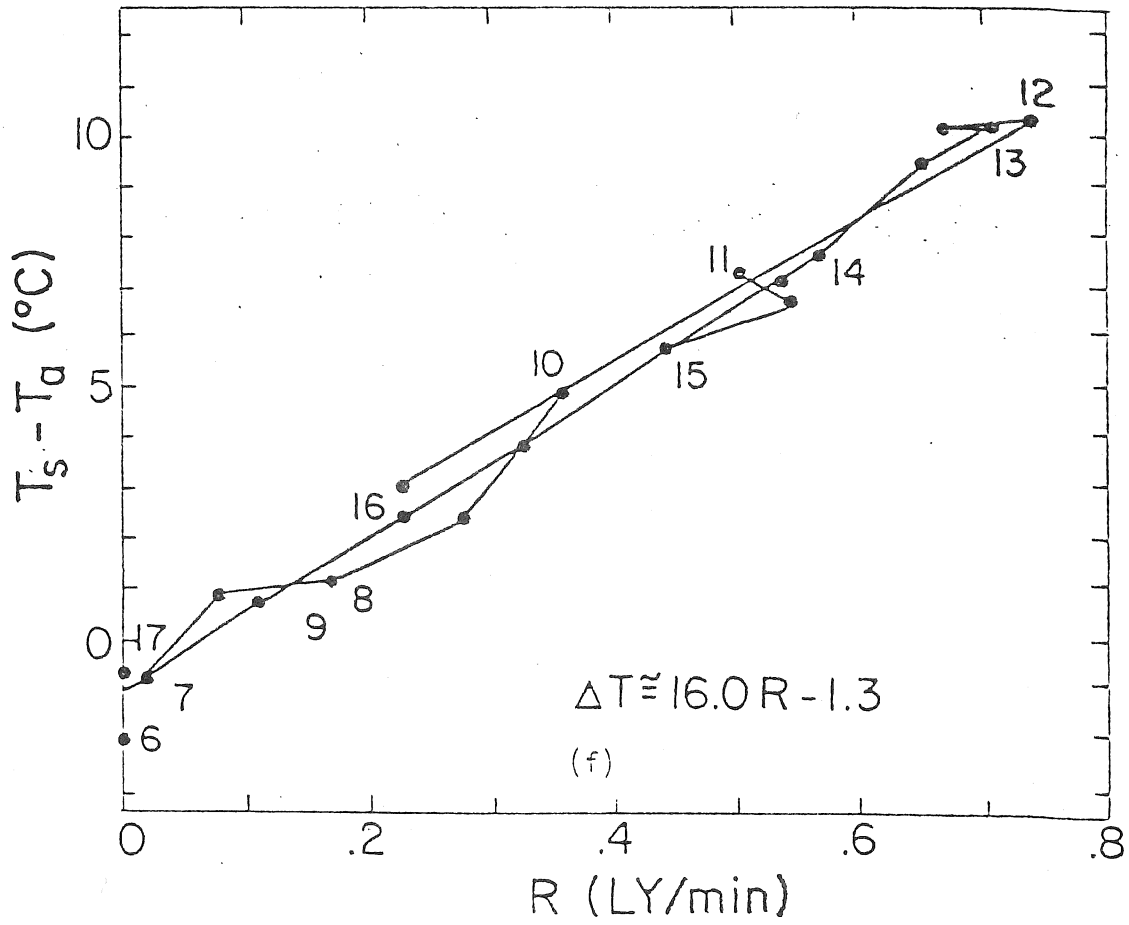

Figure 11. (cont.)

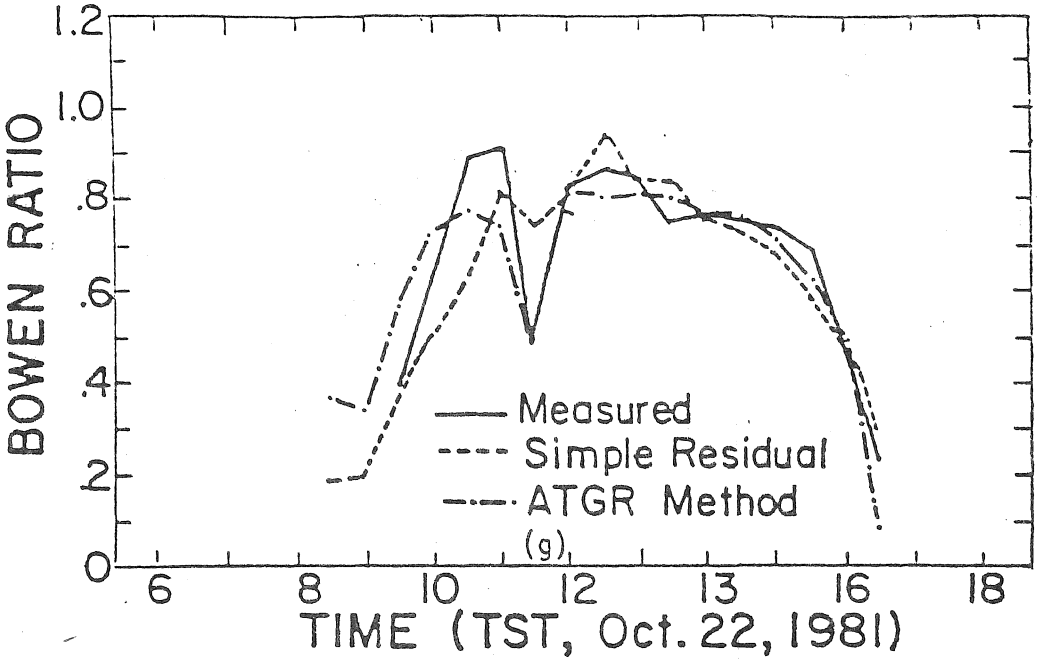

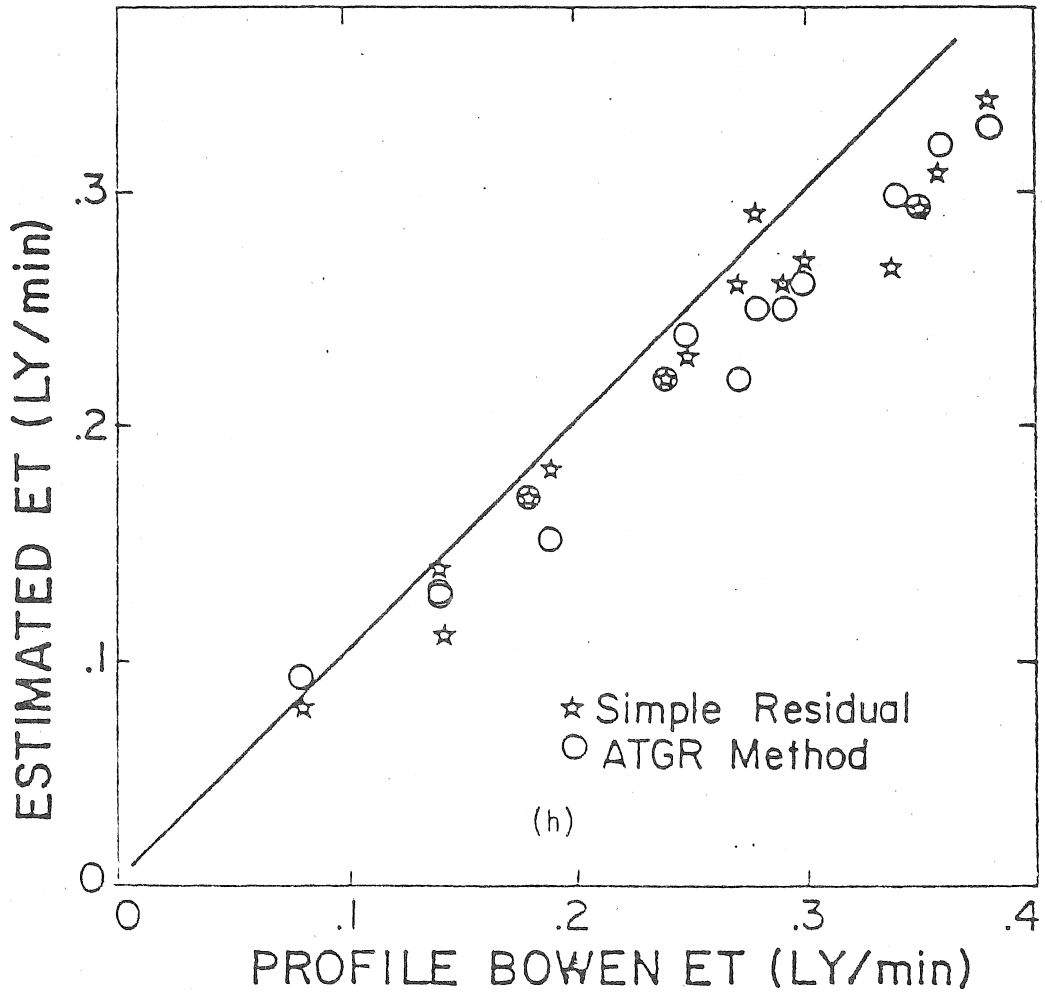

Figure 11. (cont.)

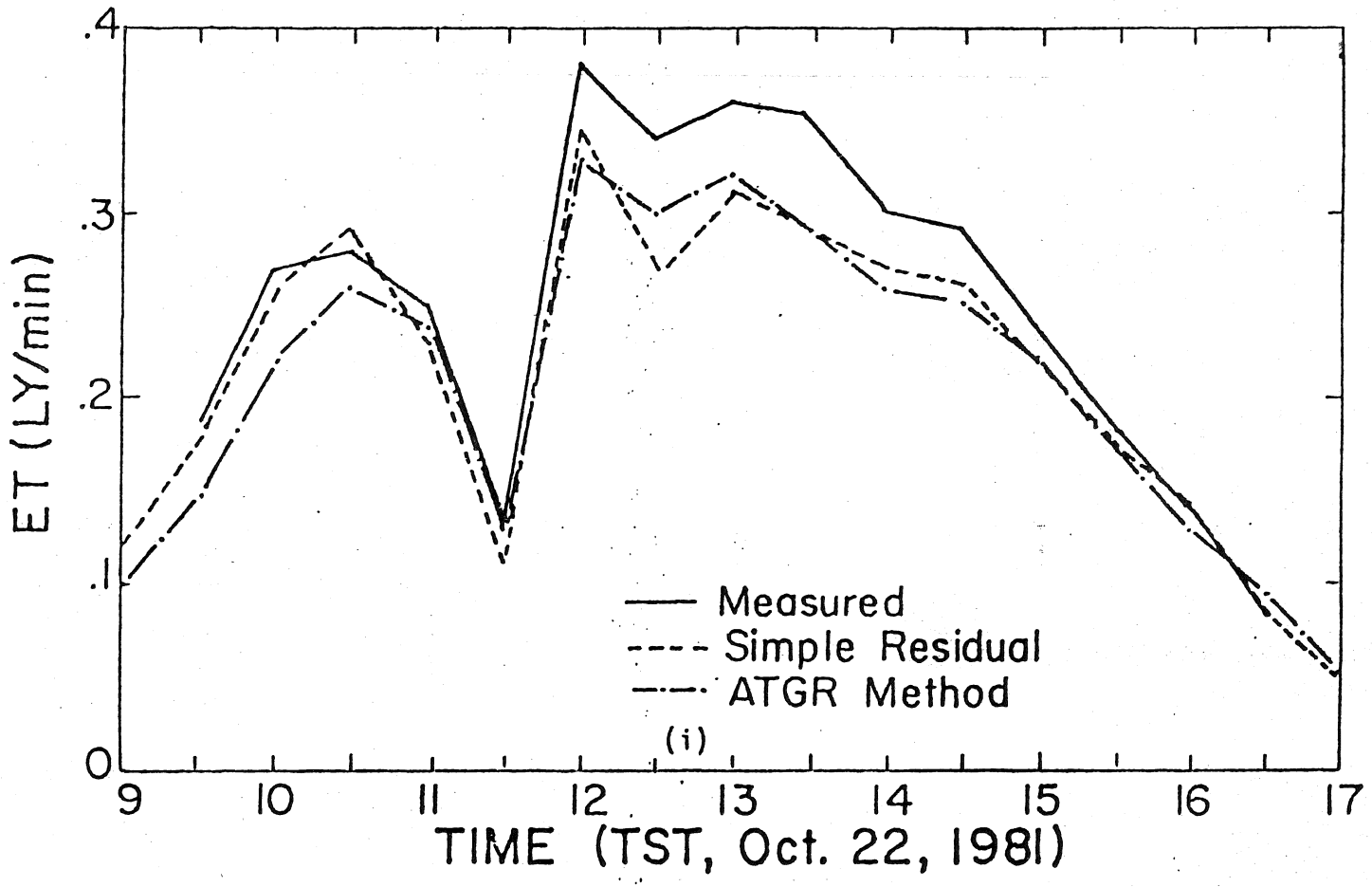

Figure 11. (cont.)

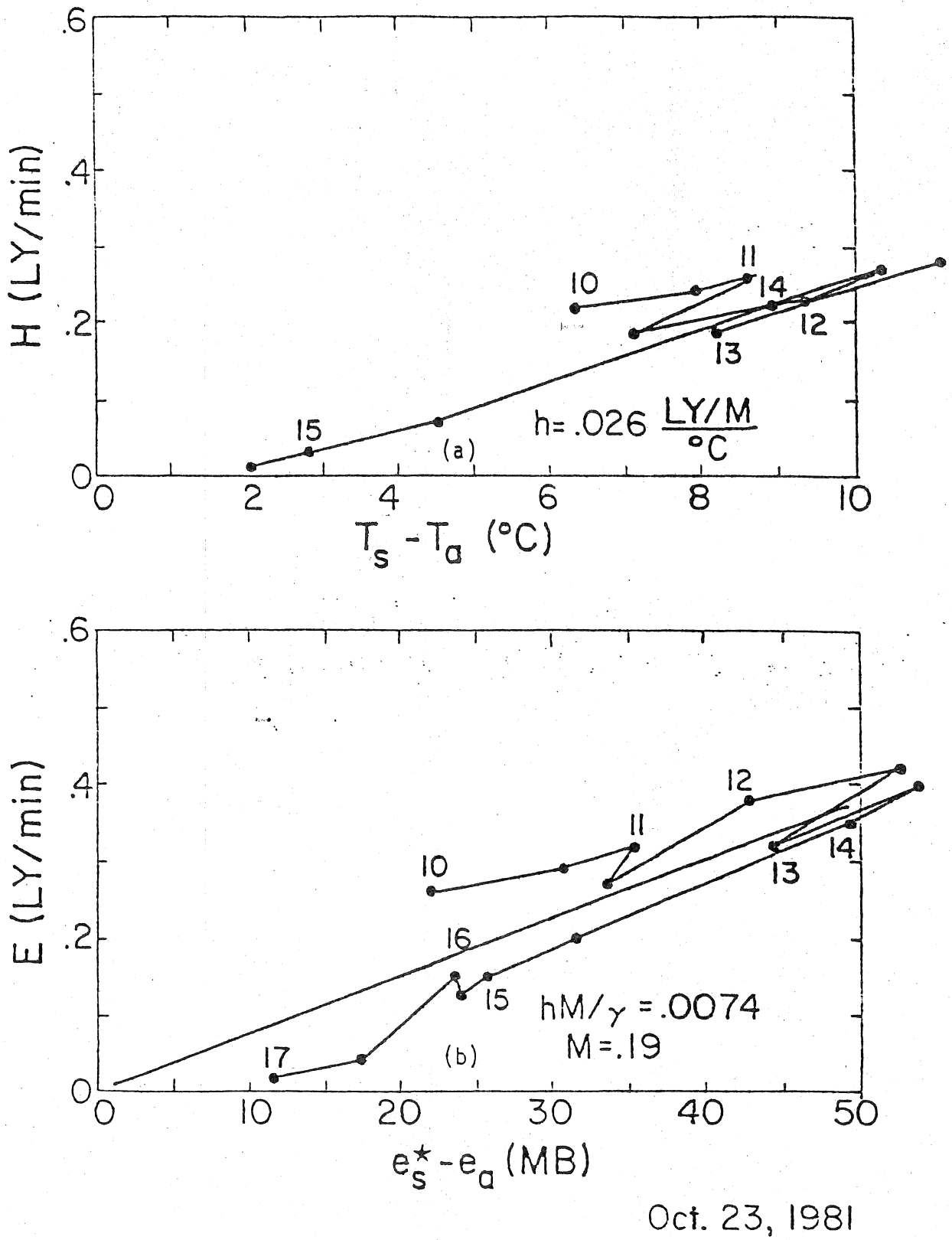

Figure 12. Data and ET Estimates for Oct. 23, 1981. See p. 185 for brief explanation of individual graphs.

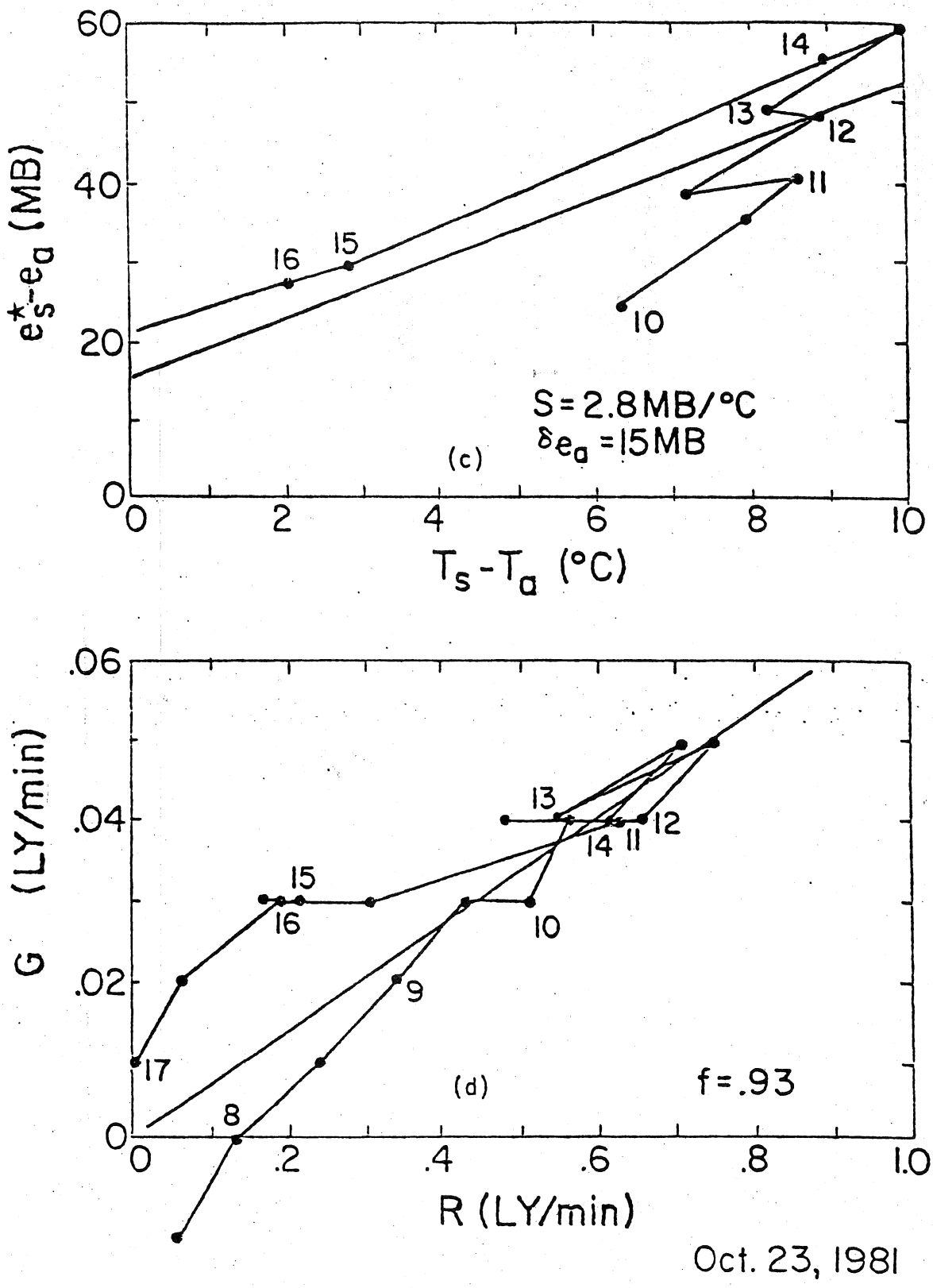

Figure 12. (cont.)

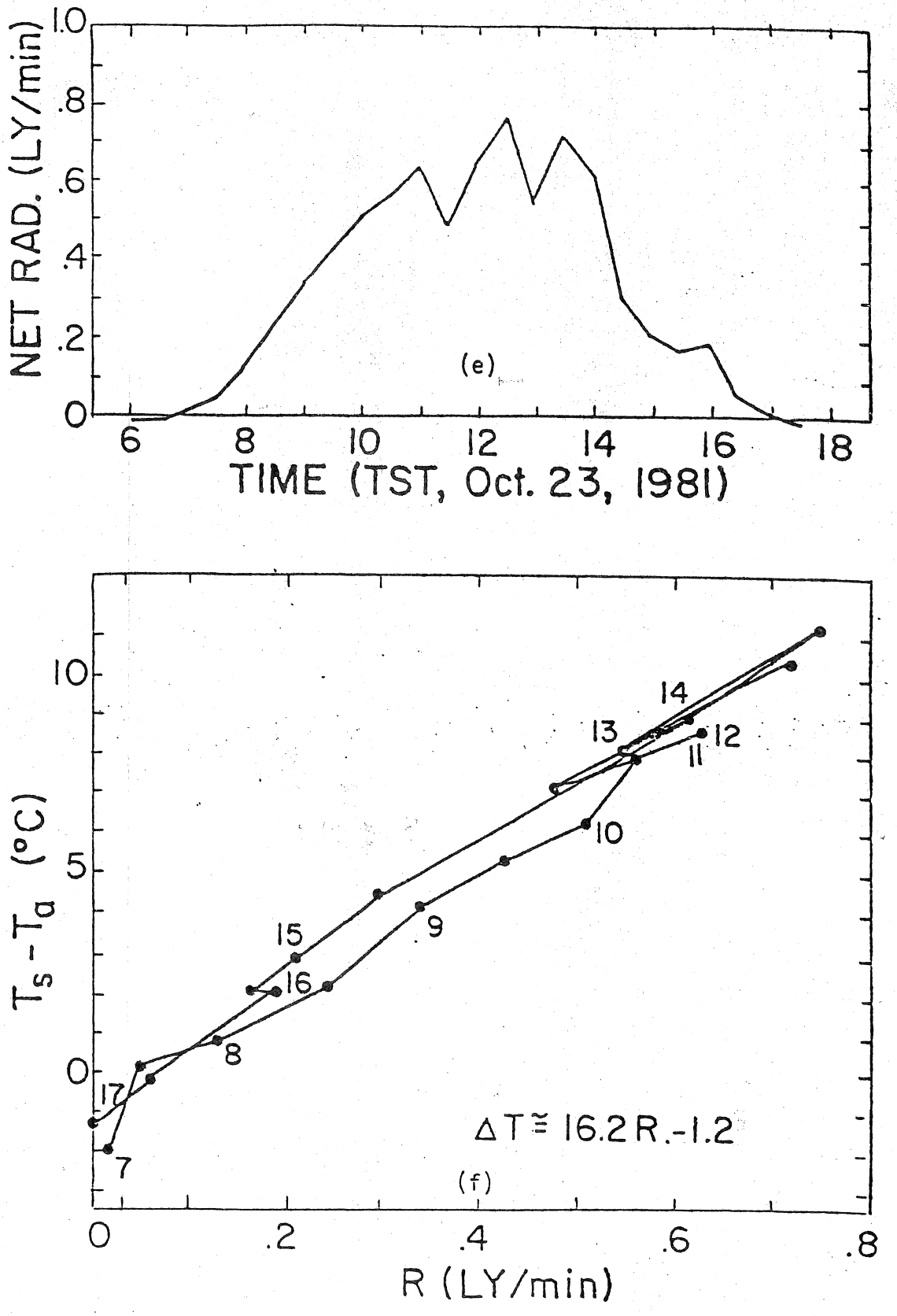

Figure 12. (cont.)

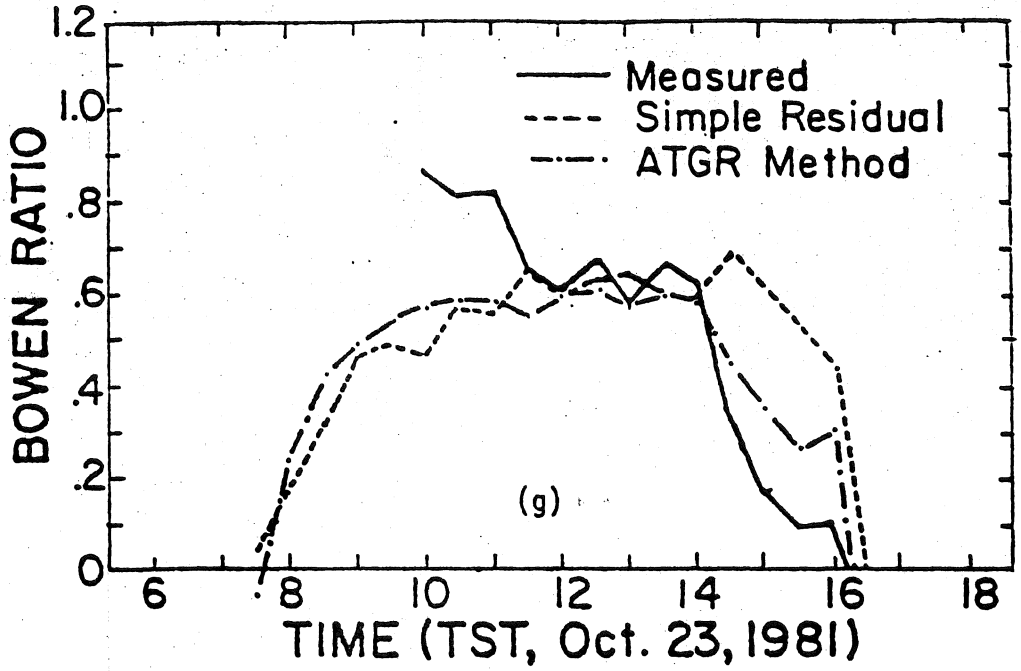

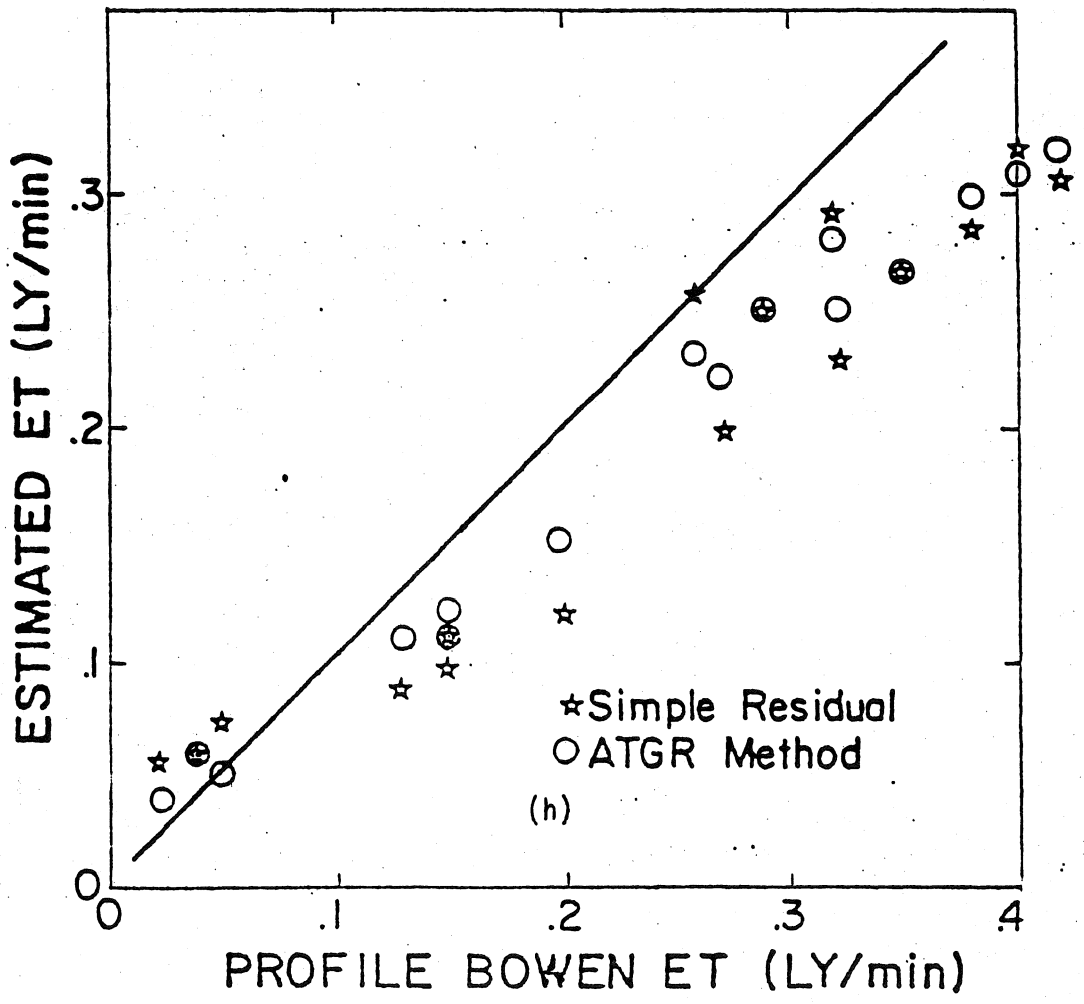

Figure 12. (cont.)

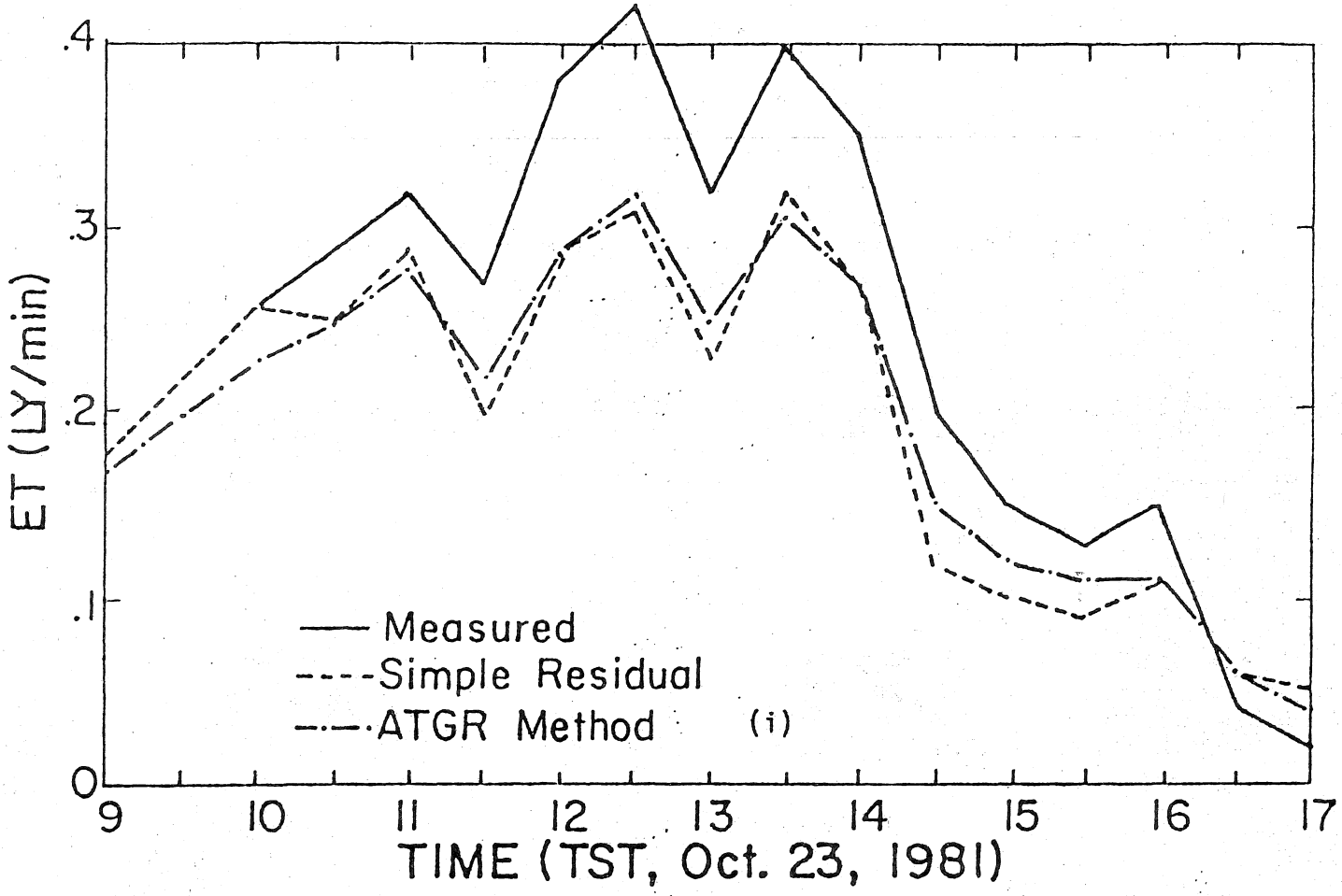

Figure 12. (cont.)